NOTICE

The quality of this microform is heavily dependent upon the quality of the original thesis submitted for microfilming. Every effort has been made to ensure the highest quality of reproduction possible.

If pages are missing, contact the university which granted the degree.

Some pages may have indistinct print especially if the original pages were typed with a poor typewriter ribbon or if the university sent us an inferior photocopy.

Reproduction in full or in part of this microform is governed by the Canadian Copyright Act, R.S.C. 1970, c. C-30, and subsequent amendments.

AVIS

La qualité de cette microforme dépend grandement de la qualité de la thèse soumise au microfilmage. Nous avons tout fait pour assurer une qualité supérieure de reproduction.

S'il manque des pages, veuillez communiquer avec l'université qui a conféré le grade.

La qualité d'impression de certaines pages peut laisser à désirer, surtout si les pages originales ont été dactylographiées à l'aide d'un ruban usé ou si l'université nous a fait parvenir une photocopie de qualité inférieure.

La reproduction, même partielle, de cette microforme est soumise à la Loi canadienne sur le droit d'auteur, SRC 1970, c. C-30, et ses amendements subséquents.

ISBN 0-315-56462-8

UNIVERSITÉ D'OTTAWA
UNIVERSITY OF OTTAWA

To my wife, Carol

and son, Ryan

"I use to be a coyote, but

I'm all right nowooooooooooo!!!"

Acknowledgements

I wish to express my gratitude to my research supervisor, Professor B.A. Morrow for his inspiration and guidance throughout my tenure at Univ. of Ottawa and for being a formidable opponent during the backgammon era.

I am equally indebted to Professor J.C. Lavalley for his enlightening discussions and comments concerning Chapters 3 to 7.

I am grateful to Dr. Henry Buijs, Garry Vail and Jean Noel Berube of Bomem Inc. for their help and encouragement in finishing this thesis.

I would like to thank my good friend, Richard McFarlane who had to put up with me for 5 years in the same lab. I don't know how I would have managed to find anything without him around.

To Professor D.M. Bishop whose organizational skills with 400 first year students was appreciated.

Thanks to Yves, Andy, Jo-Anne and Steve for help along the way.

Thanks to "The Turk", Dave "T", "Tall Dave","Dis-Abel", Germain and the coyotes for good times.

Finally, I would like to thank my best friend and wife, Carol, for typing this thesis and for everything else.

Contents

Abstract

In this thesis, infrared and Raman spectroscopy are used to study catalytic processes occurring on metal oxides. The text is divided into three sections. In Chapters 3 to 7, a comprehensive examination of the Claus reaction on several oxides has been undertaken. Secondly, the reaction of cyanogen and hydrogen cyanide on alumina and silica is discussed in Chapter 8 and 9. Finally in Chapter 10, the development of techniques and instrumentation necessary for the experiments performed in Chapters 3 to 9 is outlined.

Claus Catalysis

The removal of H_2S and SO_2 from industrial gas streams is usually accomplished over suitable catalysts by the modified Claus reaction:

$$2H_2S + SO_2 \rightarrow \frac{3}{n}S_n + 2H_2O \qquad (1)$$

Alumina itself or alumina with sodium or titania as promoters are commonly used catalysts. In an attempt to clarify the role of the catalyst in the Claus reaction, infrared and Raman spectroscopy have been used to study the adsorption of SO_2, H_2S

and H_2O in various combinations on alumina, sodium doped alumina, silica, sodium doped silica, titania and gallium oxide.

H_2S dissociatively adsorbs on the coordinately unsaturated (cus) Lewis acid/base sites of alumina giving rise to infrared bands at 3690 (AlOH) and 2570 cm^{-1} (AlSH).

$$_{cus}\,Al^{+3}\quad _{cus}\,O^{-2} \quad + H_2S \rightarrow \quad \begin{matrix} H & \\ S & H \\ | & | \\ Al & O \end{matrix} \qquad (2)$$

H_2S also forms hydrogen bonded species with AlOH sites present initially on the alumina or those created via Reaction 2. Infrared bands at 1570 and 1340 cm^{-1} are due to trace amounts of CO_2 in the H_2S or bound to the alumina as carbonates and bicarbonates.

For all oxides studied, (excluding silica) Raman bands at 480, 220 and 151 cm^{-1} characteristic of sulfur were produced only from the reaction of adsorbed SO_2 with gaseous H_2S.

On alumina, SO_2 reacts with Lewis basic sites to form a sulfite, (Al-SO_3) and with Lewis acid sites to form Al-SO_2. With a hydroxylated alumina, the reaction of Al-OH sites with gaseous SO_2 produces Al-OSOOH. Al-OSOOH is much more reactive with H_2S at room temperature than Al-SO_3 and it is the major species formed on a highly dehydroxylated alumina when trace amounts of H_2O are present during reaction. H_2O is a product of the Claus reaction and this would ensure that mainly Al-OSOOH is present as a reactive species.

A comparative study between sodium on silica, sodium on alumina and alumina was undertaken to determine the role of sodium as a promoter for the Claus reaction. Silica itself adsorbed neither H_2S nor SO_2 and hence showed no Claus activity. On the other hand, sodium doped silica adsorbed both SO_2 and H_2S and exhibited some Claus activity.

The reaction between H_2S and SO_2 on sodium doped silica resembled the reaction in aqueous solution commonly known as Wackenroder's solution. SO_2 is adsorbed as sulfite $SO_3^=$ or hydrogen sulfite (HSO_3^-). The hydrogen sulfite is in equilibrium with the pyrosulfite ($S_2O_5^=$):

$$2HSO_3^- \rightleftharpoons S_2O_5^= + H_2O \qquad (3)$$

Addition of H_2S converts both the $S_2O_5^=$ and HSO_3^- to thiosulfate $S_2O_3^=$. In Raman experiments $S_2O_3^=$ decomposed with increased laser power to produce sulfur.

Sodium doped alumina exhibits an enhanced basicity relative to pure alumina. The effect of this is to produce a larger concentration of Al-SO_3 from the adsorption of SO_2 and this is converted easily to $AlHSO_3$ in the presence of water. This type of conversion was not observed for pure alumina. The combination of higher concentrations of Al-SO_3 and the facile conversion of Al-SO_3 to a more reactive $AlHSO_3$ (with respect to H_2S) could account for the higher Claus activity.

The basic sites of titania reacted with SO_2 to form a sulfite, Ti-OSO_2, which is more labile than $AlSO_3$ on alumina. Reaction of SO_2 with hydroxyl groups of titania, or of Ti-OSO_2

with H_2O, produces several adsorbed species, all of which are reactive with H_2S.

Adsorption of SO_2 on gallium oxide produces three types of adsorbed species. The adsorbed SO_2 can be correlated with the poisoning of sites for selective catalytic processes such as cis-trans isomerization and H/D exchange reactions.

In general, we have found that several types of adsorbed SO_2, which exhibit varying degrees of Claus reactivity, can exist on alumina and other oxides. The presence of water as a product of the Claus reaction would ensure a highly hydroxylated and hydrated environment which would have a dramatic effect on the types of adsorbed SO_2 species present during Claus catalysis.

The formation of surface sulfates can cause deactivation of Claus catalysts. The oxidation of H_2S or SO_2 in excess O_2 over Al_2O_3 or TiO_2 (anatase) yields, for either catalyst under anhydrous conditions, an infrared spectrum which is characterized by an intense sharp band near 1380 cm^{-1} and a broad band or doublet near 1040 cm^{-1}. The same spectrum arises from the impregnation of Al_2O_3 with either $(NH_4)_2SO_4$ or $Al_2(SO_4)_3.18H_2O$ or of TiO_2 with $(NH_4)_2SO_4$ or $TiOSO_4$ and heating the dried mixture at 500°C under vacuum. The sulfated surface does not exchange with $^{18}O_2$ but does with $H_2{}^{18}O$ and only one new shifted high wavenumber band is produced for partial or complete oxygen-18 exchange. The infrared spectrum changes in the presence of H_2O at 20°C and resembles that of a more traditional bidentate type sulfate species and we postulate that, in the absence of OH groups or water the sulfate has a structure resembling (I) instead of (II):

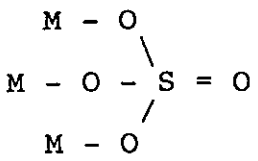

(I)

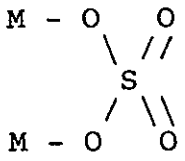

(II) (4)

In the presence of H_2O or excess surface OH groups, enhanced Bronsted acidity is due to SOH groups formed via the equilibrium:

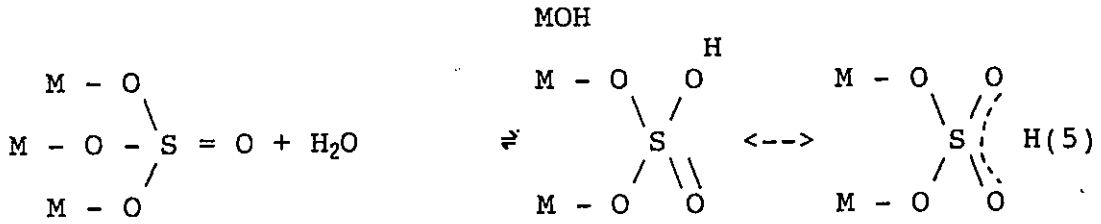

H(5)

Finally, the sulfated Al_2O_3 surface is more thermally stable and more resistant to reduction in H_2 than is the TiO_2 surface.

Hydrogen Cyanide and Cyanogen on Silica and Alumina

a. Silica

The primary reaction of C_2N_2 with silica at 420°C is;

$$SiOH + C_2N_2 \rightarrow SiNCO + HCN \qquad (6)$$

With a highly dehydroxylated silica in which reactive siloxane sites are present, a second reaction also takes place.

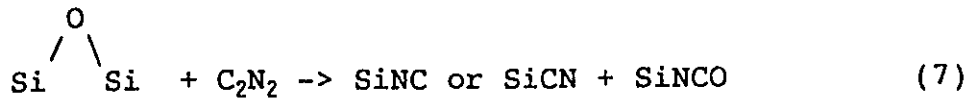

(7)

Condensation of the SiNCO to form a carbodiimide, Si-N=C=N-Si, occurs upon pyrolysis above 470°C;

$$2\ SiNCO \rightarrow SiN{=}C{=}N{-}Si + CO_2\uparrow \qquad (8)$$

The SiNC and SiCN formed in Reaction 7 are converted to a SiNC adjacent to the carbodiimide and both are stable to 900°C.

On a silica activated at 420°C, no reactive siloxane sites are present and, hence, no SiCN or SiNC formed upon reaction of C_2N_2 below 420°C. Pyrolysis above 420°C resulted in the formation of a carbodiimide and a second species similar to the carbodiimide from the reaction of SiOH and SiNCO. Small amounts of $SiNH_2$ formed during pyrolysis from the reaction of adjacent SiOH and SiNCO.

$$2SiOH + SiNCO \rightarrow SiNH_2 + CO_2 + \begin{matrix} & O & \\ / & & \backslash \\ Si & & Si \end{matrix} \qquad (9)$$

b. Alumina

Addition of HCN to alumina initially formed two types of adsorbed species, a dissociative Al-NC via the reaction;

$$_{cus}\ Al^{+3} + {}_{cus}\ O^{-2} + HCN \rightarrow \begin{matrix} C & & \\ N & & H \\ | & & | \\ Al & & O \end{matrix} \qquad (10)$$

and a nondissociative HCN coordinated to a $_{cus}\ Al^{+3}$ site;

$$_{cus}\ Al^{+3} \leftarrow :N{\equiv}C{-}H \qquad (11)$$

which is followed by rapid and extensive polymerization.

Addition of C_2N_2 to a completely dehydroxylated alumina at room temperature forms AlNCO, AlCN and AlNC.

$$_{cus}\,Al^{+3}\;_{cus}\,O^{-2} + C_2N_2 \rightarrow AlNC \text{ or } AlCN + AlNCO \qquad (12)$$

With excess C_2N_2, a polymeric buildup of paracyanogen is observed;

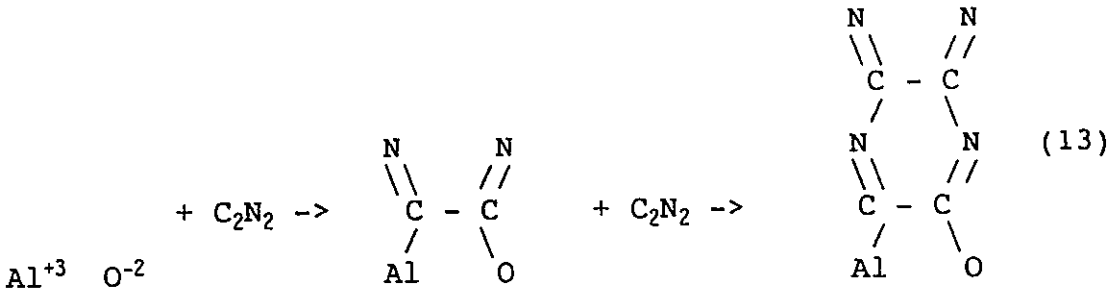

(13)

Pyrolysis of the surface at 400°C results in conversion of AlNCO to a carbodiimide structure.

COMPUTERIZATION OF A DISPERSIVE INFRARED SPECTROMETER

A major problem for infrared studies for studying the Claus process on oxides is that many characteristic vibrational modes (i.e. SO_x), lie in regions where the oxide is opaque. Thin film techniques have been developed to extend the region of transparency of the oxide. In situ measurement and computer aided subtractive programs were developed in order to extract the vibrational spectra of surface species from regions of low transparency. Therefore, much of the initial groundwork for this

thesis involved the development of instrumentation to perform such tasks. This work is outlined in Chapter 10.

Chapter 1

INTRODUCTION

During the past decade, the term "acid rain", originating from SO_x and NO_x emissions, has become synonymous with the destruction of lakes and forests of North America and Europe. Having been born and raised in Sudbury, Canada, the author is well aware of this problem. Sudbury contains large deposits of nickel and copper located in iron sulfide ores. To separate the copper and nickel from the iron sulfide, the ore is smelted, liberating SO_2 as a gas.

Ironically, before the turn of the century, Sudbury was a lumber town. The building of the Trans-Canada Railway, which led to the discovery of copper nickel ores, changed that. In the early mining years, the smelting of the ore was performed in open areas over large piles of stacked timber. The SO_2 emission from the ore simply drifted across the land, leaving a destructive path in its wake. This left Sudbury with large sections of land completely barren. Nevertheless, these areas of land did find some use. In the mid to late 1960's, the Apollo astronauts used these areas to test drive their moon vehicles. The term

"moonscape" is normally used by the local inhabitants to describe these desolated areas.

Unfortunately, the smelting of sulfur containing ores accounts for only about 20% of the total SO_x emissions in North America. About 75% of the SO_x emission originate from the combustion of fuels which naturally contain trace amounts of sulfur compounds. As a testament to the enormity of this problem, one needs only to consider the following example. A single 600 MW coal fired power plant containing a conservative estimate of 1% sulfur in the coal, would generate 50,000 tons of SO_2 per year [1].

The technology for removal of sulfur containing compounds from gas streams has been extensively developed [2,3]. In the first step, the sulfurous materials (thiols, thiophenes, etc.) are usually converted to hydrogen sulfide. This is followed by extraction of the H_2S from the gas stream over a suitable catalyst.

Once recovered from gas streams, the malodorous and toxic H_2S must be converted to either sulfuric acid, or more commonly, to sulfur. Conversion to sulfur is primarily accomplished by the well known Claus reaction.

$$H_2S + \frac{1}{2} O_2 \rightarrow H_2O + \frac{1}{n} S_n \quad \Delta H = -222 \text{ kJ mol}^{-1} \quad (1.a)$$

The reaction was first commercialized by Claus in 1890 [4]. Sulfur production involved the passage of H_2S in air over a bauxite catalyst. The high exothermicity of Reaction (1.a) made

it difficult to control the temperature and this lowered productivity.

This problem was later improved upon by using a two step reaction [5]. In the first step, one third of the H_2S is converted to SO_2 by direct oxidation.

$$H_2S + \frac{3}{2} O_2 = SO_2 + H_2O \quad \Delta H = -519 \text{ kJ mol}^{-1} \quad (1.b)$$

This is followed by the catalytic reaction over bauxite without the presence of oxygen.

$$2 H_2S + SO_2 = 2 H_2O + \frac{3}{n} S_n \quad \Delta H = -146 \text{ kJ mol}^{-1} \quad (1.c)$$

The lower exothermicity of Reaction (1.c) enabled a higher sulfur yield and it is this process, known as the modified Claus reaction, which is generally used today in Claus reactors.

The above equation (Reaction 1.c) is a simplistic view of the Claus process. In reality, sulfur formation is dependent on complex equilibrium and kinetic factors. The equilibrium in Reaction (1.c) is exothermic and thus maximum conversions are obtained at the lowest operating temperatures. However, if the temperature is lowered below 330°C, sulfur sublimation occurs which is a precursor for sulfate formation which is a poison for the Claus reaction. Consequently, a compromise in temperature is necessary giving rise to a 95 to 97% efficiency in typical Claus plants.

Because of the large quantities of sulfur normally involved, these efficiency levels do not meet the allowable emission standards that exist today. Therefore, much of the recent

technology developed has focused on the treatment of Claus tail gases where unreacted sulfur compounds such as CS_2, H_2S, SO_2 and COS exist. The high cost of tailgas treatment process has provided the impetus to achieve maximum conversions in Claus reactors. To accomplish this, a better understanding of the Claus process is needed.

Alumina is primarily used as a catalyst for the Claus reaction although, promoters such as sodium and titania are also employed [6]. The majority of information concerning the Claus mechanism on alumina has been obtained from transmission infrared spectroscopic studies. These studies have been used to observe the nature and reactivity of adsorbed SO_2 and H_2S on alumina. However, the mechanism for the Claus reaction over alumina-based catalysts is still not well understood.

Although the Claus reaction superficially appears simple (Reaction 1.b and 1.c) the fundamental chemistry is quite complex. Free SO_2 has vibrational modes at 1362(ν_a) and at 1151 cm^{-1} (ν_s) [7]. It reacts readily with basic metallic oxides and hydroxides to form a number of salts [8,9]. Sulfites are produced with polyvalent cations under basic conditions. Only salts of $H\text{-}SO_3^-$ and $S_2O_5^=$ are known, whereas several other species ($H\text{-}SO_3^-$, $HOSO_2^-$, $S_2O_5^=$) have been reported in aqueous solution.

To appreciate the complexity of sulfur chemistry one needs only to look at the reaction between H_2S and SO_2 in aqueous solution where a complex mixture of oxysulfur compounds, mainly polythionic acids, thiosulfuric acid and sulfur in various amounts can be formed depending on the conditions used. This

solution, known as Wackenroder's solution, has been the subject of several studies [10-12]. One postulated mechanism to illustrate this complexity is outlined below.

In the first step, the adsorption of SO_2 in water has been postulated to form at least five different species in equilibria as symbolized below.

$$2SO_{2(g)} + H_2O_{(l)} \overset{1}{=} 2SO_2 \times H_2O \overset{2}{=} 2\,H_2SO_3 \qquad (1.d)$$

$$\overset{3}{=} 2H^+ + 2HSO_3^- \overset{4}{=} 2SO_3^{-2} + 4H^+$$

$$\overset{5}{\rightleftharpoons} S_2O_5^{-2} + H_2O$$

Upon initial addition of H_2S in neutral solutions, almost 100% thiosulfate is formed.

$$4HSO_3^- + 2HS^- \rightarrow 3S_2O_3^{-2} + 3H_2O \qquad (1.e)$$

However, under slightly acidic conditions formation of tetrathionate occurs:

$$4HSO_3^- + 2H_2S \rightarrow 3S_2O_3^{-2} + 2H^+ + 3\,H_2O \qquad (1.f)$$

$$3HSO_3^- + H_2S + H^+ \rightarrow S_4O_6^{-2} + 3H_2O \qquad (1.g)$$

The tetrathionate can react further to form trithionate:

$$S_4O_6^{-2} + HSO_3^- \rightarrow S_3O_6^{-2} + S_2O_3^{-2} + H^+ \qquad (1.h)$$

In the second phase (when all HSO_3^- is depleted) reduction of the polythionates and thiosulfate occurs.

$$S_4O_6^{-2} + H_2S \rightarrow 2S_2O_3^{-2} + S + 2H^+ \quad (1.i)$$

$$S_3O_6^{-2} + 3H_2S \rightarrow S_2O_3^{-2} + 4S + 3H_2O \quad (1.j)$$

$$S_2O_3^- + 2H_2S + 2H^+ \rightarrow 4S + 3H_2O \quad (1.k)$$

Additional side reactions to form sulfite may occur:

$$S_3O_6^{-2} + S_2O_3^{-2} \rightarrow S_4O_6^{-2} + SO_3^{-2} \quad (1.l)$$

However, the sulfite formed also reacts to give sulfur:

$$SO_3^{=} + 2\ H_2S + 2\ H^+ \rightarrow 3S + 3\ H_2O \quad (1.m)$$

Although the overall stoichiometry of the solution reaction is the same as Reaction (1.b), we see that the chemistry is much more complex.

Similar and other oxysulfur and sulfur species may also be possible on alumina and other oxide catalysts. Vibrational assignment would require the knowledge of the group frequencies associated with S=O, S-O-S, S-S-O, SO_2, O-O, S-S, and S-H bonds in compounds of known structure.

Sato et. al. [13] employed infrared and Raman spectroscopies to identify several oxysulfur compounds. The infrared spectra are shown in Figure 1.1 and Raman spectra in Figure 1.2, 1.3. The infrared bands observed for these oxysulfur salts are much broader than the observed Raman bands. The infrared bands from 1200 to 950 cm^{-1} are associated with S-O stretching vibrations (S=O, SO_3^{-2}, SO_4^{-2}) and the bands in the 800 to 400 cm^{-1} are due to

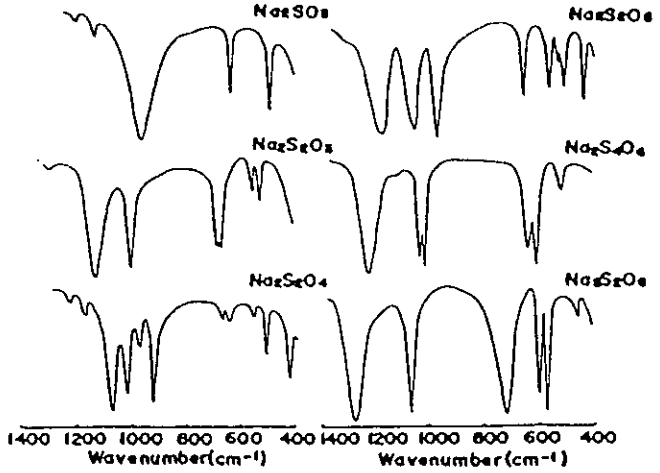

Figure 1.1

Infrared spectra of oxysulfur compounds measured in KBr disks. (from Sato et. al., ref. 13)

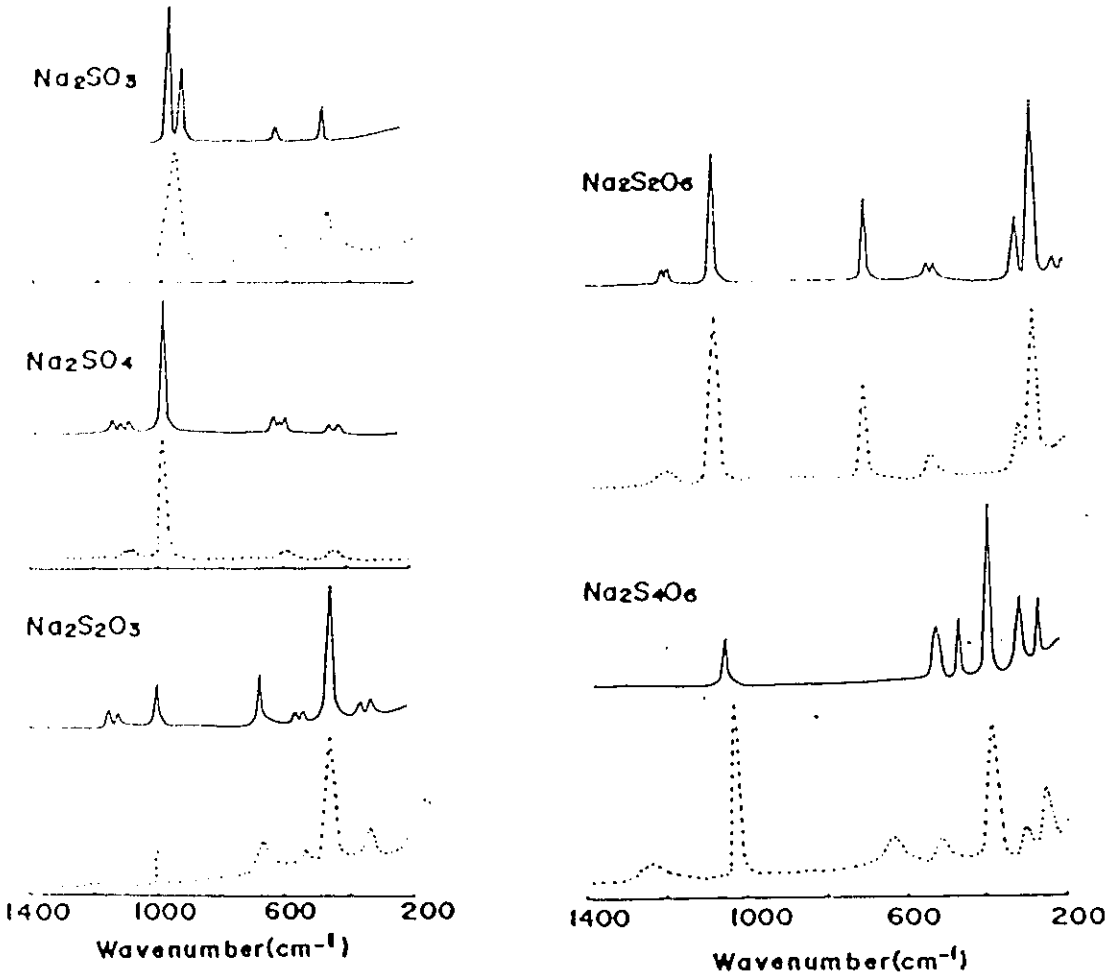

Figure 1.2

Raman spectra of oxysulfur compounds. Dashed lines denote spectrum in solution. (from Sato et. al., ref. 13)

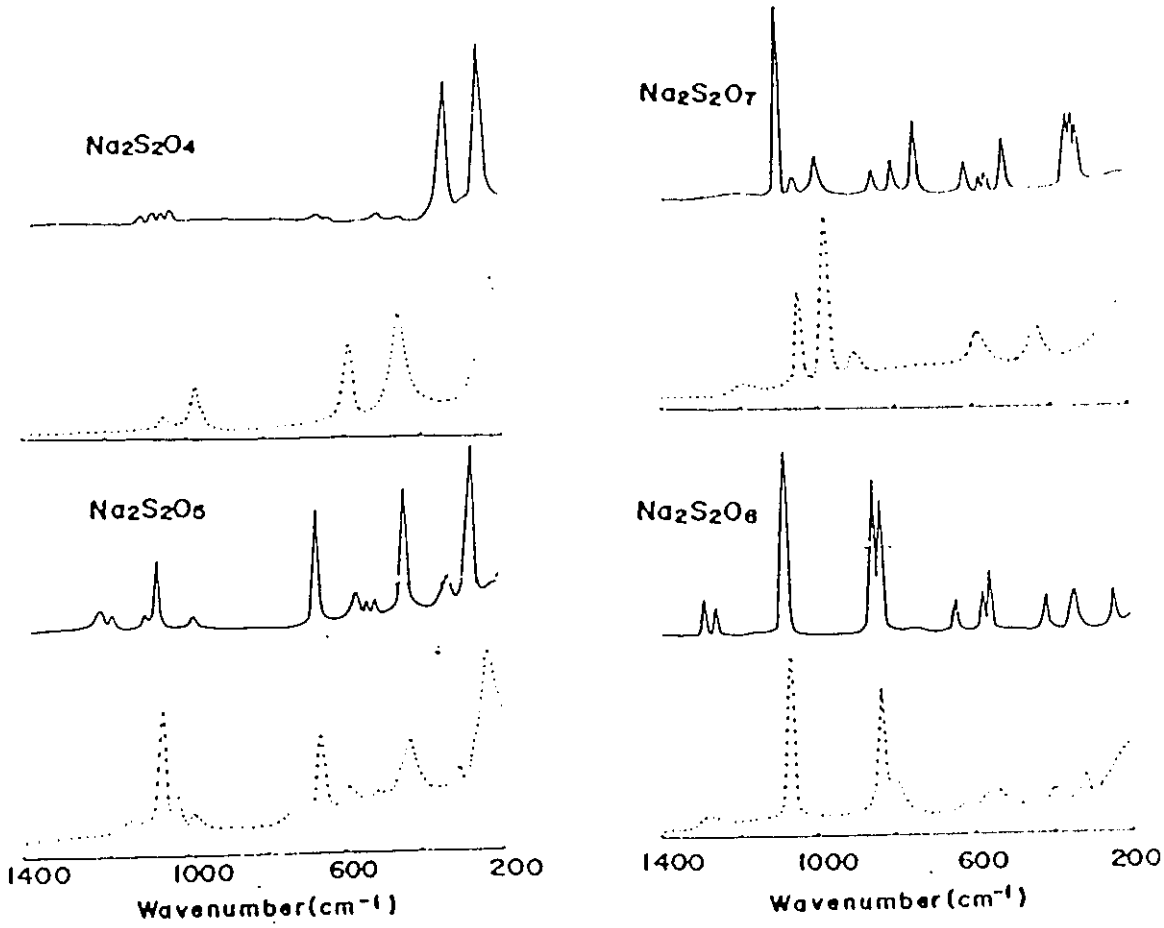

Figure 1.3

Additional Raman spectra. (from Sato et. al. ref. 13)

S-O-S and S-S-O deformation vibrational modes. The associated group Raman frequencies are shown in Figure 1.4. Raman bands due to S-S and O-O stretching modes can be observed easily, whereas in the infrared these stretching modes are very weak or are unobservable. Infrared spectra of other possible oxysulfur compounds are shown in Figures 1.5. In addition, disulfur oxide (S_2O) has been reported [15] and IR bands at 1165 and 679 cm^{-1} have been assigned to ν_1(S-O) and ν_2(S-S) stretching modes, respectively. Raman bands are located at 1157, 673 and 382 cm^{-1} [16].

The final product of the Claus process is sulfur. The group frequencies associated with S-S vibrations lie below 500 cm^{-1}. Our current configuration of our Fourier transorm infrared (FTIR) spectrometer did not allow us to examine this spectral region and, hence, these S-S bands could only be observed with Raman spectroscopy. In Figure 1.6, the Raman spectra of several polysulfides are shown. Sulfur (S_8) has strong Raman bands at 84(m), 156(s), 190(w), 220(s), 441(w) and 475(s) cm^{-1} [18].

In Chapter 3, we have reinvestigated the Claus reaction on alumina using infrared and Raman spectroscopy. Assignment of adsorbed species on alumina has been compounded by the fact that alumina is opaque below 1000 cm^{-1} where most of the characteristic SO_x modes lie. To reduce this problem, we have taken two approaches. First, by using a FTIR (previous studies mainly used dispersive IR spectrometers), where both the multiplex and throughput advantages of FTIR over dispersive systems result in the achievement of much higher signal to noise

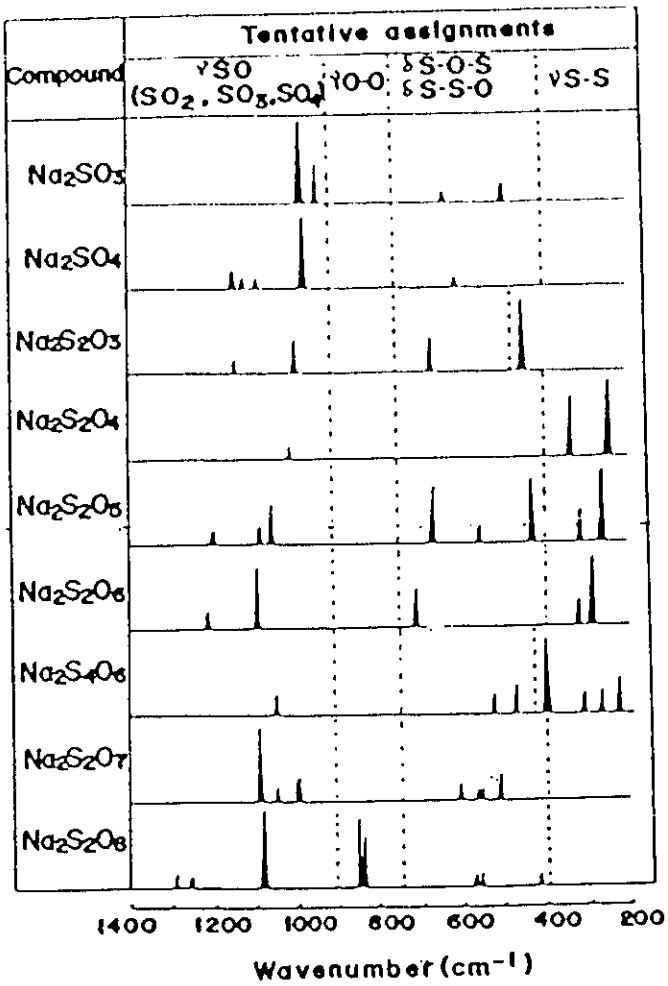

Figure 1.4

Group frequency identification of oxysulfur compounds. (from Sato et. al. ref. 13)

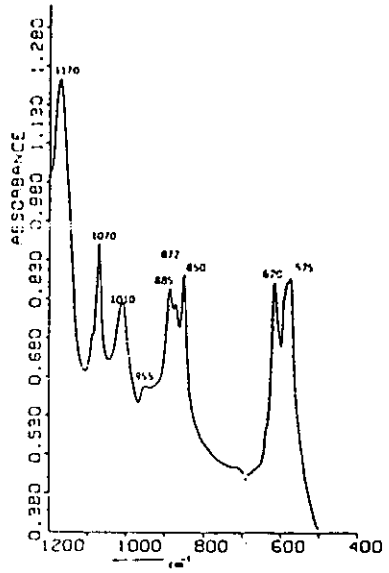

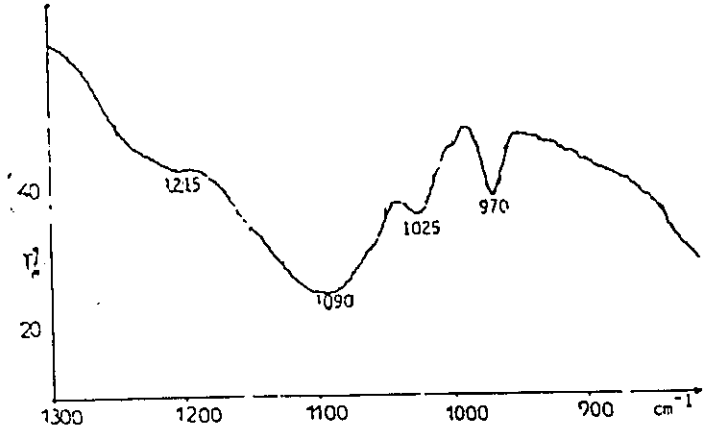

Figure 1.5

Spectra of;
a) $NaHSO_4$ in KBr
b) $NaHSO_3$ in solution (pH=5)
(from Saad, ref. 14)

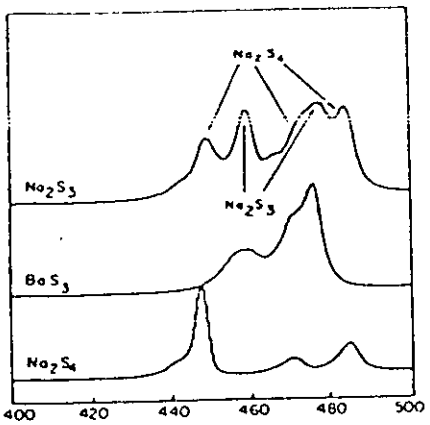

Figure 3. Raman spectra of polycrystalline Na_2S_3, Na_2S_4, and BaS_3 in the stretching region. For the Na_2S_3 spectrum the peaks are labeled to indicate their assignment to Na_2S_4 or Na_2S_3.

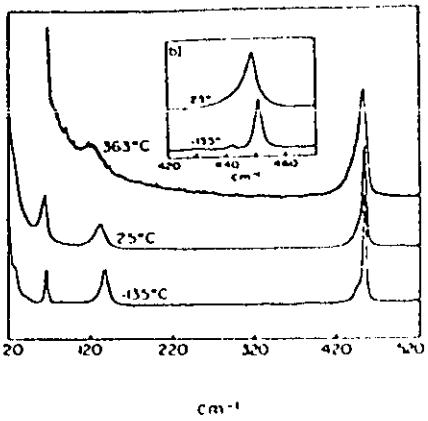

Figure 1. Raman spectra for polycrystalline β-Na_2S_3. The inset (b) illustrates the low-temperature splitting in the stretching region. All spectra were recorded with a spectral slit width of 2 cm^{-1} except the −135 °C spectrum in the inset for which the slit width is 0.7 cm^{-1}.

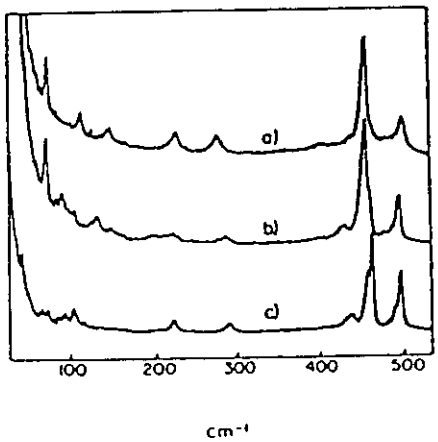

Figure 5. Room-temperature Raman spectra of the polycrystalline α (a), β (b), and γ (c) forms of Na_2S_5.

Figure 1.6

Raman spectra of polysulfur compounds.
(from Janz et. al., ref. 17)

ratios necessary for observation of bands in low transmittance regions. The high wavenumber reproducibility of an FTIR enables subtractive techniques to be accurately employed and this, coupled with thin film techniques, has permitted observation of infrared bands due to adsorbed species on alumina below 1000 cm^{-1}. Both the FTIR employed and thin film techniques used are discussed further in the experimental section.

Secondly, whereas alumina is strongly adsorbing below 1000 cm^{-1}, it is a weak Raman scatterer and hence, observation of Raman bands due to adsorbed species from 100 to 4000 cm^{-1} may be possible. Strong Raman bands are associated with S-O and S-S group frequencies.

In Chapter 4, the Claus reaction on sodium doped alumina and sodium doped silica has been examined. Silica itself is inert vis-à-vis the Claus reaction. It was our hope that a comparative study of pure alumina, Na doped alumina and Na doped silica, would clarify the role of sodium in the Claus reaction.

Titania has been used as a promoter for alumina for the Claus reaction [6]. Recently, titania has been reported to be a better Claus catalyst the alumina [19]. In Chapter 5, we have then examined this possibility.

In Chapter 6, we have studied gallium oxide as a possible Claus catalyst. Ga_2O_3 has been shown to exhibit similar surface properties and catalytic activity to that of Al_2O_3. Ga_2O_3 was an attractive oxide to study for the Claus process because the transparent region is extended to 850 cm^{-1}.

Finally, in Chapter 7, we have examined the structure and stability of sulfated catalysts. Cumulative sulfate formation results in catalytic deactivation and, therefore, costly periodic regeneration of the catalyst must be performed.

It was intended that these studies would lead to a better understanding of the mechanism of the Claus reaction and in particular, to the identification of the reactive intermediates and of the alumina sites involved in this process. With this in hand, future improvements in Claus catalysts, providing a more efficient and economical means of sulfur removal, might be achieved.

Chapter 2

GENERAL EXPERIMENTAL

2.1 INSTRUMENTATION

Infrared spectra were obtained using either a Bomem DA3-02 FTIR or a computer controlled Perkin-Elmer 283 dispersive spectrometer. The Perkin-Elmer 283 spectrometer is described in more detail in Chapter 10.

With the Bomem DA3, spectra were recorded under purge conditions operating at 4 cm^{-1} resolution employing a wide band MCT detector ($D^* = 5 \times 10^9$). Typical spectra were recorded with 100 scans requiring 39 seconds observation time.

A Vacuum Generators SX-200 or a M59 mass spectrometer was employed for gas analysis. A turbo molecular pump was provided with the SX-200.

A Jobin-Yvon HG-2 Raman spectrometer was used to obtain Raman spectra with a Spectra Physics argon or krypton ion laser. Plasma line filtering was provided by an Anaspec laser filter monochrometer. A diagram of the Raman configuration is shown in Figure 2.1. A 90 degrees scattering geometry was employed in all

cases. Spectra were usually recorded between 4000-100 cm^{-1} shift from the laser line at a resolution of approximately 6 cm^{-1} with scan times of 40 minutes.

2.2 SAMPLE CELLS

A standard sample cell used for the infrared studies has been described previously by Morrow and Ramamurthy [20] and is shown in Figure 2.2. The sample holder could be easily raised and lowered from the window to the furnace region with a magnet without breaking vacuum. The cell holder and cell bottom were made of quartz enabling furnace temperatures of 1200°C to be achieved. The cell top was made of pyrex. The two sections of the cell were connected by applying Apiezon H grease between the two ground glass joints. The furnace region consisted of asbestos paper surrounding the cell around which was wound Kanthal wire at a density of four turns per cm. This was insulated by two layers of a ceramic paper tied securely with asbestos cord. Temperatures were measured with a chromel-alumel thermocouple encased in a quartz tube inserted between the insulation and the heating wire.

To test the accuracy of the temperature measured by the thermocouple, a second thermocouple was placed at the centre of the furnace region in the evacuated cell. Temperatures were raised at equal intervals from room temperature to 1000°C and measurements were obtained thirty minutes after equilibrium. Virtually no difference was observed in the measured temperature

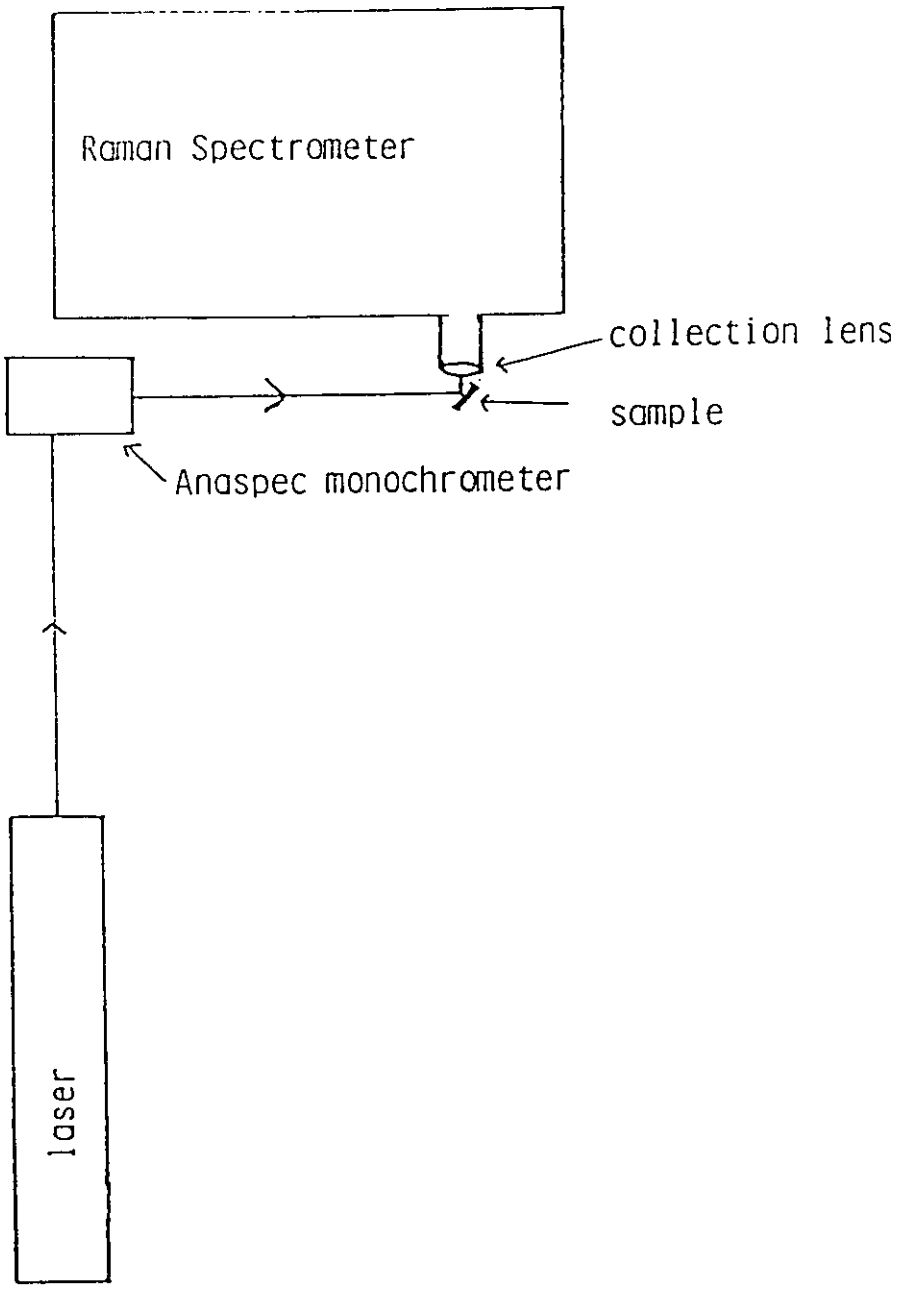

Figure 2.1

Configuration of the laser, sample and Raman spectrometer.

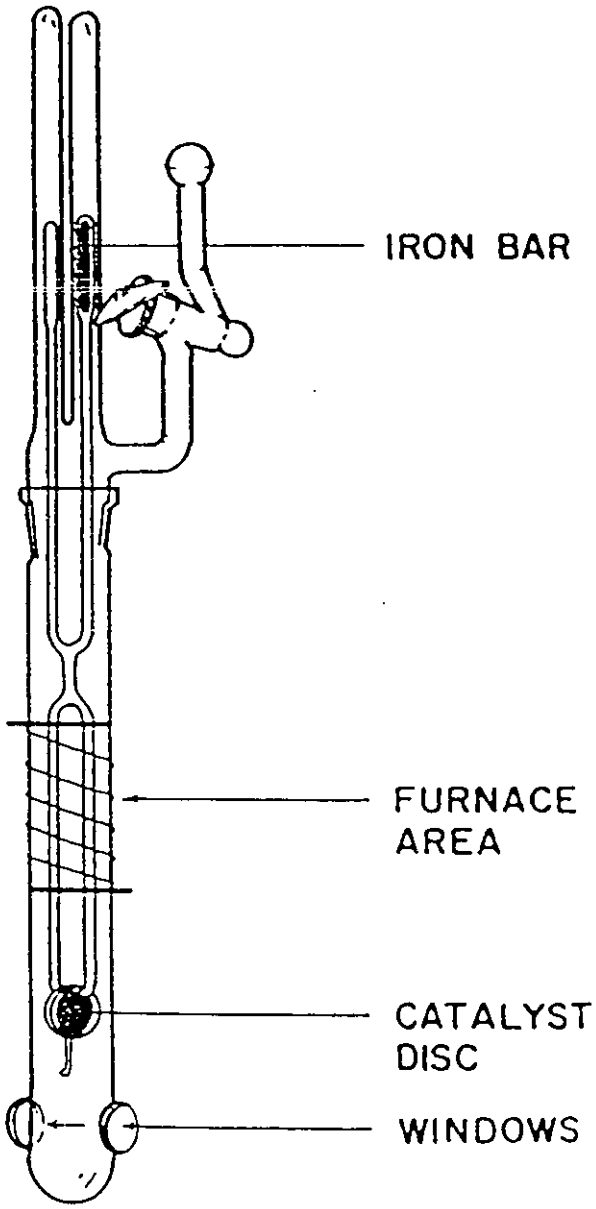

Figure 2.2

The standard infrared cell.

below 400°C. Above 400°C, a slightly lower temperature was observed for the thermocouple in the center of the furnace region. This discrepancy increased linearly with higher temperatures to a maximum of 50 degrees at 1000°C.

Cell windows were usually NaCl, KCl or CaF_2 and were held in place with an epoxy resin. Initial experiments involving SO_2 and H_2S oxidation (Chapter 7) resulted in reaction with the NaCl or KCl windows. ZnS windows were inert for all Claus experiments and, therefore, were exclusively used in these studies.

A second quartz infrared cell shown in Figure 2.3 was used when in situ heating of the sample in the IR spectrometer was required. A NaCl window was epoxyed on one end of the cell. A second NaCl window was epoxyed to a Cajon Ultra-Torr vacuum adapter which fitted over the other end of the tube.

2.3 VACUUM LINE

A standard pyrex vacuum line was used to evacuate sample cells and to manipulate and add gases. The vacuum lines were mounted on portable tables and could be moved close to the infrared spectrometers for in situ studies. A residual pressure of 10^{-6} to 10^{-7} torr was achieved with an oil diffusion pump.

2.4 RAMAN CELLS

The Raman cells were similar in construction to the infrared cells (Figure 2.4). However, the window region and sample

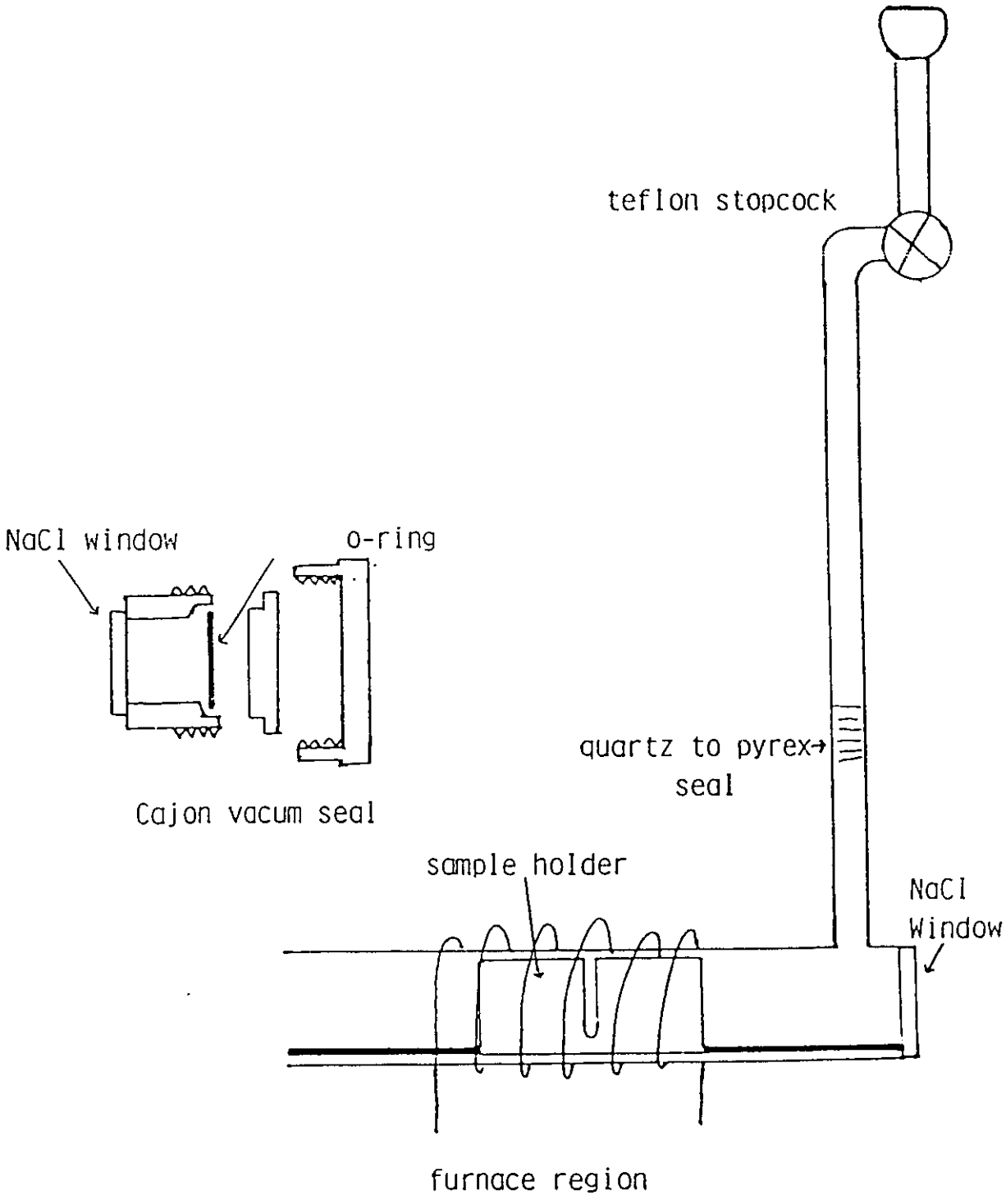

Figure 2.3

Infrared cell used for insitu studies.

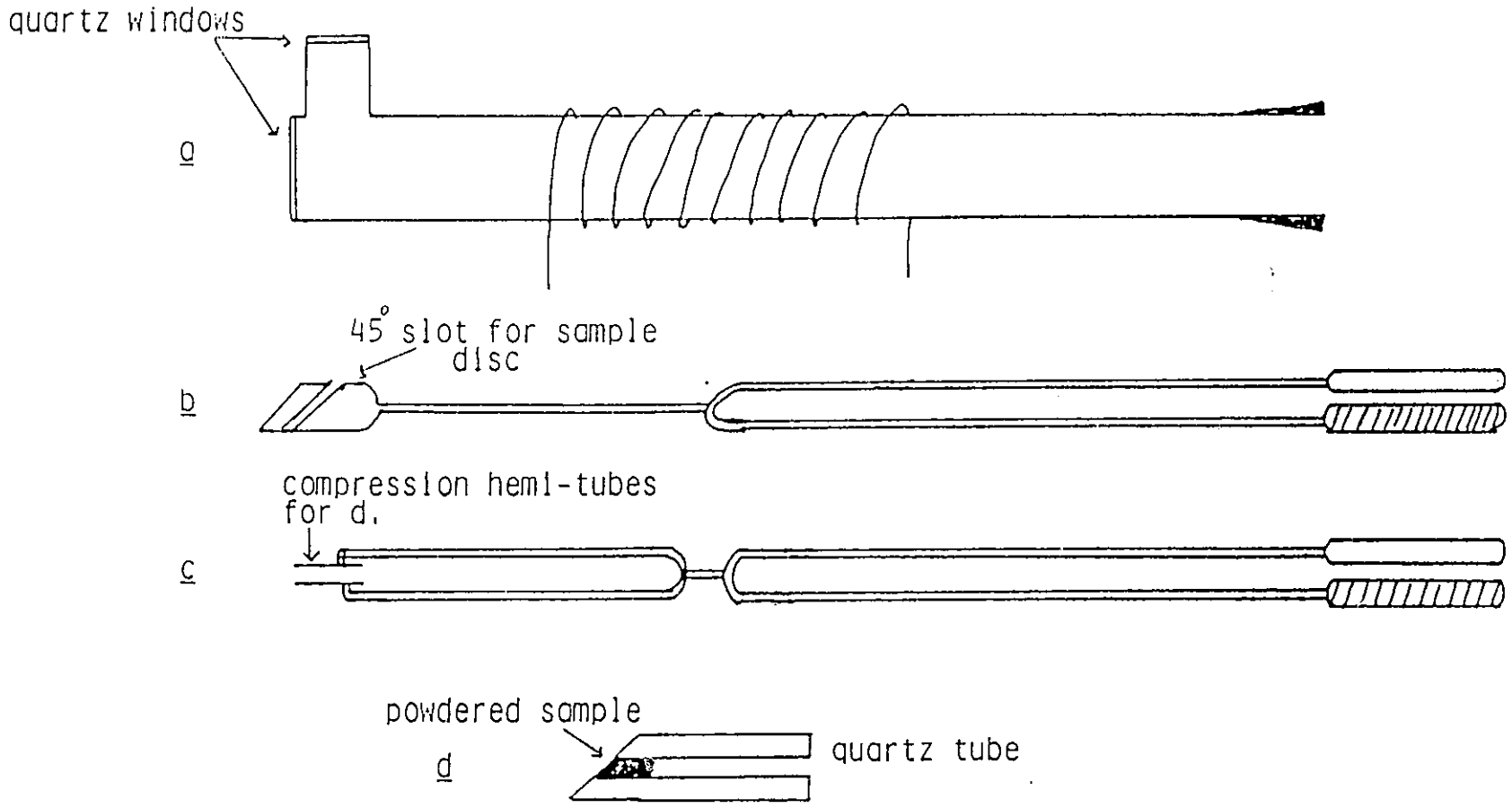

Figure 2.4

a) Bottom part of the Raman cell. The cell top is the same as that shown in Figure 2.2.
b) Conventional sample holder for Raman studies.
c) Modified Raman sample holder for small quantities of a powdered sample.
d) Sample tube from (c).

holders were modified to allow 90 degree collection geometry of scattered radiation. The cell was made from pyrex and the windows were of optical quartz. The sample holder shown in Figure 2.4(b) was used and required the use of 12 mm sample discs. For samples which were air sensitive or hygroscopic, the sample holder shown in Figure 2.4(c,d) was used. In this case, samples were pressed into the holder using a glass rod inside a nitrogen purged glove bag.

2.5 HIGH TEMPERATURE MEASUREMENTS

A method using the Perkin-Elmer 283 spectrometer for recording adsorption spectra at elevated temperatures, is described in Chapter 10. A similar technique has been developed for the DA3-02 FTIR and is also described in Chapter 10.

2.6 PROCEDURE FOR FILTER EXPERIMENTS

Under normal FTIR scanning conditions, the spectrum of a sample which contains regions of high and low transparency may contain "ripples" in the latter. Silica or 3% Na/SiO_2 satisfy both of these conditions in that a highly transparent region (4000 to 1300 cm^{-1}) and a "window" region of low transparency (1000 to 500 cm^{-1}) both exist (see Figure 4.2). The existence of these "ripples" made observation of bands due to adsorbed species in the window region difficult.

To eliminate this problem the following procedure was used. A filter which blocked out radiation in the 4000 to 1100 cm^{-1} region was placed in the FTIR filter wheel. This modification produced a single region of transparency for silica. The largest aperture available (10 mm) for the Bomem DA3-02 was used to allow the maximum amount of light to pass through the sample to achieve a better signal to noise ratio.

2.7 MATERIALS

Both the alumina (Degussa Alumin Oxid C) and titania (Degussa P25) were obtained from Deguss A.G. Frankfurt. They had a measured B.E.T. (N_2) surface areas of 105 m^2g^{-1} and 55 m^2g^{-1}, respectively. The silica used was Cab-O-Sil HS-5 obtained from Cabot Inc. of Tuscola, Illinois, U.S.A. It had a B.E.T. (N_2) surface area of 330 m^2g^{-1}. Unless otherwise specified the above catalysts were calcined at 550°C for several days in air prior to use to remove organic impurities.

For infrared studies, self-supporting discs, 2.5 cm in diameter, were prepared in a stainless steel die and compacted at a pressure of 10^7 Pa. For silica, self-supporting discs containing 5 mg cm^{-2} could be prepared in this manner.

During pressing, both titania and alumina would adhere to the die faces. To prevent this, lens paper was placed between the sample and die faces before pressing and was removed after pressing. Sample discs containing 4 mg cm^{-2} could be made in this manner. Techniques for thin films dispersed on ZnS or ZnSe

windows containing 0.1 to 0.5 mg cm^{-2} of material have been developed. In one method, the catalyst material was placed on one die face. The window was then placed over this and rotated gently to uniformly distribute the material over the window. Hand pressure was then applied to the centre of the window. A relatively uniform film usually adhered to the window.

A second method involved placing some catalyst inside a spray bomb with a suitable volatile solvent, normally methylene chloride. The ZnSe or ZnS window was then sprayed using rapid side to side motions until the desired amount of catalyst was deposited. This latter technique worked exceptionally well for titania.

Gallium oxide (99.99%) was supplied by Alpha Ventron of Danvers, Ma. and had a measured surface area of 13 m^2g^{-1}. The Ga_2O_3 was not calcined prior to use. Self supporting discs containing 20 mg cm^{-2} were normally employed.

For Raman experiments, sample discs, 12.5 mm in diameter containing 160 mg cm^{-2}, were used unless otherwise specified. To produce samples which were fluorescence-free, the following procedure was used. The furnace region of the cell and sample holder were heated in air at 480°C for six hours. The calcined samples were quickly transferred to the cell and subsequently evacuated at 25°C for ten minutes. The cell was then heated at 480°C for thirty minutes in 600 torr of O_2 followed by evacuation for ten minutes. This last step was repeated three more times. Finally the sample was cooled to room temperature with the O_2 present and then the cell was evacuated.

The above procedure was used for Al_2O_3, TiO_2, SiO_2, Na/SiO_2 and Na/Al_2O_3. For Ga_2O_3, evacuation at the desired temperatures was sufficient to generate a fluorescence-free sample. Raman studies involving NaSH, Na_2S, NaOH, Na_2O and Na_2O_2 were performed (Chapter 4) and these materials were obtained from commercial sources. Both NaSH and NaOH existed in pellet form and hence, were used with the standard Raman cell. For Na_2S, Na_2O and Na_2O_2, the second Raman cell shown in Figure 2.4(c,d) was used.

Most chemicals employed were obtained from standard commercial sources. Gases were distilled, dried and degassed as needed. Purity analysis was checked by infrared and mass spectrometry.

For SO_2 and H_2S, special care was taken to remove all traces of CO_2 [21]. After initial distillation to remove water, 30 mmoles of H_2S or SO_2 was passed through approximately 1 gram of alumina. The alumina was placed at least 4 cm from the bottom of a glass finger between two layers of glass wool. The alumina was then degassed at 150°C to remove molecular water. The SO_2 or H_2S passed through the alumina by cooling the bottom of the glass finger with liquid N_2. The H_2S or SO_2 was passed several times through the alumina until all traces of CO_2 were removed.

$S^{18}O_2$ was produced by heating uniformly and slowly the outside of a wide bottom flask containing sulfur and $^{18}O_2$ (99% ^{18}O, from Merck Isotopes) using a glass blowing torch. The sulfur was degassed at 100°C prior to use to remove water. D_2S was prepared by dripping D_2O over Al_2S_3 and was purified by distillation [22].

HCN, DCN, $H^{13}CN$ and $HC^{15}N$ was prepared by reaction of concentrated H_2SO_4/D_2SO_4 with $KCN/K^{13}CN$ or $KC^{15}N$ [23].

C_2N_2, $^{13}C_2N_2$ and $C_2{}^{15}N_2$ were also prepared from the corresponding AgCN salt [23]. AgCN was first prepared from precipitation of a solution of AgCl and KCN. Thermal decomposition of AgCN gave rise to liberation of C_2N_2.

Additional experimental sections are included in the following chapters outlining specific procedures pertinent to those sections.

Chapter 3

ALUMINA

3.1 THE CATALYST

Aluminas are mainly used as catalyst supports for metals and other oxides for a number of industrial processes [24]. Additionally, several catalytic reactions such as conversion of alcohols to alkenes and ethers, isomerizations of alkenes, ortho-para conversion of hydrogen and of course, the Claus reaction, occur with alumina itself [25,26].

Numerous attractive features of alumina have fueled its popularity and importance as a catalyst. Aluminas are relatively inexpensive, they are available in large quantities of high purity, thermally stability and a high surface area (100-300 m^2g^{-1}). Aluminas are amphoteric, containing both acidic and basic surface sites. The abundance and nature of these sites have a drastic influence on its catalytic activity and the properties of these sites can be modified by heat treatment or by addition of various additives [27].

3.1.1 STRUCTURE OF ALUMINA

Alumina exists in a number of crystalline forms of which the η and γ are most commonly used. In our studies the alumina was of the γ form. γ-alumina is obtained by thermal dehydration of boehmite (AlO(OH)) at 450°C. Additional crystalline forms arise from thermal transitions [28]:

$$2\ AlO(OH) \xrightarrow{450^{\circ}C} \gamma\text{-}Al_2O_3 \xrightarrow{750^{\circ}C} \delta\text{-}Al_2O_3 \xrightarrow{1000^{\circ}C} \theta + \alpha\text{-}Al_2O_3$$

$$\theta + \alpha\text{-}Al_2O_3 \xrightarrow{1200^{\circ}C} \alpha\text{-}Al_2O_3 \qquad (3.a)$$

γ-alumina has a defect spinel structure which is tetragonally distorted. The oxygen atoms form a cubic close packed arrangement in which the aluminum occupy both octahedral and tetrahedral sites and the defect structure arises from vacant cation sites.

Knözinger and Ratanasamy [25] have shown that hydroxyl groups form a layer at the alumina surface. By considering relative contributions of exposed crystal faces in the micro-crystallites of alumina, several models of the surface of alumina have been proposed. Lippens [29], in his model of the γ-alumina surface considered the (110) and (100) faces, whereas Peri [30] and Butt et. al. [31,32] considered only the (100) face. By examining all possible crystal faces, Knözinger and Ratanasamy [25] concluded that a maximum of five types of hydroxyl groups exist on the

surface of alumina. Their relative concentrations depend on the relative exposure of the crystal faces.

Using the same designation of Knozinger and Ratnasamy, the five hydroxyl types are: Type Ia, with a tetrahedrally coordinated Al^{+3} site; Type IIa, a bridged hydroxyl group between an octahedral and tetrahedral Al^{+3}; Type IIb, bridged hydroxyl between two octahedral Al^{+3} sites; Type III, coordination with three octahedral Al^{+3} sites; and Type Ib, which would occur at defect sites when an adjacent tetrahedral cation is missing.

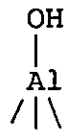

Ia 3760 cm^{-1}

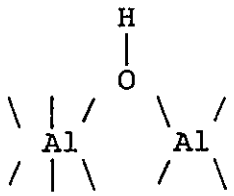

IIa 3730 cm^{-1}

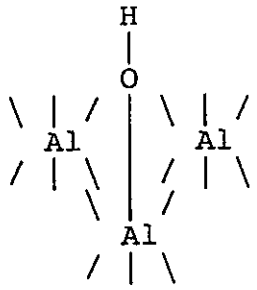

III 3700 cm^{-1}

(3.b)

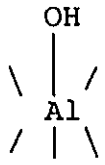

Ib 3785 cm^{-1}

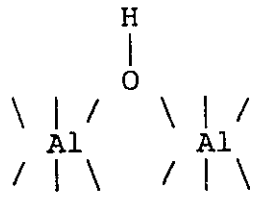

IIb 3740 cm^{-1}

By considering the residual negative charge left on the oxygen of the hydroxyl by removing the proton, Knözinger and Ratnasamy concluded that Bronsted acidity would decrease in the order III > IIa > IIb > Ia > Ib.

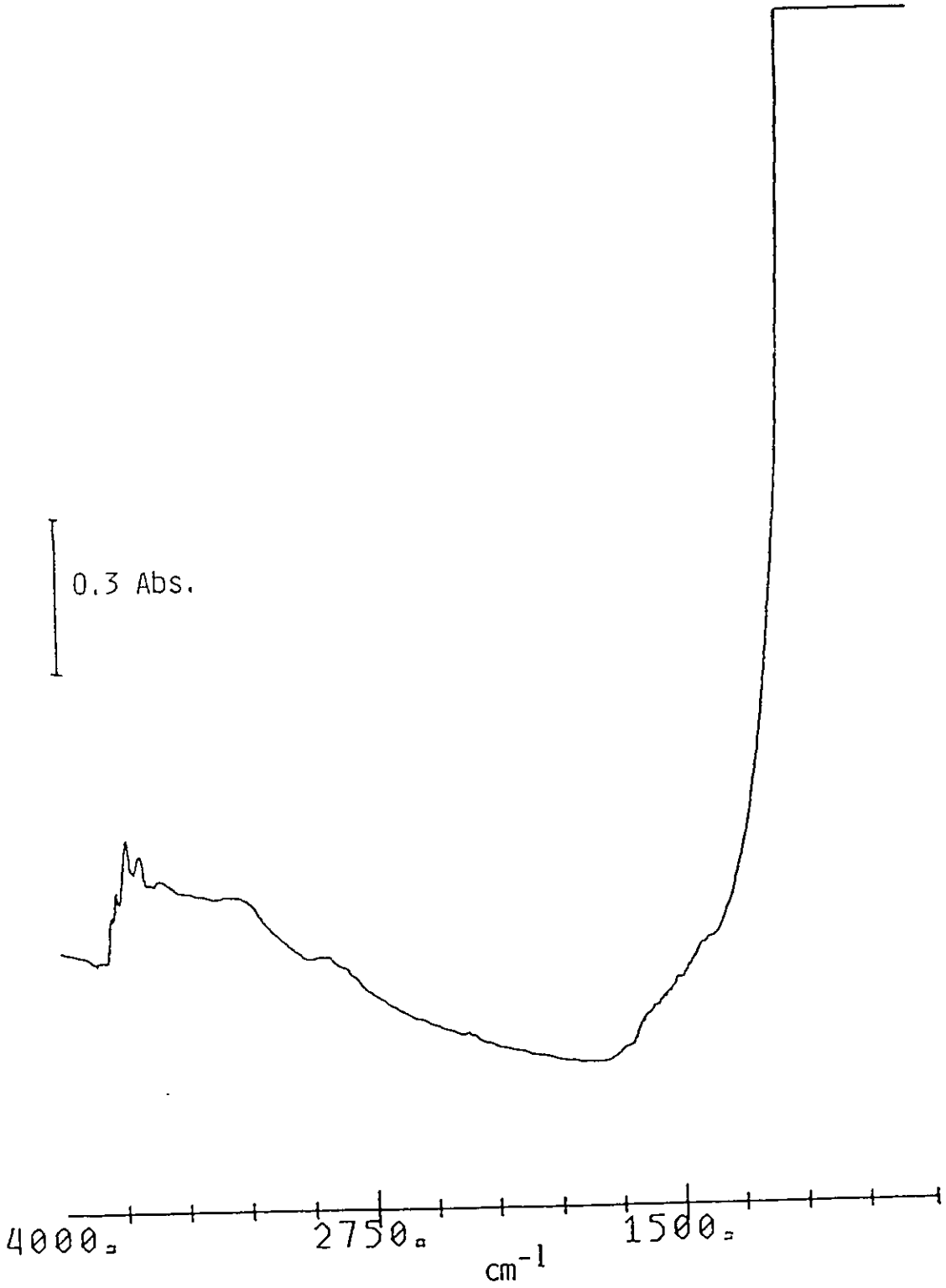

Figure 3.1

Infrared spectrum of γ-alumina (20 mg cm^{-2}) which had been degassed at 450 °C for one hour.

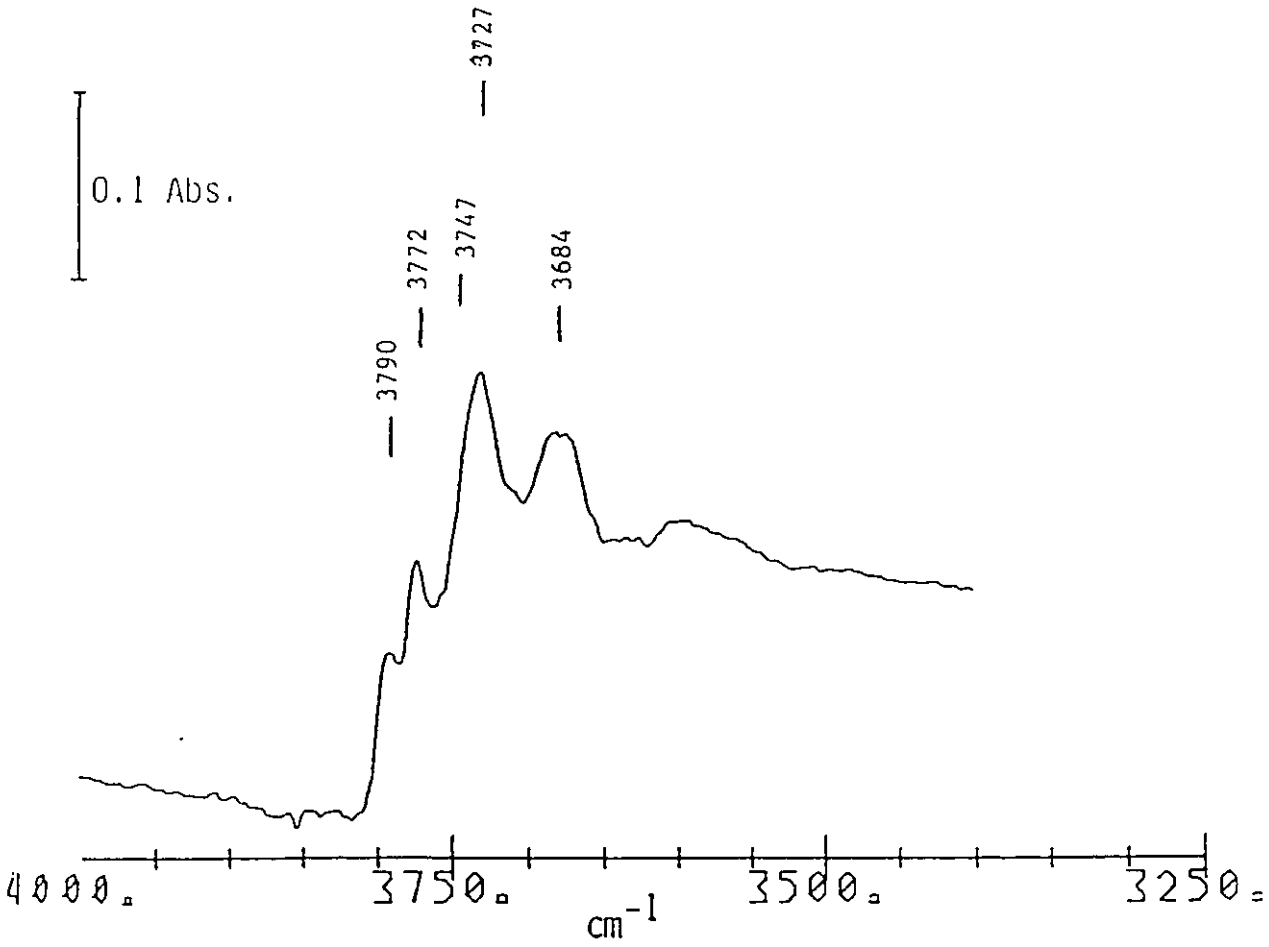

Figure 3.2

Infrared spectrum of γ-alumina sample in Figure 3.1 in the OH stretching region.

The infrared spectrum of γ-alumina is shown in Figure 3.1 and 3.2. Jones [33] reported for crystalline lithium hydroxide that the OH stretching mode, in general, increased with increasing negative charge. Hence, the bands, shown in Figure 3.2, at 3790, 3772, 3747, 3727 and 3684 cm^{-1} were assigned by Knözinger and Ratnasamy to Types Ib, Ia, IIb, IIa and III hydroxyls, respectively.

Peri [30], in his model, considered only the (100) face of alumina and assigned hydroxyl bands to Type Ib of hydroxyls. Dehydroxylation of the surface would yield hydroxyls with 0 to 4 coordinatively unsaturated (cus) oxygen neighbors giving rise to the five infrared bands. This would occur between neighbouring hydroxyls exposing various cus aluminum Lewis acid site and cus oxygen Lewis base sites.

For example, Type Ia and IIa hydroxyls occur in the same layer of a (111) face and hence would be neighbors. During dehydroxylation, the Type IIa site being more acidic would combine with a Type Ia hydrogen to form H_2O creating a cus 3-coordinate aluminum and a cus oxygen which bridges a 4 and 6 coordinated Al^{+3} site:

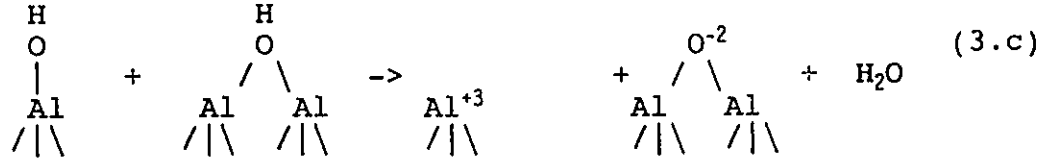

(3.c)

With this scheme, several types of cus Al^{+3} and cus O^{-2} sites were proposed. This type of dehydroxylation would give rise to cus

Al^{+3} and cus O^{-2} sites with the smallest possible charge and hence, weak Lewis acid and base sites.

However, the catalytic activity of γ-alumina for most reactions appears only after dehydroxylation above 300-400°C, even though 3.7×10^{14} cm^{-2} of cus-oxygen and cus-alumina atoms already exist. The immobility of hydroxyl groups would increase with temperature allowing further condensation above 300°C creating special defect sites with catalytic activity.

Della Gatta et. al. [34] employed CO as a probe molecule to study these defect sites. No CO was adsorbed on γ-alumina degassed below 400°C. Above 400°C, bands at 2215-2203 cm^{-1}, due to adsorbed CO, formed and increased with dehydroxylation up to 600°C. In addition, above 500°C, a second CO species with a band at 2244 cm^{-1} formed along with the perturbation of the Ia hydroxyl band. Both have been assigned to bonding to cus Al^{+3} sites with the latter site adjacent to a Ia type hydroxyl.

To conclude, dehydroxylation of alumina below 400°C produces weak cus Al^{+3} Lewis acid and cus O^{-2} basic sites. Dehydroxylation above 400°C produces strong Lewis acid sites, which can be explained by considering the crystal faces of a defect spinel structure of alumina. The Claus reaction over alumina occurs at relatively low temperatures (200°C). Water formation from this reaction would probably lead to a highly hydroxylated alumina with small numbers of cus Al^{+3} and O^{-2} sites. Nevertheless, to examine its catalytic activity, we have studied the adsorption of H_2S and SO_2 on aluminas ranging from those activated at 150°C, corresponding to a completely hydroxylated, but water free

surface, to those activated at 700°C which were virtually totally dehydroxlated.

3.2 ADSORPTION OF HYDROGEN SULFIDE

3.2.1 INTRODUCTION

Although infrared studies involving the adsorption of H_2S on alumina have previously been reported, there exists two conflicting interpretations of the observed results. Datta and Cavell [35] reported IR bands at 1624, 1570 and 1334 cm^{-1} in addition to a band near 2570 cm^{-1} which has been reported by others [36-40]. The 1624 cm^{-1} band was attributed to the formation of water via the reaction H_2S and AlO^{-2} -> AlS^{-2} + H_2O, that at 1570 cm^{-1} was assigned to an Al=O surface mode [41], and the 2570/1334 cm^{-1} pair were assigned to the H_2S stretching and deformation modes respectively of non-dissociatively adsorbed H_2S on a cus aluminum ion or cluster, represented by;

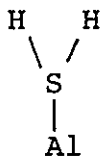

(3.d)

Lavalley et. al., however, observed bands at 3690 cm^{-1} and 3570 cm^{-1} ν(O-H) and concluded that dissociative, irreversible adsorption occurs via the reaction:

(3.e)

In addition, broad bands near 3400 cm^{-1} and a band near 2570 cm^{-1} were assigned to hydrogen bonded reversibly adsorbed

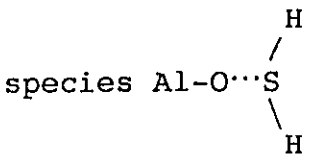

species Al-O···S and Al-O···H-S-H respectively.

Lavalley et. al. [38] suggested that bands at 1570 and 1340 cm^{-1} resulted from coadsorption of CO_2 present as an impurity in the H_2S and are not due to the stretching and deformation modes of H_2S.

In light of these contradictory views, we have undertaken a further study of the adsorption of H_2S on alumina. In particular, we have employed isotopic studies, using ($^{13}CO_2$, D_2S, $C^{18}O_2$) to determine if the bands at 1570/1340 cm^{-1} are due to CO_2 impurities, or to the H_2S bending and Al=O surface mode, respectively.

3.2.2 EXPERIMENTAL

The alumina used was pressed into self-supporting discs of 8 mg cm^{-2} or used as thin films 1 mg cm^{-2} on ZnSe windows. Although the alumina was calcined at 550°C prior to use, rehydration and hydroxylation occurred during the preparation of discs. Samples denoted Al(150°C) were prepared by further outgassing the alumina at 150°C for two hours.

Al(400°C) and Al(700°C) samples were outgassed at 400°C and 700°C for 0.5 hour. This was followed by several additions of 600 torr O_2 at 400°C or 700°C to remove organic impurities prior to use. The samples were then outgassed for an additional hour. The use of ZnSe windows did not permit in situ thin film Al(700°C) studies.

3.2.3 RESULTS AND DISCUSSION

The addition of H_2S (75 umoles g^{-1}) to alumina degassed at 700°C (Figure 3.3(b-a)) gave rise to bands at 3690 cm^{-1} v(O-H), 2570 cm^{-1} v(S-H), a broad band at 3200 cm^{-1} and a decrease in the isolated hydroxyl bands at 3790 and 3772 cm^{-1}. A further large addition of H_2S [3000 umoles g^{-1},Figure 3.3(c)] resulted in an increase in intensity of the 3200 and 2570 cm^{-1} bands and a decrease in the band at 3690 cm^{-1}. With evacuation, the band at 3690 cm^{-1} increased while the band at 3200 cm^{-1} decreased (Figure 3.3(d-c)). We conclude that the 3200 cm^{-1} band is the result of weak hydrogen bonding between H_2S and the species which gave rise

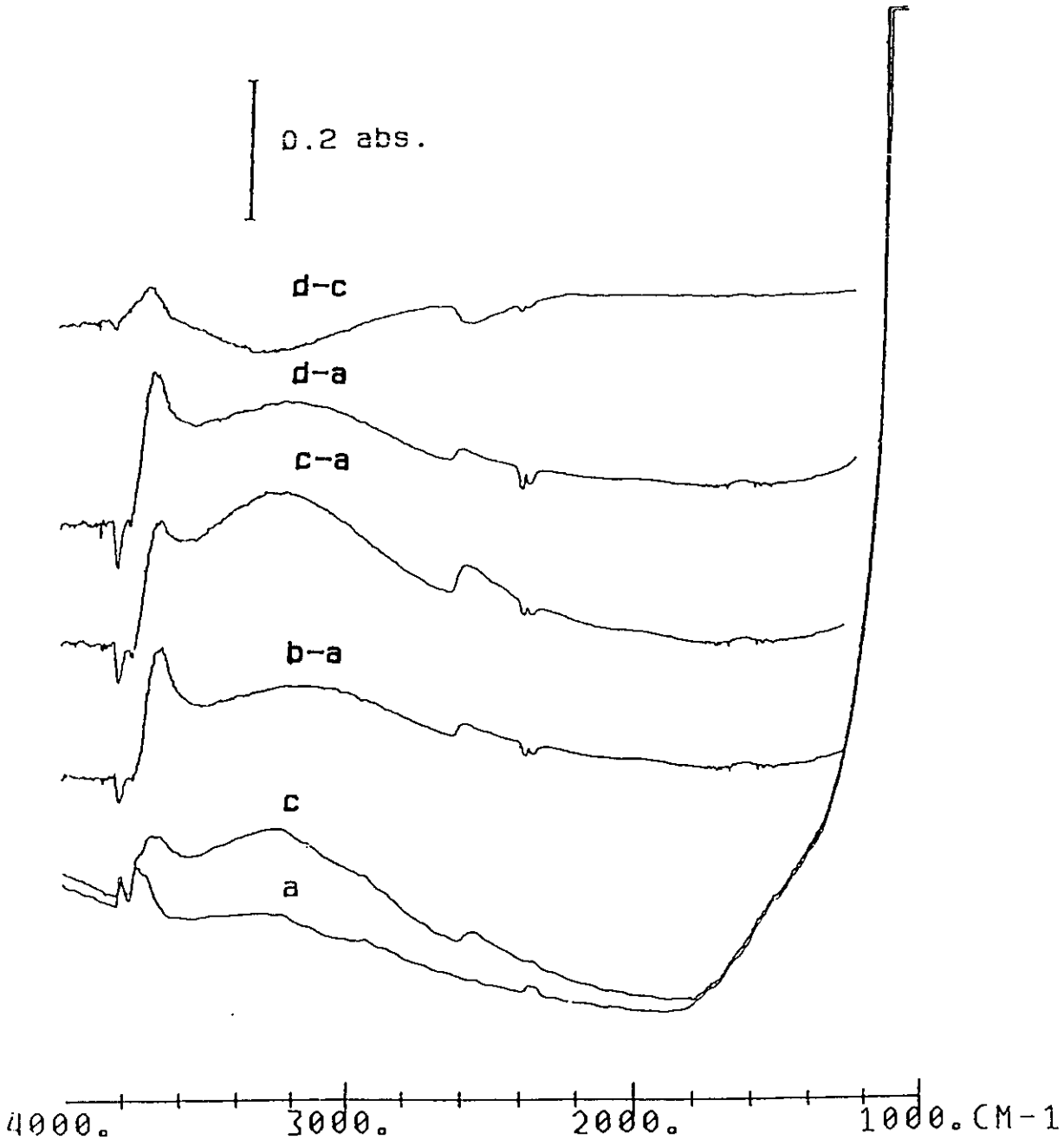

Figure 3.3

a) Al(700 °C) with the addition of
b) 75 umole g^{-1} H_2S, followed by;
c) 3000 umole g^{-1} H_2S, and
d) Evacuation for 0.5 hours.

to the OH band at 3690 cm^{-1}. After prolonged evacuation, the band at 2570 cm^{-1} was still present, which suggested that this band is partially due to dissociative adsorption of H_2S. At no time were bands at 1570 or 1340 cm^{-1} observed.

Datta and Cavell [35] have suggested that the spectral changes in the OH region of alumina could be due to water formation from the reaction:

$$H_2S + AlO^{-2} \rightarrow H_2O + Al\text{-}S^{-2} \qquad (3.f)$$

This may be possible since it has been reported [39] that the spectra observed after the adsorption of small quantities of H_2O or H_2S on alumina are similar in the 4000 to 3000 cm^{-1} region. In addition, the dissociative adsorption of H_2S on many metals to form metal sulfides occurs readily [42]. Deane et. al. also suggested the formation of water resulting from adsorption of H_2S on MgO [43].

A definite assignment in the infrared is not possible because bands due to Al-S would appear below 1000 cm^{-1} where alumina is opaque. However, Al-S Raman bands could possibly be detected (Al_2S_3 has strong Raman bands [44] at 248, 211, 191, 174 and 141 cm^{-1}). In separate Raman experiments, the adsorption of H_2S on Al(700°C) or Al(500°C) (Figure 3.4(b)) gave rise to an S-H band at 2590 cm^{-1} which was easily removed upon evacuation at 25°C and is, therefore, due to weakly adsorbed H_2S. No other Raman bands were observed.

Lavalley et. al. [39] have observed via infrared spectroscopy, that the increase in the OH intensity at 3690 cm^{-1}

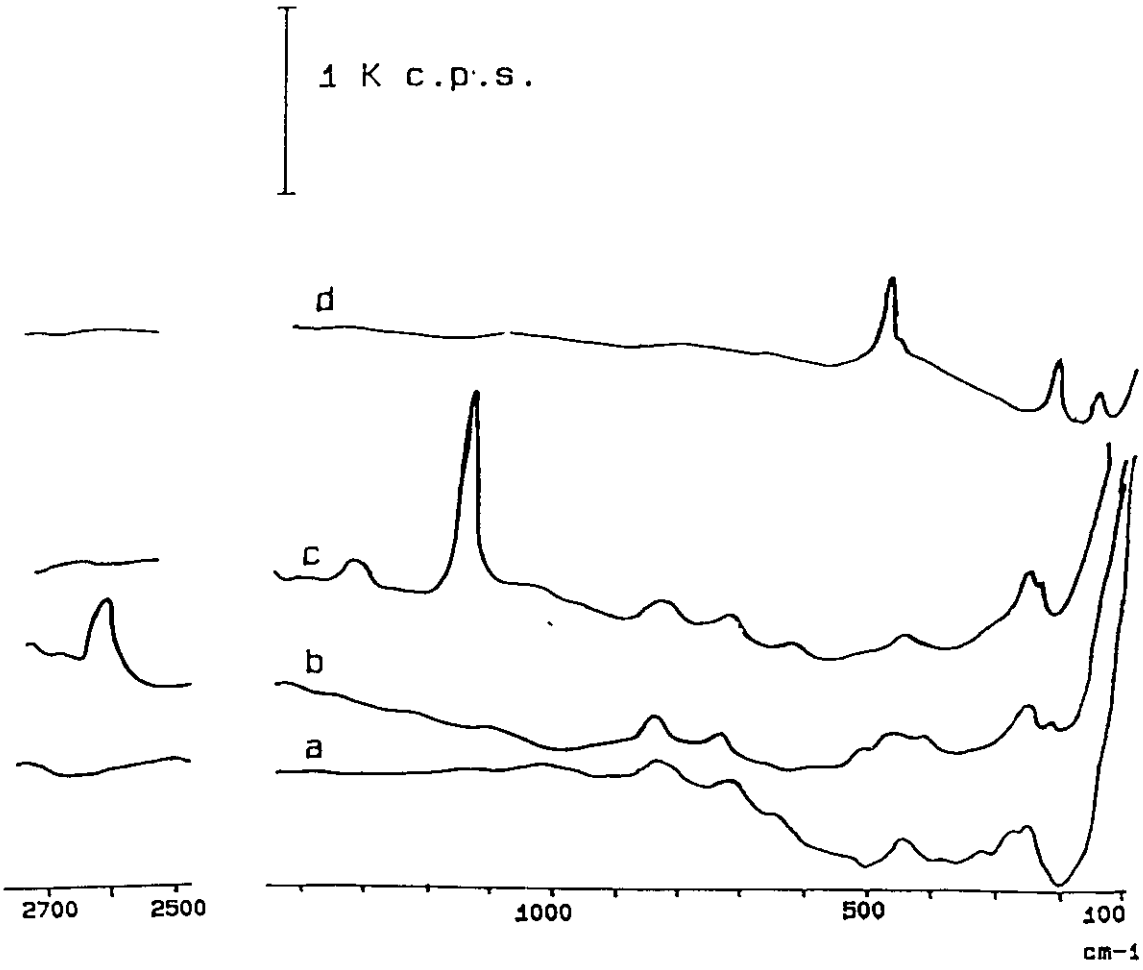

Figure 3.4

Raman spectra of;
a) Al(500 °C) with
b) 3 mmole g^{-1} H_2S added to (a).
c) 1 mmole g^{-1} SO_2 added to (a).
d) (c) evacuated 0.5 hours followed by addition of 3 mmole g^{-1} of H_2S.

per mole of adsorbed H_2S or CH_3SH was identical and that both molecules dissociatively adsorbed to yield AlOH and $AlSCH_3$ (from CH_3SH), or AlSH (from H_2S) The band at 3690 cm^{-1} cannot be due to water via Reaction (3.f) with CH_3SH replacing H_2S because water would not be a product.

Datta and Cavell have reported that an equal amount of H_2S is adsorbed on Al(400°C) or Al(700°C). Although an Al(700°C) has 45% of AlOH removed relative to Al(400°C) [27], dissociative adsorption of H_2S would result in the rehydroxylation of the Al(700°C) via Reaction (3.e) with formation of O-H at 3690 cm^{-1}. We have observed that H_2S may hydrogen bond with the species giving the 3690 cm^{-1} band. This could account for the equal amount of H_2S adsorbed on the two aluminas. Furthermore, the adsorption of $(CH_3)_2S$ and CH_3SH on alumina have been shown to form hydrogen bonded species on alumina [39].

3.3 ADSORPTION OF CARBON DIOXIDE AND HYDROGEN SULFIDE

Lavalley et. al. have reported [37-39] that commercially available H_2S usually contains traces of CO_2 and that the adsorption of this on alumina inevitably gave rise to infrared bands at 1570 and 1340 cm^{-1}. Additional weaker features are sometimes also observed near 1640, 1450 and 1230 cm^{-1} which are due to the formation of HCO_3^- surface species [38,45,46]. The 1570 and 1334 cm^{-1} bands always appear unless extreme precautions are taken to remove traces of CO_2 from commercial H_2S

(freeze-pump-thaw cycles are not sufficient) or if the alumina is not sufficiently treated to remove HCO_3^- from the surface.

On Al(400°C) with HCO_3^- bands at 1640, 1450 and 1230 cm^{-1} addition of H_2S resulted in the decrease in intensity of these bands and formation of bands at 2570, 1570 and 1334 cm^{-1}. The 1570/1340 cm^{-1} pair were produced if CO_2 or H_2S was preadsorbed followed by H_2S or CO_2 addition, or for the coaddition of both H_2S and CO_2. Upon evacuation, the 2570 cm^{-1} band decreased whereas the intensity of the 1570/1340 cm^{-1} pair remained constant. If very highly pure H_2S was used then no IR bands were observed in the 1700-1000 cm^{-1} spectral region although we always observed the peak near 2570 cm^{-1}. On this evidence, it must be concluded that the peaks in this frequency region which were observed by Datta and Cavell do not arise from the adsorption of pure H_2S.

The ratio of the intensities of the 1570/1340 cm^{-1} bands was always constant (as was found by Datta and Cavell for H_2S adsorption on an alumina activated at 700°C) and both bands shifted to lower wavenumber when H_2S was coadsorbed with $^{13}C^{16}O_2$ (1528/1314) or $^{12}C^{18}O_2$ (1548/1301) but not at all when using D_2S + $^{12}C^{16}O_2$ (Figure 3.5). Using 10% CO_2 the 1570/1340 cm^{-1} bands were much more intense than those which arose from the adsorption of unpurified H_2S. The minimum level of CO_2 which would give rise to these spectral observations has not been determined because the objective was to determine the isotopic shifts using the same conditions which were used previously [38]. Further, the adsorption of pure COS on to a similarly activated alumina gave

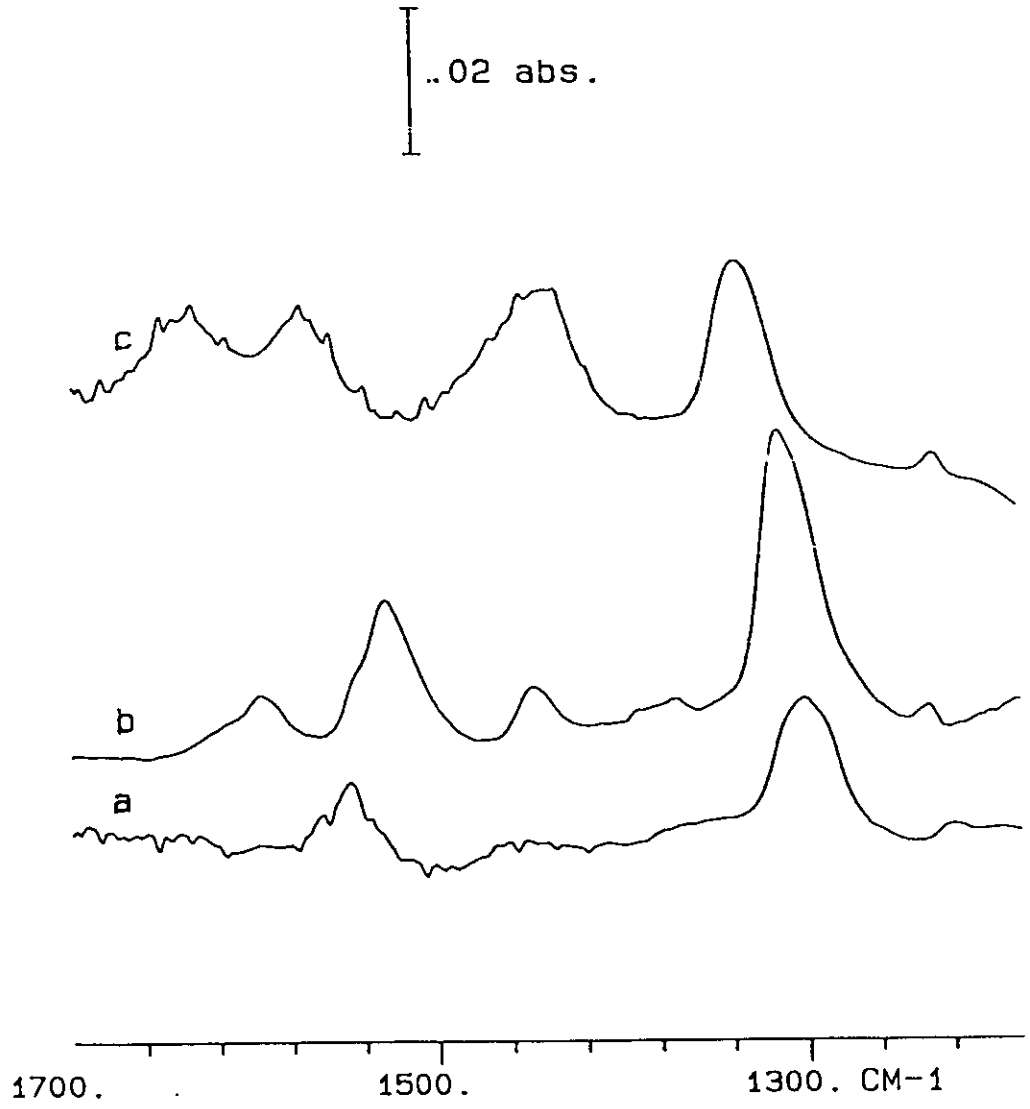

Figure 3.5

Al(700 °C) with addition of;
a) $C^{18}O_2/H_2S$
b) $^{13}CO_2/H_2S$
c) CO_2/H_2S
in a ratio of approximately 1:3, 1:2, and 10:1 respectively. For (a) and (b), CO_2 was first added, followed by evacuation ten minutes, then addition of H_2S. For (c), H_2S was preadsorbed and evacuated five minutes prior to CO_2 addition.

rise to the identical 1570/1340 cm^{-1} pair [38]. These bands have been assigned to a type of surface thiocarbonate species.

From the spectroscopic point of view, there is no doubt that alumina does not have "intrinsic" bands at 1560 and 1480 cm^{-1} and that a vibration due to Al=O at 1578 cm^{-1} does not exist, regardless of the temperature of activation. Furthermore, the deformation mode of gaseous [47] or solid [48] H_2S is near 1182 cm^{-1}, whereas that for H_2S in CCl_4 is reported [49] to be at 1172 cm^{-1}, far below the 1334 cm^{-1} band assigned by Datta and Cavell to the deformation mode of coordinated H_2S (coordination is not expected to alter the frequency significantly, as has been found for coordinated water [50]).

To conclude, the 1570/1334 cm^{-1} bands observed by Datta and Cavell must be due to thiocarbonate formation. The band at 1620 cm^{-1} observed by Cavell could be due to H_2O elimination in formation of the thiocarbonate via the reaction,

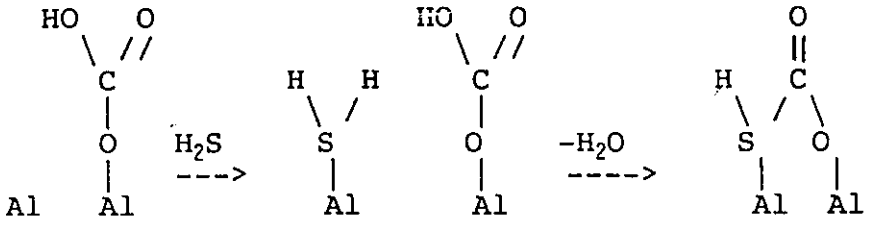

rather from the dissociative adsorption of H_2S. Similar spectral features always appeared unless extreme precautions were taken to remove traces of CO_2 from commercial H_2S. The alumina sample used in this work was different from that used by Datta and Cavell, (they did not specify the crystalline form, nor the Kaiser description) but it is to be noted that Amenomiya et .al.

[45,46] have reported little difference for the adsorption of CO_2 on and -alumina. Further, in agreement with Lavalley et. al. [39] we find that H_2S dissociatively adsorbs on alumina forming AlSH and AlOH and can hydrogen bond with hydroxyl sites.

3.4 ADSORPTION OF SULFUR DIOXIDE

3.4.1 INTRODUCTION

There have been several infrared studies of the adsorption of SO_2 on alumina. Deo et. al. [36] reported bands at 1330 cm^{-1} (ν_3 asym. stretch) and 1140 cm^{-1} (ν_1 sym. stretch) due to weakly adsorbed SO_2. Later, Chang [51] reported the formation of two additional bands at 1326 and 1050 cm^{-1}. The 1050 cm^{-1} band was difficult to detect because of the high absorbance of alumina in this region. The 1326 cm^{-1} band was stable to evacuation at 100°C while the band at 1050 cm^{-1} (assigned to a sulfite species) was only removed above 800°C. Subsequent investigations by Karge and Dalla Lana [52] suggested that the 1050 cm^{-1} band occurred following adsorption on basic cus O^{-2} sites and that bands at 1330, 1326 and 1150 cm^{-1} occurred on acidic cus Al^{+3} sites. The assignments of Karge et. al. were based on the site blocking effect of preadsorbed bases and acids on alumina.

On the other hand, Datta et. al. [53] recently assigned the 1050 cm^{-1} band to a species on an acidic surface site and the

bands at 1330 and 1148 cm^{-1} to a weakly adsorbed SO_2 on a hydroxyl group of alumina. It was observed that the 1050 cm^{-1} band increased in intensity with higher activation temperatures above 140°C. Datta et. al. assignment of this band was based on a previous study [54], which reported that the number of basic sites is a maximum for alumina at 140°C and the number of acidic sites increased up to 550°C.

E.S.R. studies by Karge et. al. [52] have demonstrated that formation of SO_2^- radicals do occur on alumina. Further investigations by Karge et. al. [55] and by Datta et. al. [53] indicated that there was no correlation between the ESR signals and observed infrared adsorption bands. It was estimated that no more than 1% of the adsorbed SO_2 formed radicals.

A large number of possible oxysulfur compounds exist (i.e. sulfite, sulfate, thionate, thiosulfate, etc.) which can usually be identified by their characteristic group frequencies (see Chapter 1). Unfortunately, most of these characteristic bands lie below 1000 cm^{-1} where alumina is opaque. Schoonheydt and Lunsford [56] observed upon addition of SO_2 to MgO (MgO is transparent to 750 cm^{-1}) a large number of bands below 1000 cm^{-1} which were assigned to several adsorbed species. In an attempt to clarify the nature of adsorbed SO_2 and the role of reactive sites on alumina, we have undertaken infrared and Raman spectroscopic studies.

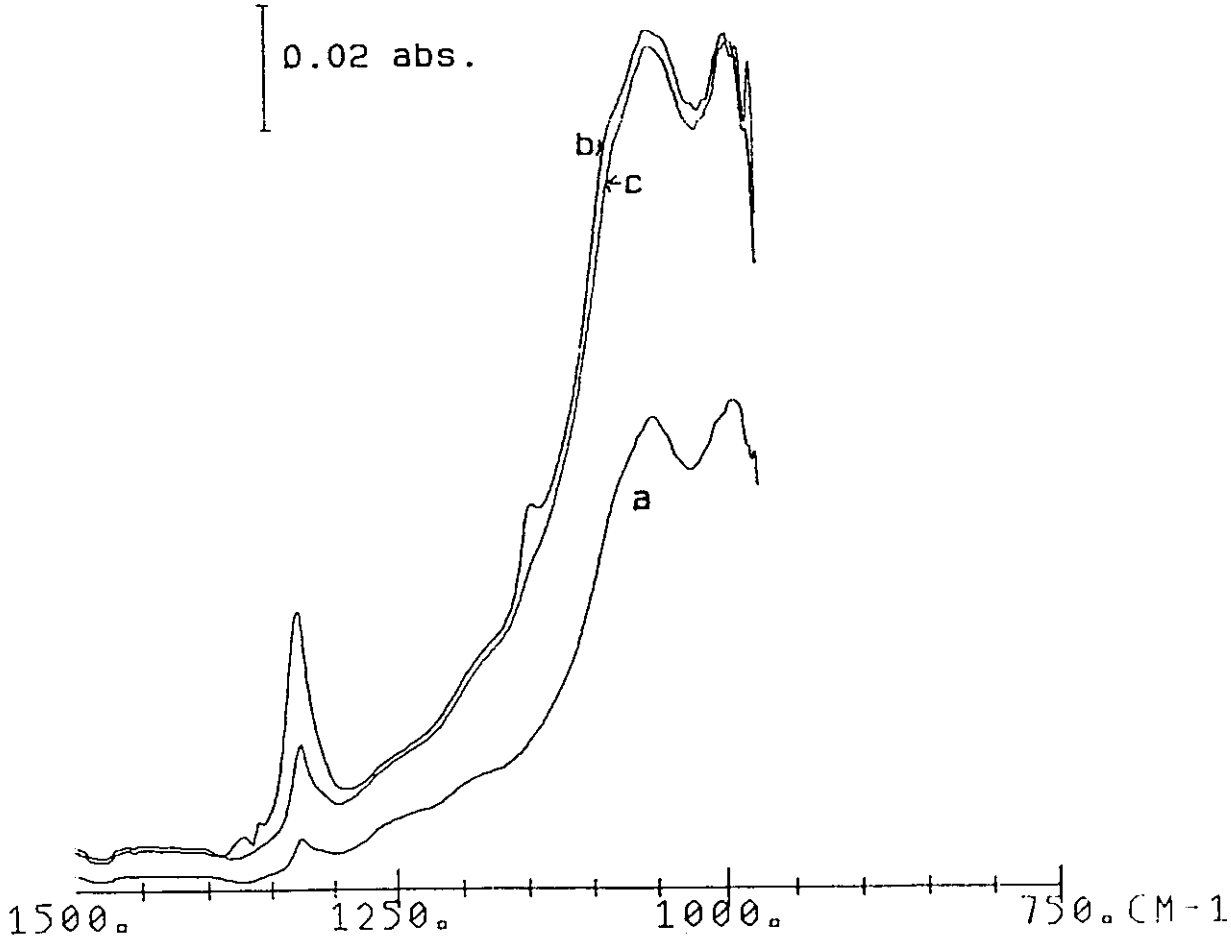

Figure 3.6

Al(400 °C) doped with SO_2;
a) 30 umole g^{-1}.
b) 300 umole g^{-1}, followed by;
c) Evacuation for five minutes.

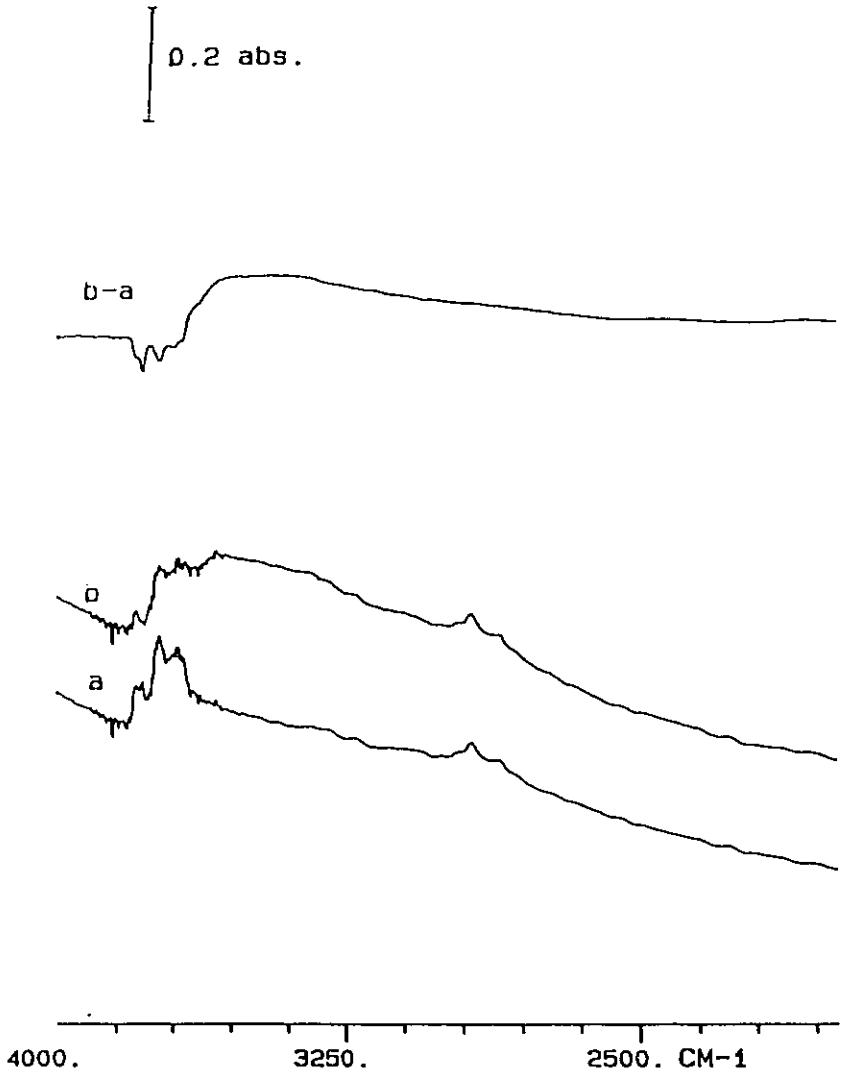

Figure 3.7

4000 to 2000 cm^{-1} region of spectra shown in Figure 3.8.

3.4.2 RESULTS and DISCUSSION

The addition of a small dose of SO_2 to Al(400°C), gave rise to a band at 1050 cm^{-1} (Figure 3.6). Further successive doses of SO_2 resulted in the appearance of a band at 1326 cm^{-1}, followed later by bands at 1330 cm^{-1} and 1150 cm^{-1}. The latter two bands increased in unison until bands due to gaseous SO_2 were observed at 1375 and 1165 cm^{-1}. The 1330 cm^{-1} and 1150 cm^{-1} bands were removed upon evacuation at room temperature and all other bands decreased slightly. In the OH region of Al(400°C) the residual hydroxyl bands disappeared and a weak but broad band between 3600 and 3000 cm^{-1} formed when SO_2 was added (Figure 3.7).

A second band at 990 cm^{-1} in Figure 3.6 may be due to a spectral artifact created as a result of the subtractive process in regions of high absorbance. The spectra shown in Figure 3.6 are difference spectra from which the alumina background spectrum had been subtracted. To illustrate the difficulty experienced in this spectral region, the measured adsorption spectra are shown in Figure 3.8. For alumina discs of 8 mg cm^{-2} an absorbance value of 1 was measured at 1000 cm^{-1} on a highly sloping background. The feature at 990 cm^{-1} was always observed using 8 mg cm^{-2} and upon subsequent addition of H_2S (see next section, Figure 3.15) it decreased at a faster rate than the band at 1050 cm^{-1}. Karge and Dalla Lana[52] have reported the formation of a shoulder at 1000 cm^{-1} with the addition of SO_2 to a dehydroxylated alumina. (They used ALON, a γ-alumina from Cabot Corp. in their study.) Therefore, it would be plausible to assign the 990 cm^{-1}

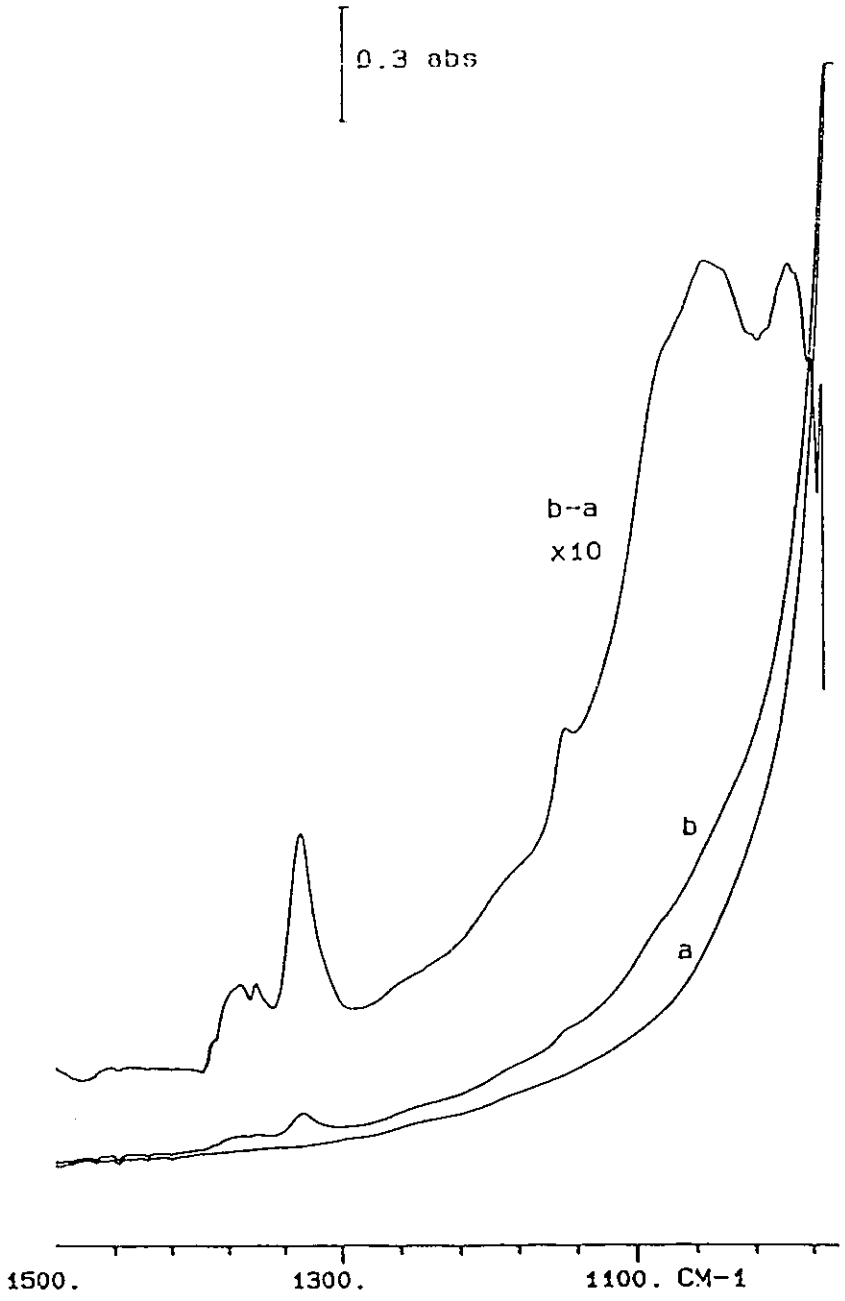

Figure 3.8

a) Al(400 °C).
b) and with 300 umole g^{-1} SO_2 added.

band to a second type of sulfite on the surface. Schoonheydt and Lunsford[56] observed bands at 955 cm^{-1}, 925 and 895 cm^{-1} upon addition of SO_2 to MgO, and assigned these bands to a more weakly adsorbed $SO_3^=$ species coordinated through the oxygen atom. (Coordination through an oxygen atom would shift the bands to lower frequencies relative to the free ion.)

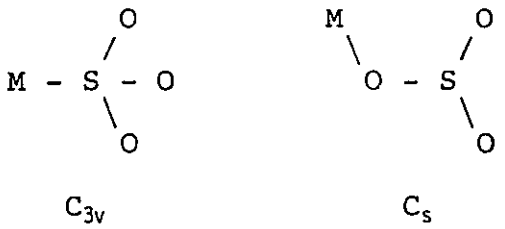

(3.h)

However, the 990 cm^{-1} feature was not observed using 4 mg cm^{-2} discs (absorbance a$^+$ 1000 cm^{-1} was 0.5) and could not be produced on 8 mg cm^{-2} discs using a second source of the Degussa alumina. In both cases a band at 1050 cm^{-1} was present and with addition of H_2S this band slowly decreased and was accompanied by a much larger decrease in the overall absorbance in the 1000-980 cm^{-1} region.

It has been reported [57] that the dehydroxylation of alumina above 400°C results in the formation of a band in the 1020 -> 1050 cm^{-1} region due to strained

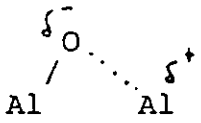

(3.i)

bridged sites. Therefore, the feature at 990 cm^{-1} may actually be due to the disappearance of these strained bridged sites giving rise to a "valley" at 1020 cm^{-1} in the subtracted spectrum.

Isotopic studies of the adsorption of SO_2 or $S^{18}O_2$ on Al(400°C) and ^{18}O exchanged Al(400°C) were employed to determine reaction sites on alumina. ^{18}O-exchanged Al(400°C) was prepared by heating Al(400°C) in $H_2{}^{18}O$ several times at 400°C. Comparison of the v(O-H) of Al(400°C) before and after exchange showed that the ^{16}OH -> ^{18}OH had occurred. The band at 1050 cm^{-1} shifts to lower frequency with Al(400°C) + $S^{18}O_2$ (1040 cm^{-1}) or ^{18}O-exchanged Al(400°C) + $S^{18}O_2$ (1018 cm^{-1}) and produced a broad band centered at 1020 cm^{-1} with (^{18}O-exchanged Al(400°C) + SO_2). The bands at 1330 and 1150 cm^{-1} do not shift to lower frequency with ^{18}O-exchanged Al(400°C) + SO_2 but they shifted to 1286/1097 cm^{-1} with either ^{18}O-exchanged Al(400°C) + $S^{18}O_2$ or Al(400°C) + $S^{18}O_2$.

The shifts in the 1050 cm^{-1} with (^{18}O-exchanged Al(400°C) + SO_2) and (^{18}O-exchanged Al(400°C) + $S^{18}O_2$) clearly indicate that the 1050 cm^{-1} band involved a reaction at basic oxide sites on alumina. The bridged sites shown in scheme (3.i) have been reported[57] to be sensitive to ^{16}O-^{18}O exchange. Exchange of oxygen atoms between ^{18}O-exchanged alumina and adsorbed SO_2 (sulfite) could account for the broad band observed at 1020 cm^{-1}.

It is evident from our isotopic data that the 1330/1150 cm^{-1} pair do not involve a reaction at basic <u>cus</u> O^{-2} sites. Furthermore, no exchange between surface oxides and gaseous SO_2 was observed. For this to occur, additional bands corresponding

to $S^{18}O^{16}O$ on the surface would have been observed for the ^{18}O-exchanged Al(400°C) + SO_2 and Al(400°C) + $S^{18}O_2$ reactions.

Datta et. al. [53] have suggested that the 1330/1150 cm^{-1} bands involve a reaction at hydroxyl sites. Although we observed some changes in the v(O-H) region of Al(400°C), Karge et. al. [58] have reported that the spectra between Al(400°C) and a totally dehydroxylated alumina show the same bands at 1330, 1326, 1150 and 1050 cm^{-1}. The 1326 cm^{-1} band has been assigned to v_3 asymmetrical stretch of SO_2 adsorbed on alumina [51]. However, the bands at 1330/1150 cm^{-1} were not observed upon addition of SO_2 to Al(150°C) (see next Section, Figure 3.11) and we conclude that these bands are due to weakly adsorbed SO_2 on cus Al^{+3} sites.

The 1050 cm^{-1} band is much lower than the expected frequencies of adsorbed SO_2 (gas phase SO_2 has vibrations at 1375(v_3) and 1165(v_1 cm^{-1}) and by virtue of its strong reactivity with basic O^{-2} sites, formation of $SO_3^=$ could be postulated. Free $SO_3^=$ ions (C_{3v}) have a doubly degenerate vibration (v_3) at 1010 cm^{-1} and a non-degenerate v_1 at 960 cm^{-1}. Newman and Powell [59] reported that the splitting of the v_3 vibration for sulfite complexes produced two bands in the region 1093-1070 and 1036-1024 cm^{-1} and a third at 988 cm^{-1}. Schoonheydt and Lunsford [56] observed bands at 975 and 1040 cm^{-1} with a shoulder at 1070 cm^{-1} upon adsorption of SO_2 on MgO and assigned these bands to a $SO_3^=$ species coordinated to the surface through the sulfur atom. Coordination through the sulfur atom would preserve the C_{3v} symmetry and would shift the S-O bands to higher frequencies relative to free $SO_3^=$ (see Scheme 3.h). Chang [51] reported that

the formation of SO_3^- on MgO or CaO (SO_3^- bands at 1050 cm^{-1} and 960 cm^{-1}) coincided with the 1050 cm^{-1} band on alumina and thus tentatively assigned it to v_3 of an adsorbed SO_3^-.

In a Raman experiment, the addition of SO_2 to Al(500°C) resulted in the appearance of a strong sharp band at 1150 cm^{-1} along with a less intense sharp band at 1330 cm^{-1} (Figure 3.4(c)). Both bands were easily removed upon evacuation. The Raman bands at 1330 and 1150 cm^{-1} were undoubtedly due to weakly adsorbed SO_2. Unfortunately, no other Raman bands were observed upon adsorption of SO_2 on alumina. This was unexpected since salts of oxysulfur compounds are known to produce strong Raman bands [13].

Lavalley et. al. [60] have reported that approximately 200 umole g-1 of SO_2 was irreversibly adsorbed on Al(500°C), which corresponds to approximately 3% by weight. Spectra of silica impregnated with Na_2SO_3 or Na_2SO_4 at concentrations of 3% to 15% by weight were recorded (silica is inert vis-a-vis the Claus reaction) to test whether, at these concentration levels Raman spectra could be observed. The strong Raman bands at 990 cm^{-1} for SO_3^- or 980 cm^{-1} SO_4^- were barely observable above the background for 3% impregnated samples. Only at 5% and higher sodium loadings were these bands observed (Figure 3.9). From this we conclude that observation of Raman bands was limited because of a lack of sensitivity in detection which was compounded because of a large fluorescence associated with the alumina itself or which generally arose after addition of an adsorbate.

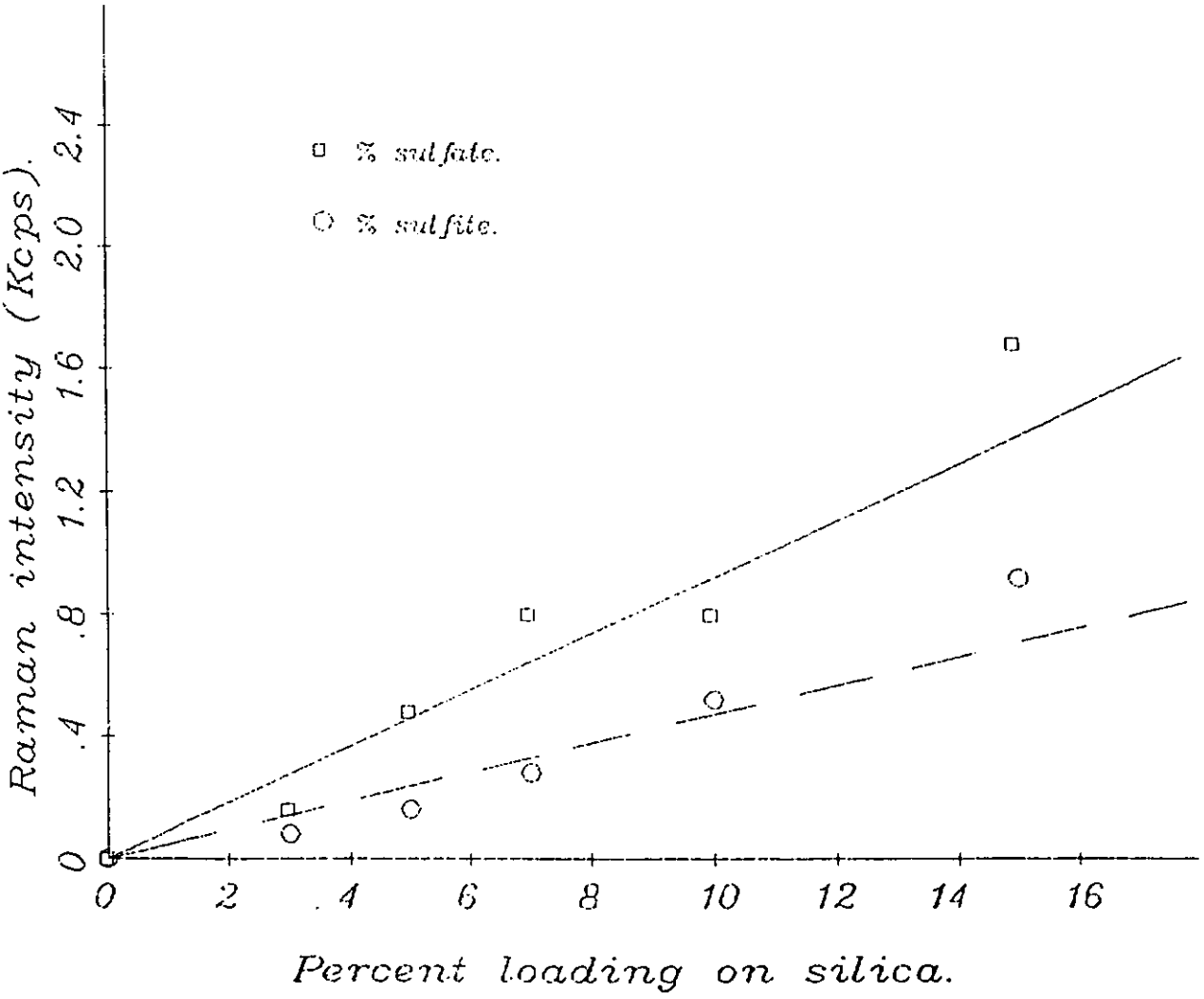

Figure 3.9

Raman intensity versus % loading on silica

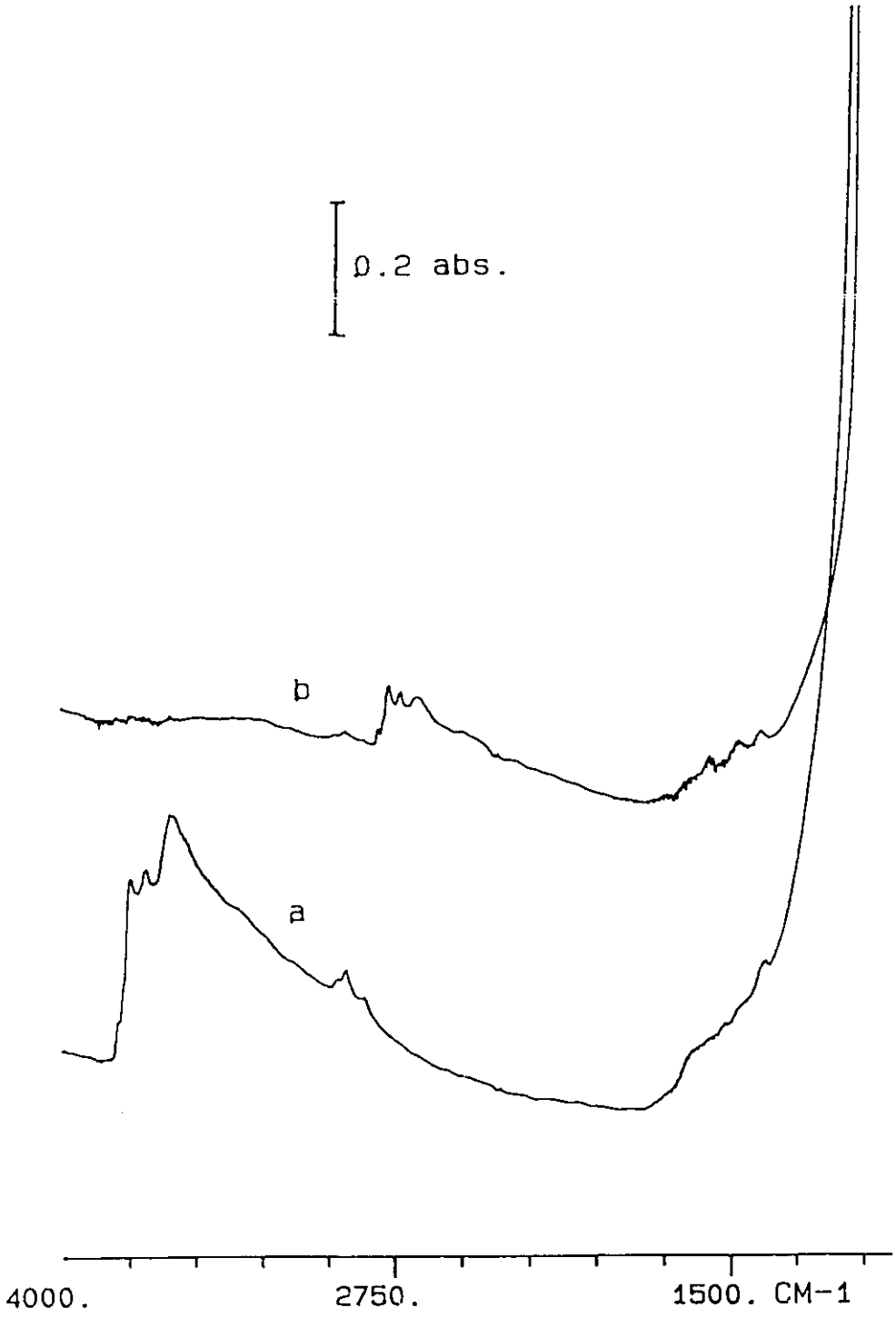

Figure 3.10

a) Al(150 °C).
b) Deuterated Al(200 °C).

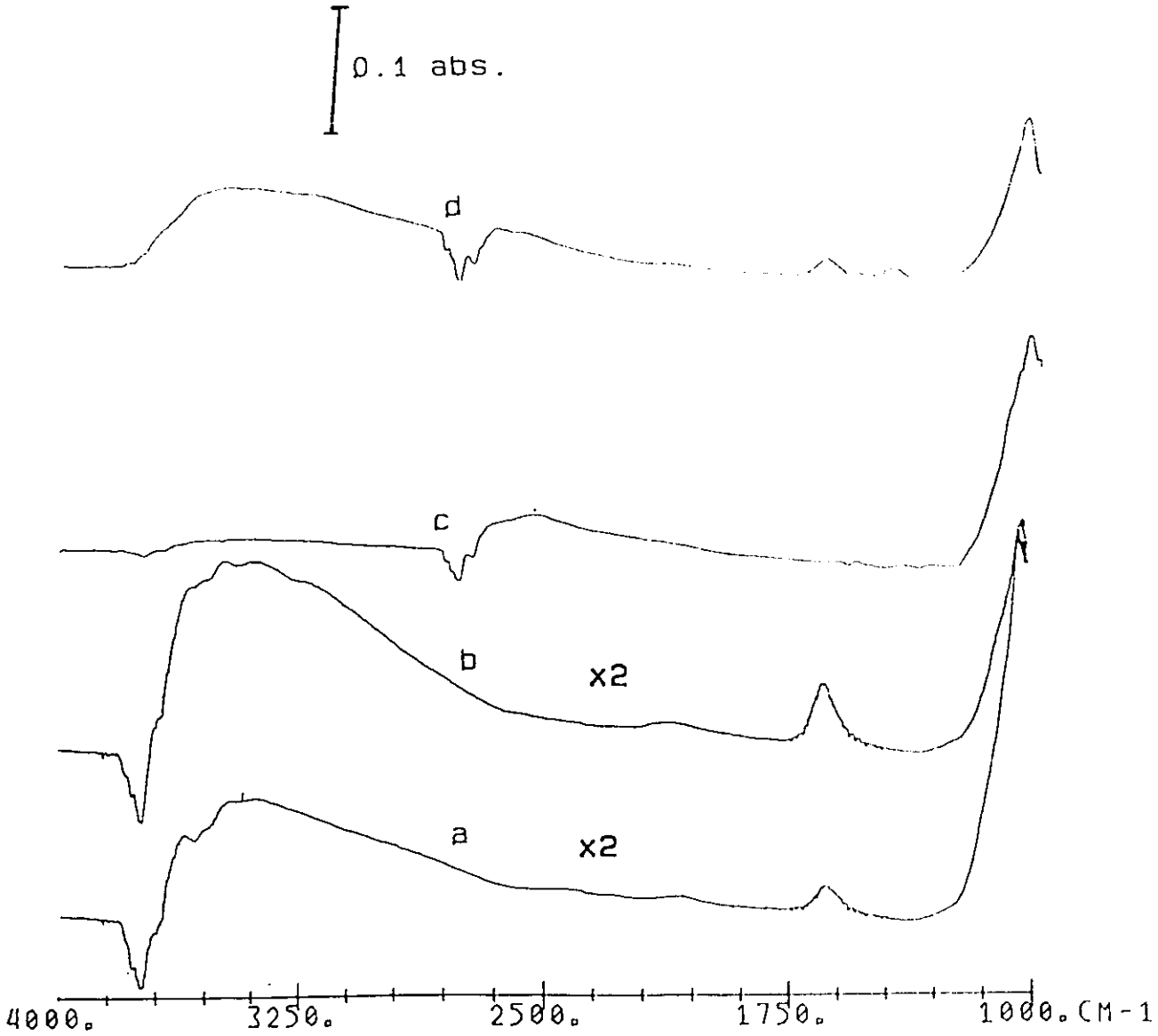

Figure 3.11

Difference spectra of the addition of:
a) 600 umole g^{-1} SO_2 to Al(150 °C), followed by evacuation and addition of;
b) 3000 umole g^{-1} H_2S.
c) 1500 umole g^{-1} SO_2 to a deuterated Al(200 °C), followed by evacuation and addition of;
d) 3000 umole g^{-1} H_2S.

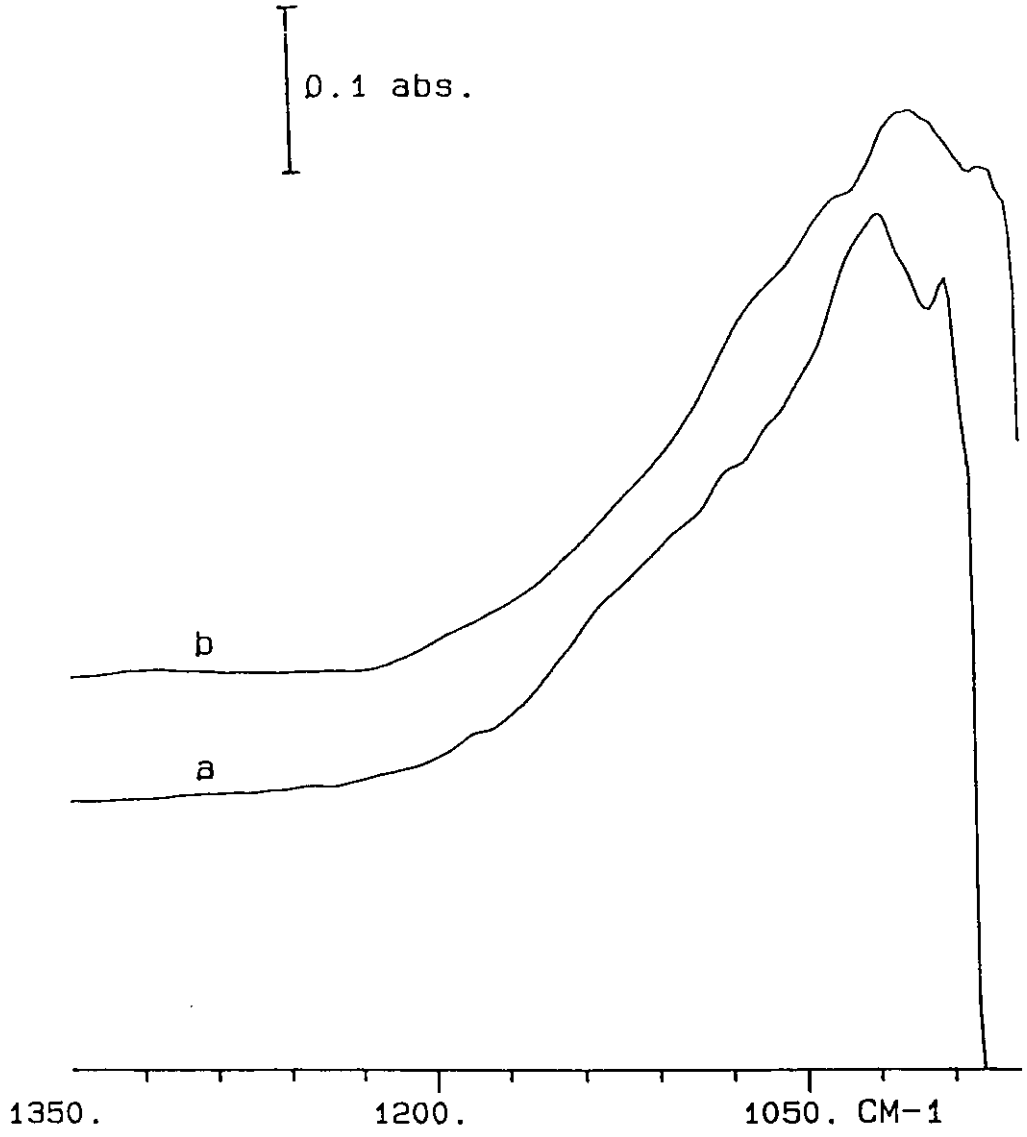

Figure 3.12

Expanded spectral region between 1350 and 960 cm^{-1} of:
a) 3.11 (a).
b) 3.11 (c).

The spectra of Al(150°C) and deuterated Al(200°C) are shown in Figure 3.10. Upon addition of SO_2 in increasing doses to Al(150°C) bands at 1620 cm^{-1} (H_2O) and 1020 cm^{-1} formed and increased along with a broad band centred at 3500 cm^{-1} while bands due to Al-OH at 3790, 3727 and 3700 cm^{-1} decreased in intensity (Figures 3.11(a) and 3.12(a)). The bands at 3500 and 1020 cm^{-1} were reduced slightly upon evacuation. On a deuterated Al(200°C) (Figures 3.11(c) and 3.12(b)), the broad 3500 cm^{-1} band shifts to 2500 cm^{-1} and the 1020 cm^{-1} band to 1005 cm^{-1}. The bands at 1330/1150 cm^{-1} did not form, confirming their assignment to adsorption on <u>cus</u> Al^{+3} sites. Evidently, the formation of a 1020 cm^{-1} band and a broad 3500 cm^{-1} band is due to reaction with hydroxyl sites on alumina.

The addition of SO_2 to Al(400°C) produced bands at 1330/1150, 1050, and the 990 cm^{-1} artifact (Figure 3.13(a)). With evacuation of excess SO_2 and subsequent addition of H_2O, the band at 1020 cm^{-1} formed (Figure 3.13(b)). In fact, we have found that the 1020 cm^{-1} band will form on Al(400°C) or Al(700°C) if traces of H_2O are not removed from the vacuum line or the SO_2 supply.

In aqueous solution, it has been found that water reacts with SO_2 to form hydrogen sulfite. Its structure has been determined to be:

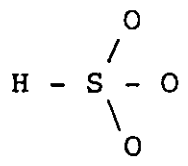

(3.j)

having a S-H linkage. No salts of the type,

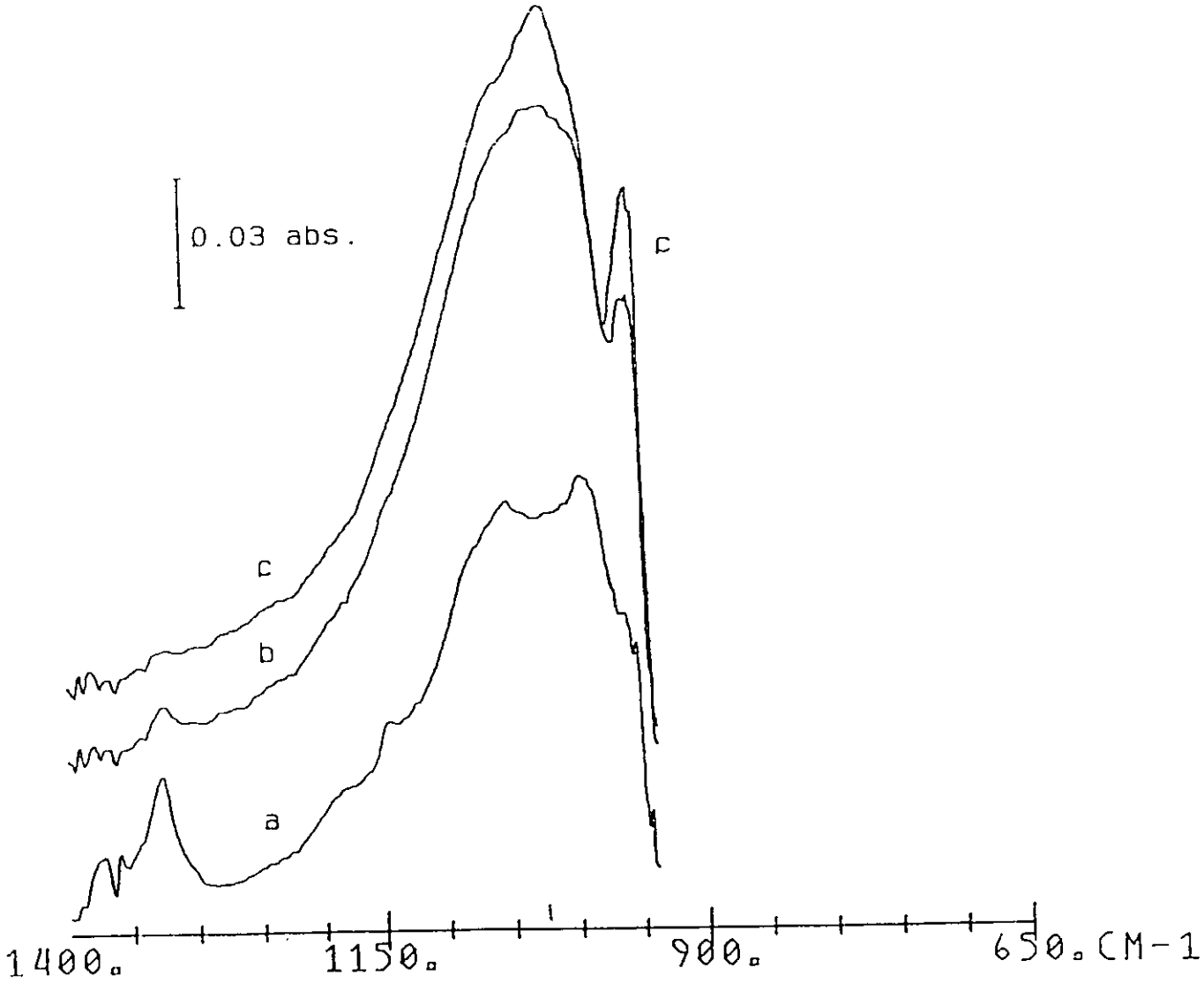

Figure 3.13

Difference spectra after the:
a) Addition of 100 umole g^{-1} SO_2 to Al(400 °C), followed by,
b) Evacuation for five minutes and addition of 15 umole g^{-1} H_2O
c) Scan ten minutes later.

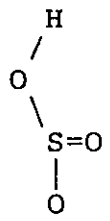

(3.k)

are known to occur in solution. However, the infrared spectrum of a species having similar structure, the $HOSO_2^-$ radical, has been recorded in an argon matrix at 11 K [61]. Bands at 3540 (O-H st.), 1309 (SO_2 asym. st.), 1097 (SO_2 sym. st.) and 759 cm^{-1} (S-OH st.) were observed.

In our case, on Al(150°C), at no time were infrared bands in the v(S-H) region observed. The appearance of hydrogen bonded OH(3500 cm^{-1}) or OD(2300 cm^{-1}) would suggest the formation of $HOSO_2^-$ rather than $H-SO_3^-$. The band at 1020 cm^{-1} can be produced on Al(700°C) by predoping the alumina with small quantities of H_2S or H_2O. (H_2S reacts to give Al-SH and AlOH). Lavalley et. al. [60] have studied the adsorption of SO_2 on highly hydroxylated alumina and reported that an additional band at 1020 cm^{-1} formed. From comparative studies of CO_2 and SO_2 adsorption, they speculated that the 1020 cm^{-1} band was due to hydrogen sulfite possessing an S-OH linkage ($HOSO_2^-$). Although no spectra were shown, they indicated that it occurred at the limit of sample transparency (a dispersive spectrometer was used). Addition of SO_2 blocked the formation of HCO_3^- with further CO_2 addition. It was also observed that HCO_3^- was displaced with SO_2 and hence, similar sites must be responsible for both reactions.

CO_2 has been shown to involve hydroxyl displacement via the reaction [62]:

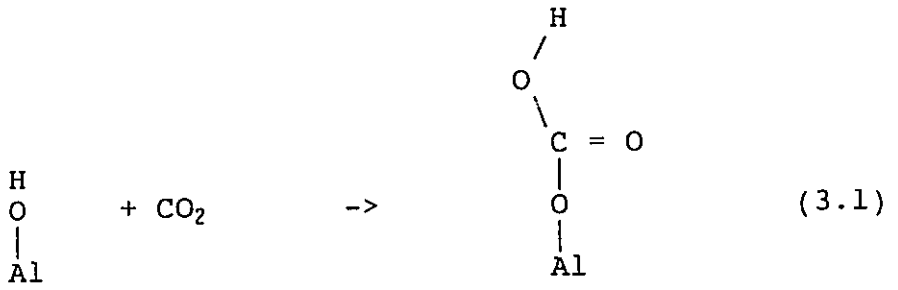

(3.1)

We conclude that SO_2 reacts with residual OH groups or with OH groups produced from H_2S dissociative adsorption.

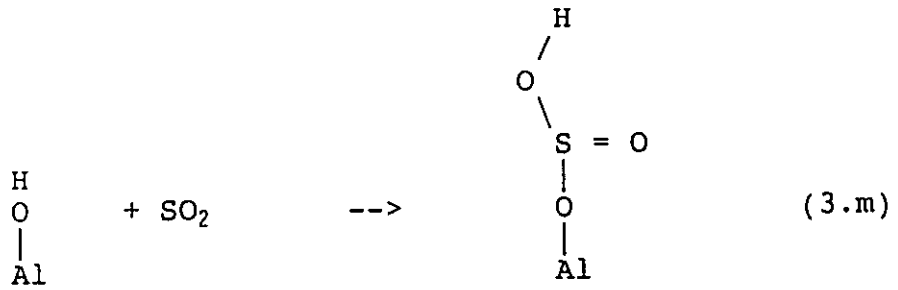

(3.m)

The formation of H_2O with SO_2 adsorption on Al(150°C) may result from condensation of two $HOSO_2^-$ or an $HOSO_2^-$ with a AlOH group. H_2O formation was not observed on Al(700°C) with SO_2 adsorption. We have found that the $HOSO_2^-$ is a hydrogen bonded species and H_2O may be produced via the reaction:

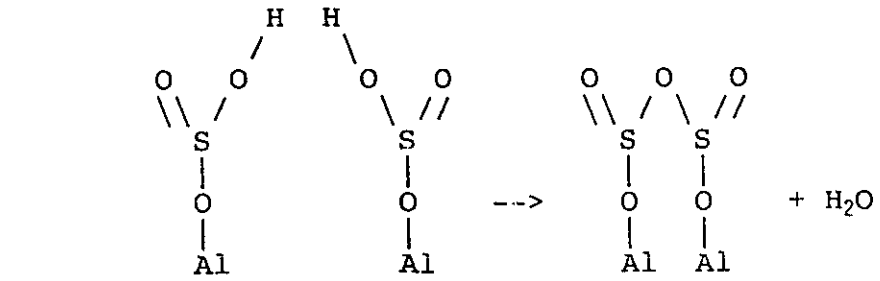

(II)

or (3.n)

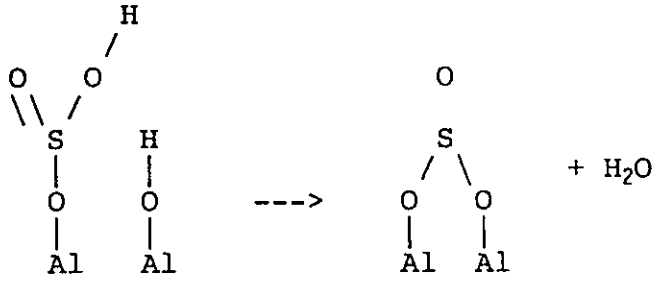

(III)

The above reactions are similar to that suggested between $HOCO_2^-$ and H_2S to form a thiocarbonate species [38]. Species (III) is very similar to the structure of the sulfate species (Chapter 7) and thus, may be a precursor for its formation.

3.5 ADSORPTION OF SULFUR DIOXIDE AND HYDROGEN SULFIDE

Previous studies using infrared spectroscopy have examined the interaction of H_2S with adsorbed SO_2 (or vice versa) or the coadsorption of H_2S with adsorbed SO_2 on the surface of alumina. Karge *et. al.* [52] observed that the H_2S band at 2570 cm^{-1} was easily eliminated upon addition of SO_2 or water and the bands at 1330/1150 cm^{-1} from SO_2 adsorption were removed when H_2S or H_2O was

added. Therefore, Karge et. al. suggested that the water formed during the Claus reaction would prevent the formation of these species and that they would not be Claus intermediates.

Karge et. al. found that the rate of reaction of the species responsible for the 1050 cm^{-1} band with H_2S increased on going from room temperature to 200°C. Because the Claus reaction on alumina typically involves temperatures over 200°C, and both sulfur and water as products, he postulated that the Claus reaction involved an interaction between gaseous H_2S and adsorbed SO_2. The 1050 cm^{-1} band was not removed from the surface when evacuated at 200°C and, therefore, the species responsible for this band would be present during the Claus process.

Lavalley et. al. [63] observed the disappearance of the 2570 cm^{-1} band and a yellow colourization of the alumina with SO_2 adsorption on alumina pretreated with H_2S. They suggested that the formation of sulfur, polysulfide or polythionates had occurred. Lavalley et. al. reported that addition of CH_3SH to Al_2O_3 activated at 800°C results in the following reaction:

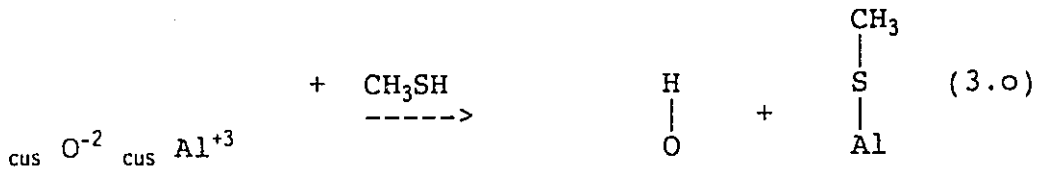

(3.o)

Upon further addition of SO_2, the band at 3690 cm^{-1} (O-H) was reduced and the bands at 2998 and 2938 cm^{-1} (SCH_3) shifted in frequency. From this, the following reaction was postulated:

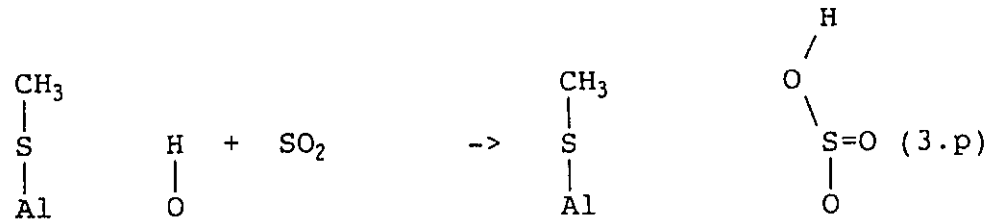

A similar mechanism was postulated for H_2S and SO_2.

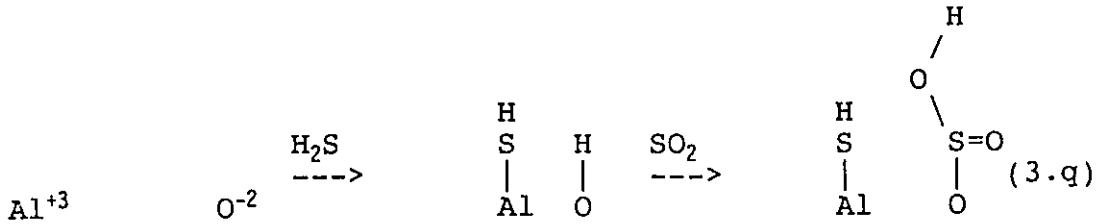

Lavalley et. al. further suggested that the yellow colourization observed with SO_2 addition to alumina predoped with H_2S may be due to the following reaction.

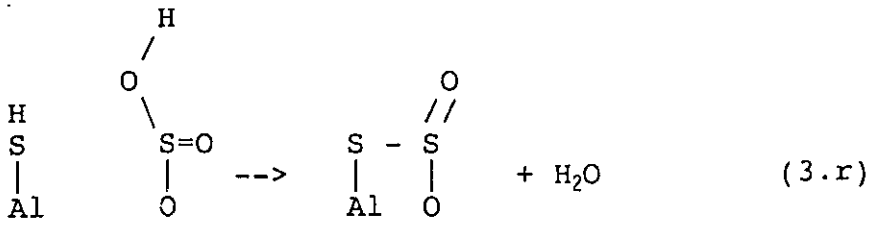

The S_2O may be a reactive intermediate and further react with H_2S to form sulfur.

More recently, Datta and Cavell [64] observed the formation of H_2O along with the disappearance of the 2570 cm^{-1} band and

concluded that some Claus activity did occur at room temperature. Datta and Cavell found that the reaction between adsorbed H_2S and gaseous SO_2 occurred to a lesser extent than the reaction of preadsorbed SO_2 with gaseous H_2S. No definite assignment could be postulated since sulfur, polysulfide and polythionate bands occur at frequencies below 1000 cm^{-1}. However, thiocarbonate impurities, which we have shown to be present in Cavell's study, may be involved in a reaction with SO_2 producing H_2O. (Cavell observed that the band at 1334 cm^{-1} decreased upon SO_2 adsorption).

Previous studies [52,64] have examined the reactions of H_2S with adsorbed SO_2 species on dehydroxylated Al_2O_3. Since on highly hydroxylated alumina, $HOSO_2^-$ was primarily formed and the alumina in a Claus reactor would be highly hydroxylated, a further infrared study is warranted. We have also used Raman spectroscopy in order to observe sulfur, polysulfide or polythionate formation to determine whether the Claus reaction procedes via reaction with adsorbed H_2S or SO_2.

3.5.1 ADDITION OF H_2S, FOLLOWED BY SO_2

The adsorption of H_2S on Al(700°C) followed by evacuation has been shown (Figure 3.3) to give rise to bands at 2570 cm^{-1} (Al-SH) and 3690 cm^{-1} (Al-OH). Upon introduction of SO_2 to Al(700°C) predoped with H_2S, the 2570 cm^{-1} band disappeared, followed by formation of a broad band centred at 3500 cm^{-1} and bands at 1050 cm^{-1} ($SO_3^=$), 1020 cm^{-1} ($HOSO_2^-$), 1620 cm^{-1} due to H_2O

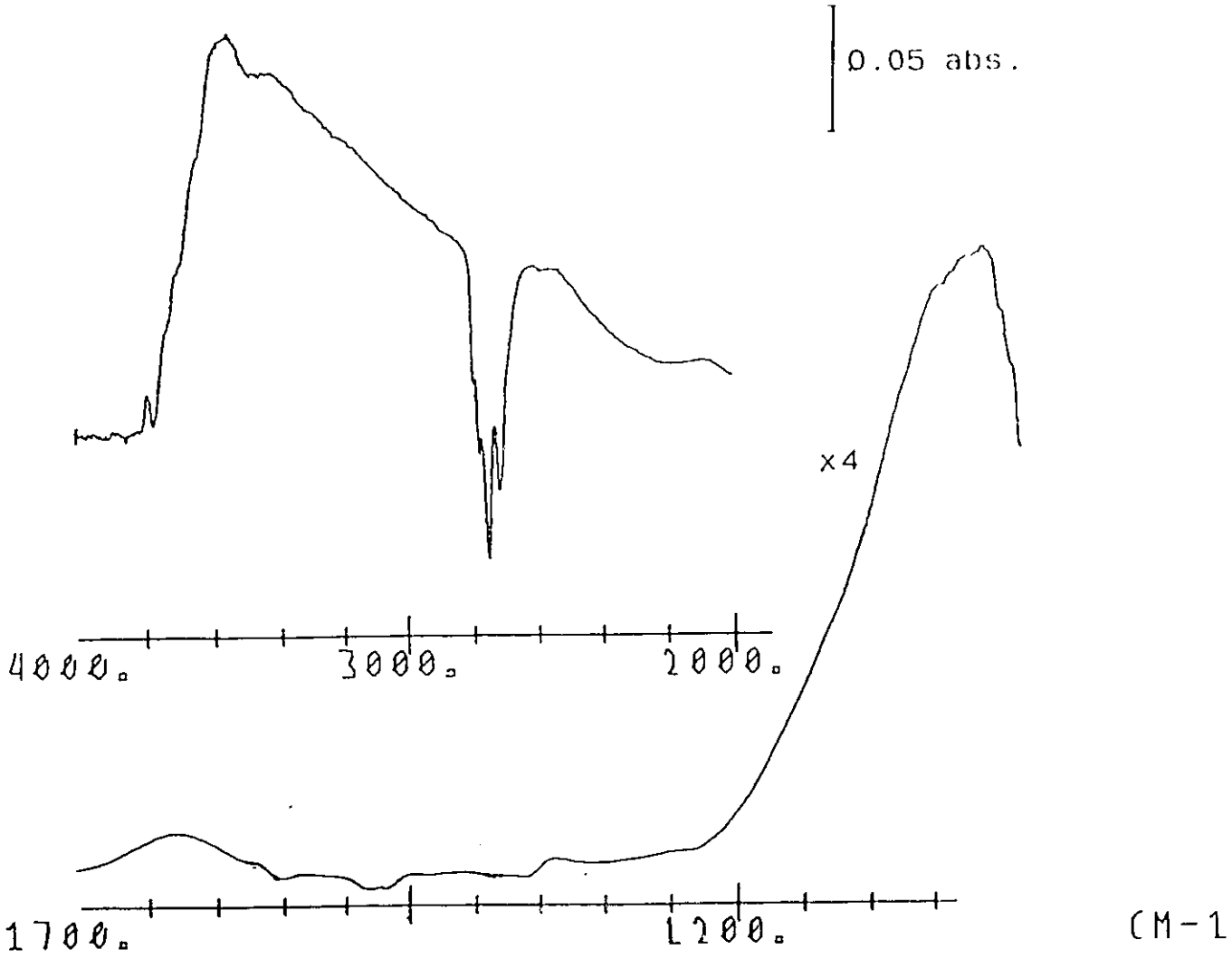

Figure 3.14

Difference spectrum of deuterated Al(400 °C) with 60 umole g^{-1} H_2S added, followed by evacuation 5 minutes, then addition of 600 umole g^{-1} SO_2 and evacuation for ten minutes.

and at higher doses, bands at 1330 and 1150 cm^{-1}. All bands, except the 1020 cm^{-1} band ($HOSO_2^-$), form on a pure Al(700°C) sample with SO_2 addition. The 1020 cm^{-1} band is due to reaction of SO_2 with Al-OH formed upon dissociative adsorption of H_2S. In a separate experiment, SO_2 was added to a deuterated Al(400°C) sample predoped with H_2S (Figure 3.14). Predoping with H_2S produced OH groups in addition to the OD groups originally on the deuterated alumina. SO_2 addition resulted in the formation of bands at 1050 cm^{-1} with bands at 1020-1000 cm^{-1} and 3500/2600 cm^{-1} while the OH band at 3690 cm^{-1} decreased and the OD bands disappeared. The results of these experiments show that both S-H and AlOH groups reacted with SO_2. We conclude that $HOSO_2^-$ is produced from this reaction and that sulfite (1050 cm^{-1}) is produced via adsorption of SO_2 on bare O^{-2} sites.

In a Raman experiment no bands other than 1338/1150 cm^{-1} were observed upon the addition of SO_2 to Al(500°C) pretreated with H_2S. However, upon evacuation of the SO_2 and further addition of H_2S, S_8 bands at 151, 220 and 480 cm^{-1} (Figure 3.4(d)) were observed. In a separate experiment, pretreatment of Al_2O_3 with SO_2 followed by H_2S also generated the S_8 bands. It has been reported from gravimetric results that 90 umole g^{-1} of H_2S [39] and 200 umole g^{-1} of SO_2 [60] were irreversibly adsorbed on Al(500°C). Therefore, if sulfur formed from reaction of adsorbed H_2S with SO_2 it should have formed in sufficient quantities to be detected.

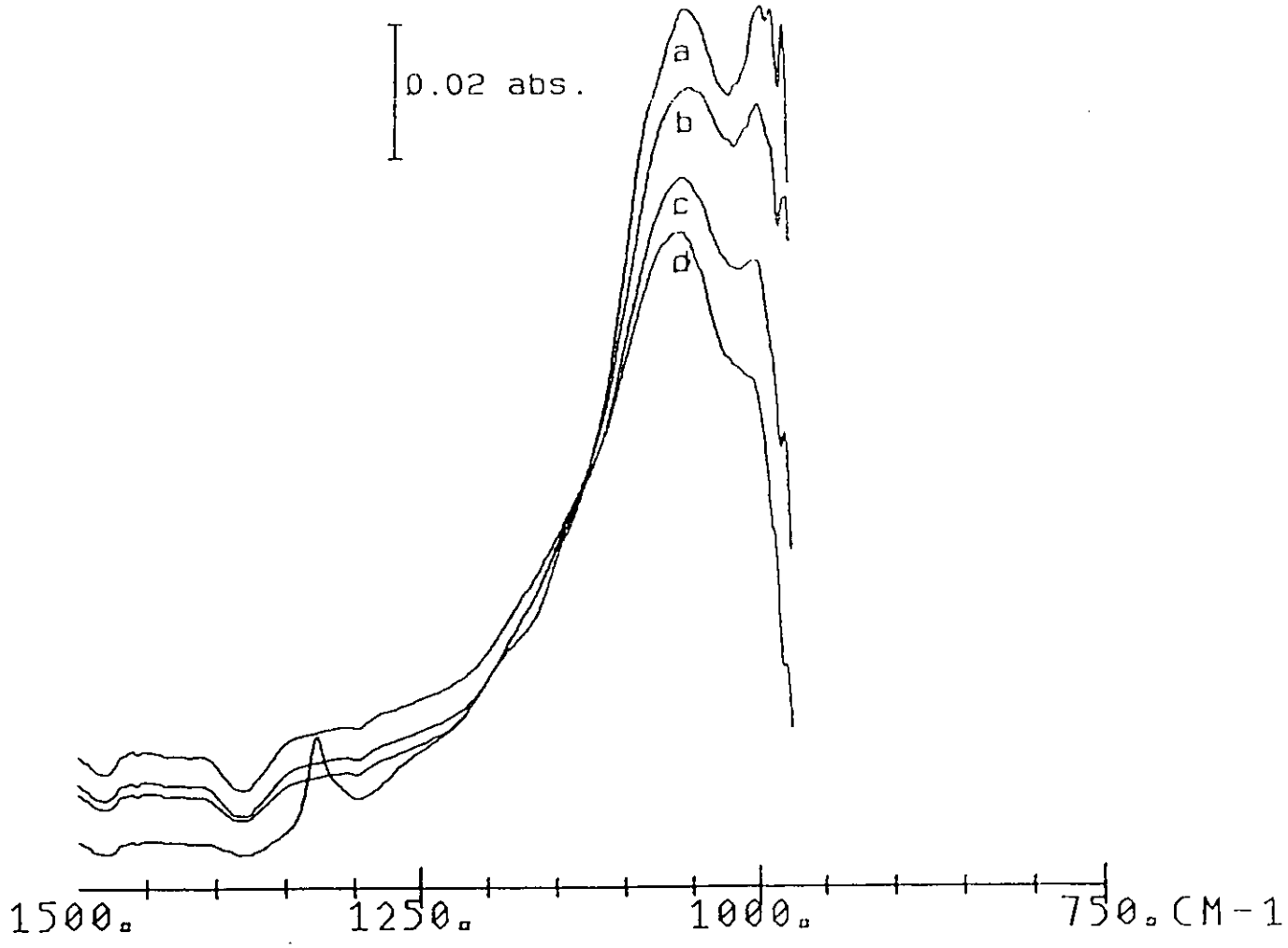

Figure 3.15

a) Same as Figure 3.4(c).
Scan immediately after adding
b) 15 umole g^{-1}, c) 90 umole g^{-1}, and
d) 3 mmole g^{-1} of H_2S.

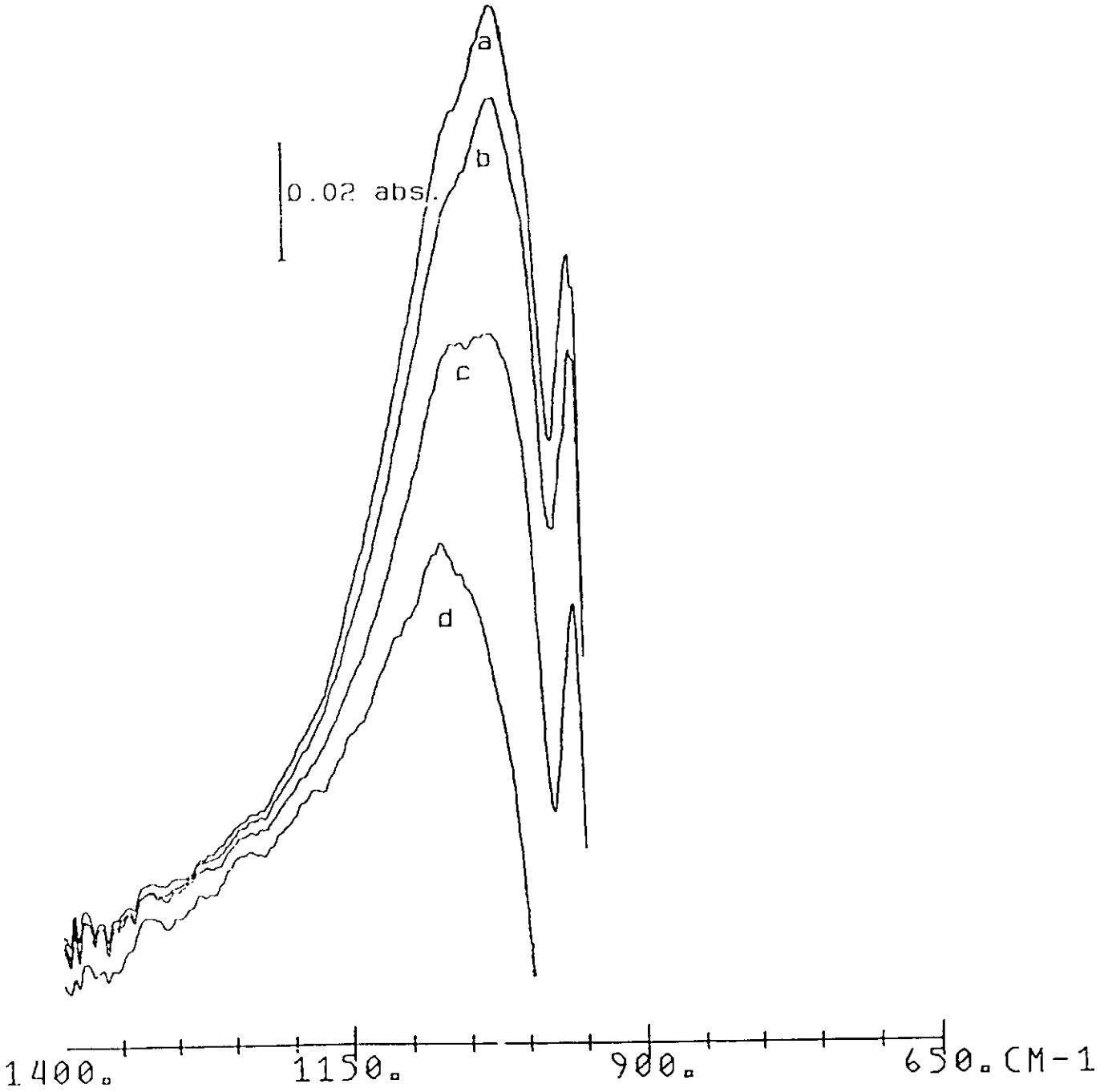

Figure 3.16

a) Sample in Figure 3.13(c) after evacuation one minute.
b) Followed by addition of H_2S (3000 umole g^{-1}).
c) Thirty minutes later.
d) Six hours later.

4.5.2 ADDITION OF SO_2, FOLLOWED BY H_2S

Spectra following the addition of H_2S in increasing doses to Al(400°C) pretreated with SO_2 are shown in (Figure 3.15). The bands due to weakly adsorbed SO_2 at 1330 and 1150 cm^{-1} first decrease in intensity while bands at 3500 and 1620 cm^{-1} (H_2O), (not shown) formed, suggesting some Claus activity. Upon further addition of H_2S, the 1050 cm^{-1} band was reduced in intensity (the 990 cm^{-1} feature has been discussed previously) and the formation of H_2O (1620 cm^{-1} band) accompanied this change. The absence of the hydrogen sulfite band at 1020 cm^{-1} indicated that some $SO_3^=$ was directly converted into sulfur and H_2O.

At no time during the addition of H_2S (even in excess) were bands due to Al-SH (2570 cm^{-1}) observed. This may be the result of blockage of reactive cus Al^{+3} acidic sites by adsorbed SO_2, or by the sulfur and H_2O. Sulfur sublimation causing catalyst deactivation is normally prevented when the reaction is carried out at temperatures above 200°C.

On Al(150°C), where addition of SO_2 primarily forms $HOSO_2^-$, addition of H_2S (Figure 3.11(b)) resulted in the decrease in the 1020 cm^{-1} band and an increase in the band at 1620 cm^{-1} (H_2O). On alumina, where both $SO_3^=$ (1050 cm^{-1}) and $HOSO_2^-$ (1020 cm^{-1}) are present, the 1020 cm^{-1} band decreased more rapidly than the 1050 cm^{-1} band (Figure 3.16). Therefore, the $HOSO_2^-$ (1020 cm^{-1}) is more reactive with H_2S than the $SO_3^=$ (1050 cm^{-1}).

We have reported that $DOSO_2^-$ (bands at 2450 and 1000 cm^{-1}) formed with exposure of SO_2 to a deuterated Al(200°C).

Subsequent addition of H_2S decreased the 1000 cm^{-1} band and the broad band located at 2450 cm^{-1}. At the same time, bands at 1620 and 1410 cm^{-1} and a broad flat band between 3500 and 2600 cm^{-1} formed indicating the formation of H_2O and HDO. HDO formation would suggest the reaction of gaseous H_2S with the hydroxyl group of the hydrogen sulfite species.

4.6 CONCLUSION

Our Raman results clearly show that the formation of sulfur on alumina involves reaction of gaseous H_2S with adsorbed SO_2. Isotopic studies suggest that both the 1330 and 1150 cm^{-1} bands were due to weakly adsorbed SO_2 on acidic sites on alumina, while the band at 1050 cm^{-1} was due to sulfite species on basic sites. On a hydroxylated alumina, SO_2 primarily forms hydrogen sulfite (1020 cm^{-1}) via direct reaction of SO_2 with hydroxyl groups.

The hydrogen sulfite reacted with H_2S and at a much faster rate than the more strongly held sulfite. The Claus reaction results in the production of H_2O which would ensure the existence of a highly hydroxylated alumina. Under these conditions, we have observed that the formation of hydrogen sulfite mainly forms and is reactive with gaseous H_2S.

Chapter 4

THE ROLE OF SODIUM IN THE CLAUS REACTION

4.1 INTRODUCTION

It has been reported that alumina impregnated with NaOH (1% by weight) resulted in an increase in the rate of the Claus reaction [58,65]. Recently, Saussey et. al. [65] have observed an enhancement in the direct conversion of H_2S to sulfur;

$$2\ H_2S + O_2 \rightarrow \frac{1}{n} S_n + H_2O \qquad (4.a)$$

by sodium loading of alumina up to 3% by weight. Higher sodium loading resulted in drastic catalytic deactivation.

It has also been observed that silica impregnated with NaOH possessed some Claus activity [66], whereas pure silica is inert vis-à-vis the Claus process [67-69]. Essentially no infrared spectral changes were observed (Figure 4.1) upon impregnation of silica with sodium (3% by weight) relative to pure silica indicating that the sodium is simply dispersed over the silica (silica behaves as a high surface area inert support). Although

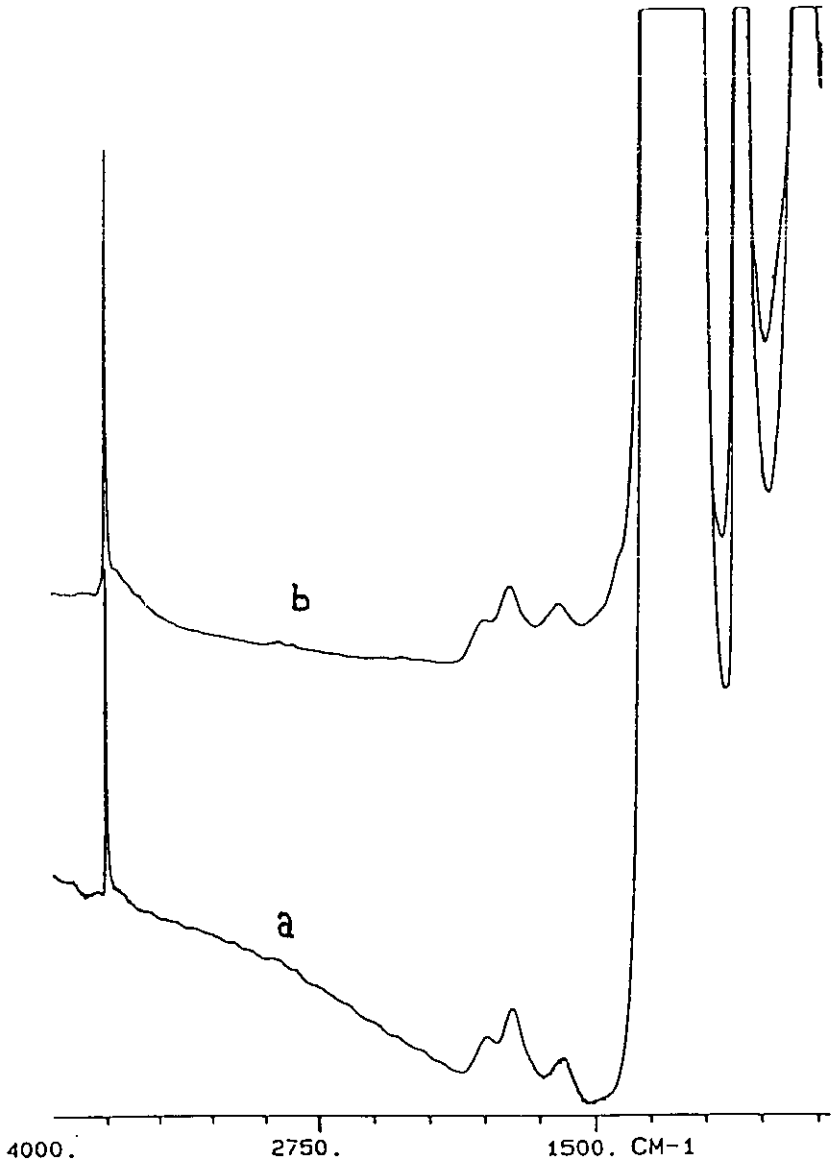

Figure 4.1

a) 3% Na/SiO_2(450 °C).
b) SiO_2(450 °C).
The spectra have been offset for clarity.

silica is opaque from 1300-1000 cm^{-1}, there are two regions of partial transparency between 1000 cm^{-1} and 500 cm^{-1} in which characteristic SO_x modes are located (Figure 4.1).

Dudzik and George [66] reported a strong correlation between the concentration of SO_2^- radicals (as measured by ESR spectroscopy) and formation of sulfur from the reaction of H_2S with SO_2 adsorbed on sodium doped silica (Na/SiO_2). The increased activity was demonstrated to be related to the electron donor properties of the Na doped catalyst with possible cus O^{-2} or OH^- sites. However, Dudzik and George observed that only as much as 10% of the total adsorbed SO_2 formed SO_2^- radicals of which only 50% reacted with H_2S at 25°C. SO_2^- radicals have also been postulated as Claus intermediates on alumina although they constitute 1% of the total SO_2 adsorbed. In this case, Claus activity has been shown to occur with other SO_2 adsorbed species. It is possible that for Na/SiO_2 the other 90% of adsorbed SO_2 will also exhibit some Claus activity.

Therefore, the aims of this chapter are twofold. In the first section, we examine the Claus activity of sodium, by itself, physically dispersed over an inert silica support. In particular, we have used IR spectroscopy to study the reactions of SO_2, H_2S and H_2O on a sodium/silica catalyst. By using spectral subtraction, we have been able to observe characteristic vibrations due to SO_x stretching and deformation modes which occur below 1000 cm^{-1}. Complementary data has also been acquired from Raman spectral studies.

In the second section, the adsorption of H_2S and SO_2 are studied on Na/Al_2O_3 catalysts. In the previous chapters, we have determined that the Claus process primarily occurred between adsorbed SO_2 on alumina and gaseous H_2S. Adsorbed SO_2 on alumina exists in a number of forms on surface sites with varying acidity. The sodium impregnation may perhaps alter the acidity of various adsorption sites which could manifest in an enhanced Claus activity. By comparison of the adsorbed species on Na/SiO_2, Na/Al_2O_3 and on pure Al_2O_3, the role of sodium in the Claus process may be better understood.

4.2 EXPERIMENTAL

Sodium doped silica or alumina, containing 3% Na by weight, was prepared by wet impregnation with NaOH, and dried at 100°C. Self supporting discs contained about 5 mg cm^{-2} of this mixture and samples were prepared under several different activation conditions. After impregnation with NaOH, samples denoted Na/O(450°C) were calcined in air at 600°C followed by activation in O_2 at 450°C for one hour, followed by evacuation at 450°C for thirty minutes. Na(450°C) and Na(150°C) samples were simply degassed in vacuum for one hour at 450°C and 150°C respectively.

Solid NaOH, Na_2O_2, Na_2O, and other sodium salts for Raman studies were obtained from commercial sources and were normally evacuated at 100°C in the standard Raman cells for one hour prior to use. H_2S and SO_2 were purified prior to use to remove traces of CO_2 [69].

4.3 PURE SILICA

The characterization of the surface of aerosil silicas has been the topic of numerous reviews and articles [70,71]. Of importance in our study are the types of sites which exist on silica which have been degassed at 150°C and 450°C.

Spectra of the hydroxyl region of aerosil silica degassed at several temperatures are shown in Figure 4.2. Infrared studies have concentrated on the study of the hydroxyl bands located in the 3800 to 3400 cm^{-1} region [70-72]. Molecular water is readily eliminated by degassing at room temperature. Silica degassed at 150°C exhibits hydroxyl bands at 3747 (sharp), 3720 and 3650 (broad), and at 3520 cm^{-1} (broad). The 3747 cm^{-1} is due to isolated hydroxyls while those at 3520 cm^{-1} and 3720 cm^{-1} are due to hydrogen bonded hydroxyls.

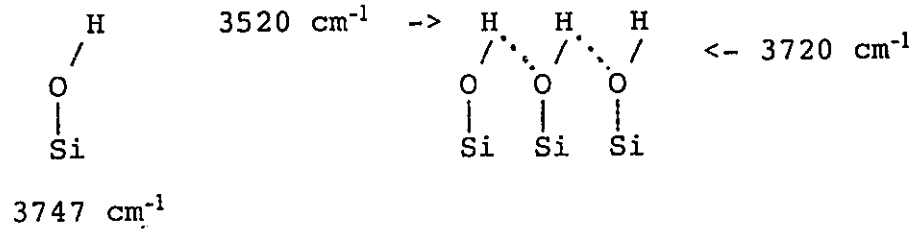

(4.b)

The broad band at 3650 cm^{-1} has been assigned to inaccessible hydroxyls resulting from the compression of adjacent silica particles.

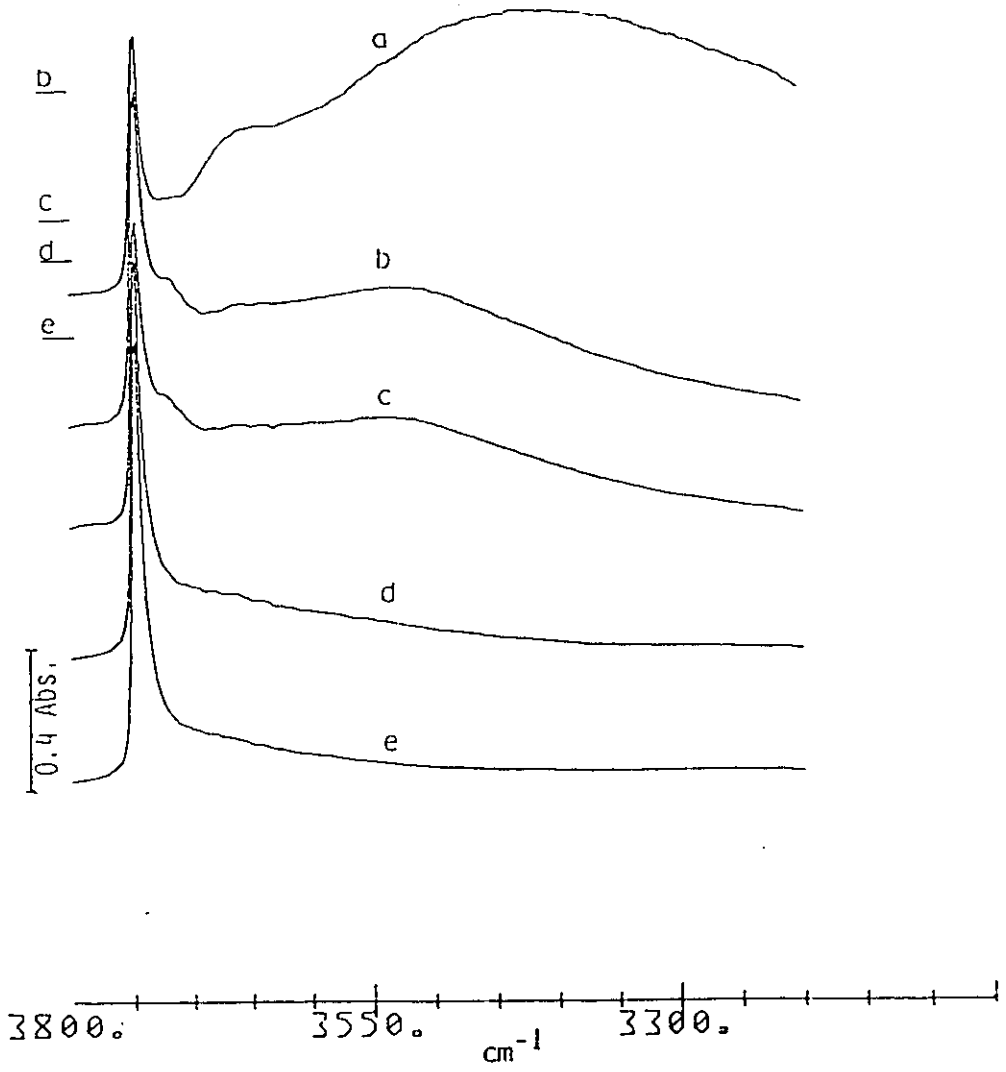

Figure 4.2

Infrared spectra of aerosil (10mg/cm^{-2}) in the OH stretching region:
a) Before degasing and after degasing for one hour at:
b) 25 °C.
c) 150 °C.
d) 300 °C.
e) 500 °C.
(from McFarlane, R.A., ref. 72).

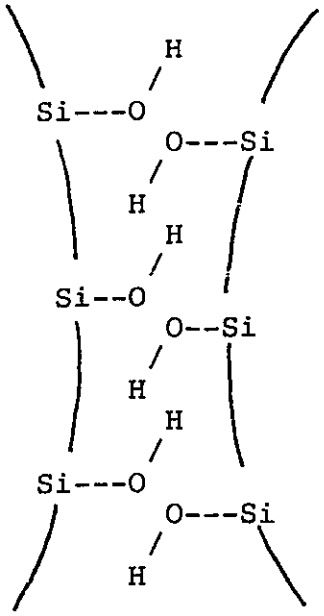

(4.c)

Evacuation at temperatures up to 400°C results in the removal of hydrogen bonded hydroxyls and isolated hydroxyl groups via condensation of adjacent hydroxyls to form siloxane sites of TYPE A.

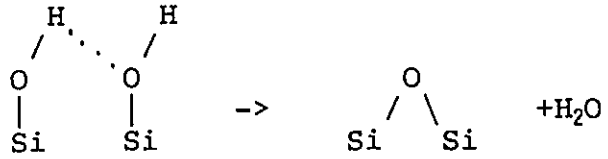

(4.d)

TYPE A

The siloxane sites are unreactive and can be completely rehydrated upon addition of water.

When silica is outgassed at temperatures above 400°C, the surface is no longer reversibly dehydroxylated. A second type of siloxane with bands at 908 and 888 cm^{-1} begins to form resulting from the migration and condensation of hydroxyl groups. Unlike the siloxane sites of TYPE A, the sites are reactive with a number of gases and upon rehydration form hydroxyl groups. The

reactive siloxane sites are very low in number even when high temperature outgassing is performed (0.15/nm^{-2} at 1200°C).

4.3.0.1 ADDITION OF SO_2 OR H_2S

The addition of SO_2 or H_2S to silica degassed at 450°C or 900°C resulted in no spectral changes whatsoever. We conclude that SO_2 and H_2S are completely unreactive with the silica surface OH groups or reactive siloxane sites at room temperature. Weakly adsorbed SO_2 (similar to that observed on alumina acidic sites with bands at 1330 and 1150 cm^{-1}) may occur in the 1300 to 1000 cm^{-1} region where silica is opaque. However, the existence of oxysulfur compounds such as sulfite, sulfate, etc. would have produced bands in the partially transparent 1000 to 600 cm^{-1} region. In addition, no Raman bands were observed in this spectral region unlike those which have been observed for alumina, and also in following chapters for titania and gallium oxide.

4.4 SODIUM SILICA CATALYST

4.4.1 NATURE OF THE CATALYST

A silica of 320 m^2g^{-1} area contains about 1.4 OH groups per nm^2 after degassing at 450°C under vacuum and for a 3% Na/SiO_2 the ratio of Na to OH is about 2. Although the SiOH intensity at 3747 cm^{-1} was slightly reduced relative to that of pure silica,

(see Figure 4.1) we conclude that surface SiOH groups have not significantly been transformed to SiONa.

The treatment of solid NaOH with oxygen at pressures greater than 1 atmosphere at 450°C slowly forms a product containing the oxide and peroxide [73]. For the NaO(450°C) samples the sodium exists in a highly dispersed state and thus the calcination process at 600°C would result primarily in the formation of sodium peroxide and oxide. However, the further outgassing of NaO(450°C) at 450°C would likely convert much of the peroxide to the oxide (Na_2O_2 begins to liberate oxygen to form Na_2O at temperatures between 311 and 400°C [73]). Therefore, we assume that this material probably corresponds to supported sodium oxide.

Consequently, for Na(450°C) or Na(150°C), outgassing at 450°C or 150°C would not alter the sodium hydroxide on the surface. We have also studied the adsorption of SO_2 and H_2S on these surfaces because, under normal Claus conditions, the water produced would preclude oxide or peroxide formation. Both Na_2O_2 and Na_2O react readily with water to form NaOH.

4.4.1.1 ADDITION OF SO_2

The addition of either H_2S or SO_2 to NaO(450°C) or Na(450°C) did not give rise to any observable Raman bands due to SO_x or HS vibrational modes. The Raman spectrum of Na(150°C) exhibited a high background fluorescence even before the addition of a reactant and this material was not used in further Raman

experiments. We have demonstrated in Chapter 3, that this inability to observe bands is partially due to fluorescence and is partially due to a sensitivity problem at the 3% loading level. To overcome this problem, we have also undertaken Raman studies using solid NaOH, Na_2O, Na_2O_2 and using sodium salts of sulfur compounds. The addition of SO_2 to solid NaOH, Na_2O or Na_2O_2 produced Raman bands at 990, 940, 630 and 490 cm^{-1} characteristic of $SO_3^=$ (Figure 4.3).

A typical infrared spectrum of the window region for Na(450°C) is shown in Figure 4.4. The addition of SO_2 to Na(450°C) or NaO(450°C) resulted in an increase in the background absorption near 600 cm^{-1} and 900 cm^{-1} which, after spectral subtraction (Figure 4.5(a,b)), revealed a broad band at 925 and a weaker band at 620 cm^{-1}. The 925 cm^{-1} band was near 915 cm^{-1} using $S^{18}O_2$. Sirinardine and Cook [74] have reported in a XPS study, that for sodium deposited on a single crystal of SiO_2, the adsorption of SO_2 resulted in the formation of $SO_3^=$. Free $SO_3^=$ in solution, has bands at 966, 933, 620 and 470 cm^{-1}. The corresponding bands for solid Na_2SO_3 and other sulfite salts are shown in Table 4.6. Both the Raman results on solid oxides and the infrared results on NaO/(450°C) suggest that $SO_3^=$ is formed upon addition of SO_2. Formation of a sulfite on Na/SiO_2 resembles more the free $SO_3^=$ rather than the Na_2SO_3 salt. This could account for the broad band observed at 925 cm^{-1} which is close to the 933 cm^{-1} band observed for free $SO_3^=$.

Finally, for Na(150°C) or Na(450°C), we also observed infrared bands at 925 and 620 cm^{-1} accompanied by a new band at

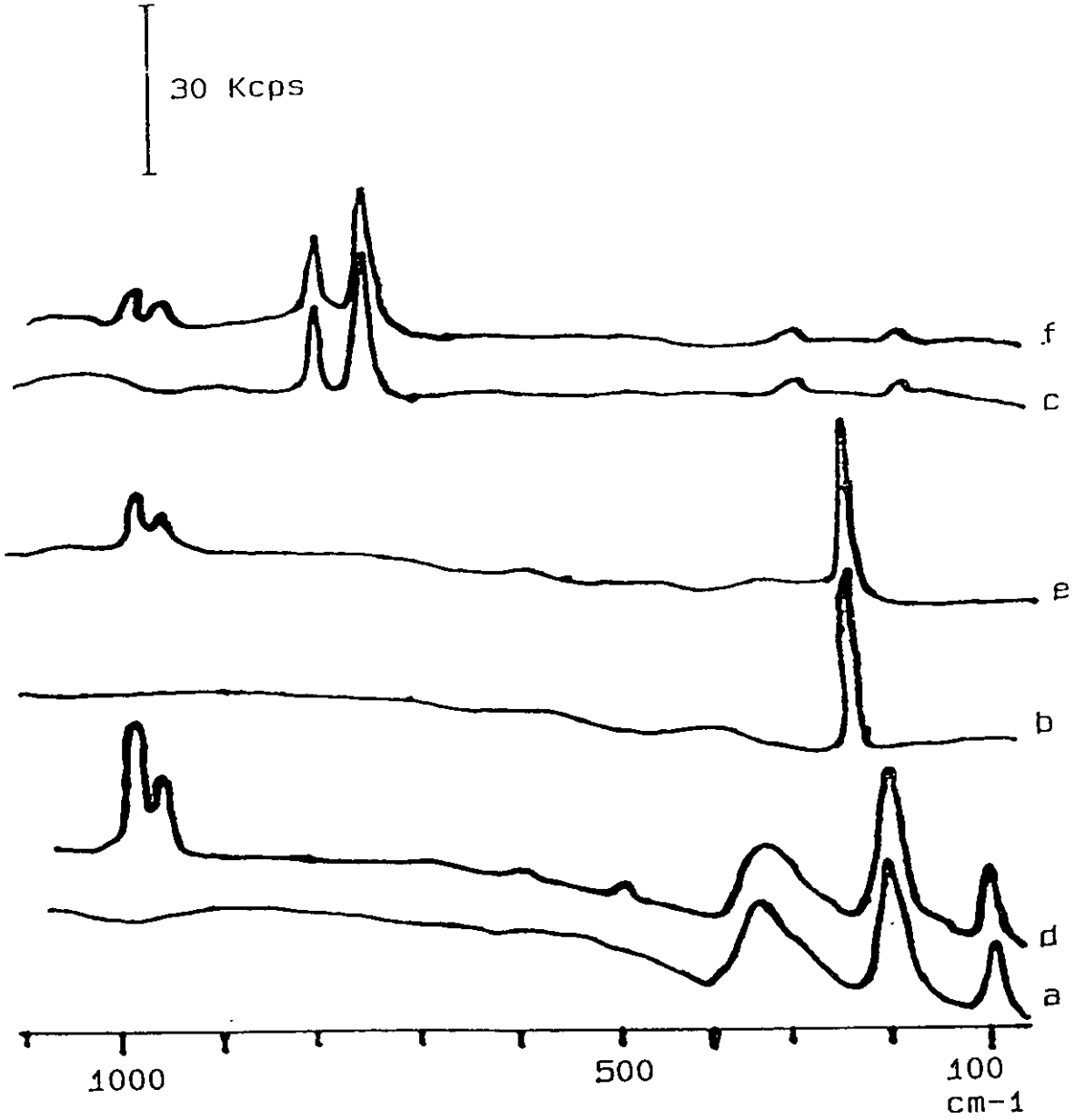

Figure 4.3

Raman spectra of;
a) NaOH, b) Na_2O, c) Na_2O_2.
Followed by addition of SO_2(600 umole g^{-1}) and evacuation thirty minutes to ;
d) NaOH, e) Na_2O, f) Na_2O_2.

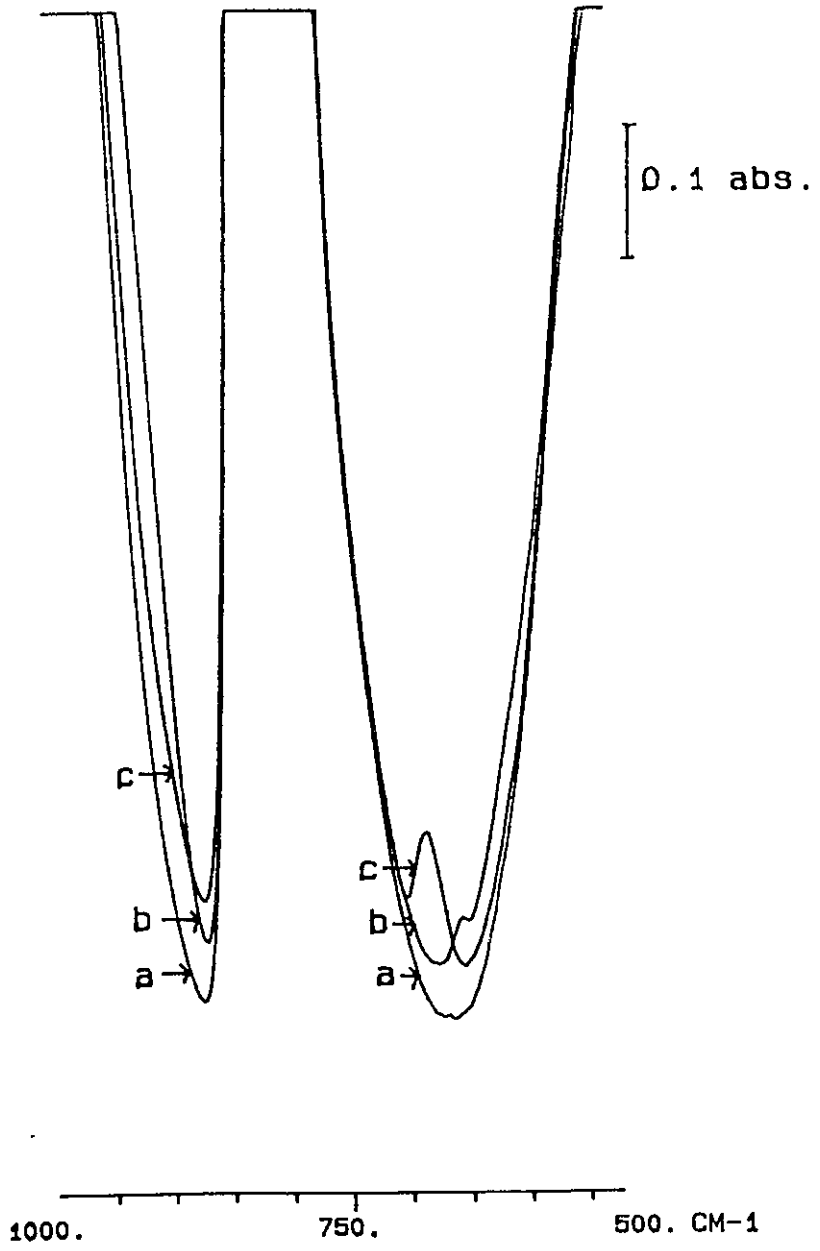

Figure 4.4

a) Na(450 °C).
b) Add 200 umole g^{-1} SO_2.
c) Evacuate five minutes, add 200 umole g^{-1} H_2S.
The difference spectra are shown in Figure 4.5(b) and (d).

TABLE 4.1

Raman frequencies for sulfite ion in solution and ionic compounds (cm^{-1}).

SPECIES	$\nu_3(A)$	$\nu_1(E)$	$\nu_2(A)$	$\nu_4(E)$
$SO_3^{=}(aq)$	966	933	620	470
Na_2SO_3	990	950	639	499
K_2SO_3	978	952	628	478
Rb_2SO_3	963	952	628	479
Cs_2SO_3	951	936	620	470
Ti_2SO_3	928	928	600	457

From Peter, L. and Meyer, B., ref. 9.

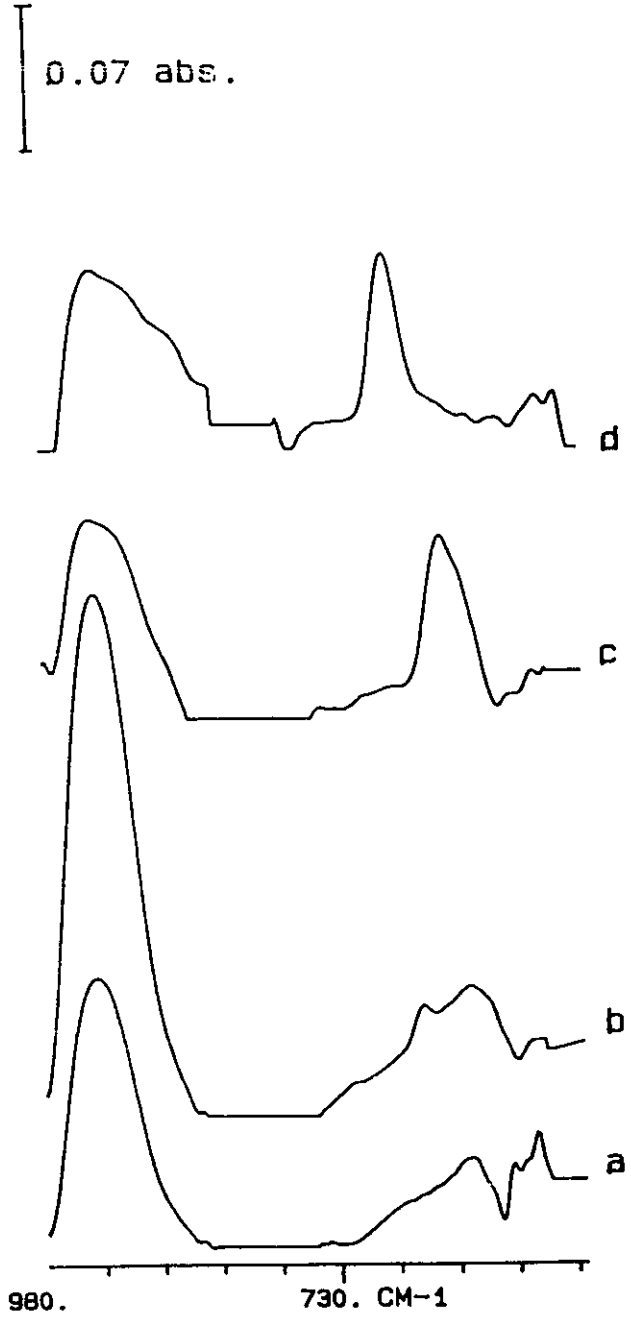

Figure 4.5

Difference spectrum after addition of SO_2(200 umole g^{-1}) to;
a) NaO(450 °C), and, b) Na(450 °C).
Followed by evacuation for ten minutes and
addition of H_2S (200 umole g^{-1}) to;
c) NaO(450 °C), and, d) Na(450 °C).

660 cm^{-1} (Figure 4.5(b)). This 660 cm^{-1} band was also observed following adsorption of SO_2 and H_2O on NaO/(450°C) and its nature will be discussed in the next section.

4.4.1.2 ADDITION OF H_2O AND SO_2

The addition of H_2O to preadsorbed SO_2 (excess SO_2 evacuated) lowered the infrared band intensity at 620 cm^{-1} (Figure 4.6) for all three samples, gave rise to a stronger band at 660 cm^{-1}, and additionally produced new bands at 2425 cm^{-1}, 960, 635 and 560 cm^{-1}. The same spectrum was observed for the reverse sequence, H_2O then SO_2 addition or for H_2O and SO_2 coadsorption (Figure 4.7). From comparison to known species in solution, the bands at 2425, 960, 635 and 560 cm^{-1} are undoubtedly due to HSO_3^-. The disappearance of the $SO_3^=$ bands and formation of HSO_3^- probably occurred via the reaction:

$$Na_2SO_3 + H_2O \rightarrow NaOH + NaHSO_3 \qquad (4.e)$$

The band at 660 cm^{-1} is characteristic of formation on a disulfite, $S_2O_5^=$. The disulfite forms in solution via the following equilibrium [11]:

$$2\ HSO_3^- \rightleftharpoons S_2O_5^= + H_2O \qquad (4.f)$$

This equilibrium could account for the relative intensities of the 660/635 cm^{-1} bands upon addition of water and upon subsequent evacuation. In Figure 4.6(f), evacuation resulted in the slight

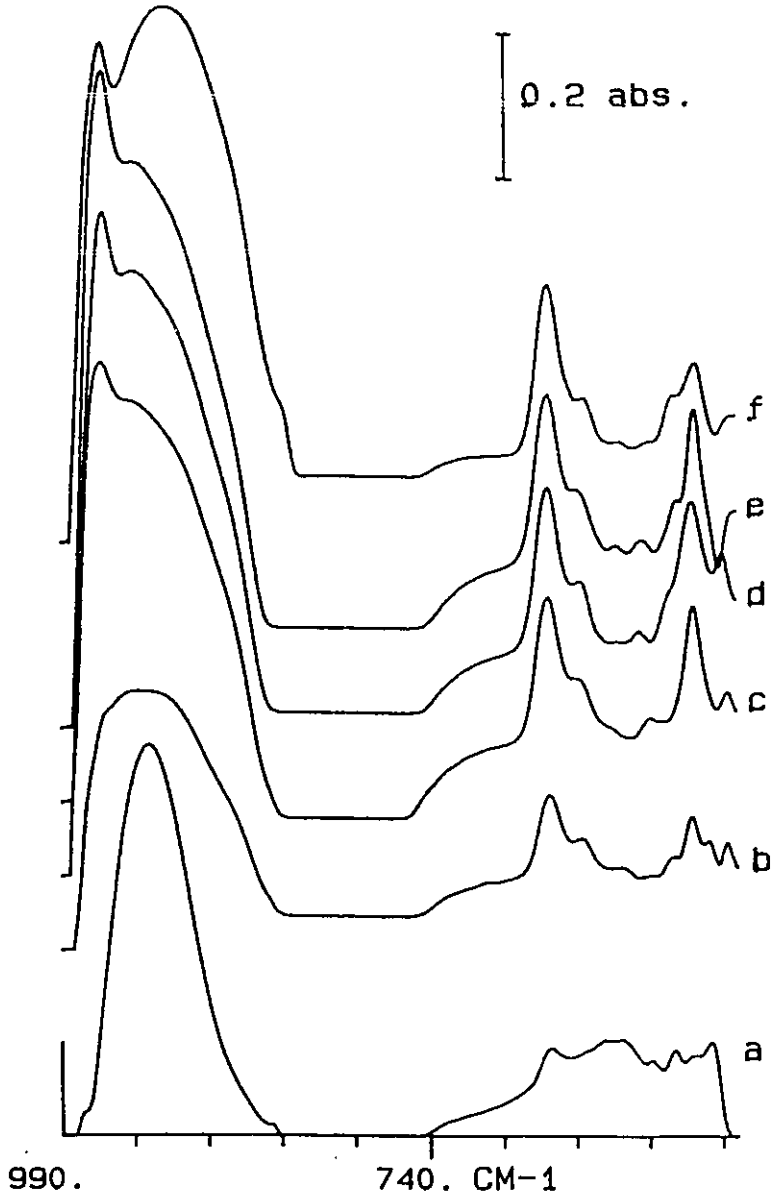

Figure 4.6

Na(450 °C) with;
a) Addition of SO_2(200 umole g^{-1}).
b) Evacuate one minute, add H_2O(200 umole g^{-1}).
c) scan ten minutes later.
d) Twenty minutes later.
e) Forty minutes later.
f) Evacuate five minutes.

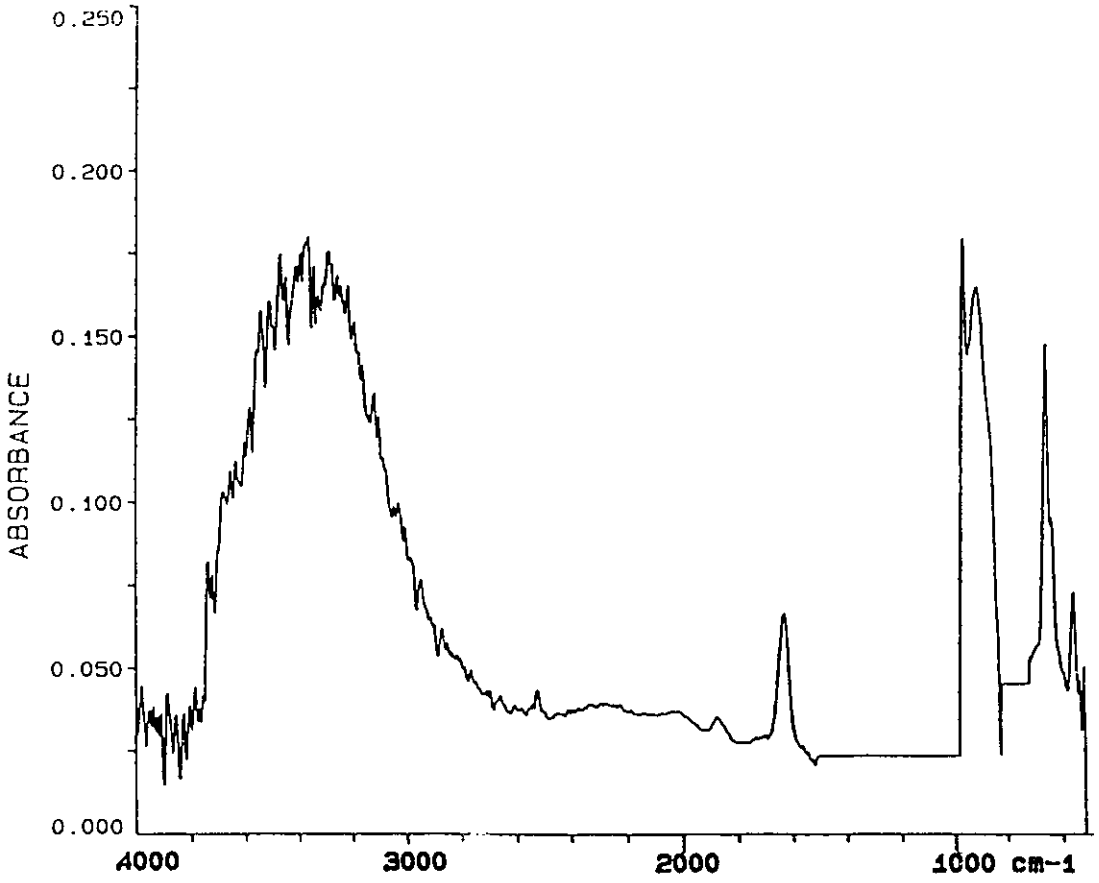

Figure 4.7

Na(450 °C) with the coaddition of SO_2(200 umole g^{-1}) and H_2O(200 umole g^{-1}).

reduction in the bands at 960, 635 and 560 cm^{-1} due to HSO_3^-, whereas the band at 660 cm^{-1} ($S_2O_5^=$) did not change appreciably.

The existence of $S_2O_5^=$ on Na(450°C) or Na(150°C), doped only with SO_2, suggests that it may also be formed via reaction with NaOH (i.e. OH^-) on the surface via the known solution reaction:

$$2\ NaOH + 2\ SO_2 \rightarrow 2\ NaHSO_3 \rightleftharpoons NaS_2O_5 + H_2O \qquad (4.g)$$

The absence of the 635 cm^{-1} band due to HSO_3^- on Na(150°C) or Na(450°C) would presumably be due to the fact that the equilibrium in Reaction (4.g) shifts to the right in the relatively anhydrous environment.

4.4.1.3 ADDITION OF H_2S

Saussey [69] observed a weak band at 2590 cm^{-1} and bands due to water (broad 3100 and 1630 cm^{-1}) upon addition of H_2S to sodium doped silica. The band at 2590 cm^{-1} was assigned to v(SH) of a dissociatively adsorbed H_2S on sodium. Water formation was suggested to occur via reaction with basic sites:

$$O^{-2} + H_2S \rightarrow S^{-2} + H_2O \qquad (4.h)$$

Our experiments with H_2S addition to Na(450°C) or Na(150°C) gave rise to spectral changes which were consistent with those reported by Saussey. However, no spectral changes were observed upon addition of H_2S to NaO(450°C). Since NaO(450°C) would contain more O^{-2} sites (i.e. Na_2O) than Na(450°C) or Na(150°C), a mechanism for water formation other than Reaction 4.h is likely.

In Raman experiments, H_2S adsorbed on NaOH produced a strong band at 2540 cm^{-1} due to an S-H vibrational mode (solid NaSH has a strong Raman band at 2540 cm^{-1}), whereas no bands were observed upon adsorption of H_2S on Na_2O. These results indicate that H_2S dissociated on Na(450°C) or on solid NaOH resulting in formation of NaSH via reaction with OH^-:

$$NaOH + H_2S \rightarrow NaSH + H_2O \qquad (4.i)$$

Additional H_2O could form by:

$$2\ NaOH + H_2S \rightarrow Na_2S + 2\ H_2O \qquad (4.j)$$

However, a Raman investigation of the reaction of H_2S with solid $Na_2S \cdot 9H_2O$ degassed at 110°C for 40 hours, resulted in the rapid disappearance of a band at 185 cm^{-1} (Na_2S) and the formation of a band at 2540 cm^{-1} (Figure 4.8(b)). Fiujii and Takeda [75] found that adsorption of H_2S on a packed column of solid NaOH produced mainly NaSH with less than 5% sodium sulfide or polysulfides. Although Reaction 4.j may occur, further reaction of the Na_2S via the reaction:

$$Na_2S + H_2S \rightarrow 2\ NaSH \qquad (4.k)$$

is probable.

The absence of water during reaction of H_2S with NaO/(450°C) or solid Na_2O suggests that a reaction with basic oxide sites (i.e Reaction 4.h) does not occur. Furthermore, if Na_2S or $S^=$ were produced via reaction 4.h it should react with H_2S to give NaSH (infrared band at 2590 cm^{-1}) and this did not occur.

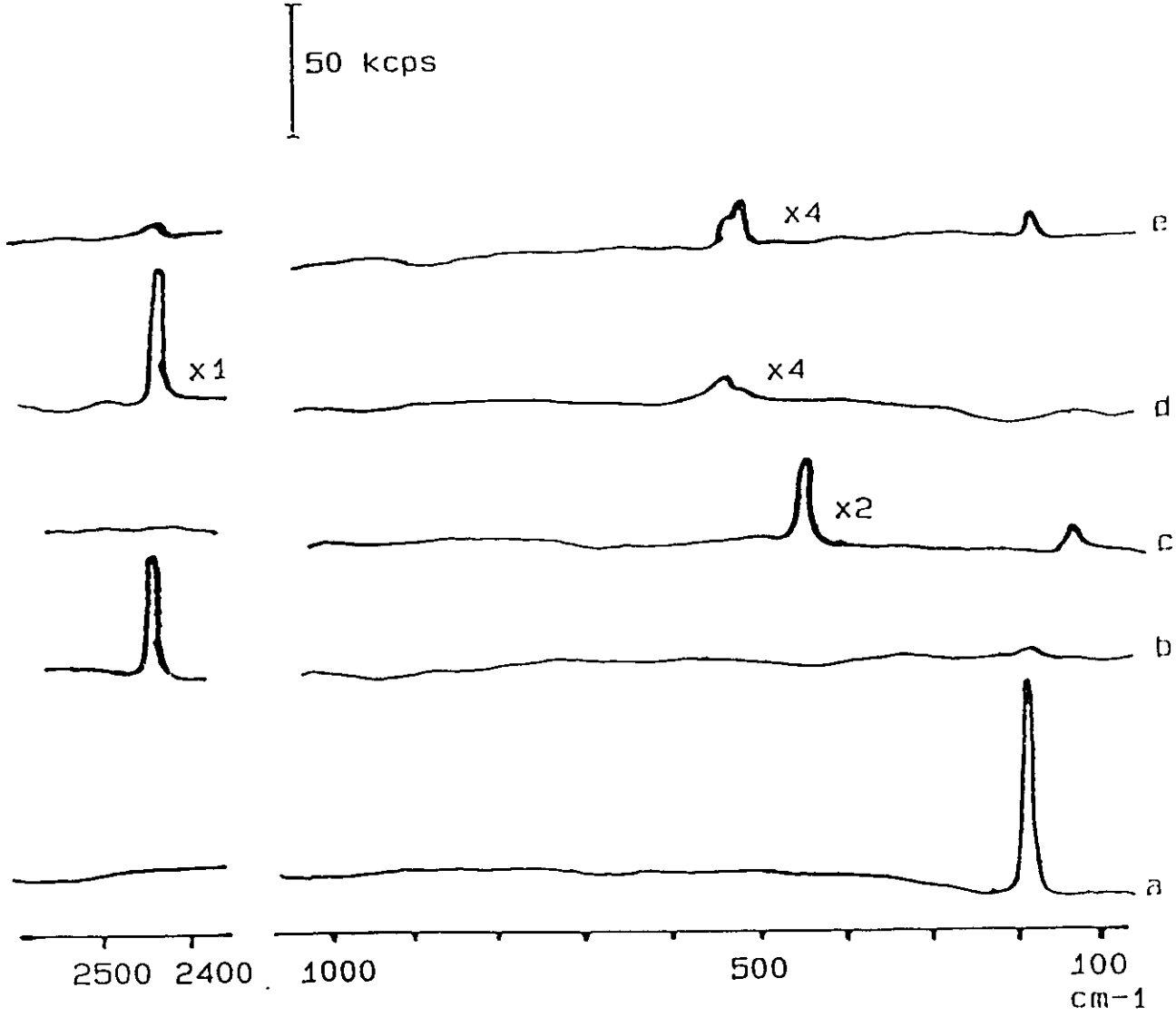

Figure 4.8

a) Na_2S + 9 H_2O evacuated 40 hours at 110 °C.
b) Add 30 umole g^{-1} H_2S to a), followed by evacuation for ten minutes.
c) Add 30 umole g^{-1} SO_2 to b).
d) NaSH evacuated 2 hours at 25 °C.
e) Add 30 umole g^{-1} SO_2 to d).

4.4.1.4 ADDITION OF SO_2, THEN H_2S

H_2S addition to Na(450°C) predoped with H_2O and SO_2 (with or without evacuation of SO_2), gave rise to a band at 680 cm^{-1} accompanied by the disappearance of the HSO_3^- (635 cm^{-1}) and $S_2O_5^=$ (660 cm^{-1}) bands (Figure 4.5(d)). Furthermore, the 1620 cm^{-1} band increased in intensity and the amount of H_2O produced for this reaction was much greater than that observed after the addition of only H_2S to Na(450°C). The 680 cm^{-1} band shifted to lower frequency with H_2S addition to Na(450°C) predoped with ($H_2{}^{18}O$ + SO_2), (H_2O + $S^{18}O_2$), but not with (D_2O + SO_2) or with D_2S addition. The intensity of the 680 cm^{-1} band diminished upon heating above 200°C and disappeared near 300°C.

In a separate experiment, 3% Na/SiO_2 prepared by wet impregnation with $Na_2S_2O_3$, also exhibited a band at 680 cm^{-1} (Figure 4.9). This band diminished above 200°C and disappeared at 300°C. We, therefore, conclude that the band at 680 cm^{-1} is due to $S_2O_3^=$ and that it is formed via the reaction of gaseous H_2S with either HSO_3^- or $S_2O_5^=$.

For NaO(450°C) predoped with H_2O + SO_2, addition of H_2S gave rise to strong Raman bands at 152 cm^{-1}, 220 cm^{-1} and 480 cm^{-1} due to S_8 when the laser power was increased from 50 mW to 200 mW. A previous Raman study [76] has reported that solid sodium thiosulfate decomposed to give sulfur with an Argon ion laser line operating at an output of 700 mW, whereas no decomposition was observed with a 90 mW He-Ne source. In our work, no Raman bands due to S_8, were observed on NaO(450°C) and Na(450°C) during

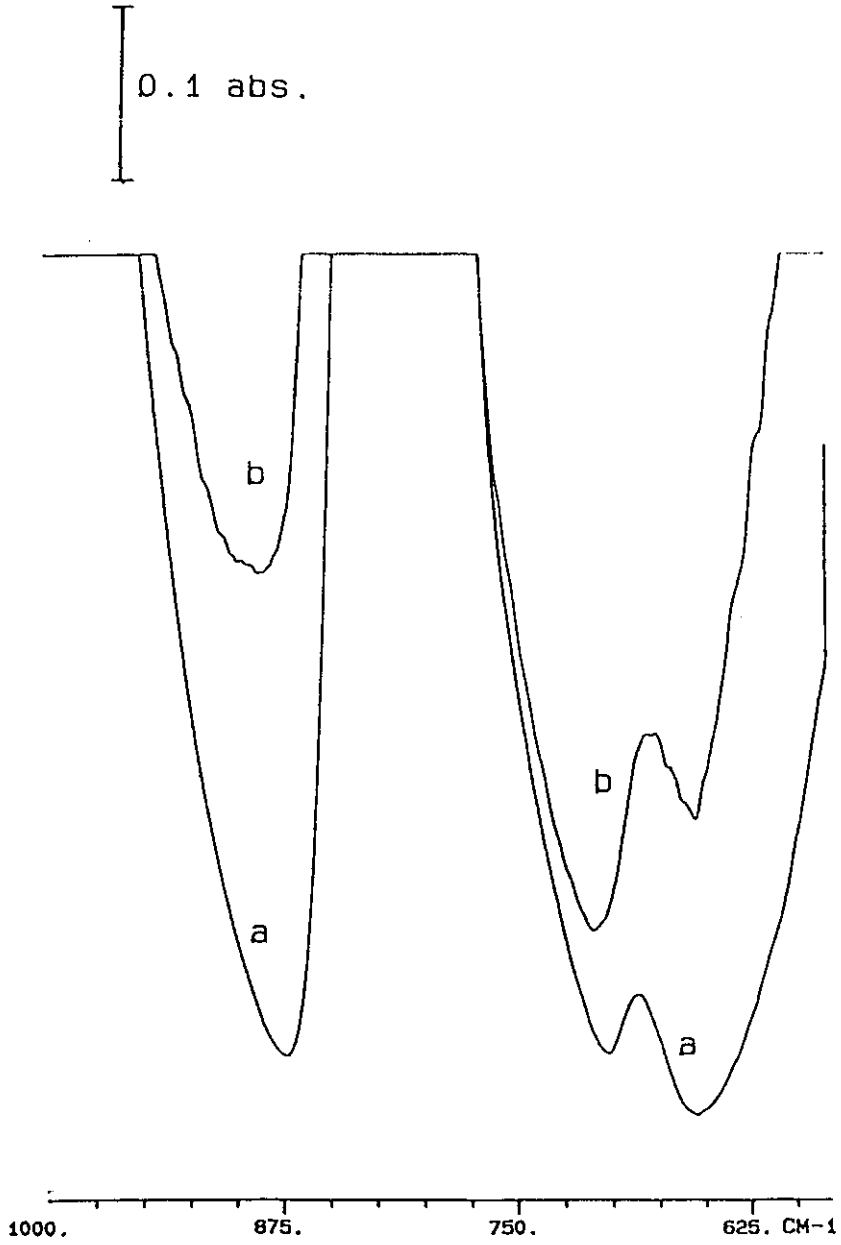

Figure 4.9

a) Spectra of Na(450 °C) predoped with SO_2(300 umole g^{-1}) followed by addition of H_2S (300 umole g^{-1})
b) 3% $S_2O_3^{=}/SiO_2$ degassed at 100 °C for one hour.

the sequence (H_2S + SO_2, evacuation then H_2O) or (H_2S + H_2O, evacuation then SO_2). However, after either of the above sequences, on further evacuation followed by addition of H_2S, S_8 bands were observed. Therefore, S_8 formation only occurred from the reaction of H_2S with either HSO_3^- or $S_2O_5^=$. The following mechanism has been proposed for the reaction between H_2S and SO_2 in water [11].

$$\begin{aligned} 2\ HSO_3^- &\rightarrow S_2O_5^= + H_2O \\ H_2S + S_2O_5^= &\rightarrow S(OH)_2 + S_2O_3^= \\ S(OH)_2 + H_2S &\rightarrow \frac{2}{n} S_n + 2\ H_2O \end{aligned} \qquad (4.l)$$

A similar reaction sequence could occur on the sodium doped silica catalysts. However to the best of the author's knowledge there is no direct evidence for the formation of the sulfoxylic acid, $S(OH)_2$. The above mechanism would account for the large amount of water formed. Formation of $S_2O_3^=$ may also originate from the direct reaction of adsorbed HSO_3^- with gaseous H_2S. In neutral solutions, almost 100% thiosulfate is formed initially via the reaction:

$$2\ HS^- + 4\ HSO_3^- \rightarrow 3\ S_2O_3^= + 3\ H_2O \qquad (4.m)$$

Further reduction of $S_2O_3^=$ to sulfur with H_2S has been reported to occur slowly [11].

The above cases involved the reaction of H_2S with HSO_3^- or $S_2O_5^=$. For NaO(450°C), addition of SO_2 results in $SO_3^=$ formation and does not give rise to either HSO_3^- or $S_2O_5^=$. In infrared

studies, the addition of H_2S to this surface produced a band at 640 cm^{-1} (630 cm^{-1} with $S^{18}O_2$ pretreatment) along with a decrease in the broad 925 cm^{-1} and 620 cm^{-1} bands (Figure 4.5(c)). With evacuation, and addition of H_2O, the band at 640 cm^{-1} was eliminated and a band at 680 cm^{-1} formed. Evidently, the 640 cm^{-1} band resulted from the reaction of SO_3^- with gaseous H_2S and is converted to $S_2O_3^=$ with H_2O. From comparison with the spectra of known sodium salts, we cannot offer a definite assignment for this band.

4.4.1.5 ADDITION OF H_2S AND O_2

The reaction of H_2S and O_2 over Na/SiO_2 has been reported by Saad [14] and the infrared spectra observed are shown in Figure 4.10. No spectral changes were observed when H_2S and O_2 were added at room temperature. Upon heating, two bands at 680 and 635 cm^{-1} were observed along with formation of water. Based on our findings, the reaction can be rationalized by the initial production of SO_2 via the reaction:

$$H_2S + (3/2)O_2 \rightarrow SO_2 + H_2O \qquad (4.n)$$

Further reaction would proceed as before, with adsorbed HSO_3^- or $S_2O_5^=$ reacting with H_2S to form $S_2O_3^=$ (680 cm^{-1} band). Since H_2S is needed to form both SO_2 and to react with the adsorbed HSO_3^- or $S_2O_5^=$, SO_2 would be in excess and, in a highly hydrated environment, would exist primarily as hydrogen sulfite (HSO_3^-, 635 cm^{-1}).

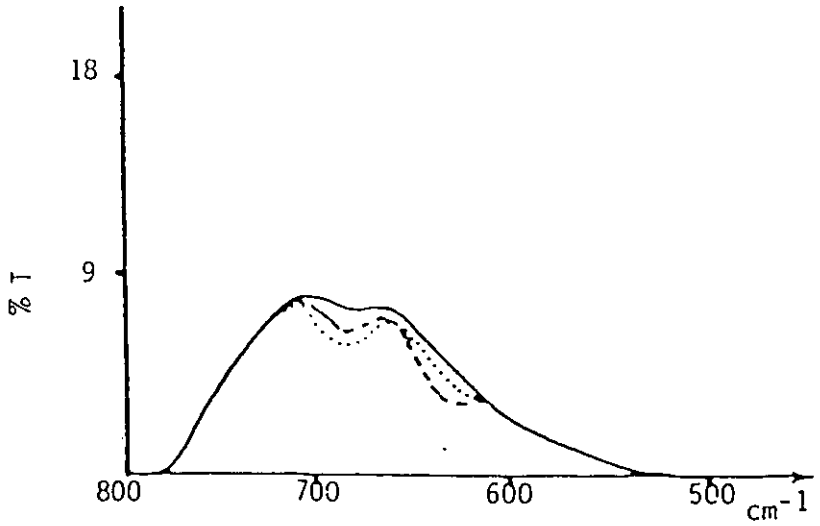

Figure 4.10

Spectra of Na(450 °C) after addition of H_2S (500 umole g^{-1}) and O_2 in excess
Heated at a) 50 °C ——
b) 100 °C ----
c) 200 °C ·····

4.5 SODIUM ON ALUMINA

4.5.1 INTRODUCTION

The initial rates of sulfur formation via the reaction of H_2S and SO_2 over several sodium doped or undoped aluminas and silicas have been measured by George [77]. George observed no change in catalytic activity upon doping the oxides with acids (i.e. HCl, H_2SO_4) but significant increases were observed with bases (i.e. NaOH, KOH). Impregnation of alumina with NaOH (3% by weight) denoted Na/Al, resulted in a small increase (approximately 20%) in initial rate, whereas with silica a thousand fold increase was observed. George concluded that basic sites are responsible for Claus activity. NaOH doping would increase slightly the number of basic sites which exist naturally on alumina, whereas similar basic sites on pure silica do not exist. George observed that a maximum in Claus activity occurred at approximately 1-3% loading of the Na/SiO_2 catalysts. A maximum activity was also observed recently on Na/Al for 3% loading by Lavalley et. al. [65] for direct oxidation of H_2S to sulfur with O_2. At higher Na loading, a rapid decrease in activity occurred which was associated with the formation of a nonporous sodium aluminate. Its formation resulted in a

decreased surface area and, hence, reduced activity of the catalyst.

The background spectra of pure alumina and of 3% Na/Al(400°C) are shown in Figure 4.11. Na impregnation of alumina resulted in the removal of OH alumina bands at 3790 and 3730 cm^{-1} and a shift in the 3690 band to 3740 cm^{-1}. These spectroscopic changes have been attributed to ion exchange between Na ions and acid OH groups on alumina [78,79]. The broad bands at 1560 and 1380 cm^{-1} have been attributed to carbonates on the surface [65]. Na impregnation has also been shown by Fledorow and Dalla Lana [78] to poison cus Al^{+3} Lewis acid sites.

4.5.1.1 ADSORPTION OF H_2S

Upon H_2S addition to Na/Al(600°C) bands at 3675, 3300(broad), 2585 and 2300 cm^{-1}(broad) appeared (Figure 4.12(b)). These results are similar to those reported by Lavalley et. al. obtained following addition of H_2S to Na/Al(450°C) [65]. Lavalley et. al. reported that dissociative adsorption of H_2S resulted in AlOH (3675 cm^{-1}) and NaSH (2585 cm^{-1}). The 2585 cm^{-1} band intensity increased with Na loading and was assigned to Na-SH species rather than Al-SH. The 2585 cm^{-1} band was located near the 2590 cm^{-1} observed in this work for H_2S adsorption on Na/SiO_2.

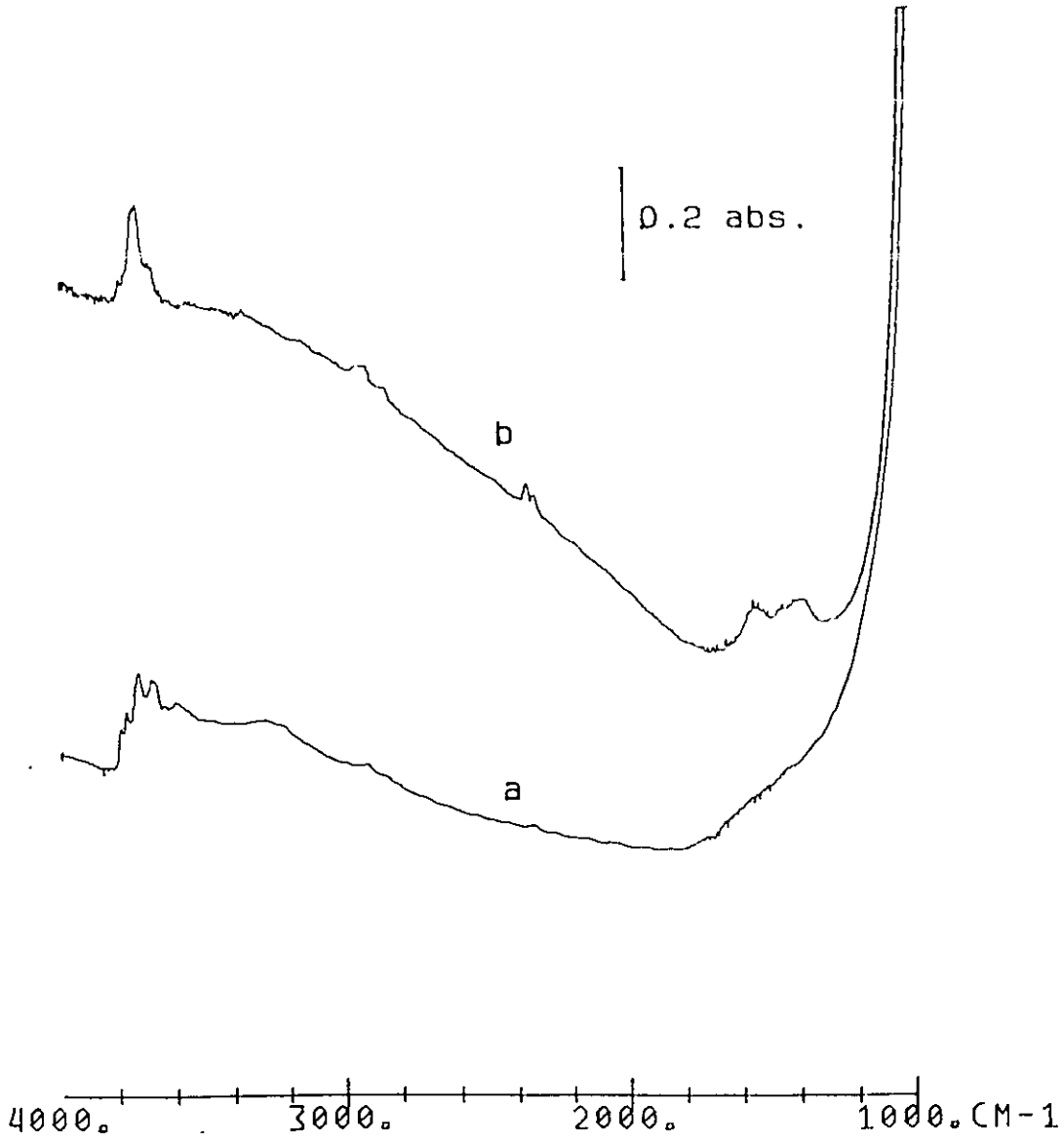

Figure 4.11

a) Al(400 °C)
b) 3% Na/Al(400 °C)
Both samples were calcined in air at 600 °C, followed by heating in O_2 1 hour, then evacuated for 0.5 hours at 400 °C.

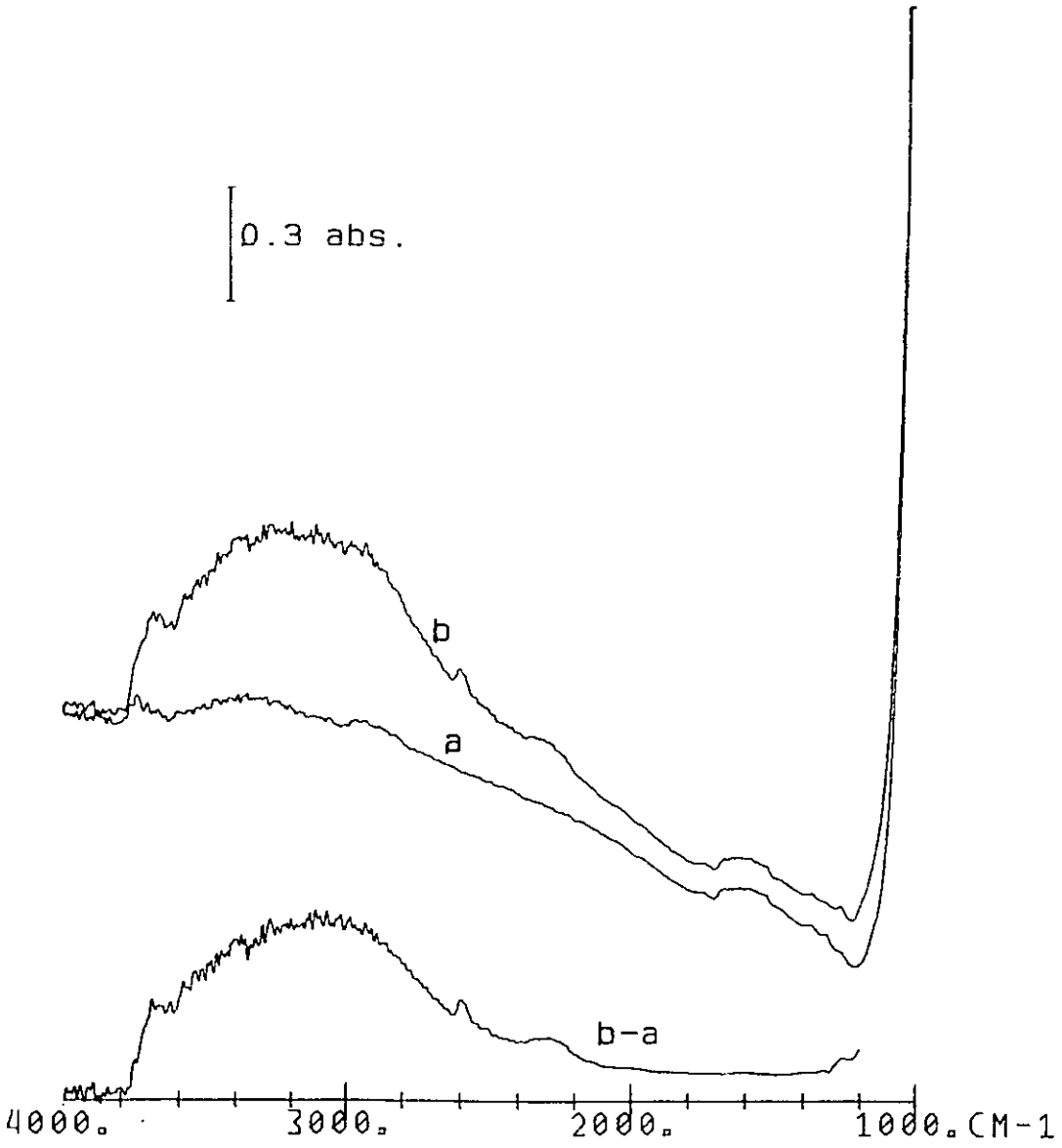

Figure 4.12

a) 3% Na/Al(600 °C).
b) Add 600 umole g^{-1} H_2S.

Additional reversibly adsorbed species were assigned by Lavalley et. al. to hydrogen bonded species:

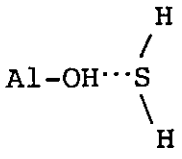

(3300 cm^{-1}) (4.o)

and to Al-O···HSH (2300 cm^{-1}).

They observed that the reversible species was converted to sulfur in O_2, whereas NaSH was oxidized to sulfate, a poison for the Claus process. The dissociative adsorption of H_2S on Na/Al(600°C) would yield AlOH (3675 cm^{-1}) which could further hydrogen bond to produce the 3300 cm^{-1} band. This would account for the similarity in spectra observed for both Lavalley's Na/Al(450°C) and our Na/Al(600°C).

4.5.1.2 ADDITION OF SO_2

Exposure of Na/Al(400°C) to SO_2(40 umole g^{-1}) gave rise to a strong infrared band at 1060 cm^{-1} (Figure 4.13). In addition, a weak band at 2050 cm^{-1} and 3200(broad) were observed along with the disappearance of the OH band at 3740 cm^{-1}. Further SO_2 addition resulted in the formation of bands at 1338/1150 cm^{-1} due to weakly held adsorbed SO_2. The 1338/1150 cm^{-1} bands disappeared upon evacuation, whereas all other bands remained unchanged.

Sodium doped alumina is known to have enhanced Lewis basicity. From a comparison of SO_2 adsorption on pure alumina to

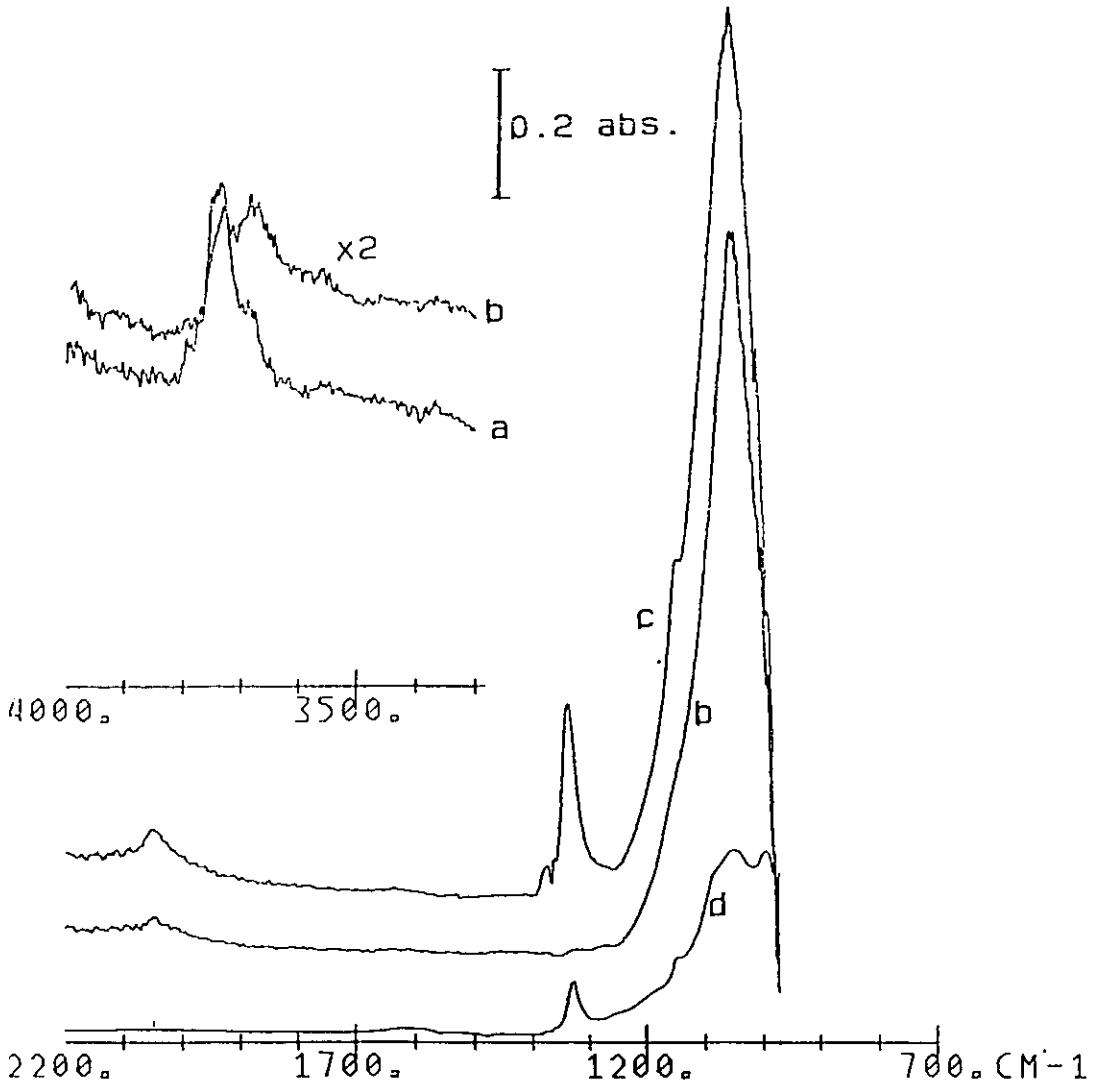

Figure 4.13

a) 3% Na/Al(400 °C).
b) Addition of 45 umole g^{-1} SO_2.
c) Addition of 600 umole g^{-1} SO_2.
d) Addition of 300 umole g^{-1} SO_2 to Al(400 °C).
Spectra shown between 2200 and 700 cm^{-1} have had the 3% Na/Al(400 °C) background subtracted.

that on Na/Al (Figure 4.13(c,d)), we found that the 1060 cm^{-1} band was much more intense on Na/Al(450°C). This result was further verified with a Raman experiment. Addition of SO_2 in this case gave rise to a Raman band at 1150 cm^{-1}, as was observed on pure alumina, but there was also a new weak band at 1060 cm^{-1}. Our isotopic studies in Chapter 3 with pure alumina have led us to conclude that the 1050 cm^{-1} band (SO_3^-) involve basic O^{-2} sites. Thus the increase in number of basic sites with Na doping would manifest itself in an increase in intensity of this band.

The 1338 cm^{-1} infrared band was shifted 8 cm^{-1} to higher frequency than was observed on pure alumina. The 8 cm^{-1} shift indicates that weaker cus Al^{+3} Lewis sites on Na doped alumina are present.

The 2050 cm^{-1} infrared band is too low in frequency for a ν(S-H) stretching mode (NaSH is at 2590, Al-SH at 2570 and H-SO_3^- at 2525 cm^{-1}). This band is not hindered in its formation by doping of the Na/Al with water and does not shift in frequency on a deuterated Na/Al(450°C) sample. Therefore, we conclude that the 2050 cm^{-1} band is the overtone of the 1060 cm^{-1} band. This band is not seen on pure alumina which is reflective of the less intense bands in the 950 -> 1100 cm^{-1} region.

The disappearance of the OH band at 3740 cm^{-1} and formation of a weak broad band at 3200 cm^{-1} suggests some reactivity with hydroxyl groups. Comparison with alumina would suggest this was due to formation of a hydrogen bonded $HOSO_2^-$. To investigate this possibility, we have studied the adsorption of SO_2 on

Na/Al(150°C). The reactivity of adsorbed SO_2 species with water (a normal Claus byproduct) was also examined.

The Na/Al(150°C) contained as an impurity, HCO_3^- with bands at 1568 and 1358 cm^{-1}. Addition of SO_2 removed these HCO_3^- bands (negative peak at 1358 cm^{-1} in Figure 4.14(b)) and formed a 1060 cm^{-1} band with shoulders at 1100 and at 1025 cm^{-1} (Figure 4.14(a)). The formation of 3200 and 2050 cm^{-1} bands and the disappearance of OH bands were also observed. The 3200 and 1100 cm^{-1} bands were more intense on Na/Al (150°C) than on Na/Al (450°C). The formation of 1340/1150 cm^{-1} bands was almost completely hindered on Na/Al(150°C). The bands at 1100 and 1025 cm^{-1} were reduced upon evacuation (Figure 4.14(b)).

Addition of water resulted in the formation of a 1100 cm^{-1} band (1040 cm^{-1} with D_2O) and a 1025 cm^{-1} shoulder with an additional weak broad band centred at 1220 cm^{-1} (Figure 4.14(c)). The spectrum is very similar to that of commercial $NaHSO_3$ solution (Figure 1.5). Therefore, we assign the 1100, 1025 and broad 1200 bands to a $H\text{-}SO_3^-$ species formed via reaction with OH groups on alumina or by reaction of H_2O with SO_3^-(1060 cm^{-1}). This $H\text{-}SO_3^-$ species is different from the $HOSO_2^-$ postulated to form on pure alumina.

4.5.1.3 ADDITION OF SO_2, THEN H_2S

In contrast to what was observed using Al_2O_3, the 1060 cm^{-1} SO_3^- band on Na/Al(450°C) showed virtually no reactivity with gaseous H_2S (Figure 4.15). Addition of excess H_2S for two hours

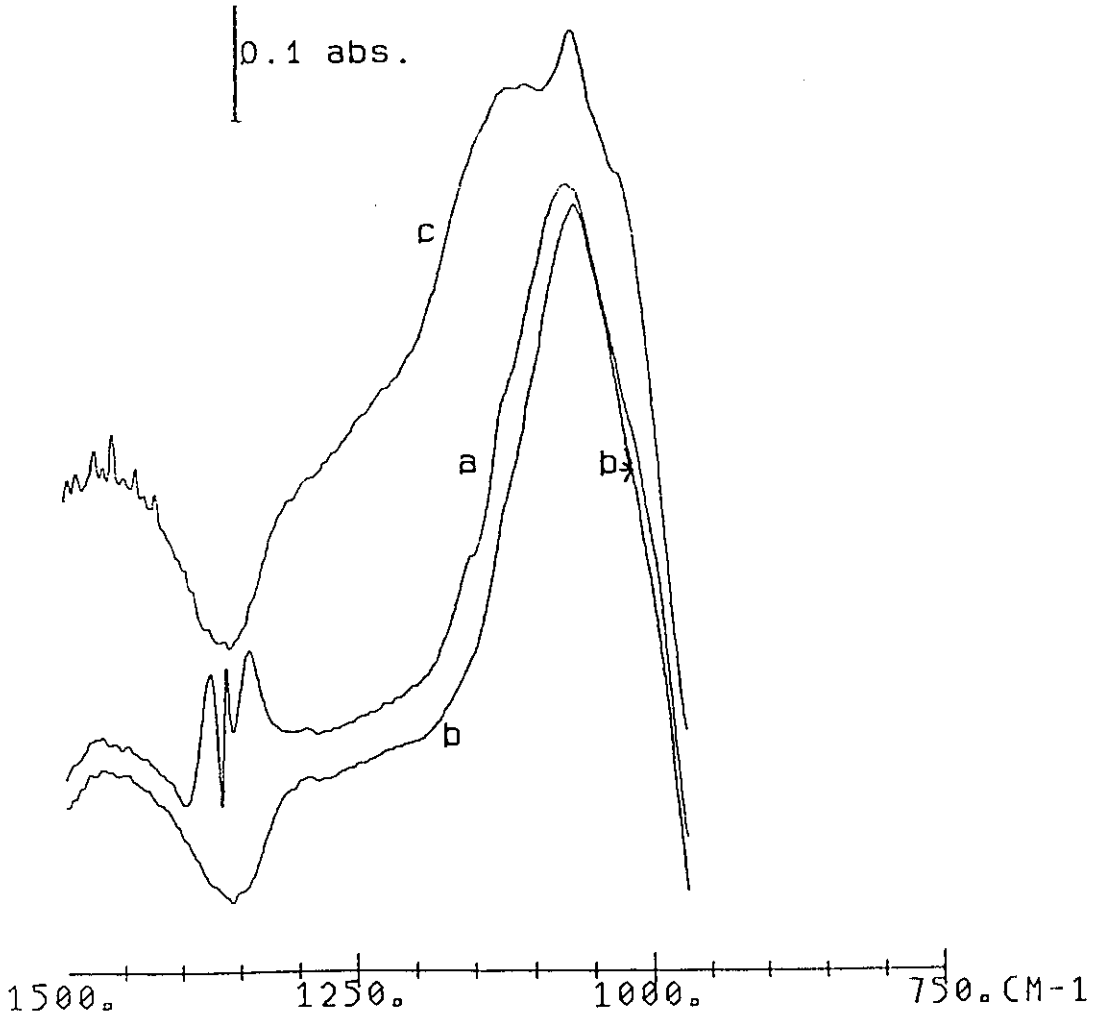

Figure 4.14

Na/Al(150 °C) with the;
a) Addition of 1.5 mmole g^{-1} SO_2, followed by;
b) Evacuation five minutes, and;
c) Addition of 600 umole g^{-1} H_2O.

resulted only in a slight decrease in this band. For the same reaction sequence on Al(150°C), there was also only a slight decrease in the intensity of the 1100, 1060, and 1025 cm^{-1} bands.

As with Al_2O_3, Raman experiments showed that the formation of sulfur occurred only when gaseous H_2S was added to adsorbed SO_2. The sulfur bands were more intense on Na/Al than on pure alumina.

4.6 CONCLUSION

The transparency of silica in the 1000 to 600 cm^{-1} range has allowed us to observe bands due to a number of adsorbed species. H_2S dissociatively adsorbs on the OH^- sites on Na/SiO_2 forming SH^- + H_2O. Upon adsorption of SO_2 on Na/SiO_2, sulfite ($SO_3^=$) species are formed on O^{-2} sites, whereas on OH^- sites, a hydrogen sulfite (HSO_3^-) species formed which is in equilibrium with a disulfite ($S_2O_5^=$). As observed for Al_2O_3, the primary reaction of H_2S and SO_2 on Na/SiO_2 is a reaction between gaseous H_2S with adsorbed SO_2. H_2S reacts with either HSO_3^- or $S_2O_5^=$ to produce water and thiosulfate ($S_2O_3^=$). The thiosulfate upon heating is converted to sulfur.

In our studies with SO_2 and H_2S adsorption on Na/SiO_2, Na/Al and pure alumina, trends exist which may lead to a better understanding of the role of sodium in the Claus reaction. Of primary importance is the effect of sodium on the nature of the adsorbed SO_2 since our results for all three catalysts have shown

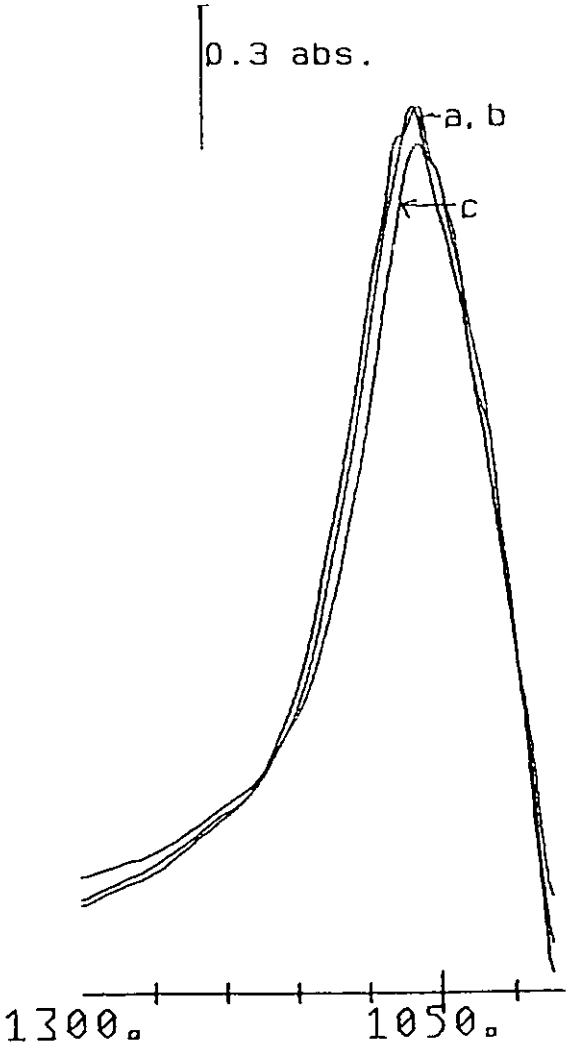

Figure 4.15

a) Na/Al(450 °C) + 600 umole g^{-1} SO_2, evacuated 0.5 hours followd by;
b) addition of H_2S (3000 umole g^{-1}) and,
c) Rescan two hours later.

that sulfur and H_2O are formed mainly due to reaction of gaseous H_2S with adsorbed SO_2.

Both Na/Al and pure alumina exhibit the same type of adsorbed species on basic Lewis sites. The enhanced basicity of sodium doped alumina gave rise to a more intense 1060 cm^{-1} band than on pure alumina which in turn indicated that a larger number of $SO_3^=$ formed (assuming extinction coefficients are equal). This may not in itself account for the increased activity since our results have shown that $SO_3^=$ on Na/Al was less reactive at room temperature with H_2S than its counterpart on alumina.

On Na/SiO_2, we have observed that the addition of H_2O converts $SO_3^=$ into a more reactive $H\text{-}SO_3^-$ or $S_2O_5^=$. This is similar for Na/Al where the 1060 cm^{-1} band ($SO_3^=$) upon H_2O addition, forms $H\text{-}SO_3^-$. This is in contrast to pure Al_2O_3 where no reaction between H_2O and the species responsible for the 1050 cm^{-1} band is observed. Therefore, enhanced activity with sodium impregnation of alumina may be due to (a) an increase in the total amount of $SO_3^=$(1060 cm^{-1}) adsorbed and (b) the fact that sodium facilitates the conversion of the less reactive $SO_3^=$ to a more reactive $H\text{-}SO_3^-$ in the presence of H_2O. The $H\text{-}SO_3^-$ was observed on both Na/SiO_2 and Na/Al, but not on alumina ($HOSO_2^-$ was observed instead on alumina).

Our results with Na/SiO_2 catalysts have shown that the Claus reaction is very complex with $SO_3^=$, $H\text{-}SO_3^-$, $S_2O_5^=$ and $S_2O_3^=$ as possible intermediates. It is possible that $S_2O_5^=$ and $S_2O_3^=$ occur as reactive intermediates on alumina but spectroscopic proof of this is unavailable because of the opacity of alumina below 1000

cm^{-1}. Perhaps techniques such as ESCA or FT-Raman may prove helpful in this respect. Recently, FT-Raman [80-83], employing a Nd/:YAG laser operating at 1.06 um, has been shown to produce fluorescence-free spectra for a wide variety of compounds. Fluorescence was the major drawback in our ability to observe SO_x Raman bands.

Chapter 5

ADSORPTION ON TITANIA

5.1 INTRODUCTION

Titania based catalysts are, at present, the best catalysts [19] for reduction of NO_x with NH_3 from flue gases and have been very promising in other catalytic areas, such as, hydrodesulfurization, coal liquidfaction, Claus tail gas treatment and CO oxidation.

Titania has three crystalline forms; anatase, brookite and rutile, of which anatase and rutile are the common forms. Anatase is stable below 700°C at which point it is converted to rutile accompanied by a significant decrease in surface area.

Both anatase and rutile have a 6-3 configuration where the Ti^{+4} ion is octahedrally coordinated, by six O^{-2} ions, with slight distortion and the O^{-2} ions are trigonally coordinated to three Ti^{+4} ions. Anatase and rutile are easily reduced relative to alumina. A change in colour during reduction from white to blue-grey is associated with loss of lattice oxygen to form reduced Ti^{+3} sites.

There have been several studies concerning the surface properties of titania [19,84,85], however, comparisons between results from different laboratories are difficult at best. The characteristics and catalytic activity of titania varied with different preparations. Titania is usually prepared by oxidation or hydrolysis of titanium tetrachloride or by hydrolysis of $TiOSO_4$ and in both methods the presence of the Cl^- or SO_4^- as an impurity significantly affects the surface chemistry. For example, a very strong Bronsted acidity for the surface hydroxyl groups is generated by the presence of sulfate impurities [84]. Even when care is taken to produce high-purity titanias, different results have frequently been observed. Variation in temperatures involved in preparation of TiO_2 affects the particle size and, hence, the concentration of defect sites and the relative abundance of exposed crystal planes.

The titania used in our experiments was commercially available Degussa P25, henceforth denoted DT, prepared by flame hydrolysis of $TiCl_4$. It consisted of 90% anatase, 10% rutile with 0.2% SiO_2, 0.3% Al_2O_3 and 0.3% Cl^- as the main impurities.

Infrared studies have been used to establish the acidity and basic behavior of the surfaces of several types of titania [85,87]. We will limit our discussion to DT employed in this work.

The infrared spectrum of DT degassed at 450°C is shown in Figure 5.1. The lower limit of transparency is below that observed for alumina, being 900 cm^{-1}. The OH region of DT degassed at 150°C and 450°C is also shown in Figure 5.1. The

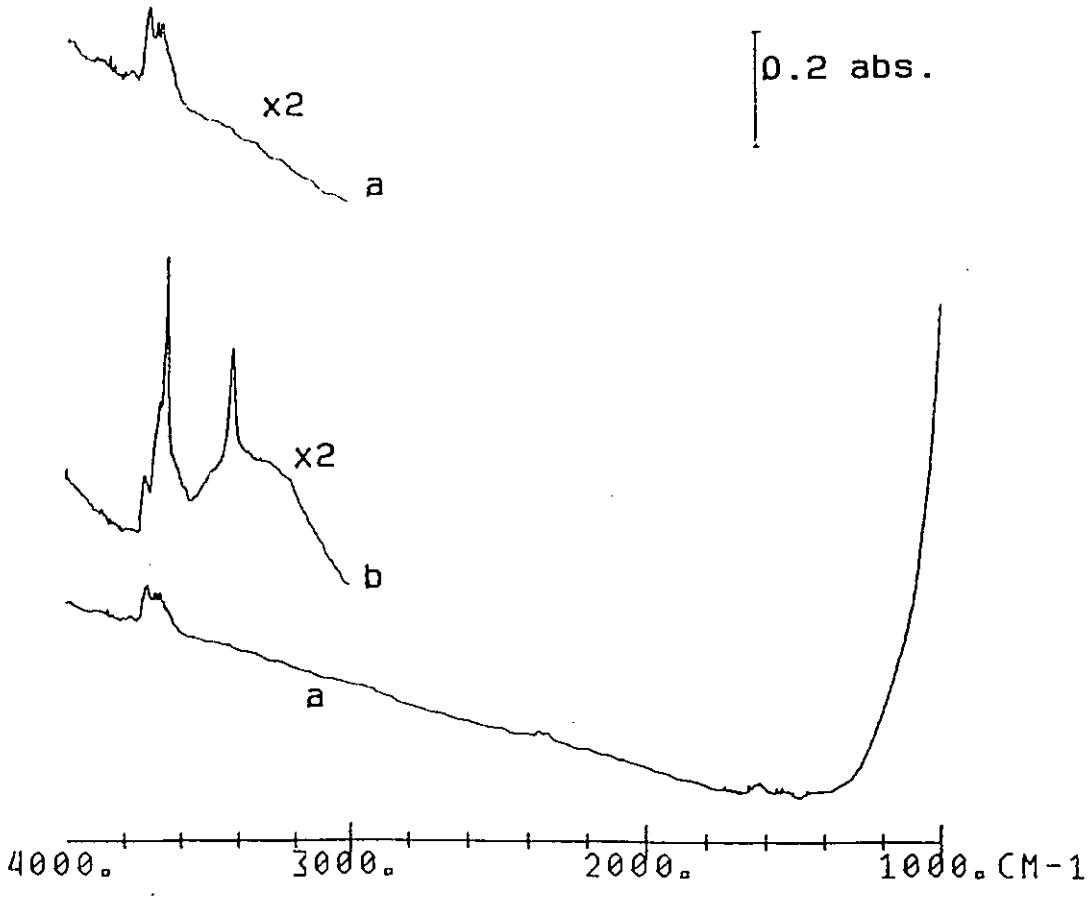

Figure 5.1

a) DT(450 °C).
b) DT(150 °C).

sharp band at 3420 cm^{-1} observed on DT(150°C), was absent on DT(450°C). The 3420 cm^{-1} band has been assigned to OH groups associated with a chloride impurity [87]. Jackson and Parfitt [87] have observed this band on rutile prepared from $TiCl_4$ by calcination at 700°C. This was attributed to migration of chloride ions from the bulk to the surface. The 3420 cm^{-1} band is not observed on titania prepared from $TiOSO_4$. Chloride impurities on DT are removed by degassing at 450°C, resulting in the elimination of the 3420 cm^{-1} band.

On both DT(450°C) and DT(150°C), OH bands at 3730, 3662 and 3640 cm^{-1} were observed (Figure 5.1). The band at 3730 cm^{-1} does not change in intensity for both samples, whereas the band at 3660 cm^{-1} is slightly reduced and that at 3640 cm^{-1} is substantially reduced on the more highly dehydroxylated titania. The 3730 cm^{-1} band exhibits some Bronsted acidity and has been assigned to SiOH impurities by several authors [85,88,89]. Degassing the DT at (700°C) removed all hydroxyl bands.

Boehm [89,90] suggested that two types of OH groups exist on pure anatase, terminal OH bound to one Ti^{+4} site (I) and bridged OH bound to two Ti^{+4} sites (II).

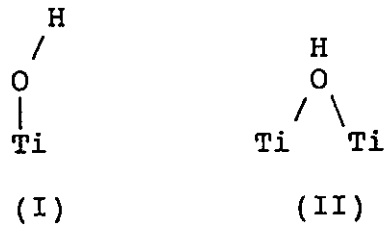

(I) (II) (5.a)

The bridged groups (II) would be acidic in character and the terminal (I) groups would be basic in nature. Boehm found that

half of the OH groups on DT reacted with 0.01 M NaOH and had a pk of 2.9; the remainder had a pk of 12.7 and also exchanged with $H_2PO_4^-$ and F^- anions.

Jackson and Parfitt [87] observed two OH bands on rutile at 3700 cm^{-1} and 3670 cm^{-1} indicative of two types of hydroxyls, with the former showing greater thermal stability. They assigned the 3700 cm^{-1} to bridged OH (II) and the 3670 cm^{-1} to terminal OH (I). The terminal groups would be sufficiently close together to enable them to hydrogen bond and condense upon heating to produce a Ti-O-Ti bridge site. Jackson and Parfitt also postulated that adjacent isolated OH groups would react to form cus surface titanium and oxide ions.

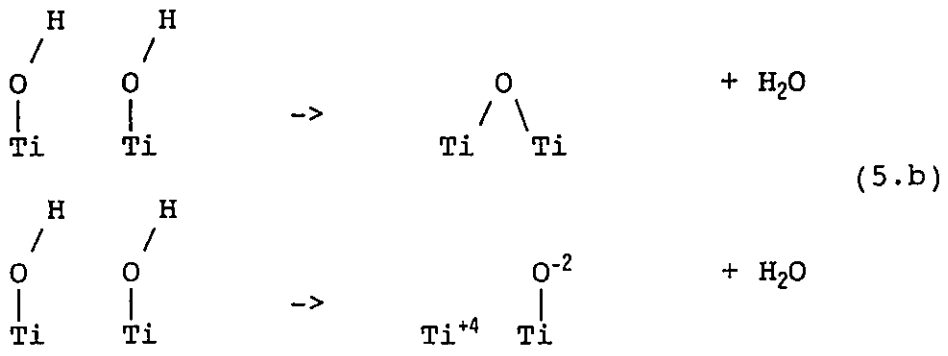

Condensation between bridged OH sites or bridged and terminal OH sites would not be favorable due to the nature of the surface attachment and the large distances between the species. Adsorption and desorption studies of H_2O on both anatase and rutile have indicated that there is little difference between the two forms in hydroxylation or dehydroxylation behavior. Therefore, a similar situation would be expected to exist for DT

(see Figure 5.1) in which the 3667 cm^{-1} would be due to bridged hydroxyls and 3647 cm^{-1} to isolated hydroxyl groups.

It has been reported [92] that approximately 3 $\pm$ 1 OH nm^{-2} are present on DT upon evacuation at 200°C and that outgassing at temperatures greater than 500°C results in total dehydroxylation. Rehydroxylation of DT(500°C) by exposure to the saturated water vapor pressure at temperatures between 25°C and 300°C, then degassed at 100°C, resulted in about half of the OH being reformed [92]. However, the same sample immersed in liquid water gave rise to a fully hydroxylated sample.

The presence of Lewis acid sites on DT has also been demonstrated [85]. Infrared studies involving adsorption of Lewis bases such as NH_3, CO, and $(CH_3)_2S$ have indicated that two types of acidic sites exist on DT. Weak Lewis acidity was assigned to single cus Ti_v^{+4} sites and strong lewis acidity to doubly cus Ti_{iv}^{+4} defect sites.

Titania and titania based catalysts are being used increasingly in heterogeneous catalysis [19,83]. In commercial Claus reactors, alumina is the primary catalyst although titania is sometimes added as a promoter for this reaction [5]. It has been suggested that TiO_2 is, in fact, a more reactive Claus catalyst than alumina [92]. In addition, we have shown that sulfate poisoning is less severe on TiO_2 than on Al_2O_3 [93].

In previous infrared studies, Lavalley et. al. [94] have observed that the dissociative adsorption of H_2S on DT was accompanied by the formation of H_2O. ESR studies [95] have shown that SO_2^- radicals form following SO_2 adsorption on TiO_2. SO_2^-

radicals, exhibiting high thermal stability, remained upon evacuation at temperatures of 150°C. However, the authors of [95] reported that the SO_2^- radicals accounted for a small fraction of the total SO_2 adsorbed.

Although there have been several infrared studies of the simultaneous adsorption of SO_2 and H_2S on alumina there exist, to the best of the author's knowledge, no similar studies with titania. Therefore, in this chapter we have undertaken a study of the Claus reaction on titania. With a similar study to that of alumina, a clearer role of titania as a promoter or as a substitute catalyst for the Claus reaction may be achieved.

5.2 EXPERIMENTAL

Preparation of titania sample disks was the same as that described for alumina. However, for DT(450°C), the sample was not evacuated for one half hour at 450°C in the final step in order to avoid reduction. Instead, the oxygen was left in contact with the sample until the temperature dropped to at least 200°C, before final evacuation.

5.3 RESULTS AND DISCUSSION

In Raman experiments, upon SO_2 addition, a band due to weakly adsorbed SO_2 at 1150 cm^{-1} was observed on DT(450°C) and was easily removed upon evacuation (Figure 5.2(b)). Subsequent H_2S addition gave rise to the formation of S_8 bands at 220 and 480

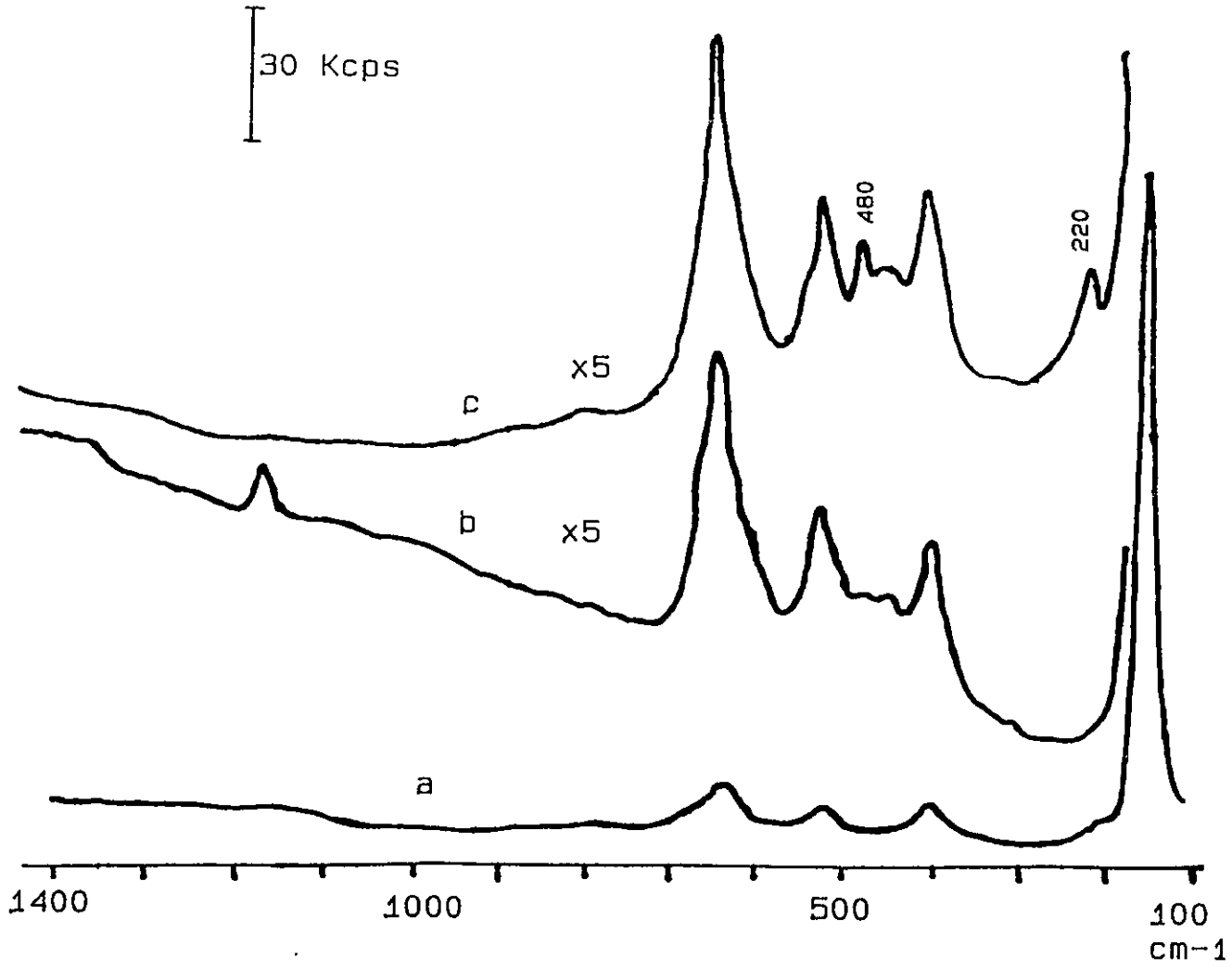

Figure 5.2

Raman spectrum of;
a) DT(450 °C).
b) a) after addition of 200 umole g^{-1} SO_2, followed by;
c) evacuation for five minutes and
addition of H_2S (200 umole g^{-1}).

cm^{-1}. The S_8 band at 151 cm^{-1} was masked by the strong titania Raman band at 150 cm^{-1}. The reverse reaction (i.e. SO_2 with preadsorbed H_2S) did not produce bands due to sulfur. However, further evacuation, followed by readdition of H_2S, did give rise to the S_8 bands. We conclude that, as with Al_2O_3, Na/Al_2O_3 and Na/SiO_2 the formation of sulfur on titania proceeds mainly via the reaction of gaseous H_2S with adsorbed SO_2.

5.3.1 ADDITION OF H_2S

Infrared spectra resulting from the addition of H_2S to DT(450°C) are shown in Figure 5.3. Initial H_2S addition gave rise to infrared bands at 3660 v(O-H), 3300 (broad), 2525 v(S-H) and 1625 cm^{-1}. With an introduction of excess H_2S(3 mmole g^{-1}) the 3300 and 2525 cm^{-1} bands increased. The 2525 cm^{-1} band was removed upon evacuation at room temperature.

These results are in agreement with Lavalley et. al. [94] and Beck et. al. [96]. The 2525 cm^{-1} band was assigned to reversibly adsorbed H_2S. Its appearance or disappearance had virtually no effect on the v(O-H) bands on DT(450°C). Comparative studies involving the addition of $(CH_3)_2S$, CH_3SH and H_2S on titania, indicated that H_2S reversibly adsorbs on acidic Ti^{+4} sites [94]. Both the 1625 cm^{-1} and 3300 cm^{-1} bands are characteristic of water formation on a dehydroxylated titania surface. Water production would result from dissociative adsorption of H_2S via the reaction:

$$O^{-2} + H_2S \rightarrow H_2O + S^{=} \qquad (5.c)$$

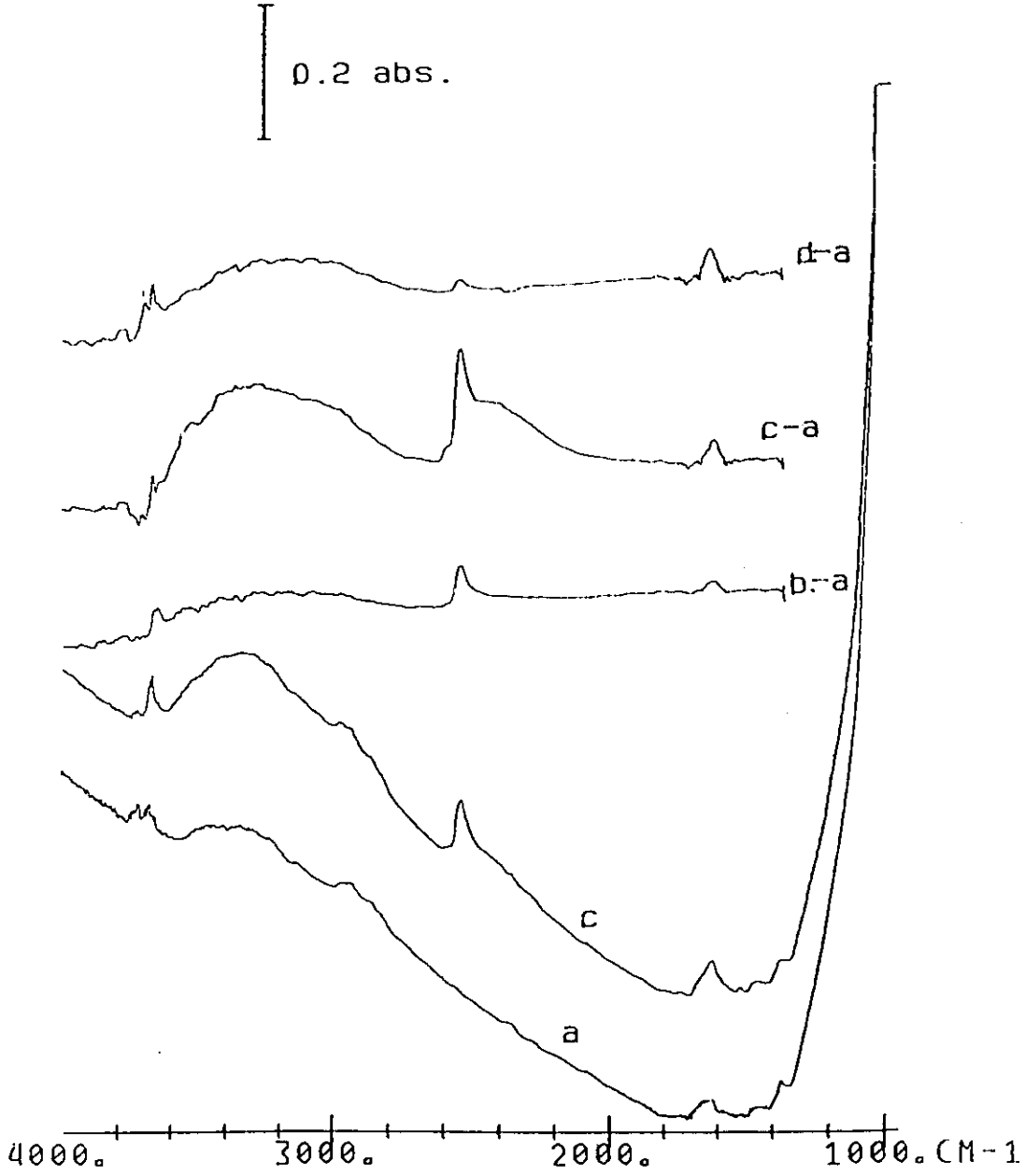

Figure 5.3

a) DT(200 °C).
b) Add 60 umole g^{-1} H_2S
c) Add 3000 umole g^{-1} H_2S.
d) Evacuate five minutes

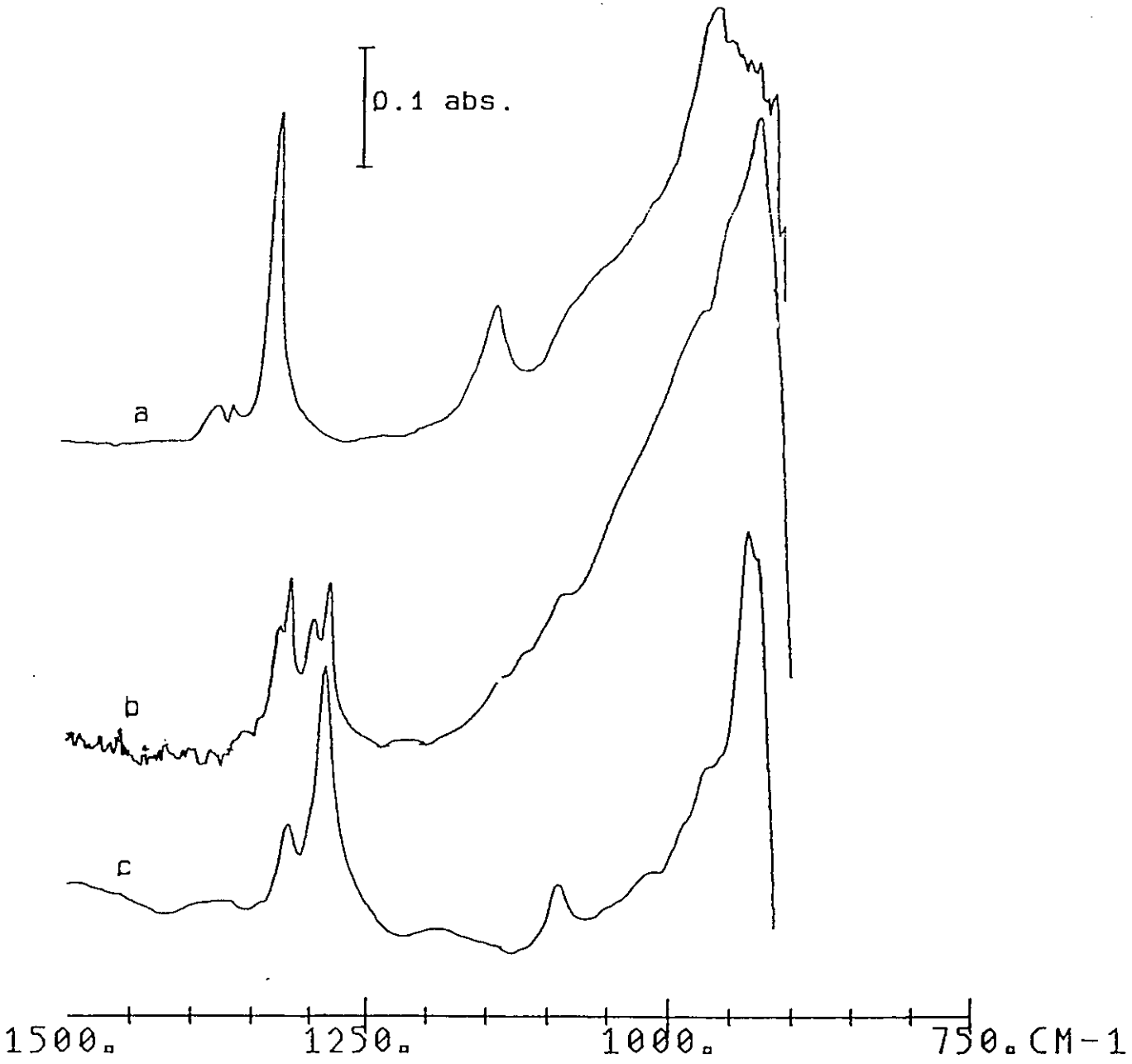

Figure 5.4

Difference spectrum for the addition of;
a) SO_2 to DT(450 °C).
b) $S^{18}O_2$ to DT(450 °C).
c) $S^{18}O_2$ to ^{18}O-exchanged DT(450 °C).

5.3.2 ADDITION OF SO_2

Addition of SO_2 to DT(450°C) first gave rise to a band at 965 cm^{-1} with a broad ill-defined shoulder between 1100 and 1000 cm^{-1}, followed by formation of sharp bands at 1326 and 1140 cm^{-1} (Figure 5.4(a)). The latter two bands were removed upon evacuation at room temperature. The residual v(O-H) bands at 3730, 3672 and 3647 cm^{-1} on the surface of DT(450°C) were completely removed and a weak broad band at 3300 cm^{-1} formed (not shown).

The 965 cm^{-1} band shifts to approximately 935 cm^{-1} with ^{18}O-exchanged DT(450°C) + $S^{18}O_2$ and the 1326/1140 cm^{-1} bands shifted to 1283/1090 cm^{-1}. The 1326/1140 cm^{-1} bands are undoubtedly due to weakly held SO_2 on cus Ti^{+4} Lewis acid sites.

An interesting result was observed when $S^{18}O_2$ was added to Ti(450°C) (Figure 5.4(b)). For the 1326/1140 cm^{-1} band combination, three bands were observed (the band at 1310 cm^{-1} is due to gas phase $S^{18}O_2$) with their relative intensities being 1283/1090 > 1295/1110 > 1326/1140 cm^{-1}. These bands represent weakly held $S^{18}O_2$, $S^{18}OO$ and SO_2, respectively.

On several oxides, sulfite formation involving reactions with basic sites are characterized by bands in the 1100 to 850 cm^{-1} region. On Al_2O_3, a strongly held sulfite with a band at 1050 cm^{-1} has been observed. On MgO[56] and CaO[97], two types of sulfites have been reported; a strongly held sulfite having bands at 1040(MgO) and 1060 cm^{-1} (CaO) and a weakly held sulfite with bands at 975 (MgO) and 960 cm^{-1} (CaO). In contrast, on TiO_2, only

a single band in this region, located at 965 cm^{-1}, is observed. We assign the 965 cm^{-1} band to a weakly held sulfite coordinated to the surface via an oxygen atom.

For the exchange with $S^{18}O_2$ on DT(450°C) to occur, an equilibrium must exist between gaseous SO_2 and adsorbed SO_2 on both basic and acidic sites along with an easy exchange between oxygens in the adsorbed sulfite . Such an equilibrium may be represented by the following sequence:

$$TiO^{-2} + SO_2 = TiOSO_2 = Ti^{+4} + SO_3^{=}$$
$$Ti^{+4} + SO_2 = TiSO_2 \qquad (5.d)$$

This type of exchange was not observed for alumina. Therefore, the sulfite on titania is more labile than that on alumina.

The addition of H_2O to DT pretreated with SO_2 gave rise to a sharp band at 3690 cm^{-1} ν(O-H) and a band at 1053 cm^{-1} along with a decrease in intensity of the 965 cm^{-1} band and removal of the 1326/1140 cm^{-1} bands (Figure 5.5). Upon evacuation of this sample, the above bands decreased and a new broad band at 1138 cm^{-1} formed (Figure 5.5(c)). The formation of bands at 3690 and 1053 cm^{-1} may be due to the following reaction:

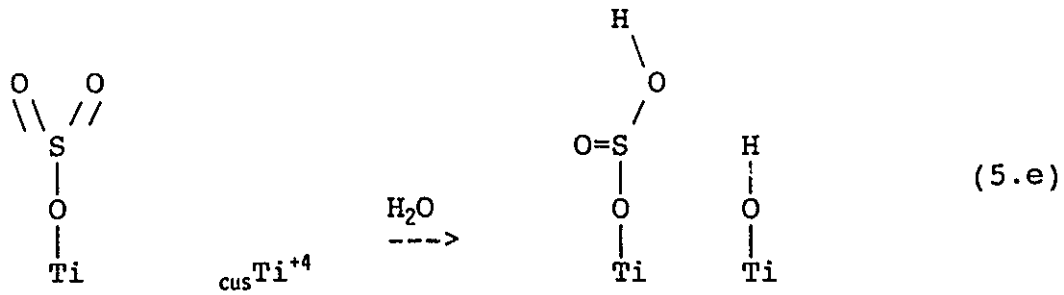

(5.e)

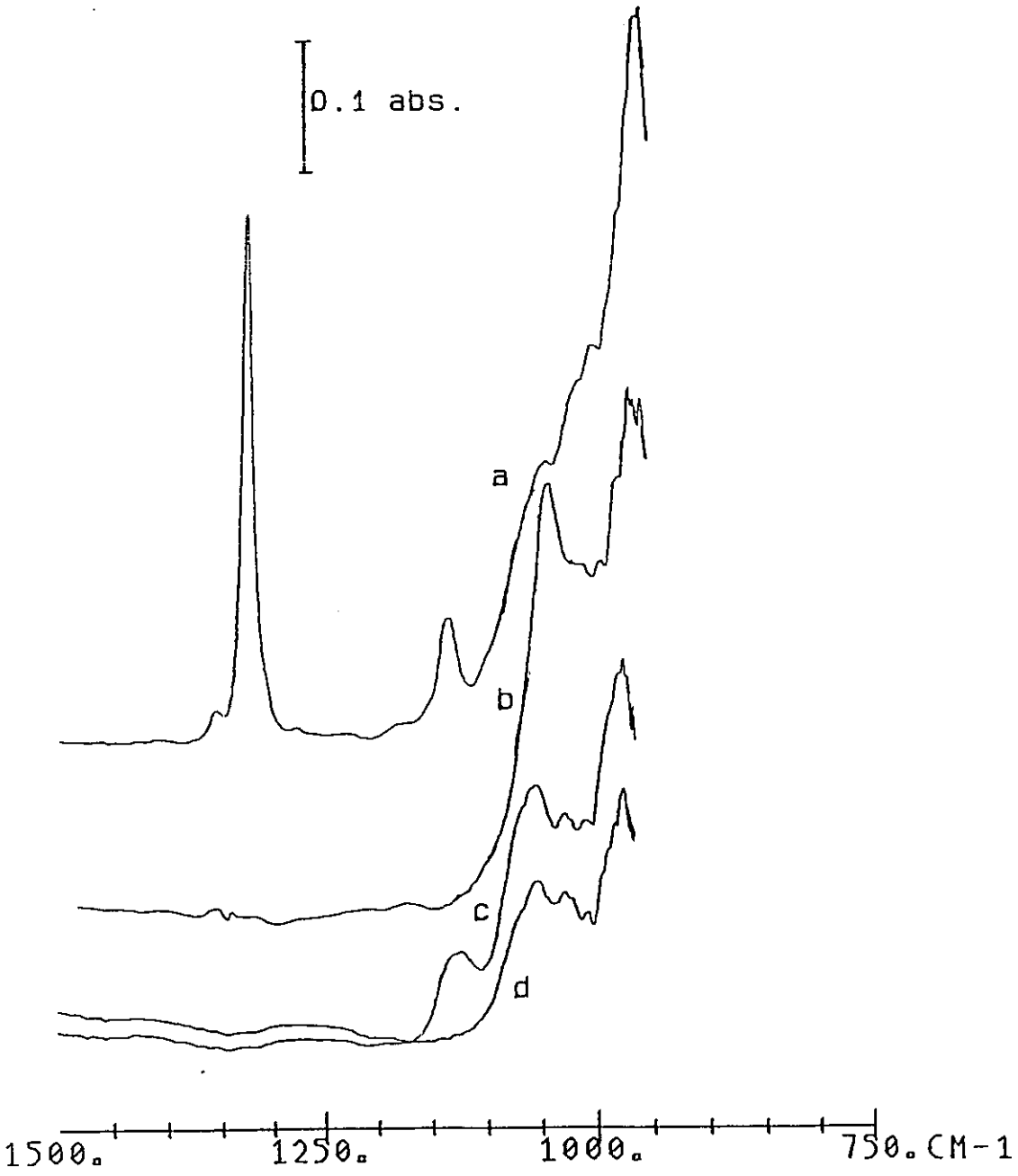

Figure 5.5

DT(450 °C) with the;
a) Addition of 600 umole g^{-1} of SO_2, followed by;
b) Evacuation five minutes and addition 300 umole g^{-1} H_2O.
c) (b) evacuated ten minutes, followed by;
d) Addition of 300 umole g^{-1} of H_2S.

A 3690 cm^{-1} band was not observed in the background spectrum of pure DT, however, the formation of an OH group adjacent to an $HOSO_2$ would be shifted in frequency relative to the pure oxide.

The 1138 cm^{-1} band disappeared upon further addition of H_2O and returned upon evacuation of the H_2O. Its formation may be the result of an equilibrium between two adjacent $HOSO_2^-$ species.

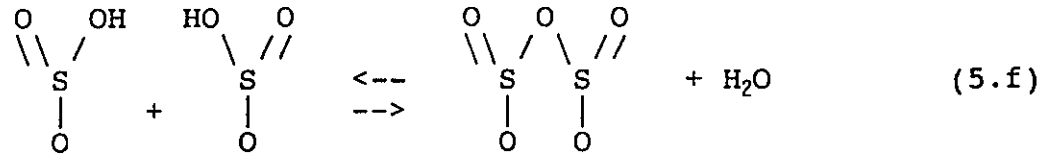

(5.f)

The addition of H_2S to DT pretreated with SO_2 resulted in numerous and complex spectral changes in the 1400-950 cm^{-1} region. This complexity in spectral changes varied from sample to sample and was probably due to the combination of the direct reaction of H_2S with the adsorbed SO_2 species and by the water that was generated from H_2S dissociation or via the Claus reaction. Nevertheless, in general, all bands due to adsorbed SO_2 decreased in intensity with addition of H_2S (e.g. Figure 5.5(d)).

5.4 CONCLUSION

The adsorption of H_2S on titania and alumina are markedly different. This is due to the fact that TiO_2 is more easily reduced than alumina. On alumina, reversible adsorption occurs at AlOH sites and dissociative adsorption at Lewis basic/acidic sites resulting in formation of AlSH and AlOH. In contrast, on TiO_2, reversible adsorption occurs at Lewis acid sites and

dissociative adsorption involves reduction of the surface producing S" and H_2O.

This difference in the nature of the preadsorbed H_2S on titania and alumina would not likely account for the observed difference in Claus activity between the two catalysts. Our Raman results have shown that Claus activity mainly involves the reaction of adsorbed SO_2 with gaseous H_2S for both alumina and titania. We believe that the variation in Claus activity would mainly originate from the differences in the mode or strength of adsorption of SO_2 between TiO_2 and alumina.

On alumina there exists a strongly adsorbed sulfite (band at 1060 cm^{-1}) which is less reactive toward H_2S than the more weakly held sulfite (960 cm^{-1}) on titania. The sulfite on titania is converted easily with water to other reactive species (with respect to H_2S) whereas the sulfite on alumina is unreactive with water. This in itself may account for the enhanced Claus activity observed for TiO_2. In addition, the 1060 cm^{-1} band on alumina might be a precursor for sulfation in the presence of O_2 causing deactivation of the catalyst. Sulfation of TiO_2 does occur to some extent, although the sulfate formed is thermally less stable than observed for alumina [Chapter 7].

Chapter 6

GALLIUM OXIDE

6.1 INTRODUCTION

Gallium lies below aluminum in the periodic table. Therefore, the surface chemistry gallium oxide (Ga_2O_3) would be similar to that of alumina but its basicity would be expected to be greater. In previous studies, both alumina and (Ga_2O_3) have been shown [98-100] to exhibit similar catalytic activities.

Activation of Ga_2O_3 above 300°C makes the catalytic properties similar to those of Al_2O_3, whereas with mild activation below 300°C the properties are quite different. Rooney et. al. [98-100] have shown that upon mild activation of Ga_2O_3 both cis-trans isomerization and H/D exchange of alkenes occur, whereas after activation at 300°C or higher, double bond migration and cis-trans isomerization resulted.

It was also observed that the addition of either SO_2 or NO_2 can selectively poison the sites responsible for double bond migration on Ga_2O_3 or Al_2O_3. ESR studies [58,101,102], at that time, had indicated that SO_2^- radicals were formed on alumina basic sites. From this, Rooney et. al. concluded that the sites responsible for double bond migration were basic sites, distinct

from the sites causing cis-trans isomerization or H/D exchange. Furthermore, on mildly activated Ga_2O_3 (300°C), SO_2 coadsorption poisoned the sites for H/D exchange, whereas cis-trans isomerization was partially (50%) restored upon evacuation of SO_2. Experiments involving deuterated Ga_2O_3 had shown that hydroxyl sites were involved in the H/D exchange reaction. It was concluded that both hydroxyl and oxide sites catalyze the exchange reaction, whereas oxide ions alone catalyze cis-trans isomerization.

However, Parkyns [103] observed that NO_2 is also strongly adsorbed on acidic sites as well as basic sites on alumina and our studies [Chapter 3] have shown that SO_2 may also react with hydroxyl and Lewis sites on alumina. A similar spectroscopic study on Ga_2O_3 has not been reported. Therefore, the role of SO_2 as a poison for selective catalytic reactions on Ga_2O_3 remains unclear.

We have undertaken a study of SO_2 adsorbed on Ga_2O_3 activated at 200, 300 and 400°C (denoted Ga(200°C) etc.) to determine the nature of the adsorbed species in relation to selective poisons for catalytic reactions of alkenes. Furthermore, Ga_2O_3 is transparent to 800 cm^{-1} and it was thought that a study of the adsorption of SO_2 and H_2S on Ga_2O_3 might lead to a better understanding of the Claus reaction on Al_2O_3.

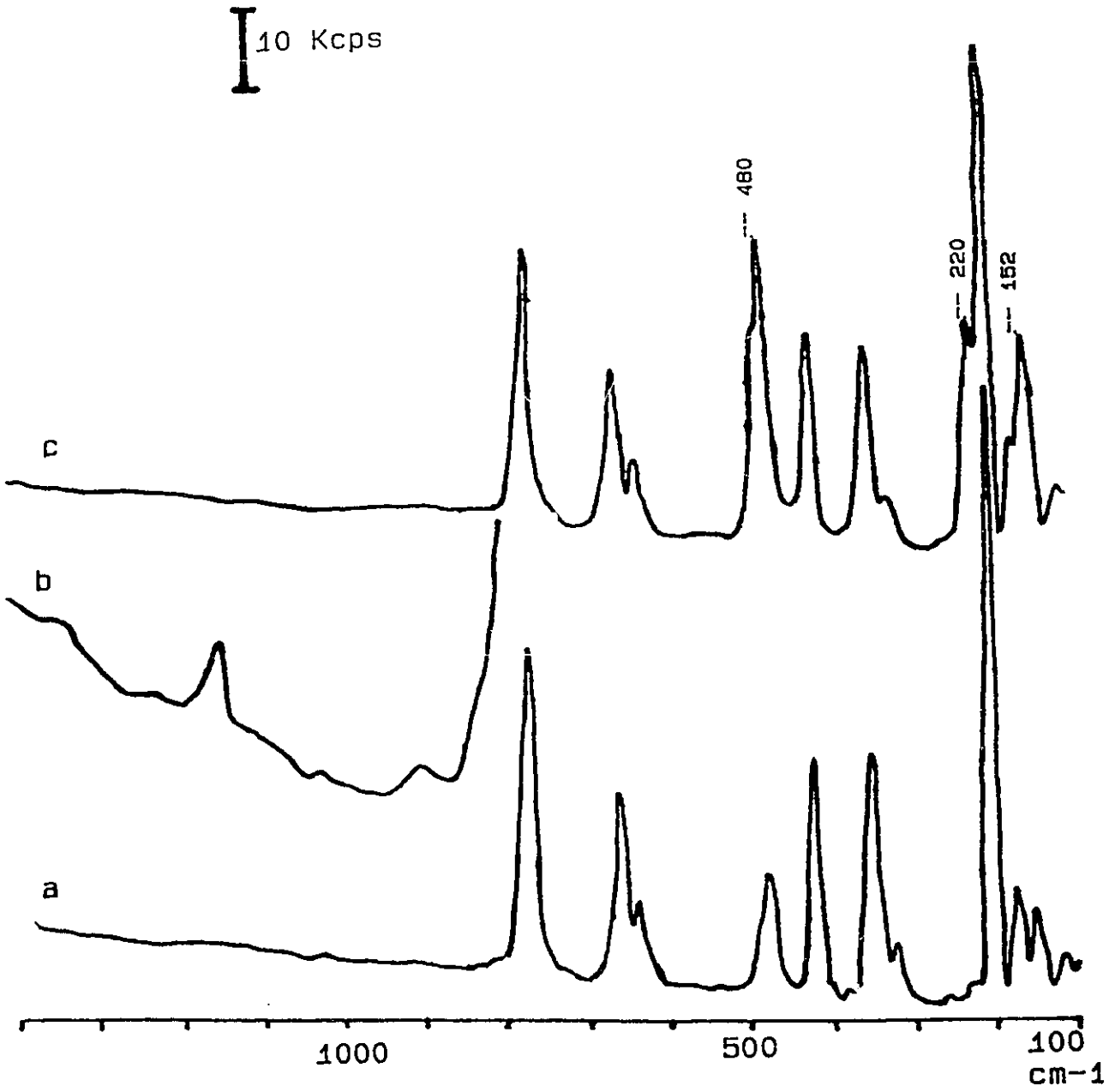

Figure 6.1

Raman spectrum of;
a) Ga_2O_3 degassed at 300 °C, followed by;
b) Addition of 300 umole g^{-1} SO_2, and;
c) Evacuation ten minutes, followed by addition of 300 umole g^{-1} H_2S.

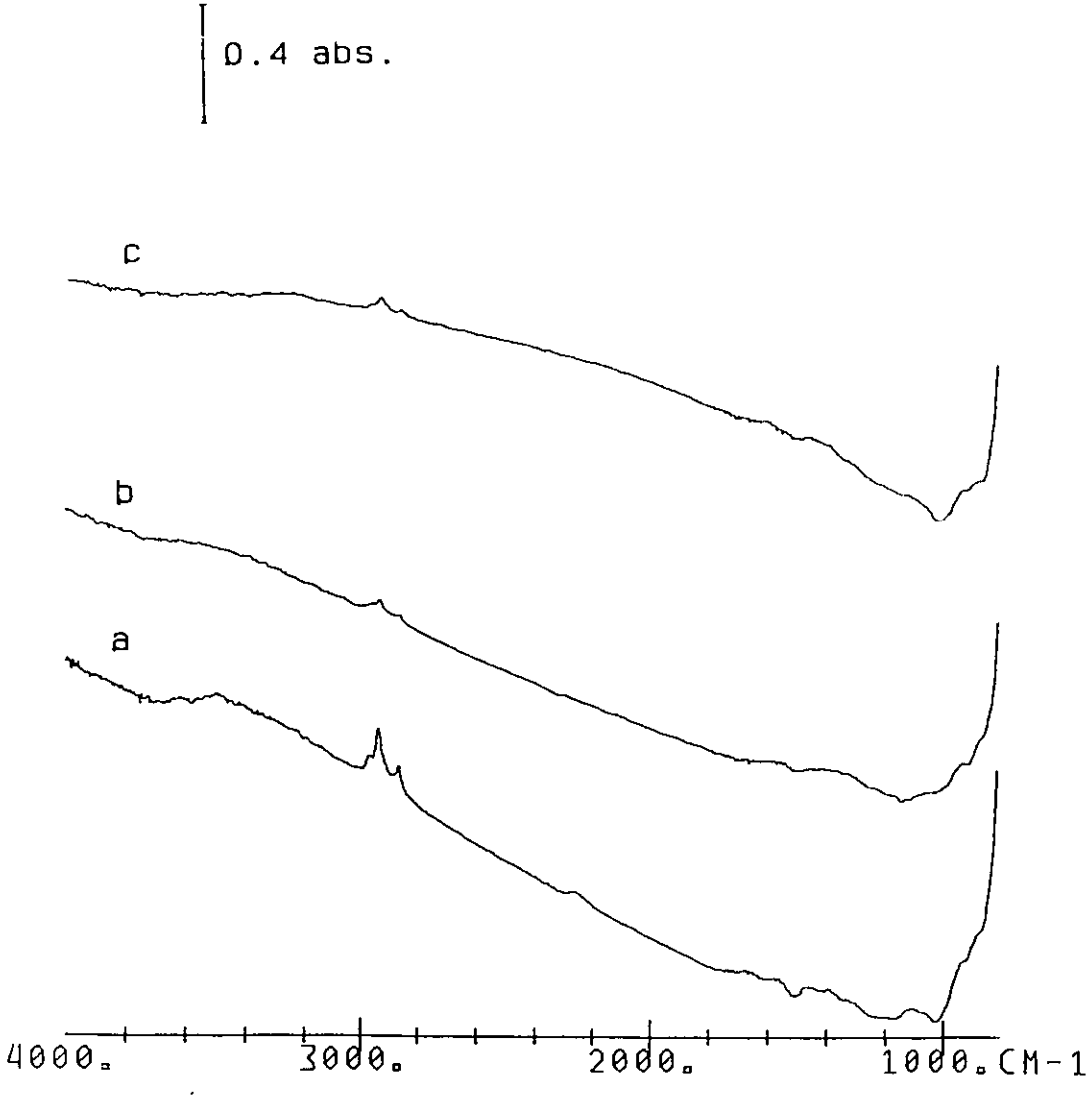

Figure 6.2

Ga_2O_3 degassed for one hour at;
a) 200 °C.
b) 300 °C.
c) 400 °C.

6.2 RESULTS AND DISCUSSION

6.2.1 RAMAN

The background Raman spectrum of Ga(300°C) is shown in Figure 6.1. Dohy and Lucazeau [104] have reported the Raman spectra of a single crystal βGa_2O_3 (our sample was a powdered crystalline βGa_2O_3). Our results are in accord with those reported with strong bands located at 763, 660, 480, 420, 350, 318, 199, 169, 155, and 115 cm^{-1} assigned by Dohy and Lucazeau to various lattice modes. As observed with Al_2O_3, the addition of SO_2 produced only a band at 1150 cm^{-1} due to weakly physisorbed SO_2 which was easily removed upon evacuation. Upon subsequent addition of H_2S sulfur bands at 151, 220 and 480 cm^{-1} formed, indicating Claus activity. In the reverse experiment, the addition of H_2S to Ga(300°C) produced a weak band at 2570 cm^{-1} ν(S-H) due to weakly adsorbed H_2S which was easily removed upon evacuation. No bands due to sulfur formed upon subsequent addition of SO_2. Once again, upon evacuation of the SO_2 and further H_2S addition, the sulfur bands appeared. As with Al_2O_3, and TiO_2, Ga_2O_3 is also a catalyst for the Claus reaction via a reaction of adsorbed SO_2 with gaseous H_2S.

6.2.2 IR STUDIES

The infrared spectrum of Ga(200°C) showed a very weak ν(O-H) band at 3620 cm^{-1} and a broad weak band at 3500 cm^{-1}. These bands

diminished upon degassing at 300°C, were completely removed at 400°C (Figure 6.2) and did not reform upon addition of water. In a previous study [100], it was reported that activation of Ga_2O_3 at temperatures above 300°C resulted in the liberation of both water and oxygen. It was suggested that the H_2O liberated was due to condensation of adjacent hydroxyls which exposed oxide and Ga sites similar to that observed for alumina [27]. This is plausible since transition from the oxyhydroxide GaO(OH) liberating water, giving rise to Ga_2O_3, is known to occur at 300°C [98].

Spectra observed after the addition of SO_2 to Ga_2O_3 are shown in Figure 6.3. For Ga(200°C) a band at 925 cm^{-1} formed along with a shoulder at 990 cm^{-1} and there was a reduction in the v(O-H) band at 3620 cm^{-1}. This 925 cm^{-1} band was also observed to occur with Ga(300°C) but not with Ga(400°C). This suggests that the SO_2 reaction with the hydroxyl groups of Ga_2O_3 gave rise to the 925 cm^{-1} band.

In contrast, addition of SO_2 to Ga(400°C) resulted first in two sharp bands at 1040 and 1010 cm^{-1}, bands whose intensity increased in unison with increasing SO_2 coverage, followed eventually by bands due to weakly adsorbed SO_2 at 1330 and 1150 cm^{-1} (Figure 6.3(c)). These bands also formed on Ga(300°C) (Figure 6.3(b)) but not on Ga(200°C) and therefore, were probably due to a reaction with either acidic or basic sites created upon dehydroxylation. The 1330/1150 cm^{-1} bands occurred at weakly acidic sites on both alumina and titania.

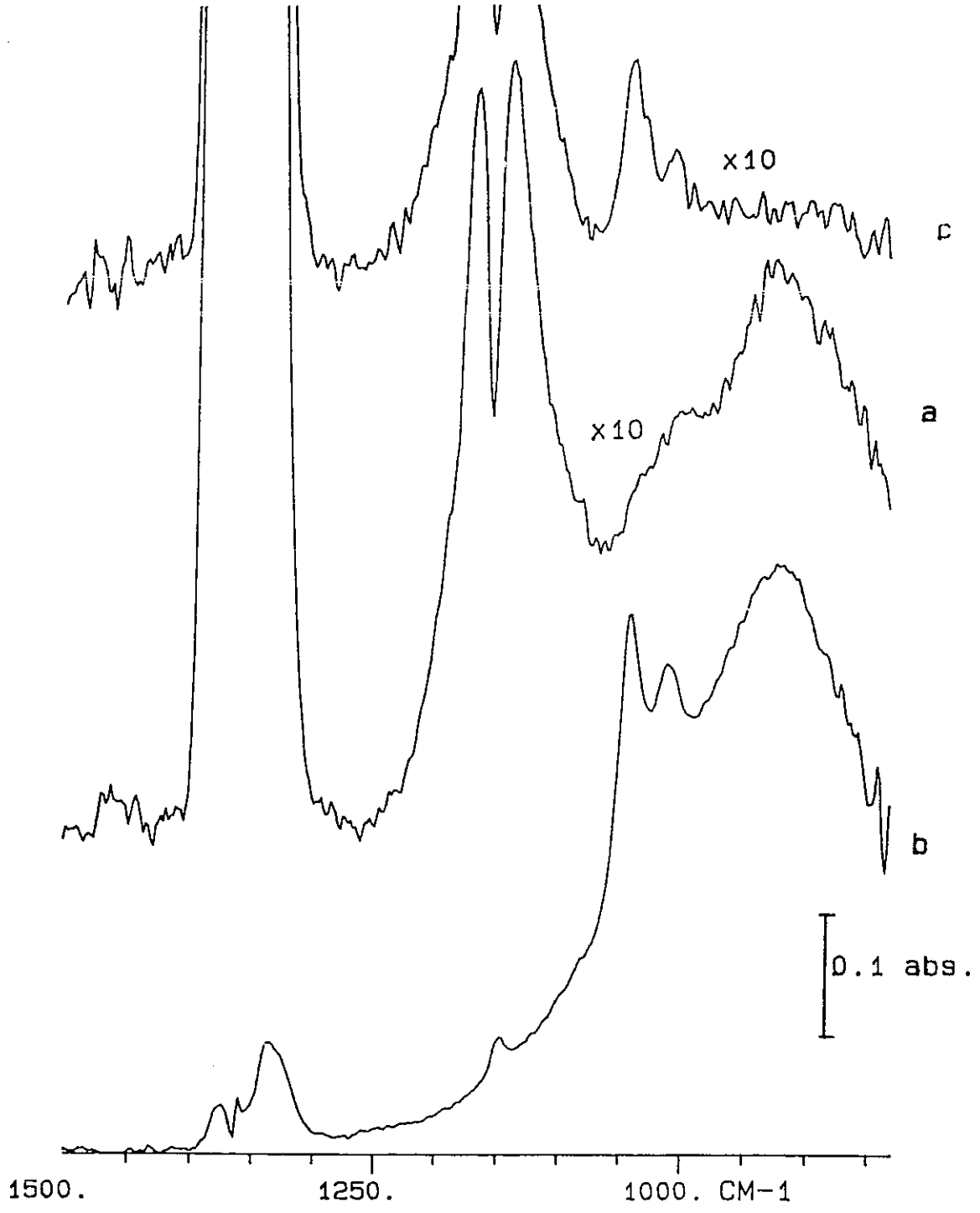

Figure 6.3

Addition of SO_2 to Ga_2O_3 initially degassed at;
a) 200 °C.
b) 300 °C.
c) 400 °C.

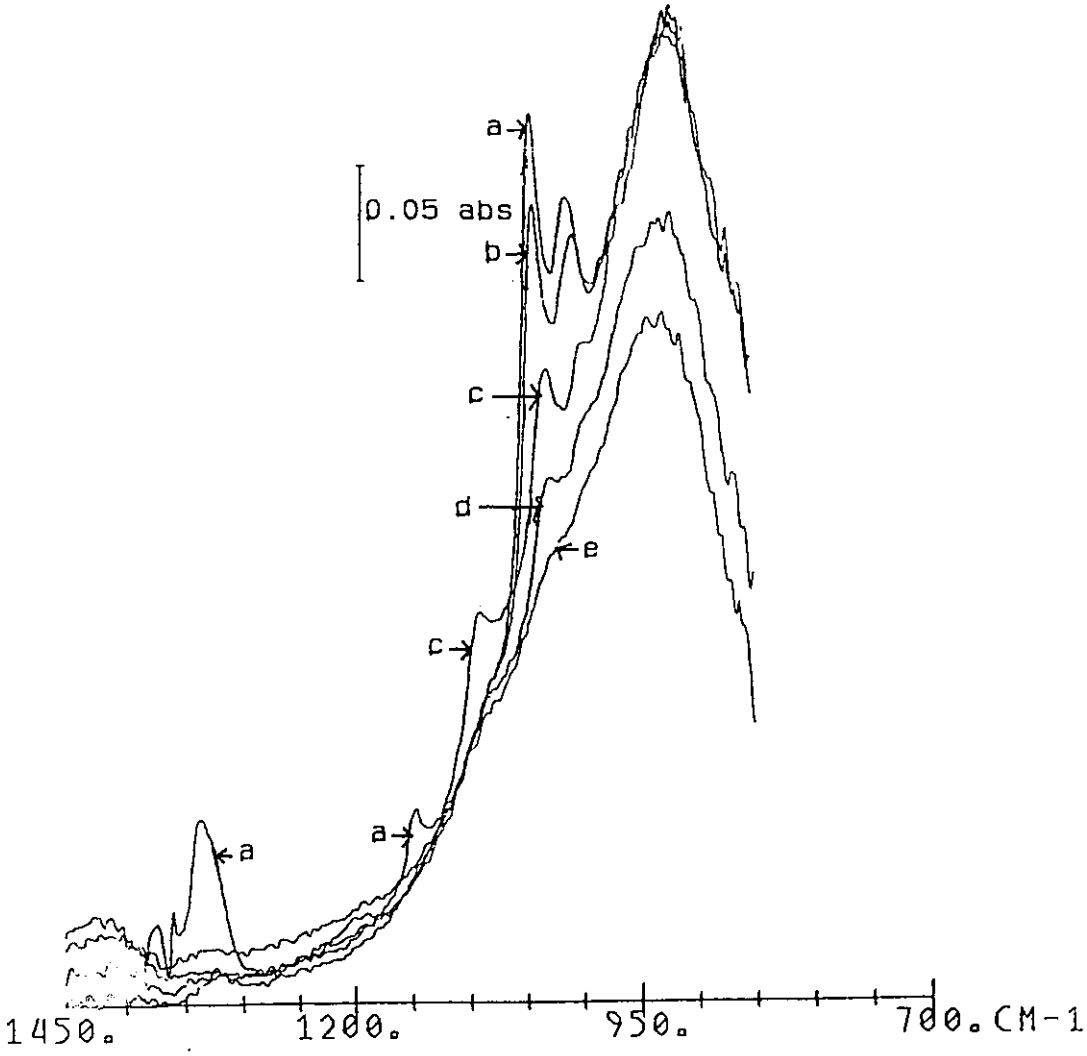

Figure 6.4

a) Same as Figure 6.3(b).
b) Evacuate one minute.
c) Add 300 umole g^{-1} D_2O
d) Add 600 umole g^{-1} H_2S.
e) Add 3000 umole g^{-1} H_2S.

The evacuation of Ga(300°C) pretreated with SO_2 first resulted in removal of weakly adsorbed SO_2 with bands at 1330 and 1150 cm^{-1} followed by reduction of the bands at 1040 and 1010 cm^{-1}, whereas the band at 925 cm^{-1} remained unchanged. The 925 cm^{-1} band was not affected by addition of D_2O, whereas bands at 1040/1010 cm^{-1} were reduced in intensity, and a band at 1080 cm^{-1} formed. On titania, a similar result was observed in which the 965 cm^{-1} band (Ti-OSO_2) decreased in the presence of H_2O and a band at 1040 cm^{-1} appeared.

The 1040/1010 cm^{-1} bands are too low in frequency and separation to be due to weakly coordinated SO_2. However, a band due to ($SO_3^=$) via reaction with O^{-2} sites occurs in this frequency region titania (965 cm^{-1}) which were also found to be reactive with H_2O. Sodium sulfite in solution has ν_1 at 967 cm^{-1} and ν_3 at 933 cm^{-1} while for the solid the ν_1 is at 1010 cm^{-1} and the ν_3 is at 961 cm^{-1}. The separation between the ν_1 and ν_3 is consistent with the observed 1030/1000 cm^{-1} bands.

On Ga(300°C), H/D exchange is irreversibly poisoned whereas cis-trans isomerization is partially (50%) reversible upon SO_2 preadsorption and evacuation. The ν(O-H) band at 3620 cm^{-1} for Ga_2O_3 has been shown to exchange with D_2O [98]. Furthermore, on Al_2O_3, the addition of CO_2 selectively poisons H/D exchange reactions but not cis-trans isomerization [105]. It is well known that the addition of CO_2 to Al_2O_3 results in the reaction of hydroxyl groups forming HCO_3^- bicarbonate species [45]. Therefore, H/D exchange would likely involve some reaction with the same sites which are poisoned by SO_2 giving rise to the band

at 925 cm^{-1}. Double bond migration (poisoned by SO_2) on Ga(400°C) would, therefore, involve basic sites (O^{-2}), represented by the 1040/1010 cm^{-1} bands.

The addition of H_2S to Ga(200, 300 or 400°C) generated no observable infrared spectral changes. Addition of H_2S to the sample represented by the Figure 6.4(c) resulted in an immediate decrease in the intensity of the bands at 1040 and 1010 cm^{-1} and 925 cm^{-1} and a disappearance of the band at 1080 cm^{-1}. In a large excess of H_2S 1040/1010 cm^{-1} bands disappeared and the 925 cm^{-1} band further decreased. Even though all species exhibit some Claus activity, H_2O formed as a product in the Claus reaction would prevent formation of the weakly adsorbed species with bands at 1330/1150 cm^{-1} or 1030/1000 cm^{-1}. The H_2O would also react with the species responsible for the 925 cm^{-1} band to produce a second very reactive species with H_2S (band at 1080 cm^{-1} with D_2O in Figure 6.4(c)).

Chapter 7

THE STRUCTURE AND STABILITY OF SULFATED CLAUS CATALYSTS

7.1 ALUMINA AND TITANIA

7.1.1 INTRODUCTION

In this chapter, we embark on a variation of the theme discussed in the preceding chapters concerning the Claus reaction. We have examined up to now, catalysts and promoters for the Claus reaction and in this chapter we look at one of the main causes of deactivation of Claus catalysts, namely, sulfate formation [106].

In a recent study, Lavalley et. al. [107] investigated the sulfation of alumina by the oxidation of H_2S or SO_2 and proposed, depending on the temperature, two mechanisms for the oxidation of H_2S. At low temperatures, below 200°C, sulfate formation occurred with chemisorbed H_2S either as Al-SH or with S^{-2}. However, at temperatures greater than 200°C, SO_2 was found in the gas phase, suggesting a mechanism involving direct oxidation with SO_2. With SO_2 alone, Lavalley et. al. have shown that the presence of hydroxyl groups or water on alumina favours sulfate

formation. They have suggested a mechanism involving a hydrogen sulfite intermediate.

$$SO_2 + OH^- \rightarrow HSO_{3(ads)}^- \qquad (7.a)$$

$$HSO_{3(ads)}^- + 1/2O_2 \rightarrow H^+ + SO_{4(ads)}^=$$

A maximum of 220 umoles g^{-1} of sulfate was formed with excess SO_2 and O_2 at all temperatures employed (400°C to 800°C). It was suggested that this maximum was achieved via destruction of the catalytic OH^- groups in Reaction 7.a.

The infrared spectrum of the sulfated Al_2O_3 was the same as that which was observed after impregnation of Al_2O_3 with $Al_2(SO_4)_3.18H_2O$ [108] or $(NH_4)_2SO_4$ suggesting that a common surface species is present. Sulfated titania [85] and alumina [109] also have an augmented acidity and it has recently been shown [110-112] that TiO_2, Zr_2O and Fe_2O_3 which contain sulfate ions have an increased catalytic activity for isomerization of hydrocarbons or dehydration of alcohols. Finally, Al_2O_3 has been proposed as an $SO_x(SO_2,SO_3)$ transfer catalyst for removal of SO_x during the regeneration of fluidized catalytic cracking (FCC) catalysts [113-115] and it is known that alumina based Claus catalysts are poisoned as a result of sulfate formation [116]. In view of the diverse interest and importance in sulfate/metal oxide systems we have undertaken a study of sulfated alumina and titania (anatase) using infrared and Raman spectroscopy with the aim of determining the structure of the surface sulfate, its thermal stability, and its reducibility in H_2. Preliminary results on the sulfation of Na/Al_2O_3 are also reported.

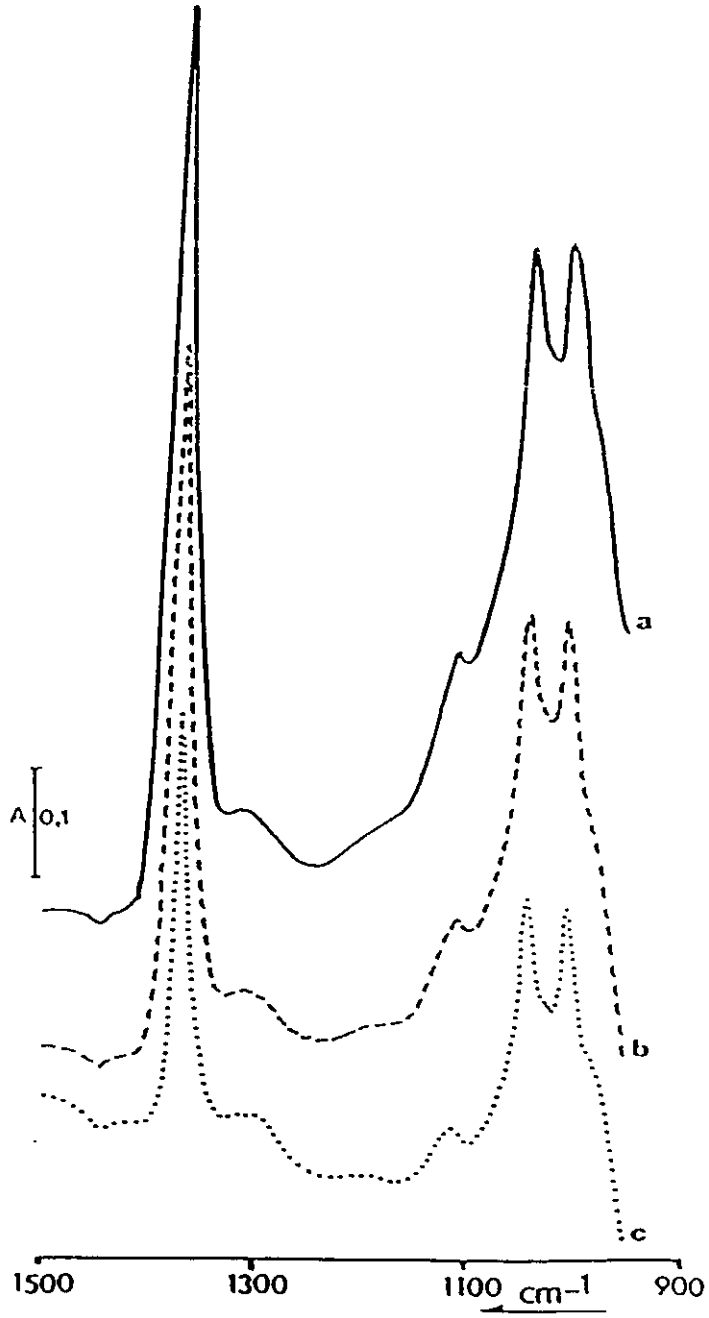

Figure 7.1

Spectra observed after sulfation of TiO_2 which had been activated at 450 °C, then reacted with SO_2 + O_2 at 450 °C (150 umole g^{-1} SO_2), then evacuated at:
a) 450 °C.
b) 550 °C.
c) 600 °C.
In all cases, the background spectrum of the activated TiO_2 has been subtracted.

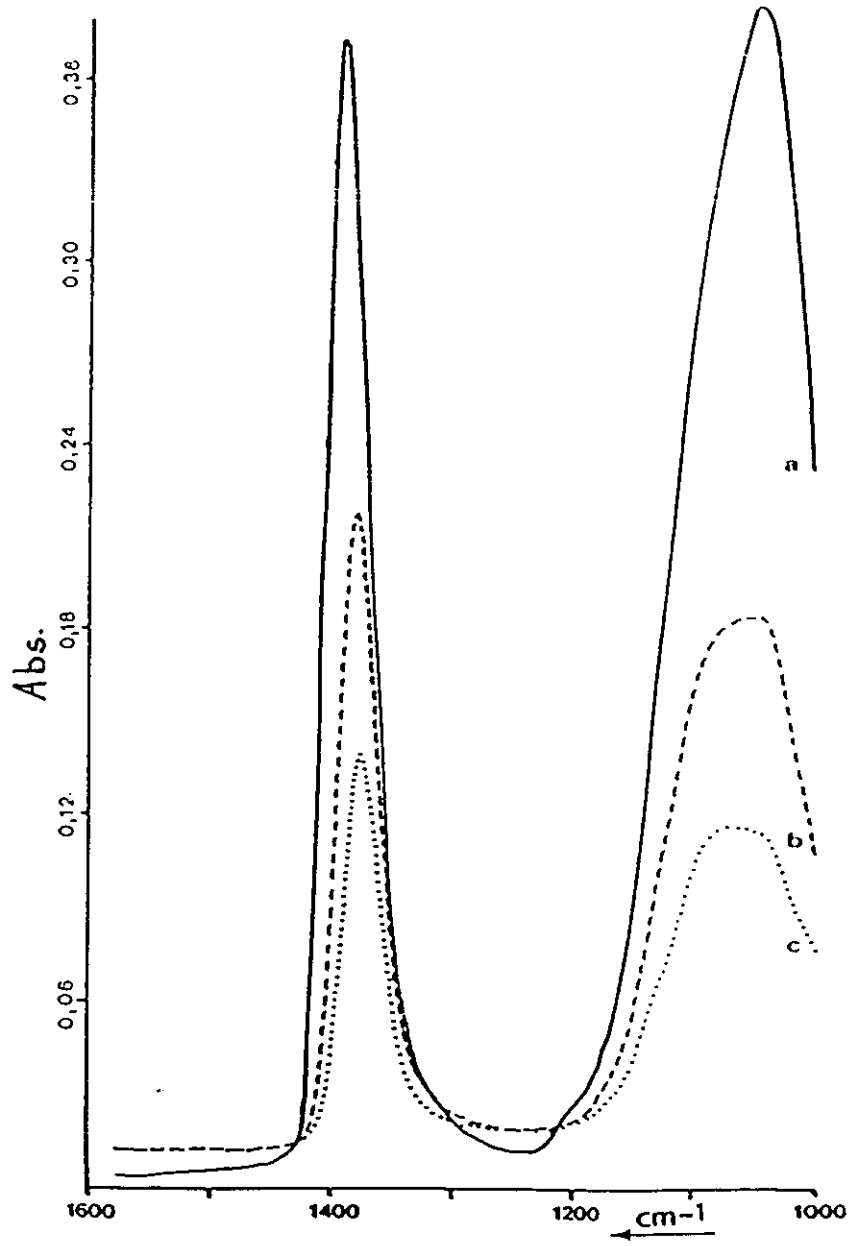

Figure 7.2

a) Spectrum observed after sulfation of Al_2O_3 as for Figure 7.1(a).
The sample was then heated in the presence of 200 torr of H_2 for two hours at:
b) 550 °C, then evacuated.
c) 600 °C, then evacuated.

7.1.2 RESULTS AND DISCUSSION

The infrared spectra observed after the adsorption of SO_2 and oxidation in excess O_2 at 450°C on titania or alumina are shown in Figure 7.1 and Figure 7.2 respectively. There is an intense sharp band at 1380 cm^{-1} accompanied by an intense but broad band near 1045 cm^{-1} for Al_2O_3; for TiO_2 the spectrum is dominated by a similar sharp peak at 1370 cm^{-1} and a broad doublet at 1045 and 1005 cm^{-1} in addition to weaker features at 1315 and 1110 cm^{-1}. The same spectra could equally be produced by oxidizing adsorbed H_2S at 450°C, by simply heating a mixture of SO_2 or H_2S in excess O_2 at 450°C, or by heating Al_2O_3 or TiO_2 which had been impregnated with $(NH_4)_2SO_4$ from aqueous solution at 450°C. Following the oxidation of excess SO_2, the maximum number of sulfate groups formed was 1.3 nm^{-2} for Al_2O_3 [108] and 3.2 nm^{-2} for TiO_2 [117] (determined gravimetrically by assuming that the mass increase is due to adsorption of SO_3). Finally, Lavalley et. al. [108] has previously shown that for Al_2O_3, the same spectrum can be produced by impregnation with $Al_2(SO_4)_3.18H_2O$ and heating in vacuum at 450°C and that the intensity of the 1380 cm^{-1} band can give a quantitative measure of the amount of sulfate present (In this previous study, using a dispersive spectrometer, they were not able to specify the frequency of the low wavenumber band as clearly as is now possible using FTIR spectrometers.) They could also produce the same spectrum by heating $TiOSO_4$ impregnated TiO_2 to 450°C under vacuum [117].

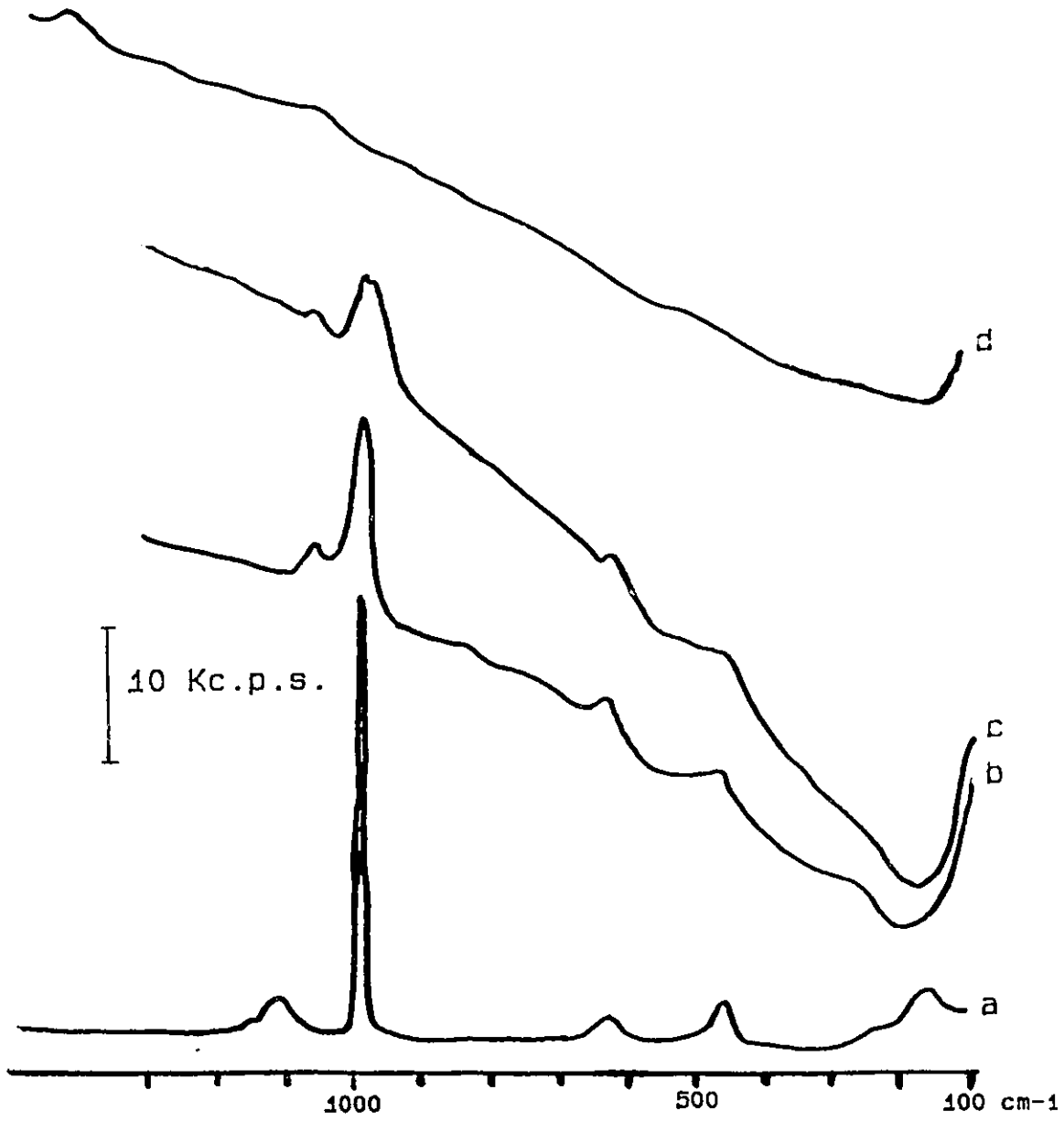

Figure 7.3

Raman spectra of:
a) Pure Na_2SO_4.
b) Sulfated 3% Na/Al(400 °C).
c) (b) after heating in $H_2{}^{18}O$ at 400 °C for one hour, evacuated 0.5 hours.
d) Sulfated Al(400 °C).

Additional bands may form below 1000 cm^{-1}. To investigate this possibility further, the formation of sulfate has been studied with Raman spectroscopy. Heating adsorbed SO_2 with O_2 on alumina only produced weak Raman bands at 1380 and 1050 cm^{-1} (Figure 7.3(d)).

In order to assess the thermal stability of the surface species generated, we heated each sulfated surface at increasing temperatures while evacuating the cell. In both cases, the IR bands decreased in intensity more or less in unison (Figure 7.1 shows a typical series of spectra for TiO_2). All peaks disappeared in the case of Al_2O_3 after prolonged heating at 800°C, whereas the disappearance occurred near 650°C for TiO_2. Since there was a severe decrease in IR transmission when TiO_2 was heated beyond 600°C due to reduction of TiO_2, we could not determine the disappearance temperature accurately.

The IR bands above were observed under normal scanning conditions at room temperature and thus, may not truly reflect the species that formed at 450°C. We have been able to study this by recording <u>in situ</u> spectra at elevated temperatures on a computer controlled dispersive IR. SO_2 (100 umol g^{-1}) was first added to Al(400°C) at room temperature. The cell temperature was raised to 400°C and excess O_2 was added. Spectra were recorded as a function of time from initial addition of the O_2 (Figure 7.4). Observation of the 1390 cm^{-1} band was hampered by the presence of gas phase SO_2. Nevertheless, the 1390 and 1050 cm^{-1} bands initially formed rapidly (Figure 7.4(a)) and increased uniformly with time. A contact time of greater than 35 minutes

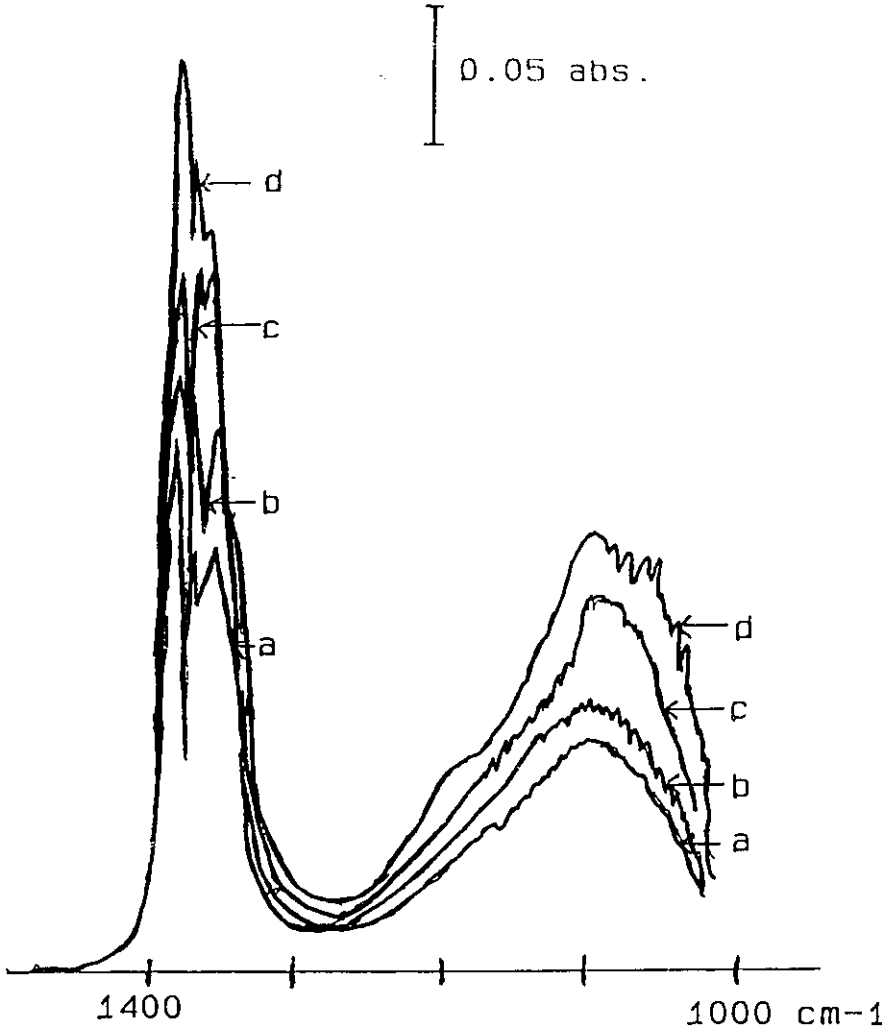

Figure 7.4

Formation of sulfated Al(400 °C) recorded at 400 °C.
a) Addition of 100 umole g^{-1} SO_2 at room temperature, followed by 2000 umole g^{-1} O_2 at 400°C.
b) Scan 14 minutes later.
c) Scan 35 minutes later.
d) Scan 90 minutes later.

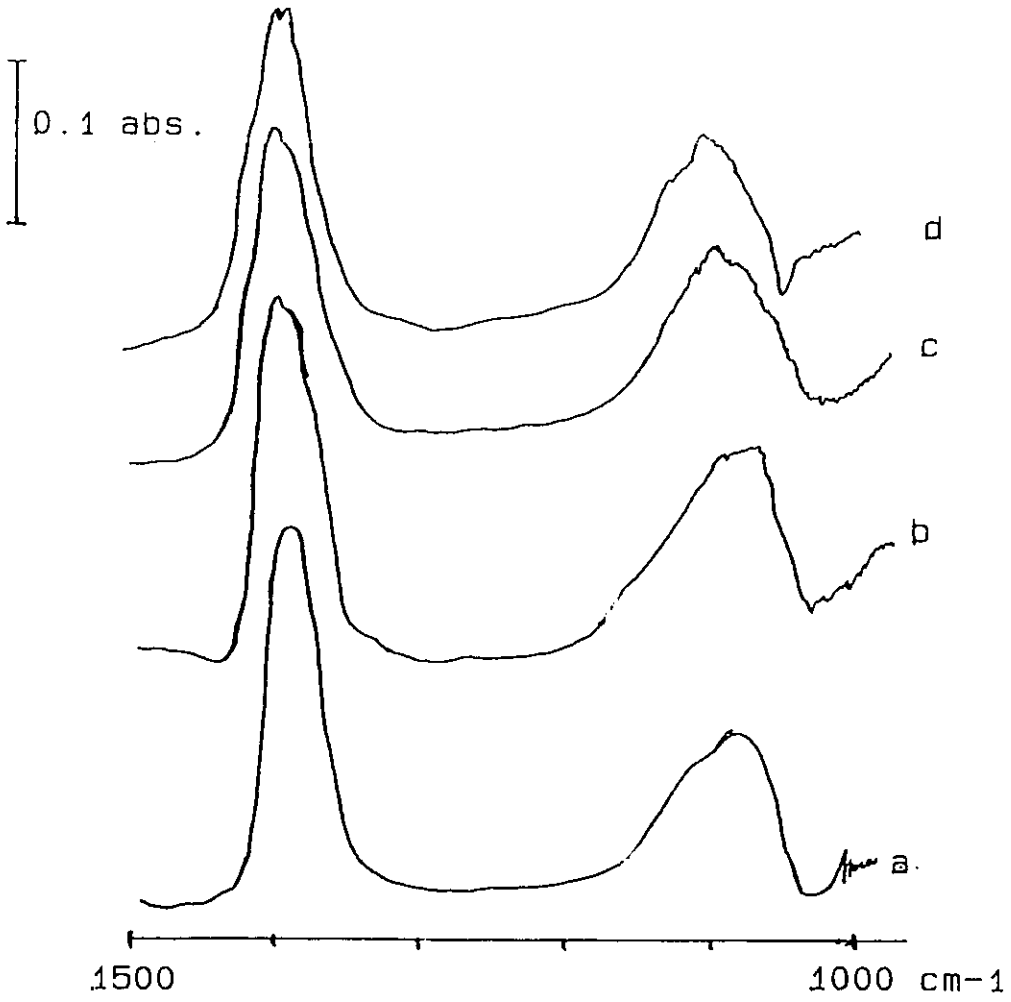

Figure 7.5

In situ infrared spectra of a sulfated alumina recorded at:
a) 25 °C.
b) 200 °C.
c) 600 °C.
d) 800 °C.

was required to obtain maximum band intensity. The sample was then evacuated and in situ spectra were recorded at several temperatures between 25 and 800°C. Over this temperature range the integrity of the bands was preserved and their integrated intensity did not change appreciably until the highest temperatures (Figure 7.5). Therefore, we conclude that the 1390 and 1050 cm^{-1} bands are due to the same adsorbed species which was the same at 800°C as at room temperature.

Lavalley et. al. have also measured the weight change during decomposition with a McBain balance. For TiO_2 (Figure 7.6) most of the mass decrease occurred between 650-720°C, and after heating at 750°C the mass of the sample was the same as it was before the sulfation with $SO_2 + O_2$. With sulfated Al_2O_3, the weight loss was slight between 600-800°C (the maximum achievable with their apparatus), but they observed a decrease in weight over eight hours at 800°C, after which the weight remained constant. When the weight change due to loss of water was taken into account (for both surfaces), they determined that all sulfate had been removed. Finally, for both sulfated TiO_2 and Al_2O_3, after the McBain experiment, each sample was examined by infrared spectroscopy. After reevacuation at 450°C, as well as after reoxidation at 450°C, no sulfate bands were observed, clearly showing that all sulfur species had left the surface.

The reduction of the sulfated surfaces in H_2 as a function of temperature was also studied. A typical set of spectra for Al_2O_3 are shown in Figure 7.2 where it can be seen that all bands decrease simultaneously while approaching 600°C. In the case of

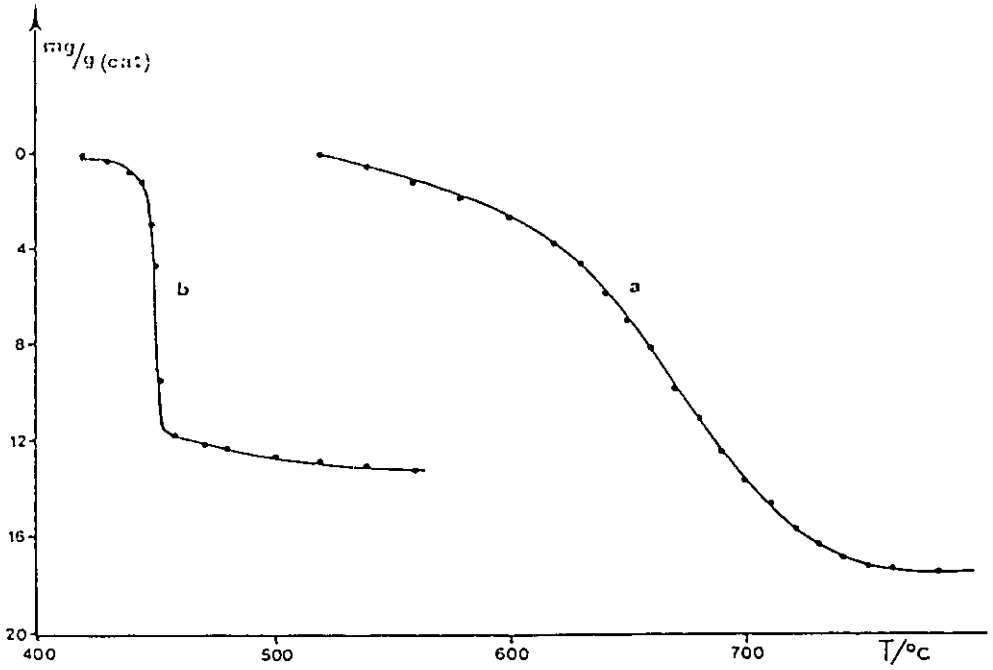

Figure 7.6

Weight loss of a sample of sulfated TiO_2 (SO_2 + O_2 at 450 °C):
a) By heating under vacuum from 450 °C to 800 °C at 1 °C min^{-1}.
b) By heating in the presence of H_2 from 400 °C to 600 °C at 1 °C min^{-1}.
(From Saur et. al. Ref. 93)

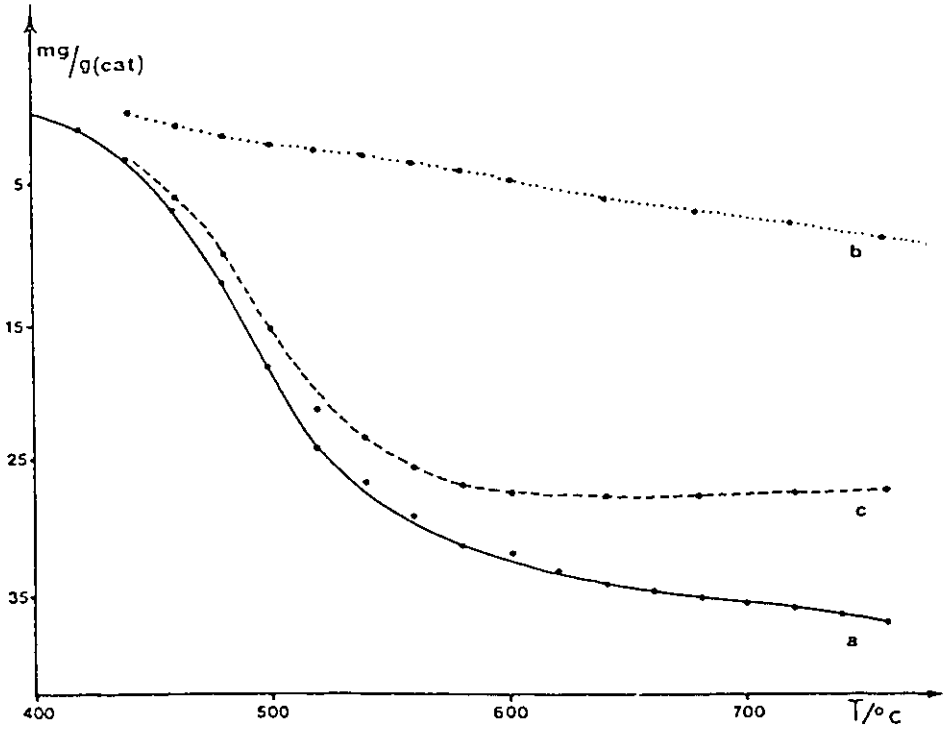

Figure 7.7

Weight loss of a sample of sulfated Al_2O_3 (SO_2 + O_2), then heated in the presence of H_2 (200 torr) from 400 °C to 700 °C:
a) Variation for a sulfated sample.
b) Variation due to loss of water from an unsulfated Al_2O_3.
c) (a)-(b): weight loss due to reduction of surface sulfates.
(Saur et. al. Ref. 93)

TiO_2, severe reduction of TiO_2 occurred beyond 400°C, reducing the transmission of the sample, and we were not able to determine the exact temperature at which the bands disappeared. However, after heating for one hour at 400°C in H_2, all IR bands disappeared but upon reoxidation in O_2 at 450°C the sulfate bands returned, thus indicating that some sulfur species remained on the surface. Lavalley et. al. were able, however, to measure the weight loss for sulfated TiO_2 and Al_2O_3 (see Figure 7.7 for Al_2O_3) during heating in H_2 and they found that constant mass was reached using Al_2O_3 near 600°C, and at 440°C with TiO_2.

In order to characterize more fully the species present on the sulfated surfaces we have used oxygen-18. We found that with either sulfated surface, (produced either by oxidation of adsorbed H_2S or SO_2, or by impregnation with a sulfate), the high frequency band shifted by about 40 cm^{-1} to lower wavenumber when the sample was heated at 450°C in $H_2{}^{18}O$ vapor and that this shifted band returned to the original frequency if $H_2{}^{16}O$ was subsequently added (see Figure 7.8 for TiO_2). The shifts in the low frequency region were complicated and difficult to assess accurately due to poor transmission near 1000 cm^{-1} (Al_2O_3) or 950 cm^{-1} (TiO_2). The spectrum shown in Figure 7.8 could also be produced following the adsorption of $S^{18}O_2$ and oxidation with $^{18}O_2$. The important point to note is that regardless of whether we used $H_2{}^{18}O$, or $S^{18}O_2$ plus $^{18}O_2$ for oxidation, only one new high frequency band was ever observed, for either Al_2O_3 or TiO_2, for any degree of partial exchange.

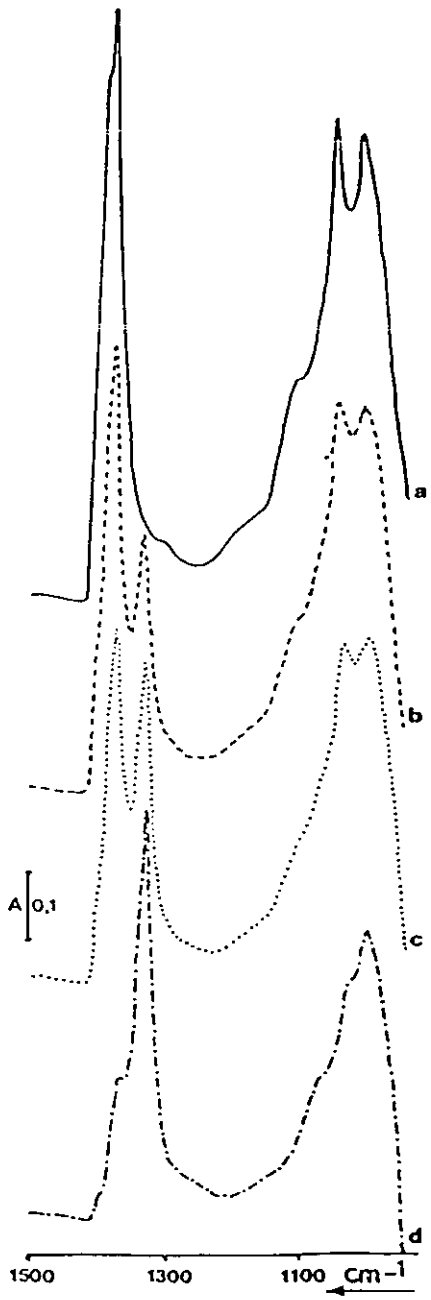

Figure 7.8

Spectra of sulfated TiO_2 during exchange with $H_2{}^{18}O$ at 450 °C.
a) Sulfated sample after oxidation of 200 umole g^{-1} of SO_2.
b) After one hour exchange in 50 umole g^{-1} $H_2{}^{18}O$, then evacuation for thirty minutes at 450 °C.
c) An additional one hour exchange in 100 umole g^{-1} $H_2{}^{18}O$.
d) An additional one hour exchange in 225 umole g^{-1} $H_2{}^{18}O$.

Finally, we found that for either oxide, once the sulfate was formed (using oxygen-16), this did not exchange with $^{18}O_2$ even when the sample was heated at 450°C in oxygen-18.

The infrared spectra of sulfated Al_2O_3 and TiO_2 resemble that reported for sulfated Fe_2O_3 [110,111]. Morterra et. al. have also shown that a spectrum similar to ours arises from anatase which had been prepared from titanyl sulfate [118]. We will first consider the structure of the sulfate species and then its stability.

Although one might suppose that sulfates are created under our oxidation conditions the infrared spectra shown in Figures 7.1 and 7.2 are very different from those of normal ionic sulfates which have bands from 1200 to 950 cm^{-1} [7,119,120]. However, covalent organic sulfates [112] show a strong band near 1400 cm^{-1} and another one between 1212 to 1190 cm^{-1} which led Tanabe et. al. [110,111] to suggest that sulfated Fe_2O_3 might contain a surface species as shown in Structure I. By analogy, one could suppose that the same

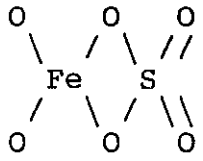

(I) (7.b)

species might also exist on TiO_2 and Al_2O_3, substituting Ti or Al for Fe. Tanabe found [110], as we do, that the spectrum changes completely if H_2O vapor is added to sulfated Al_2O_3 or TiO_2 insofar as the high frequency band disappears and new bands are created

between 1300 and 1150 cm^{-1} [108]; that is, the spectrum now more closely ressembles that of an ionic sulfate or a bidentate sulfate [7,119,120]. He also found that the sulfated anhydrous catalyst had a greater Lewis acidity and that this was largely diminished upon the addition of water. This lead him to suggest that in Structure I the surface iron atoms were electron deficient and could therefore, act as Lewis acid centres for the coordination of water. With Al_2O_3 and TiO_2, it has been observed that sulfation does not particularly increase the Lewis acidity but it creates a Brönsted acidity when the sample is not completely dehydroxylated [85,117].

In view of the spectral and chemical similarities between our systems and Fe_2O_3, we believe that a common interpretation is possible. However, our experiments with oxygen-18 exchange lead us to reject Structure I for sulfated Al_2O_3 or TiO_2. Assuming that the high wavenumber band is the antisymmetric S-O stretching mode of a terminal SO_2 group, a shift of about 40 cm^{-1} would be expected for 100% oxygen-18 exchange. For partial exchange there should be an intermediate peak due to $S^{16}O^{18}O$, as has been observed for bidentate metallic sulfates [116, 119, 122-124], and for SO_2 gas [7,122]. Since no intermediate peak was observed for either sulfated oxide, we conclude that a single S=O is formed. (It is always possible that if the bond angle in an SO_2 group were near 90 degrees, and for an appropriate interaction force constant between the two S=O groups, then only one new peak would be observed on partial or total oxygen-18 exchange. However, it seems unlikely that this coincidental combination would arise for

both sulfated TiO_2 and Al_2O_3.) We, therefore, postulate that sulfated TiO_2 or Al_2O_3 has Structure II where three oxygens are

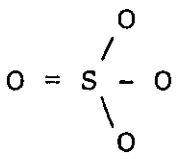

(II) (7.c)

bonded to Al or Ti. In support of this assignment, we note that in covalent organic sulfates, sulfones and sulfonates, there is a constant shift of about 200 cm^{-1} between the symmetric and antisymmetric stretching modes of the SO_2 group [121]. In our case, the broad, low wavenumber band is about 340 cm^{-1} below the high wavenumber band and can probably be attributed to the stretching motions of the M-O-S framework. We also point out that the infrared spectrum of aluminum sulfate (hydrated or anhydrous) is very different from that of the sulfated Al_2O_3 in that its v(S-O) absorption bands lie between 1250-1000 cm^{-1} [125], the normal region for ionic sulfates. Similarly, the spectrum of solid $TiOSO_4$ is also very different from that of sulfated TiO_2 [117]. Finally, although structure II is unusual, this type of structure has been reported for niobium oxide on TiO_2[126] and for sulfated ZrO_2[127].

Both the high and low frequency bands shifted when exchanged with $H_2{}^{18}O$. In order to account for this we assume that the addition of water causes the breaking of M-O-S bonds of II and propose the following scheme:

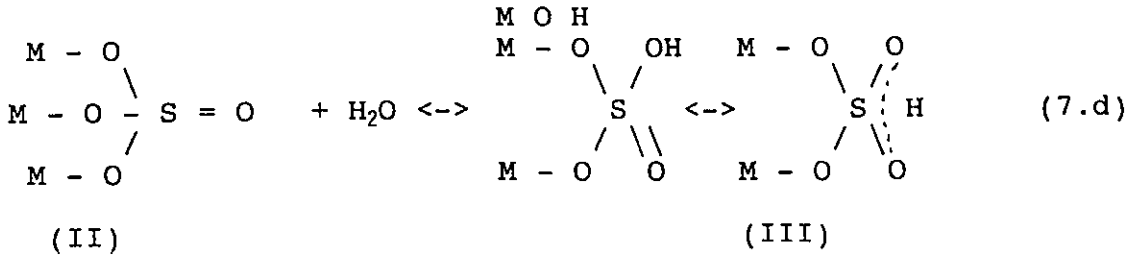

(II) (III) (7.d)

This explains in part why the terminal S=O group so easily exchanges with $H_2{}^{18}O$, but not with $^{18}O_2$; it also accounts for the increase in Bronsted acidity [85,109] which is almost certainly due to the formation of SOH groups. Further, the infrared bands of species III are very close to those which have been reported for bridged and bidentate metal sulfates [7,115-121,123,124]. Finally, Prudhomme et. al. have shown that an equilibrium between II and III exists for Al_2O_3 [108] and we have verified in this study that this is also true for TiO_2.

Concerning the thermal stability and reducibility in H_2, the infrared and microbalance results are in accord and clearly demonstrate that the sulfated alumina surface is both more thermally stable and more resistant to reduction in H_2 than is sulfated titania. This is perhaps not surprising since sulfates of titania are known to be relatively unstable [19,128-130], whereas pure $Al_2(SO_4)_3$ decomposes to yield the oxide at temperatures near 880-900°C [125]. The high thermal stability of sulfated Al_2O_3 would explain why alumina based catalysts are useful for trapping SO_x since the resultant sulfate species must be stable to near 700°C [113-115]. On the other hand, TiO_2 based catalysts which are used for NO_x reduction or CO oxidation are

particularly useful because of the relative instability of the sulfate which avoids poisoning by SO_x species [19].

7.2 Sodium on Alumina

Lavalley et. al. have reported that sulfate formation is enhanced by sodium loading of alumina [65]. Their study has shown that for direct conversion of H_2S to sulfur with O_2, reversible hydrogen bonded species are active, leading to sulfur, while NaSH irreversible species are oxidized directly to sulfate. The sulfate species were found to be stable and act as poisons for the direct oxidation Claus reaction.

The infrared spectrum of sulfate which was formed by heating adsorbed H_2S or SO_2 with O_2 at 400°C on 3% Na/Al(400°C) is shown in Figure 7.9(a). Strong bands at 1255, 1167 and 1065 cm^{-1} were observed along with weaker bands at 1380, 1360 and 1308 cm^{-1}. Upon hydration, the above bands disappeared and a broad band formed at 1130 cm^{-1} with a shoulder at 1080 cm^{-1} (Figure 7.9(c)). When heated at 400°C with $H_2{}^{18}O$ followed by evacuation at 400°C, the 1380 cm^{-1} band disappeared and the 1255, 1167 and 1065 cm^{-1} bands shifted 5 cm^{-1} to lower frequencies. The 1380, 1360 and 1308 cm^{-1} bands were observed for 1 to 3% Na/Al_2O_3. At higher Na loading (4% and greater) only bands at 1255, 1167 and 1065 were observed.

In a Raman experiment, the oxidation of adsorbed SO_2 on 3% Na/Al_2O_3 gave rise to bands at 470, 640, 995 and 1080 cm^{-1} (Figure 7.3(b)). Upon comparison with Raman spectra of known sodium

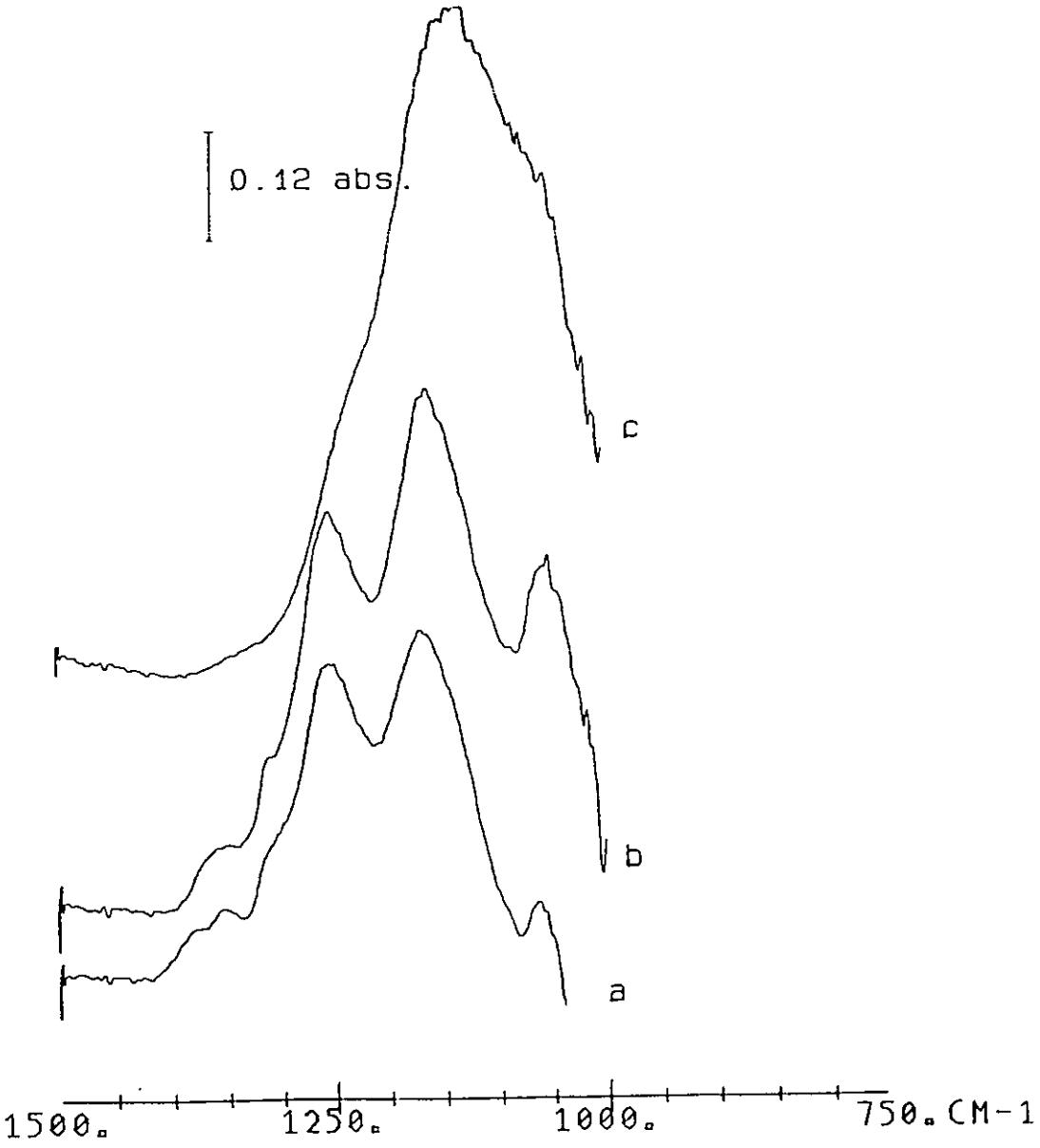

Figure 7.9

Difference spectra of 3% Na/Al(400 °C) background with;
a) 9 umole g^{-1} SO_2 and excess O_2 heated at 400 °C one hour, evacuated at 400 °C one hour.
b) (a) after heating in $H_2{}^{18}O$ at 400 °C one hour, evacuated one hour.
c) (b) after H_2O addition at room temperature.

salts, we assign these bands to Na_2SO_4. The $SO_4^=$ Raman bands did not shift with addition of $H_2^{18}O$ at room temperature. However, when heated at 500°C with $H_2^{18}O$, followed by evacuation at 400°C, the 995 cm^{-1} band partially shifted to 980 cm^{-1}.

A 3% Na loading of alumina corresponds to approximately a monolayer coverage. This, along with our Raman results, would imply that the 1255, 1180 and 1065 cm^{-1} infrared bands are the result of sulfate formation on Na sites, whereas the 1368 and 1308 cm^{-1} bands (observable only at partial monolayer coverage) involve both Na and Al sites. The infrared spectrum of solid Na_2SO_4 gives rise to a single broad band at 1125 cm^{-1} and sharp bands at 640 and 620 cm^{-1} [131].

The Raman spectrum of free $SO_4^=$ ion in solution (T_d symmetry) has bands at $\nu_1(A)$ 981, $\nu_2(E)$ 451, $\nu_3(F_2)$ 1104 and $\nu_4(F_3)$ 613 cm^{-1} [119]. The sulfate ion in solid Na_2SO_4 has D_2 site symmetry resulting in the removal of degeneracy of the ν_3 and ν_4 modes [B + B_2 + B_3(all ir, R)]. Because of the highly dispersed nature of the Na_2SO_4 on the 3% Na/Al the broad ν_3 band at 1125 cm^{-1} for solid sodium sulfate may be resolved into the observed bands at 1255, 1180 and 1065 cm^{-1}. Sulfate formation on pure alumina produces a strong band at 1390 cm^{-1} and because this band was so weak in the present case (band at 1380 cm^{-1}) we assume that most of the normal sites for formation of species II are blocked by Na.

Chapter 8

REACTION OF HYDROGEN CYANIDE AND CYANOGEN ON SILICA

8.1 INTRODUCTION

The reaction of C_2N_2 with silica has been the focus of a number of reported studies [132-135]. The main reaction of C_2N_2 with silica involved the formation of Si-NCO [132,133]. Recently, Petit and James [134,135] have studied the pyrolysis of C_2N_2 adsorbed on silica using temperature programmed desorption (TPD). For their TPD experiments, sample pretreatment consisted of outgassing silica at either 1000°C (Si(1000°C)) or 470°C (Si(470°C)) followed by cyanogen reaction at 420°C. The nature and quantity of gases evolved during pyrolysis of these two samples were very different and provided the basis for their interpretation about the types of surface species present.

Petit and James assumed that SiNCO, SiCN and SiNC initially existed on Si(1000°C), whereas only SiNCO formed on Si(470°C). Although the nature of adsorbed C_2N_2 reacted at 420°C on highly degassed silica, Si(1000°C), has been extensively studied by Ruttenburg and Low [132] and by Morrow and Cody [133], no comparative spectroscopic studies for Si(470°C) have been

undertaken. In addition, the mechanism for the C_2N_2 reaction at 420°C on Si(1000°C) remains unclear. Petit and James recognized the need for infrared studies of the products of the pyrolysis on Si(1000°C) and Si(470°C) as an accompaniment to their mass spectroscopic and thermogravametric data. Nevertheless, they proposed several mechanisms in which, at the highest pyrolysis temperatures employed (1000°C), formation of Si_3N occurred on the surface of both Si(1000°C) and Si(470°C). Furthermore, they reported that the pyrolysis of Si(1000°C) after reaction with C_2N_2 at 1000°C [135] resulted in the formation of Si_3N_4 via the overall reaction:

$$3\ C_2N_2 + 3\ SiO_2 \rightarrow Si_3N_4 + 6\ CO + N_2 \qquad (8.a)$$

Infrared and E.S.C.A. analysis of the sample by Petit and James after final pyrolysis, did not provide collaborative results.

The formation of silicon nitride is an important material in the production of integrated circuits. Ito et. al. [136] have reported that SiO_2 films can be converted to silicon nitride at the surface by heating in anhydrous ammonia at a temperature of 1200°C. Consequently, cyanogen may offer an alternative route for Si_3N_4 formation on SiO_2 films. Therefore, we have undertaken an infrared spectroscopic study to determine the nature and mechanism of C_2N_2 reaction at 420°C and during the subsequent pyrolysis using both Si(1000°C) and Si(420°C).

8.2 REACTION OF CYANOGEN AT 420°C

Ruttenburg and Low [132] observed only a weak infrared band at 2310 cm^{-1} upon addition of C_2N_2 to a highly degassed silica at 25°C, whereas numerous strong bands in the region 2400 to 2000 cm^{-1} were observed at higher contact temperatures. The disappearance of the Si-OH band at 3747 cm^{-1} was also reported and, from comparison to known silyl isocyanates, they assigned the 2310 and 1465 cm^{-1} bands to SiNCO produced via the reaction:

$$SiOH + C_2N_2 \rightarrow SiNCO + HCN \qquad (8.b)$$

Additional bands at 2218 and 2098 cm^{-1} were similarly assigned to surface cyanide species via the reactions:

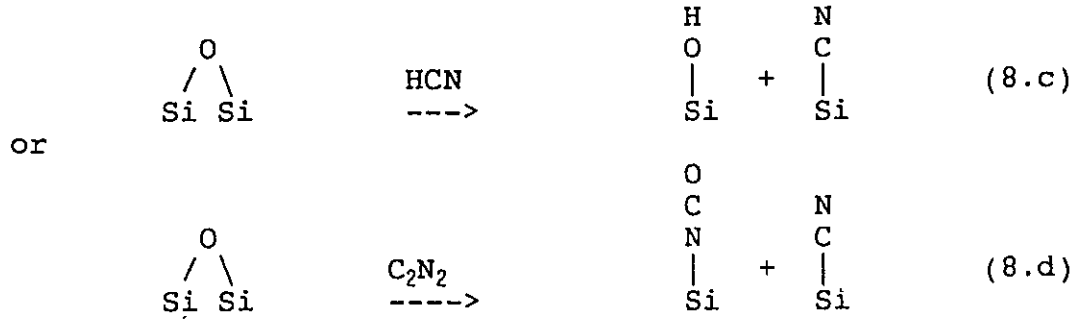

As the reaction temperature was increased above 450°C to a maximum of 600°C, an additional band, composed of two overlapping bands at 2190 cm^{-1} and at 2170 cm^{-1} formed and increased in intensity with reaction temperature. It was suggested that they could be the result of HCN polymerization or copolymerization of HCN and C_2N_2.

Morrow and Cody [133] used isotopic substitution data and force constant calculation to characterize the nature of surface species when cyanogen, hydrogen cyanide or acetonitrile reacted with highly degassed silica. Morrow and Cody were able to definitely assign bands at 3070 (ν_1 and ν_4), 2353 (ν_1 and ν_5), 2313 (ν_1), 1505 (2 ν_4) and 1470 cm^{-1} (ν_2) to a linear Si-NCO surface compound (Table 8.1). Bands at 2218 and 2100 cm^{-1} were assigned to SiCN and SiNC, respectively. The isotopic shifts observed for a 2080 cm^{-1} band did not fit either Si-CN or Si-NC and therefore, no definitive structure was assigned.

The differences between Si(1000°C) and Si(420°C) surfaces has been discussed in Section 4.3 and parts of their infrared spectra are shown in Figure 8.1(a) and Figure 8.2(a), respectively. Si(1000°C) has a symmetric SiOH band at 3747 cm^{-1}, whereas on Si(420°C), an asymmetric tail is observed on the low frequency side indicating the presence of some hydrogen bonded or perturbed silonols. In addition, Si(1000°C) has two bands at 908 and 888 cm^{-1} due to the presence of reactive siloxane sites.

The addition of C_2N_2 at 420°C to Si(1000°C) and Si(420°C) (denoted Si-cy(1000°C) and Si-cy(420°C)) is shown in Figures 8.1(b) and 8.2(b), respectively. For Si(1000°C), the reaction of C_2N_2 gave rise to the formation of SiNCO(2313/1470 cm^{-1}), SiCN(2218 cm^{-1}) and SiNC(2100 cm^{-1}). A decrease in the SiOH band at 3747 cm^{-1} and the reactive siloxane bands at 908 and 888 cm^{-1} was observed and the ratio of C_2N_2 consumed/HCN formed, was approximately one. The gas pressure measured in the cell after 20 minute contact time was equal to the initial pressure of C_2N_2

TABLE 8.1

Observed wavenumbers and isotopic shifts for the reaction of C_2N_2 on silica[b].

OBSERVED	^{13}C	^{15}N	^{18}O	ASSIGNMENT
2353	60	10	-	-NCO
2313	60	10	13	-NCO
2174[a]	70	28	-	N≠C=N
2218	51	30	0	-CN
2100	39	36	0	-NC
2078	58	20	0	
1505	0	25	-	-NCO
1470	0	30	34	-NCO

[a] from this thesis.

[b] from Morrow and Cody, ref. 133.

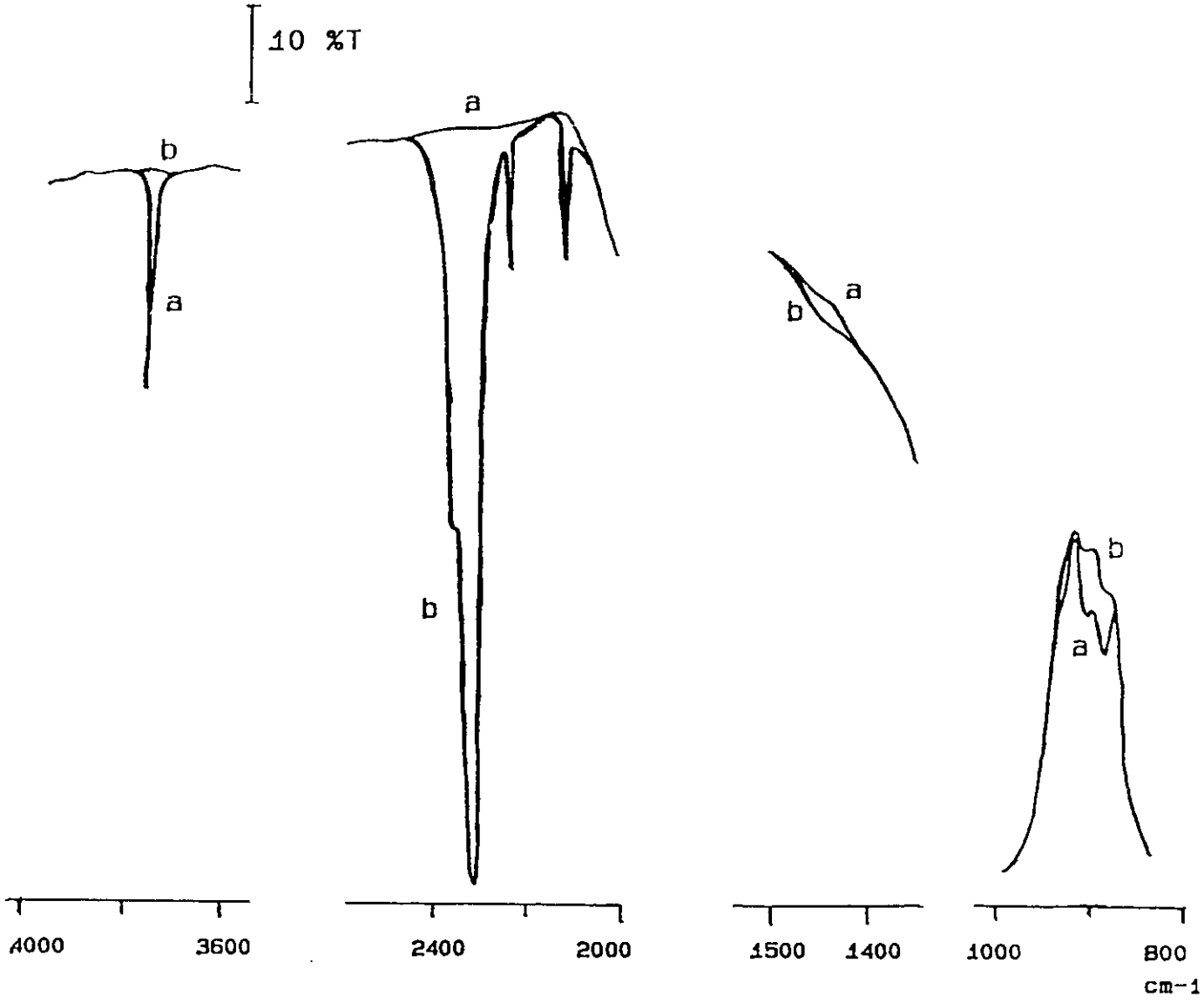

Figure 8.1

a) Silica degassed at 1000 °C 5 hrs., followed by;
b) addition of 100 umole g^{-1} C_2N_2 at 420 °C for 2 hrs.

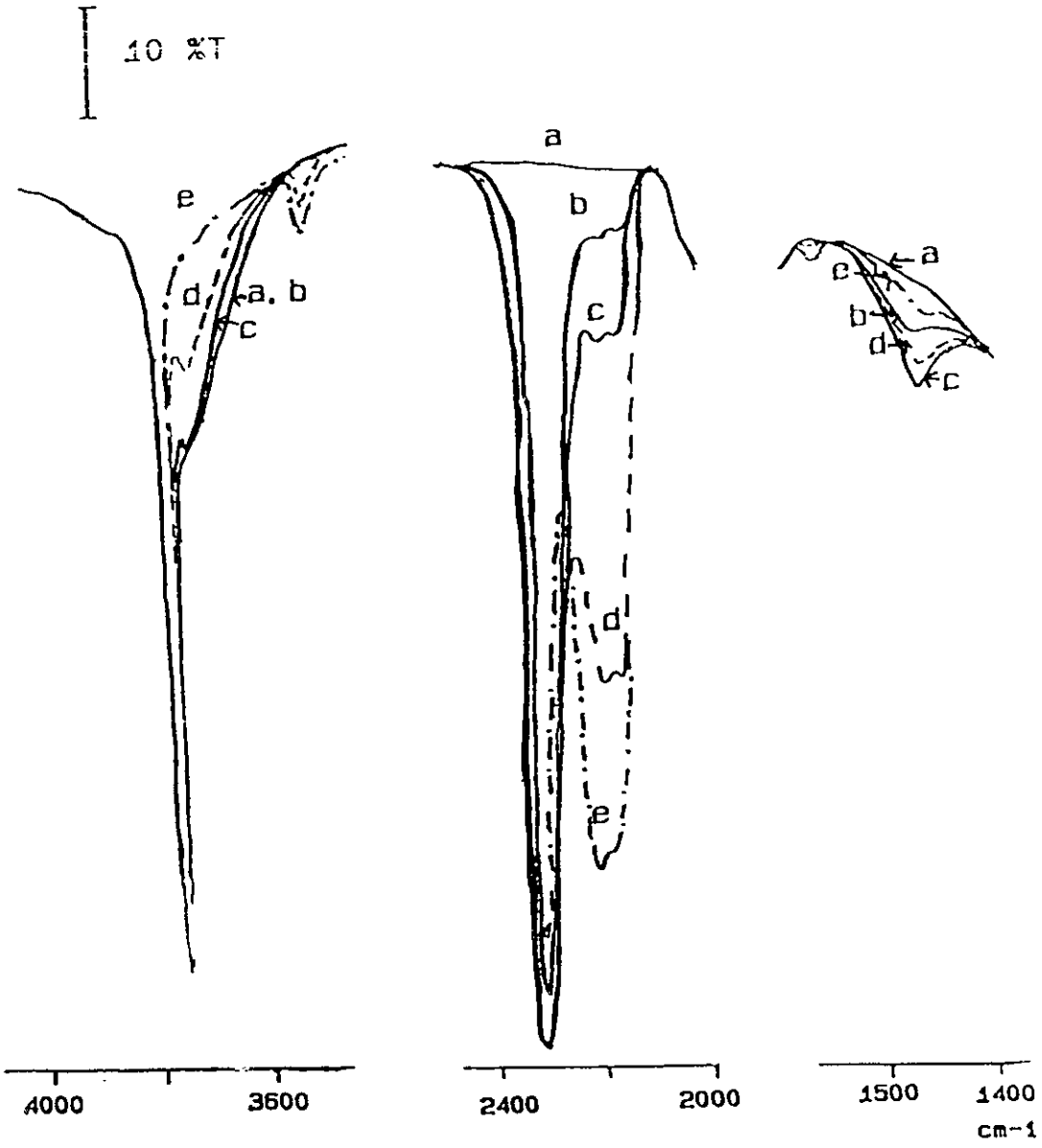

Figure 8.2

a) Silica degassed at 420 °C for one hour with;
b) 100 umole g^{-1} C_2N_2 added
at 300 °C for 14 hours followed by,
c) Heating at 420 °C for one hour.
d) Evacuation at 550 °C for one hour.
e) evacuation at 750 °C for one hour.

added and by mass spectroscopic analysis was shown to be HCN. Once all SiOH were removed no further spectroscopic changes were observed.

For Si-cy(420°C), the spectrum obtained was quite different from that of Si-cy(1000°C). The amount of SiNCO formed with Si-cy(420°C) was much greater than obtained with Si-cy(1000°C) and no bands due to SiNC or SiCN were observed. Additional overlapping broad bands centered at 2200 and 2174 cm^{-1} appeared even at contact temperatures as low as 300°C. In contrast, no spectral changes were observed on Si(1000°C) when C_2N_2 was added and heated to 300°C.

As observed for Si-cy(1000°C), with Si-cy(420°C) a decrease in the SiOH at 3747 cm^{-1} along with formation of SiNCO did occur and the ratio of C_2N_2 consumed/HCN produced was one. The latter, along with the decrease in the SiOH band, would suggest that the primary reaction with both surfaces occurs via Reaction (8.b).

The absence of SiNC or SiCN bands on Si-cy(420°C) confirms that formation of these involve reactions with the reactive siloxane sites. These sites are known to form only at outgassing temperatures greater than 450°C and, therefore, would not be present on Si(420°C). The formation of the 2218 and 2100 cm^{-1} bands were observed when Si(420°C) was heated in the presence of C_2N_2 at temperatures greater that 450°C. In additional experiments, it was observed that the intensity of the 2218 and 2100 cm^{-1} bands after reaction of C_2N_2 at 420°C, was proportional to the initial outgassing temperature of the silica. The number of siloxane sites created, represented by the 908 and 888 cm^{-1}

bands, is also proportional to the initial outgassing temperature.

Reaction with siloxane sites may occur with C_2N_2 or HCN via Reactions (8.c) and (8.d), respectively. However, the C_2N_2/HCN ratio of 1 would imply that HCN is not involved in further reactions with the surface. To confirm this, HCN(200 umole g^{-1}) was added to Si(1100°C) and after heating to 420°C, no infrared bands due to chemisorbed species were observed. However, when heated at 480°C, very weak bands at 2313, 2218 and 2100 were observed.

Therefore, reaction of C_2N_2 with Si(1000°C) at 420°C proceeds via Reactions (8.b) and (8.d) and not Reaction (8.c). For Si-cy(420°C), reactive siloxane sites were not initially present and, therefore, SiNCO mainly forms via Reaction (8.b). However, additional bands at 2200 and 2174 cm^{-1}, previously assigned to unspecified polymers [132,133], also exist on this surface. These bands also formed to some extent on Si-cy(1000°C) when intense bands due to SiNCO were present. Consequently, Petit and James' assumption that only Si-NCO was present initially when C_2N_2 was reacted at 420°C with Si-cy(420°C), is not correct.

8.2.1 ISOTHERMAL PYROLYSIS

The amount and type of gases evolved in the isothermal pyrolysis (IP) of Si-cy(1000°C) and Si-cy(470°C) obtained by Petit and James, is shown in Figures 8.3(a) and 8.3(b). They

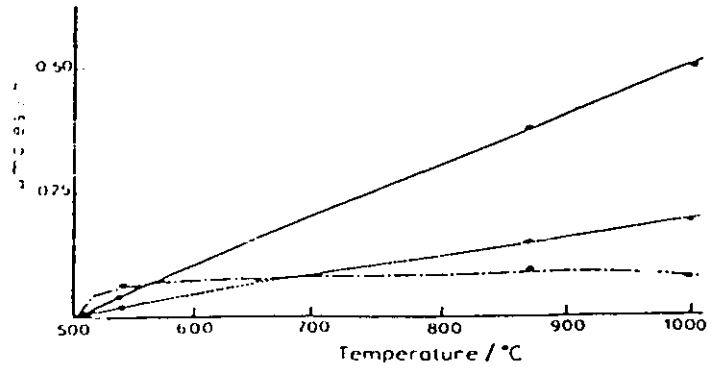

Figure 8.3(a)

Isothermal pyrolysis of Si(1000 °C). Average rate of ——, CO; ·····, N_2; and —·—· , CO_2 evolution at different temperatures.

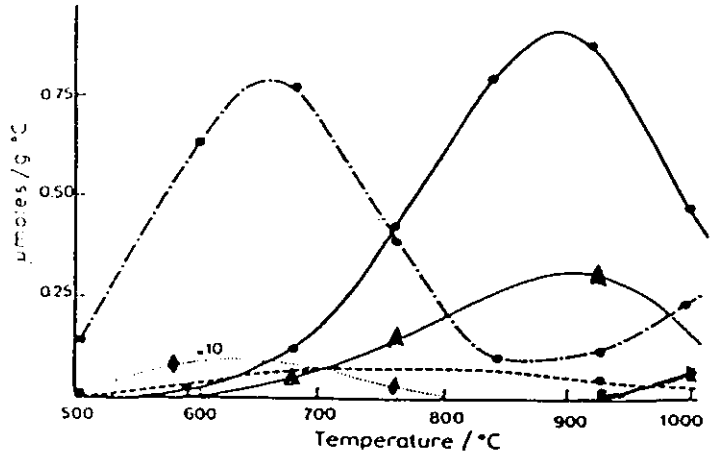

Figure 8.3(b)

Isothermal pyrolysis with Si(470 °C). Average rate of —●—, CO; —▲—, N_2; and —·—·, CO_2; ----, HCN; ···◆···, HNCO; and —■—, H_2 evolution at different temperatures.

From Petit and James. Ref. 134.

concluded that the differences must be due to the higher concentration of surface hydroxyls on Si(470°C).

On Si-cy(1000°C), when only SiNCO was presumed to be present, it was postulated that pyrolysis resulted in the thermal decomposition of SiNCO by two possible pathways. The first pathway was:

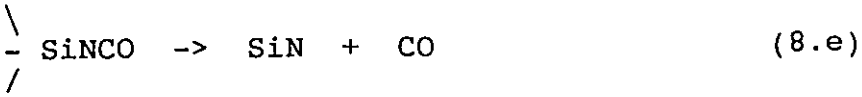

followed by SiN reorganization at the highest temperature to form Si_3N by:

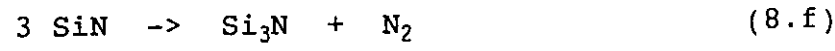

The second pathway involved destruction of two adjacent SiNCO:

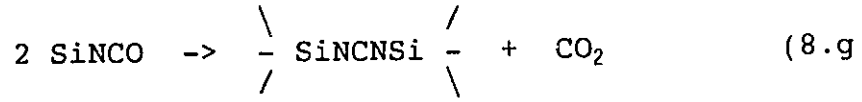

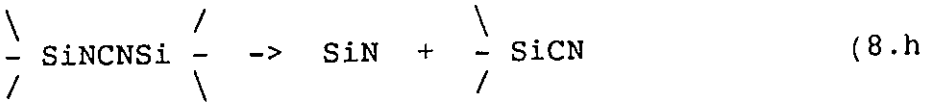

The SiN formed, would be converted to Si_3N via Reaction (8.f), leading to the overall stoichiometry:

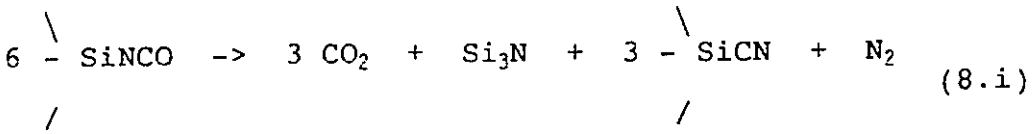

(8.i)

On Si-cy(470°C), decomposition of Si-NCO could occur with SiOH via the reaction:

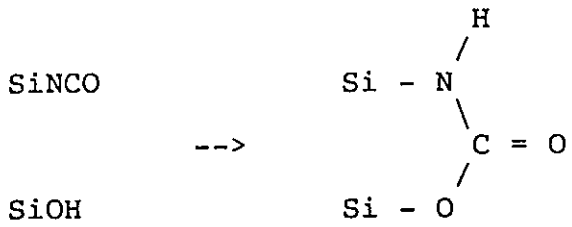

(8.j)

which, during TPD is followed by:

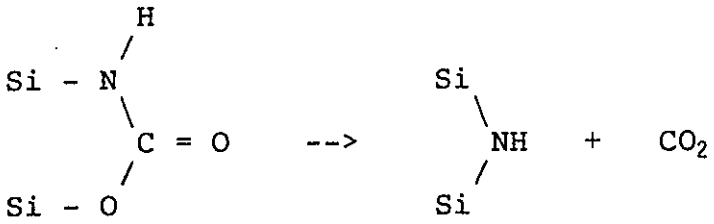

(8.k)

At the highest temperature, Si_3N would form by the reaction:

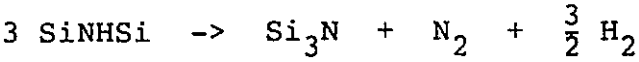

(8.l)

We have determined from spectroscopic studies that additional species exist at 420°C on Si-cy(420°C) or Si-cy(470°C) other than Si-NCO which would influence the pyrolysis mechanisms proposed. Therefore, we have used spectroscopic methods to study the pyrolysis of these surfaces. If formed, the products in Reactions (8.g), (8.h), (8.j) and (8.k) should produce characteristic infrared bands.

8.2.2 PYROLYSIS OF Si-cy(1000°C)

The infrared spectra observed after pyrolysis of a deuterated Si-cy(1000°C) at various temperatures are shown in Figure 8.4. No shifts in frequency were observed for the bands formed as a result of using a deuterated silica. Because of the complexity in the observed spectra, the changes in band intensities are shown for clarity in Figure 8.5. (The band at 2313 cm^{-1} (SiNCO) was totally absorbing during most of the pyrolysis. Intensity changes in this band was monitored by changes in the 2365 cm^{-1} band.) In general, the outgassing of Si-cy(1000°C) samples from 450°C to 900°C resulted in the decrease of the 2313/1470 cm^{-1} bands and formation of a band at 2174 cm^{-1}. This was also accompanied by the appearance of a sharp band at 2080 cm^{-1} and by the decrease and eventual disappearance of bands at 2218 and 2100 cm^{-1}. The 2080 cm^{-1} band was removed only upon evacuation at temperatures above 900°C. The 2174 cm^{-1} band remained after evacuation at 1000°C, with only a slight reduction in intensity. The same results were observed if the pyrolysis was carried out in a

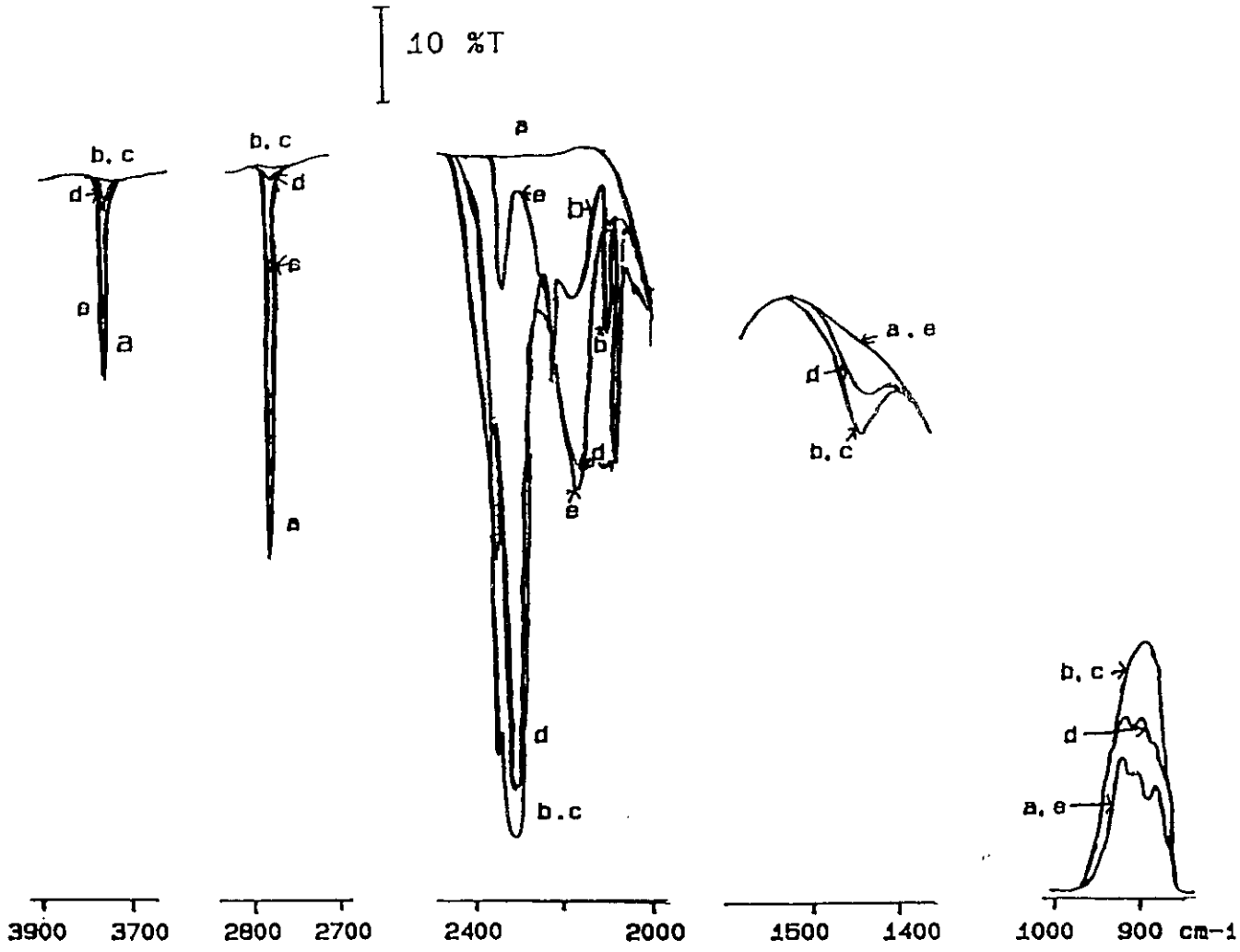

Figure 8.4

Pyrolysis of a deuterated Si(1000 °C).
a) Si(1000 °C) heated with 100 umole g^{-1} C_2N_2 at 420 °C for 2 hrs. followed by;
b) evacuation at 515 °C 18 hrs.
c) evacuation at 800 °C 2 hrs
d) evacuation at 1000 °C 2 hrs.

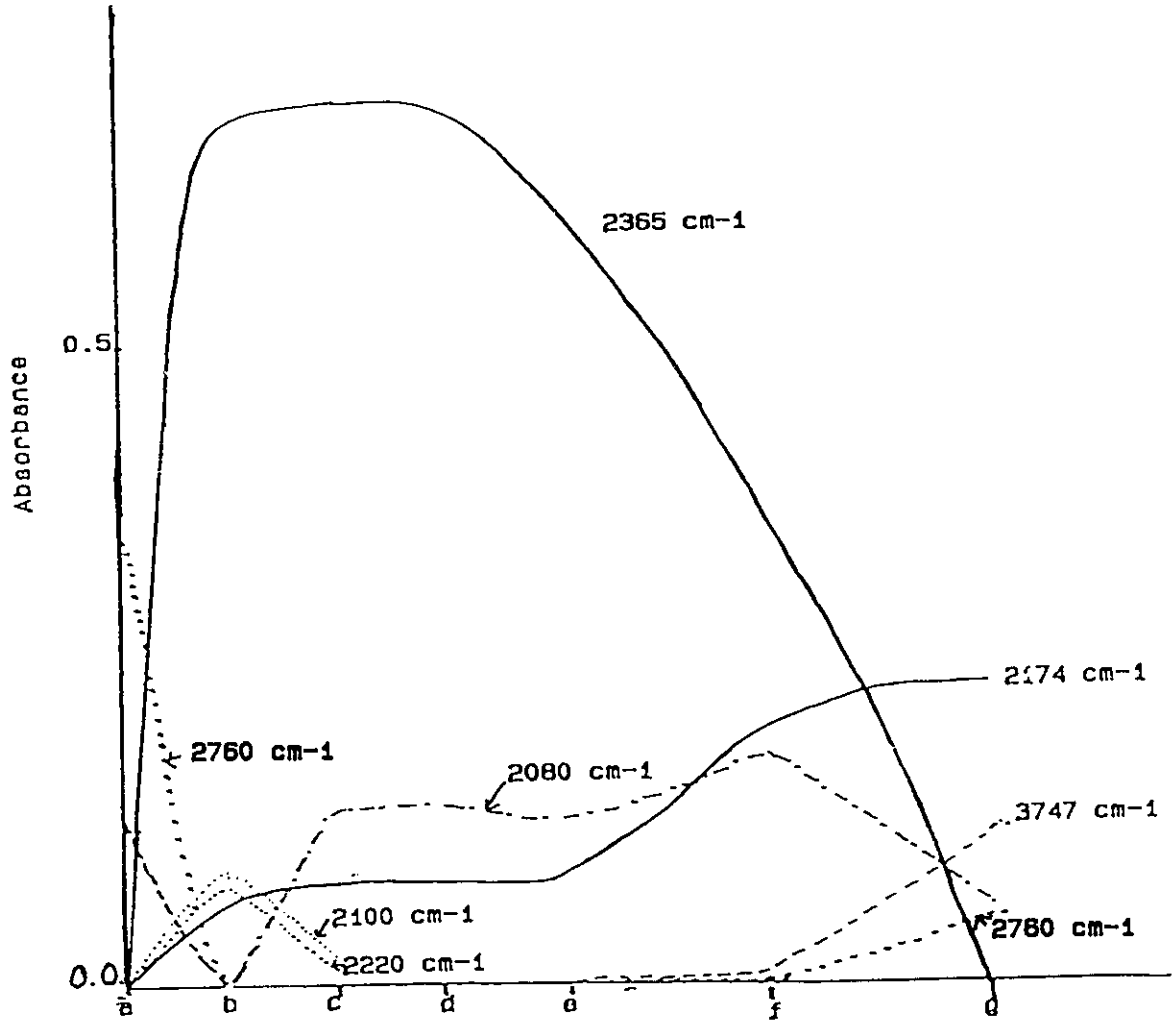

Figure 8.5

Band intensity changes for the spectra shown in Figure 8.4
a) Si(1000 °C), b) add 100 umole g^{-1} C_2N_2 at 420 °C
for 2 hrs. followed by evacuation at c) 515 °C, 18 hrs.;
d) 515 °C, 36 hrs. e) 595 °C, 2 hrs.;
f) 800 °C, 2 hrs.; and g) 1000 °C, 2 hrs.

closed cell. With the closed cell, mass spectroscopic analysis of the gas phase at 600°C showed that CO_2 had formed.

The SiOH/SiOD bands which were eliminated prior to pyrolysis returned (although reduced in intensity) at the highest pyrolysis temperatures employed. It was initially thought that this was due to the slight decomposition of the species responsible for the 2174 cm^{-1} band. However, this band did not shift on the deuterated Si-cy(1000°C) and therefore this species did not contain hydrogen. In addition, the relative SiOH/SiOD intensity after pyrolysis did not match the initial SiOH/SiOD ratios. We conclude that residual H_2O from the quartz cell or small leakages associated with the long pyrolysis times at high temperatures would result in some rehydroxylation of the surface.

Formation of the 2174 cm^{-1} band occurred even when bands at 2218 or 2100 cm^{-1} were not present. Both SiNC and SiCN bands are converted to SiNCO by heating in O_2 at 420°C [133]. In this case, no band at 2080 cm^{-1} was observed to form during pyrolysis. Hence, the formation of the 2174 cm^{-1} band along with CO_2 only involved conversion of SiNCO groups. This was also observed for Si-cy(420°C) where no SiCN or SiNC bands were present before pyrolysis.

To further clarify the nature of the 2174 cm^{-1} band, isotopic studies were employed. A 1:1 mixture of $^{13}C_2N_2/^{12}C_2N_2$ was added to Si(1000°C) and heated to 420°C. The resulting spectrum gave rise to bands of equal intensity at 2313 and 2253 cm^{-1} due to $SiN^{12}CO$ and $SiN^{13}CO$, respectively. The same result could be achieved by heating Si(1000°C) sequentially with either ^{13}C or ^{12}C labelled

C_2N_2. Upon pyrolysis above 500°C, two bands at 2174 and 2105 cm^{-1} were observed. Both the 2174/2105 cm^{-1} bands and the evolved $^{12}CO_2/^{13}CO_2$ ratios, were equal to the initial $SiN^{12}CO/SiN^{13}CO$ ratio on the silica surface.

A similar experiment with $C_2{}^{15}N_2/C_2{}^{14}N_2$ was also attempted. However, a FWHH of 40 cm^{-1} for the 2174 cm^{-1} band did not permit resolution of the overlapping bands. After pyrolysis in a closed cell at 1000°C, mass spectroscopic analysis of the gas phase revealed that no $^{15}N_2$ or $^{15}N^{14}N$ formed, indicating that dinitrogen was not evolved.

The ^{13}C results suggest that the 2174 cm^{-1} species contains only one carbon atom. Formation of organic carbodiimides is known to occur readily via the reaction [137]:

$$2\ R\text{-}NCO \xrightarrow{\text{catalyst}} R - N = C = N - R + CO_2 \qquad (8.m)$$

Carbodiimides exhibit strong bands in the 2200 to 2100 cm^{-1} region. Hence, the formation of a carbodiimide from the condensation of two adjacent isocyanates is plausible via the reaction:

$$2\ SiNCO \rightarrow Si\text{-}N = C = N - Si + CO_2 \qquad (8.g)$$

After pyrolysis at 1000°C, Petit and James [134] reported that 68.4% C, 32% N_2 and 96% O_2 (assuming 100% O_2 originates from SiNCO) was restored to the gas phase. The remaining surface species would contain a N/C ratio of two, consistent with a carbodiimide structure.

Morrow and Cody [133] reported the formation of a sharp band at 2080 cm^{-1} with C_2N_2 but not with HCN. The isotopic shifts observed (Table 8.1) did not fit SiNC or SiCN structures and remained unassigned although it was suggested that this band was a precursor for polymer formation.

We are in agreement with the isotopic results observed for the 2080 cm^{-1} band; however, we have found that the 2080 cm^{-1} band can form if large quantities of HCN are used and after prolonged heating. The HCN reaction on Si(1000°C) occurs to a much lesser extent than with C_2N_2.

Eley et. al. [138] have reported a band at 2210 cm^{-1} for C_2H_5NCO adsorbed on silica which was stable upon evacuation at temperatures up to 900°C. This stability was also observed for both the 2218 and 2100 cm^{-1} bands with HCN reacted on silica. However, for C_2N_2, upon formation of the carbodiimide (~ 500°C) the bands at 2218 and 2100 cm^{-1} decreased and this was paralleled by the formation of an equally intense and sharp band at 2080 cm^{-1}. The 2080 cm^{-1} band increased in intensity at the expense of the 2218 and 2100 cm^{-1} bands and remained stable up to temperatures of 900°C. For several silica samples initially degassed at progressively higher temperatures above 500°C, the band at 2080 cm^{-1} was always of the same relative intensity as the 2218 (SiCN) and 2100 cm^{-1} (SiNC) bands and was only present when the band at 2174 cm^{-1} formed. The 2080 cm^{-1} band did not form upon pyrolysis of Si-cy(420°C).

Evidently, the 2080 cm^{-1} band is due to a SiCN or SiNC type species which is generated at the expense of the SiCN and SiNC

species, and it is observed only when there is a band at 2174 cm^{-1} due to the carbodiimide. A plausible reaction might be;

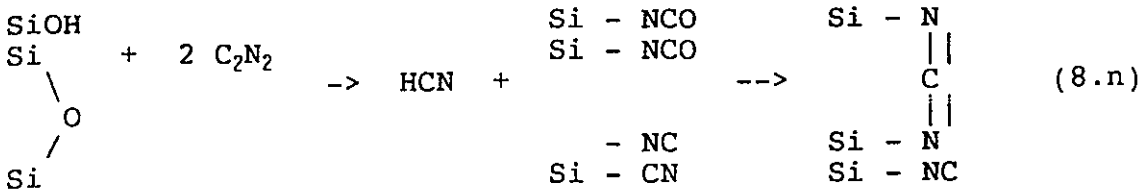

(8.n)

An additional increase in intensity of the 2080 cm^{-1} band was observed when both the 2218 and 2100 cm^{-1} bands were already eliminated. This may be due to a partial decomposition of the carbodiimide as shown in Reaction 8.h.

8.2.3 PYROLYSIS OF Si-cy(420°C)

The spectrum observed during pyrolysis of Si-cy(420°C) is shown in Figure 8.2. With increasing temperature from 420 to 900°C, the SiOH band at 3747 cm^{-1} decreased along with the SiNCO bands, whereas the 2200/2174 cm^{-1} bands increase in intensity. In addition, the broad asymmetric SiOH shoulder due to hydrogen bonded or perturbed hydroxyls between 3700 and 3500 cm^{-1} was completely eliminated above 750°C. Concurrent with this elimination was the formation of two bands at 3450 and 1550 cm^{-1} which are undoubtedly due to $SiNH_2$ [139,140]. The 3450, 2200, 2174 and 1550 cm^{-1} bands are stable to 900°C. At 1000°C, the 2200 and 2174 cm^{-1} bands decrease slightly in intensity and the 3450 and 1550 cm^{-1} bands were eliminated.

The 2174 cm^{-1} band can be observed on Si-cy(1000°C) during pyrolysis of that surface, whereas the 2200 cm^{-1} band is unique to the Si-cy(420°C) surface. In further experiments, it was observed that the intensity of the 2200 cm^{-1} band relative to the 2174 cm^{-1} band decreased when the silica was initially degassed at progressively higher temperatures from 300°C to 800°C. We conclude that the 2200 cm^{-1} band involves some reaction of SiNCO with surface hydroxyls.

The presence of the small amount of $SiNH_2$ is due to a secondary reaction. This was formed only on Si-cy(420°C) and occurred when the asymmetric SiOH tail (between 3700 and 3500 cm^{-1}) was diminished. Once this hydrogen bonded SiOH was removed, no further increase in the $SiNH_2$ bands were observed. We conclude that $SiNH_2$ formation results from the reaction of H_2O with SiNCO by:

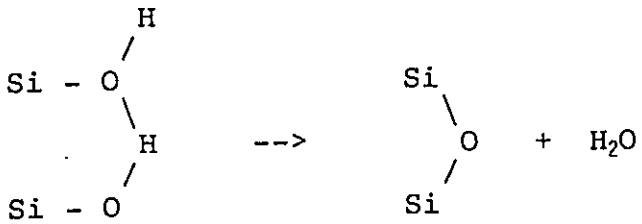

(8.o)

$$H_2O + SiNCO \rightarrow SiNH_2 + CO_2 \qquad (8.p)$$

The above reaction is known to occur with organic isocyanates [140]:

$$R\text{-}NCO + H_2O \rightarrow R\text{-}NH_2 + CO_2 \qquad (8.q)$$

At no times were bands due to Si_2NH or $SiO\text{-}\overset{\overset{O}{\|}}{C}\text{-}\overset{\overset{H}{|}}{N}\text{-}Si$ observed. Hence, the large differences between the pyrolysis results observed by Petit and James must be due to the presence of the 2200 cm^{-1} bands and H_2O formation from condensation of adjacent hydroxyls on Si-cy(420°C).

8.3 SUMMARY

Reaction of C_2N_2 with Si(1000°C) at 420°C, produces SiNCO via reaction with SiOH sites and SiCN or SiNC with reactive siloxane sites. Pyrolysis of this surface results in the formation of a carbodiimide Si-N=C=N-Si, via reaction of adjacent SiNCO. SiCN or SiNC are not involved in the carbodiimide formation. The carbodiimide is stable to 900°C and diminishes slowly at 1000°C. The 2080 cm^{-1} band is probably due to SiNC or SiCN adjacent to the carbodiimide.

Addition of C_2N_2 at 420°C to Si(420°C) forms only SiNCO which further reacts with other SiNCO to produce a carbodiimide or with SiOH groups to produce a polymeric species with a band at 2200 cm^{-1}. The reaction of C_2N_2 occurs more readily with Si(420°C) than with Si(1000°C). This can be attributed to the higher initial hydroxyl concentration on Si(420°C). No SiCN or SiNC are formed

on this surface. During pyrolysis, a small amount of $SiNH_2$ is formed from the reaction of H_2O with SiNCO.

Chapter 9

REACTION OF HYDROGEN CYANIDE AND CYANOGEN WITH DEHYDROXYLATED ALUMINA

9.1 INTRODUCTION

The removal of NO_x pollutants from automobile exhaust has been the subject of intense research and development [141-145]. Normally, this is carried out by catalytic reduction of NO_x with CO over a suitable catalyst, particularly noble metals such as platinum or ruthenium impregnated on alumina. Ruthenium is preferred because it exhibits a high selectivity for formation of N_2 as a product while other noble metals produce undesirable byproducts, such as NH_3 [146-149].

In the reaction of NO with CO, formation of NCO is a main intermediate in the process. It is postulated that reaction of the NCO with H_2O leads to the formation of NH_3 [144]. Although initial formation of isocyanate occurs at the noble metal, rapid migration of the isocyanate to the support is observed. This quick migration has been reported for several oxides including TiO_2, MgO, Al_2O_3 and SiO_2 [150].

In the previous chapter, we have reported that formation of Si-NCO is the main product in the reaction of C_2N_2 or HCN with SiO_2. By analogy, this may also be true for other oxides, such as alumina, and therefore, a study of this reaction may lead to a better understanding on the formation and reactivity of NCO on alumina. However, to the best of the writer's knowledge, the reaction of C_2N_2 with alumina has not been studied.

The reaction of C_2N_2 on silica mainly occurred with SiOH sites, liberating HCN as a product in the process. The presence of the SiOH groups also yielded at least one type of polymeric species on the surface. Al_2O_3, on the other hand, can be totally dehydroxylated by heating above 800°C. Therefore, the reaction of C_2N_2 with AlOH, Lewis acidic or basic sites and subsequent polymerization can be studied independently. The absence of Al-OH sites ensures that surface species do not contain hydrogen and that HCN as a product does not form. C_2N_2 may then be a useful probe molecule for studying reactive sites on alumina. This may also lead to additional information regarding polymeric species which forms on SiO_2.

9.2 RESULTS AND DISCUSSION

9.2.1 HCN

Kortum and Delfs [151] first reported that HCN polymerized on several oxides, including Al_2O_3, MgO, CeO_2, but not on SiO_2. Low and Ramamurthy [152] using infrared spectroscopy found that

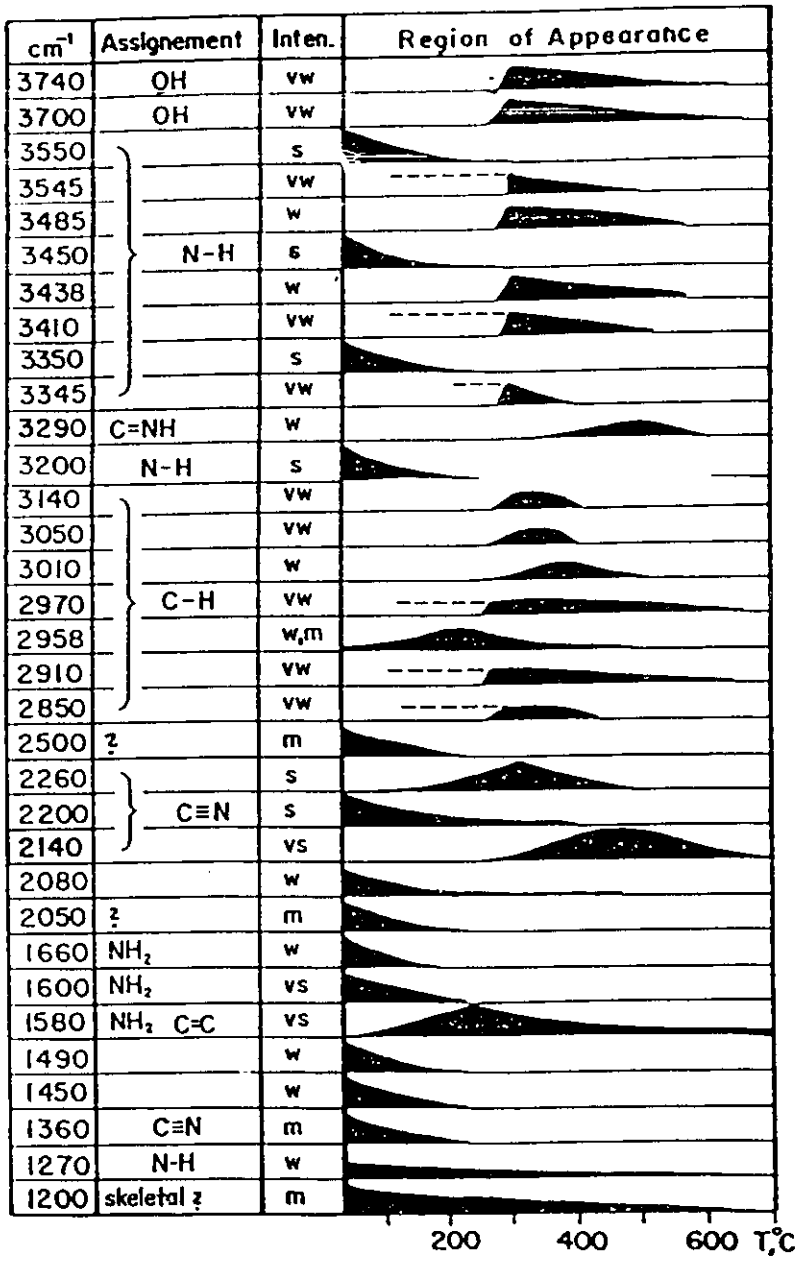

Table 9.1

Addition of HCN to alumina.
Intensities: vw, very weak; w, weak; m, medium; s, strong vs, very strong. Dashed lines indicate uncertainty.
(From Low and Ramamurthy. Ref 152.)

HCN adsorbed and polymerized rapidly at room temperature on alumina. Rapid polymerization was indicated by an immediate orange-red colourization of the alumina upon HCN addition. In their experiments, large quantities of HCN (47 umoles g^{-1}) were left in contact with the Al_2O_3 for two hours prior to recording of spectra. The alumina was degassed, treated with oxygen, then degassed at 750°C for twenty hours prior to HCN addition. Three types of HCN polymers were postulated, which were based upon various spectral changes that occurred after evacuation at elevated temperatures. Bands were assigned from the comparison of observed spectral frequencies to group frequencies of known cyano compounds. A summary of Low and Ramamurthy's spectroscopic results and band assignments is shown in Table 9.1.

HCN has been shown to form a tetramer, diamminomaleonitrile (I) [153]. Bands at 3450, 3350 and 3200 cm^{-1} were assigned to hydrogen bonded N-H, 2220 cm^{-1} to $-C\equiv N$, 1700-1500 cm^{-1} to $-NH_2$ deformations and C=C, 1360 cm^{-1} to -C-N and 1270 cm^{-1} to $-NH_2$ of (I). The existence of other bands in the C-H and N-H regions were assigned to other polymeric structures (II) and (III).

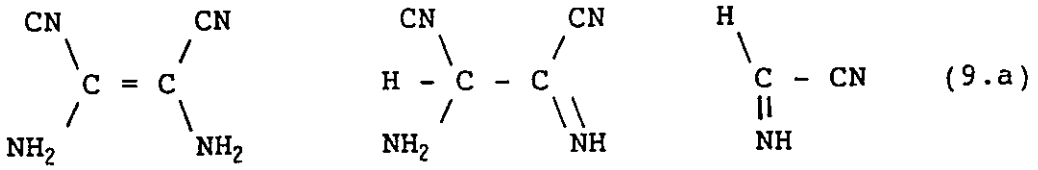

I II III (9.a)

Since both large quantities of HCN and long reaction times were employed, no information on the initial reaction of HCN with

Al_2O_3 or the mechanism of formation of polymeric species was obtained.

In Figure 9.1, 1.9 umole g^{-1} HCN was added to Al(800°C) and spectra were acquired at ten-second intervals. Initial contact of HCN gave rise to broad bands at 3662(-OH), sharp bands at 3298 (NC-H) and at 2154 and 2094 (-CN), and by weak bands at 1600, 1464 and 1323 cm^{-1}. A new band at 2226 cm^{-1} along with a broad band containing several ill-defined shoulders from 3600 to 2900 cm^{-1}, and bands at 1660, 1624, 1600, 1378, 1323, 1286 and 1241 cm^{-1} formed within one minute of initial contact time and continued to increase uniformly for the entire duration of the experiment (See Figures 9.2 and 9.3). Concurrent to this, the bands at 2154, 2094 and 1323 cm^{-1} decreased in intensity and this was accompanied by an orange-red colourization of the alumina. Similar results were observed for HCN on Al(400°C). Little or no change occurred in the OH region of Al(400°C).

The above result showed that HCN rapidly adsorbed on alumina and that polymeric species rapidly formed. The different rate of disappearance of the 2154 and 2094 cm^{-1} bands indicated that at least two types of adsorbed HCN species are present initially.

Alumina degassed at 800°C is essentially devoid of any surface hydroxyls. The dehydroxylation process exposes both catalytically active cus Lewis acid Al^{+3} and cus basic O^{-2} sites. To examine the reactivity of HCN with these sites, we have used pyridine and BF_3 as selective poisons. Pyridine has long been used as a probe and selective poison for acidic sites on alumina [27]. Coordination of pyridine to Lewis acid sites occurs via

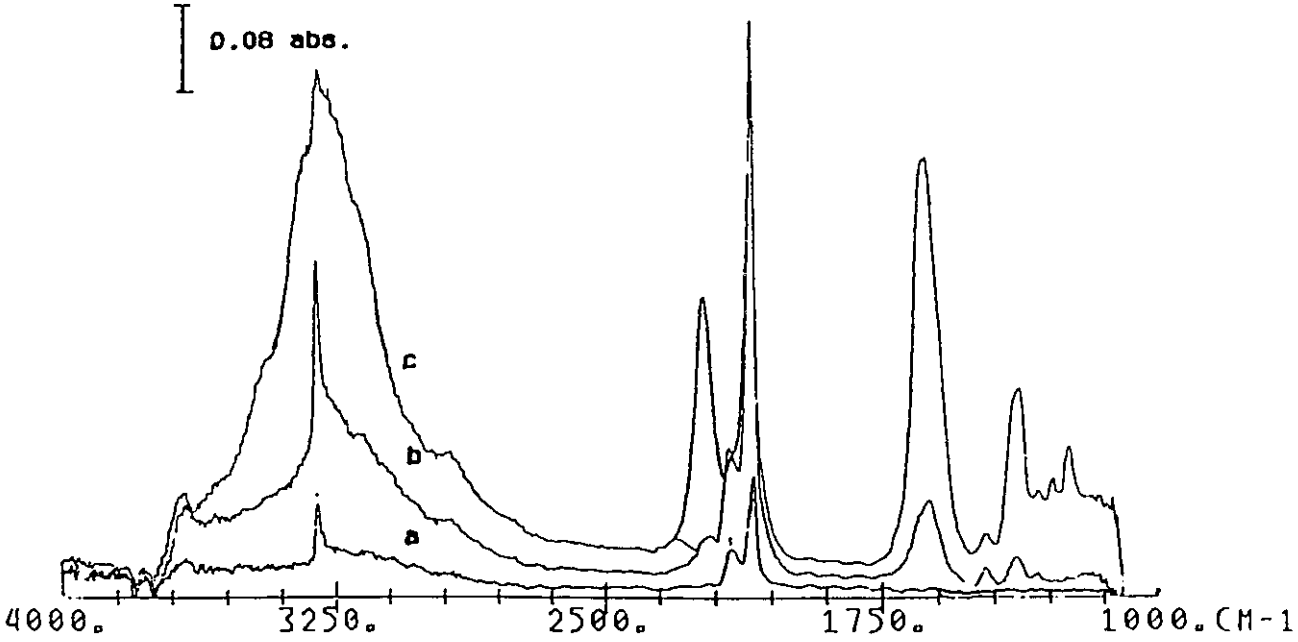

Figure 9.1

Addition of HCN to Al(800 °C).
Spectra were recorded at 10 second intervals.
a) 10 seconds
b) 20 seconds
c) 190 seconds

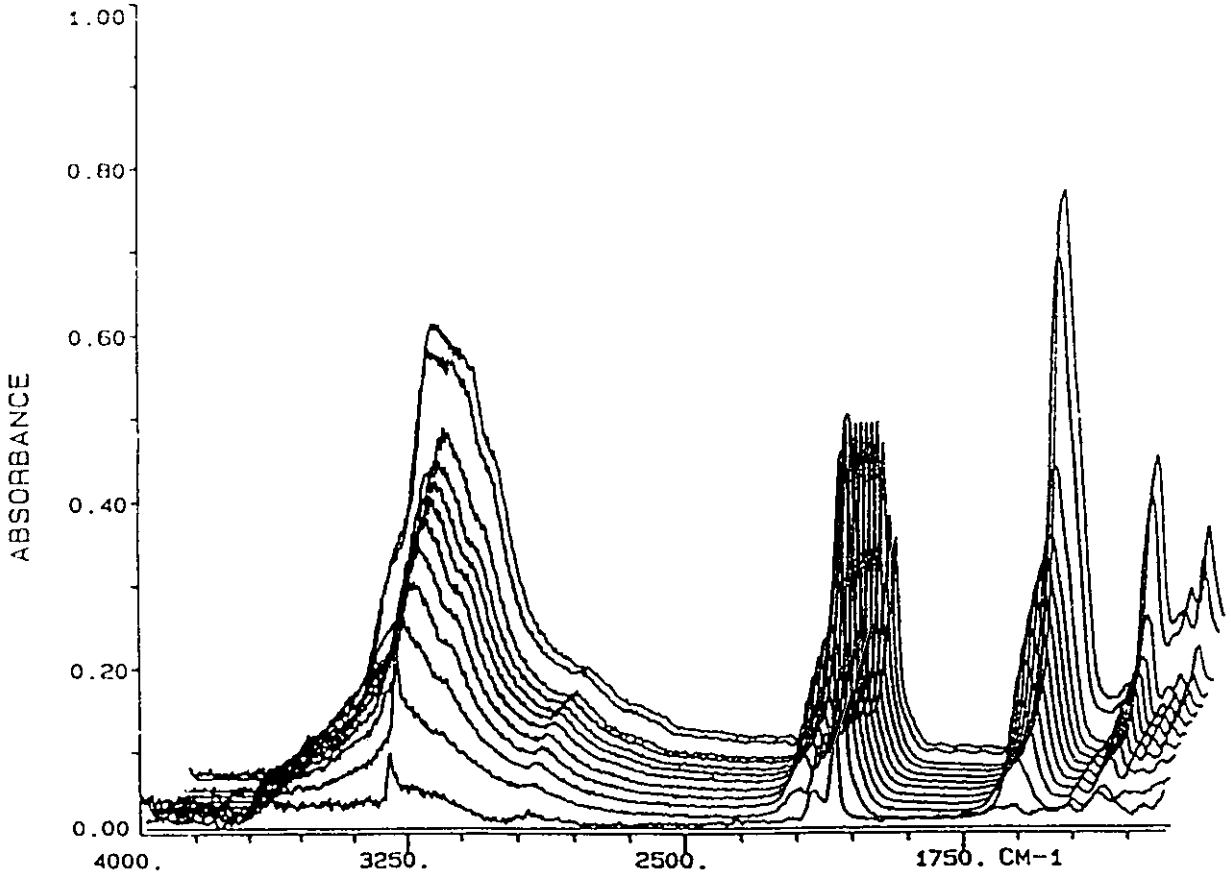

Figure 9.2

Addition of HCN to Al(800 °C). Spectra were recorded in ten second intervals. The last two spectra represent ten minutes and twenty minutes, respectively. Spectra are offset horizontally.

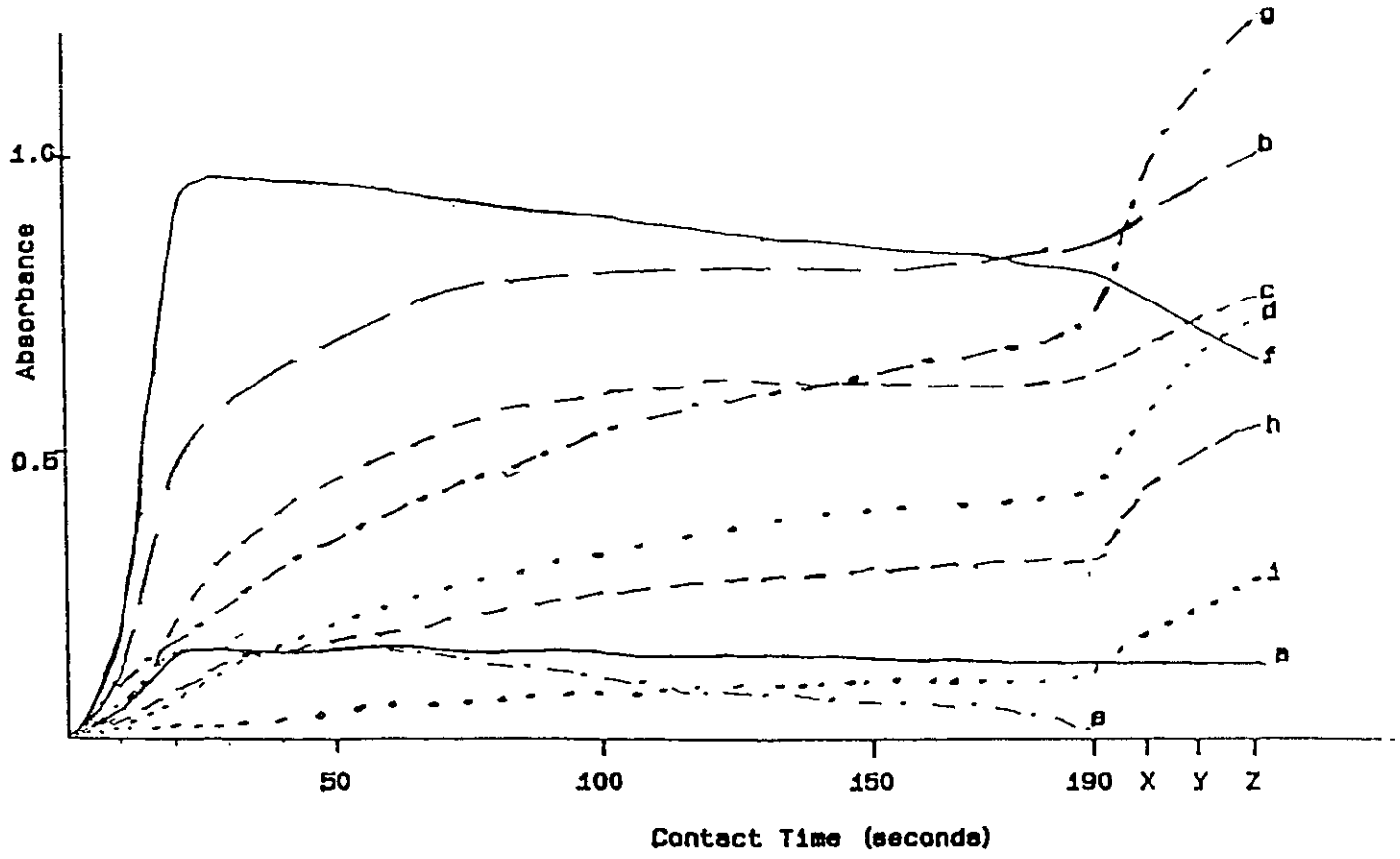

Figure 9.3

Band intensity versus HCN contact time for Figure 9.2. Plots are for bands located at:
a) 3660 cm^{-1}, b) 3298 cm^{-1}, c) 3188 cm^{-1},
d) 2226 cm^{-1}, e) 2154 cm^{-1}, f) 2094 cm^{-1},
g) 1624 cm^{-1}, h) 1378 cm^{-1}, and i) 1286 cm^{-1}.

X, Y and Z refer to ten, twenty and thirty minute contact time, respectively.

reaction with the lone pair electrons on the nitrogen atom and is characterized in the spectrum by bands located at 1632 and 1459 cm^{-1}.

Rhee and Basila [154] reported that BF_3 reacted with surface hydroxyls of alumina according to:

$$AlOH + BF_3 \rightarrow Al - \underset{\displaystyle H}{O} : \underset{\displaystyle F}{BF_2} \rightarrow Al\text{-}OBF_2 + HF \qquad (9.b)$$

Reaction with a completely dehydroxylated alumina gave rise to the same spectral bands in the 1800 to 900 cm^{-1} region. Reaction with basic oxygen anions was suggested to occur via:

$$_{cus}Al^{+3} \; _{cus}O^{-2} + BF_3 \rightarrow \underset{\displaystyle Al}{\overset{\displaystyle F}{|}} \quad \underset{\displaystyle O}{\overset{\displaystyle F_2B}{|}} \qquad (9.c)$$

Schwab and Kral [155] have reported the use of BF_3 as a probe for basic sites on alumina. Later, Karge and Dalla Lana [52] examined the site blocking effects of BF_3 on centers for adsorption of SO_2. Two types of adsorbed SO_2 are observed on a dehydroxylated Al_2O_3, one a 1065 cm^{-1} band due to a strongly adsorbed SO_3^- with basic oxygen sites and, a weakly held SO_2 to Lewis Al^{+3} sites located at 1330 cm^{-1}. On a dehydroxylated Al_2O_3, the intensity of the 1065 cm^{-1} band diminished when increasing amounts of BF_3 was preadsorbed, whereas the band at 1330 cm^{-1} showed a slight increase. Hence, basic O^{-2} sites were blocked by

BF_3, whereas Al^{+3} sites, responsible for weak adsorption of SO_2, were not poisoned.

On Al(800°C), predoped with pyridine addition of HCN, gave rise to the OH band at 3660 cm^{-1}, a weak band at 2200 cm^{-1}, and the sharp band at 2100 cm^{-1} (Figure 9.4(d)). No bands at 3298 or 2154 cm^{-1} were observed. All other bands were due to preadsorbed pyridine and virtually did not change when HCN was added. In contrast, on Al(800°C) predoped with BF_3, addition of HCN resulted in a large band located at 3298 cm^{-1} (Figure 9.4(b)) along with a band at 2186 cm^{-1}. No polymer bands were observed to form for either case.

These results confirm the existence of two types of adsorbed HCN on Al_2O_3 prior to the onset of polymerization. One species involves the dissociative adsorption of HCN on cus O^{-2} sites giving rise to bands at 3660 and 2094 cm^{-1} (the 3660 cm^{-1} band is undoubtedly due to a hydroxyl group) and a second physisorbed species on cus Al^{+3} sites characterized by sharp bands at 3298 and 2154 cm^{-1}.

A 2094 cm^{-1} band has also been observed for C_2N_2 adsorption on Al_2O_3. An identical isotopic shift of 42 cm^{-1} was observed for this band for either $H^{13}CN$ or $^{13}C_2N_2$ addition and is assigned to Al-NC (see next section). Therefore, the dissociative adsorption of HCN may proceed via the reaction:

$$_{cus}Al^{+3} \quad _{cus}O^{-2} + HCN \rightarrow \begin{matrix} C \\ N \\ | \\ Al \end{matrix} + \begin{matrix} H \\ | \\ O \end{matrix} \qquad (9.d)$$

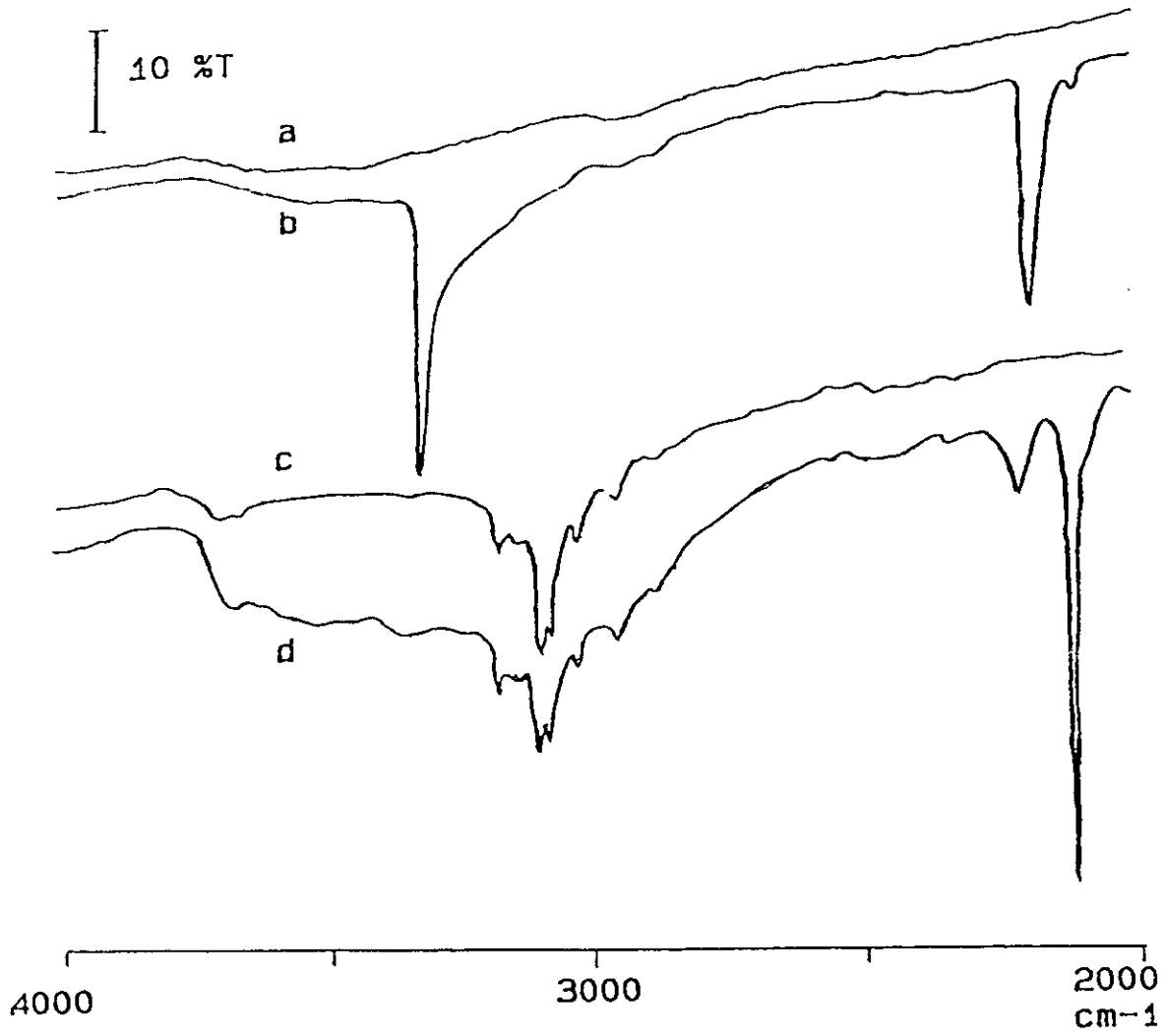

Figure 9.4

Addition of:
a) BF_3 to Al(800 °C), evacuated 0.5 hrs., followed by
b) Addition of HCN.
c) Pyridine to Al(800 °C), evacuated 0.5 hrs., followed by
d) Addition of HCN

Gaseous HCN has bands located at 3311, 2097 and 712 cm^{-1} [7]. The 3311 cm^{-1} band is at 3295 cm^{-1} with $H^{13}CN$ [7]. The band located at 3298 cm^{-1} shifted to 3277 with $H^{13}CN$ addition to alumina. Therefore, we assign the 3398 and 2154 cm^{-1} bands to a weakly adsorbed HCN on acidic Al^{+3} sites.

$$_{cus}\dot{A}l^{+3} + HCN \quad \rightarrow Al \leftarrow :N\equiv C-H \qquad (9.e)$$

Coordination through the lone pair on the nitrogen would increase the frequency of the C-N mode and lower the C-H mode relative to the gas phase.

The onset of polymerization is concurrent with formation of the broad band from 3300 to 2900, and bands at 2226, 1624, 1378, 1286 and 1241 cm^{-1}. The uniform increase in intensity of these bands with time suggests that they result from the same species.

Low and Ramamurthy [152] monitored the changes which occurred when the sample was degassed at progressively higher temperatures. Their results indicated that the band at 1600 cm^{-1} was composed of two strongly overlapping bands at 1600 and 1580 cm^{-1} and a shoulder at 1660 cm^{-1}. Both the 1660 and 1600 cm^{-1} bands decreased in intensity upon evacuation at 250°C and the band maxima shifted to 1580 cm^{-1}. On this basis, Low and Ramamurthy concluded that both NH_2 and C=C vibrational modes were present. Of the three polymer structures postulated, only species (I) contained C=C bonds. Upon addition of $HC^{13}N$ to Al(800°C) the 1660 cm^{-1} band did not shift in frequency, whereas the 1600 cm^{-1} band split into two bands located at 1600 and 1580

cm^{-1}. Therefore, the 1660 cm^{-1} band is due to NH_2 mode and the 1600 cm^{-1} band to NH_2 and C=C modes, confirming the presence of species (I).

9.2.2 ADSORPTION OF C_2N_2 ON Al_2O_3

The addition of C_2N_2 to Al(800°C) is shown in Figures 9.5 and 9.6. An intense band located at 2254 cm^{-1} with a shoulder at 2274 cm^{-1} formed, along with bands located at 2365, 2315, 2094, 1620, 1570 and 1340 cm^{-1}. No change was observed in the hydroxyl region of alumina. The 2365 cm^{-1} band reached a maximum in intensity within the first five seconds, whereas all other bands increased uniformly in intensity with contact time. After twenty minutes contact time, no changes in band intensities were observed and no residual gases were detected. All bands increased in intensity with additional doses of C_2N_2 (up to 1000 umole g^{-1} was used). Upon evacuation at room temperature, the bands at 2365, 1620 and 1560 cm^{-1} decreased slightly, whereas the bands at 2315, 2274, 2254 and 2094 cm^{-1} increased slightly.

In a separate experiment, 25 umole g^{-1} C_2N_2 was added to Al(800°C) for thirty minutes and subsequently degassed at progressively higher temperatures. The results of this experiment are shown in Figure 9.7. The band at 2365 cm^{-1} diminished with room temperature evacuation, and was completely eliminated between 200 and 300°C. The bands at 2315, 2274, 2254 and 2090 cm^{-1} increased in intensity with evacuation up to 300°C. This increase was paralleled by the decrease in intensity of

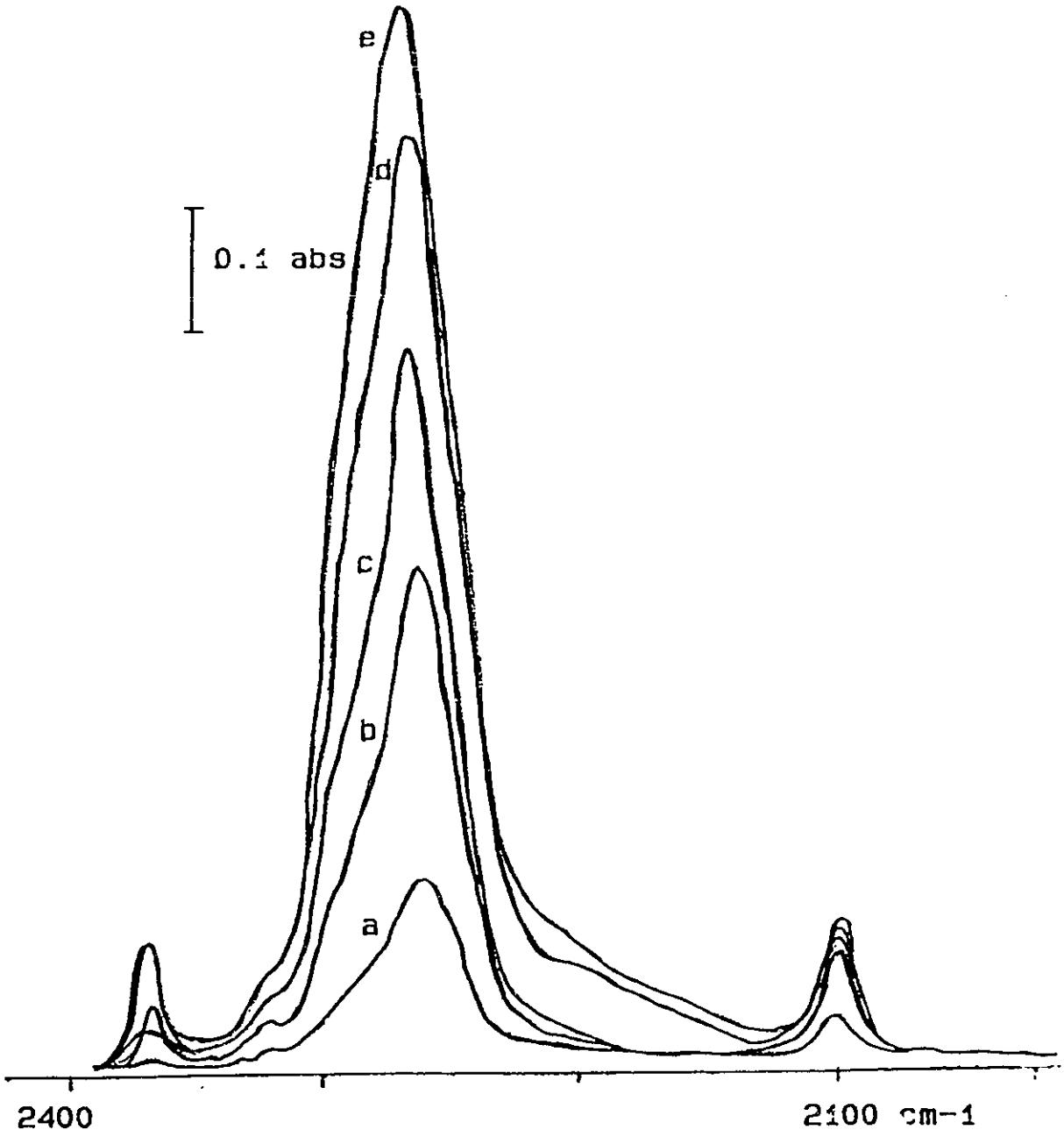

Figure 9.5

Addition of C_2N_2 to Al(800 °C).
Sequential addition of;
a) 10, b) 20, c) 34,
d) 170, and e) 750 umole g^{-1} C_2N_2.
Spectra were recorded after 0.5 hrs. contact time.

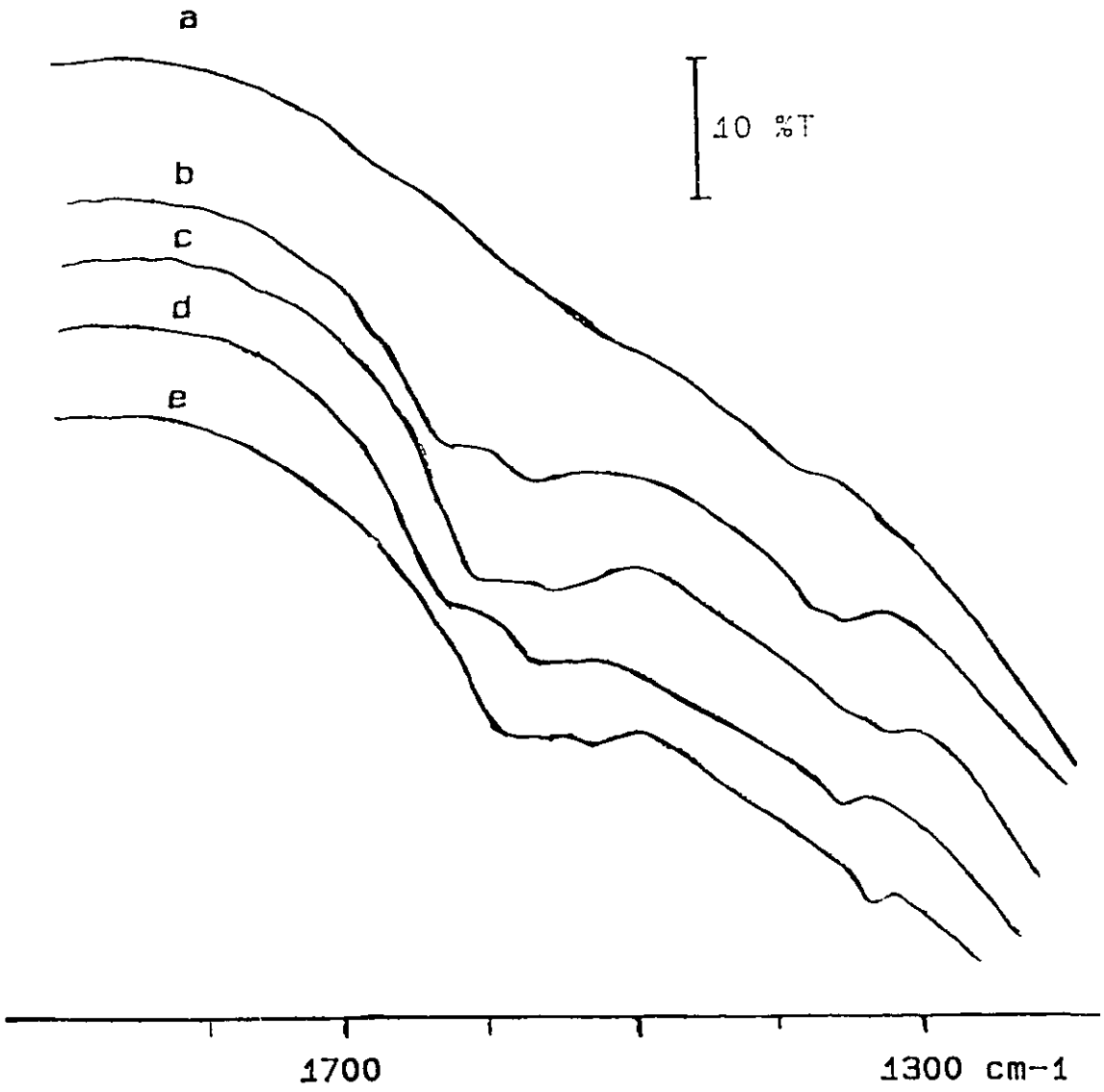

Figure 9.6

Lower spectral region (1900 to 1300 cm^{-1}) for;
a) Al(800 °C).
b) 24 umole g^{-1} C_2N_2 added to (a),
c) $C_2{}^{15}N_2$ added to (a),
d) C_2N_2 added to ^{18}O exchanged Al(800 °C),
e) $^{13}C_2N_2$ added to (a).

bands at 1625,1570 and 1340 cm^{-1}. At 300°C, the 2274/2254 cm^{-1} bands were of equal intensity, and at 400°C, the band at 2254 cm^{-1} had substantially decreased in intensity. The 2094 cm^{-1} band increased in intensity up to 300°C. At 400°C, all bands diminished, giving rise to a weak band at 2200 cm^{-1} and a broad band centred at 2140 cm^{-1}. The 1625, 1560 and 1340 cm^{-1} bands were completely removed at 400°C. Solymosi and Bansagi [150] have reported the formation of a single band at 2272 cm^{-1} upon addition of HNCO to Al_2O_3 which was attributed to an isocyanate species on alumina and a similar assignment undoubtedly applies here.

In an attempt to determine the nature of the other observed bands, we have used preadsorbed pyridine and BF_3 as selective site poisons along with isotopic studies. The addition of 40 umole g^{-1} C_2N_2 to Al(800°C), predoped with pyridine, is shown in Figure 9.8(a). No observable changes in the bands due to adsorbed pyridine occurred. In contrast with pure alumina, the band at 2274 cm^{-1} was more intense than the 2254 cm^{-1} band , the band at 2094 cm^{-1} had shifted to 2100 cm^{-1} and the 2365 cm^{-1} band did not appear. A broad band centred at 1620 cm^{-1} formed but was ill-defined because of the presence of strong pyridine bands.

C_2N_2 was also added to Al(800°C) pretreated with BF_3 (Figure 9.8(c)). Only a single band located at 2365 cm^{-1} formed. We conclude that the bands at 2274, 2254, 2094, 1640 and 1560 cm^{-1} require the presence of basic cus O^{-2} sites and the band at 2365 cm^{-1} with acidic cus Al^{+3} sites.

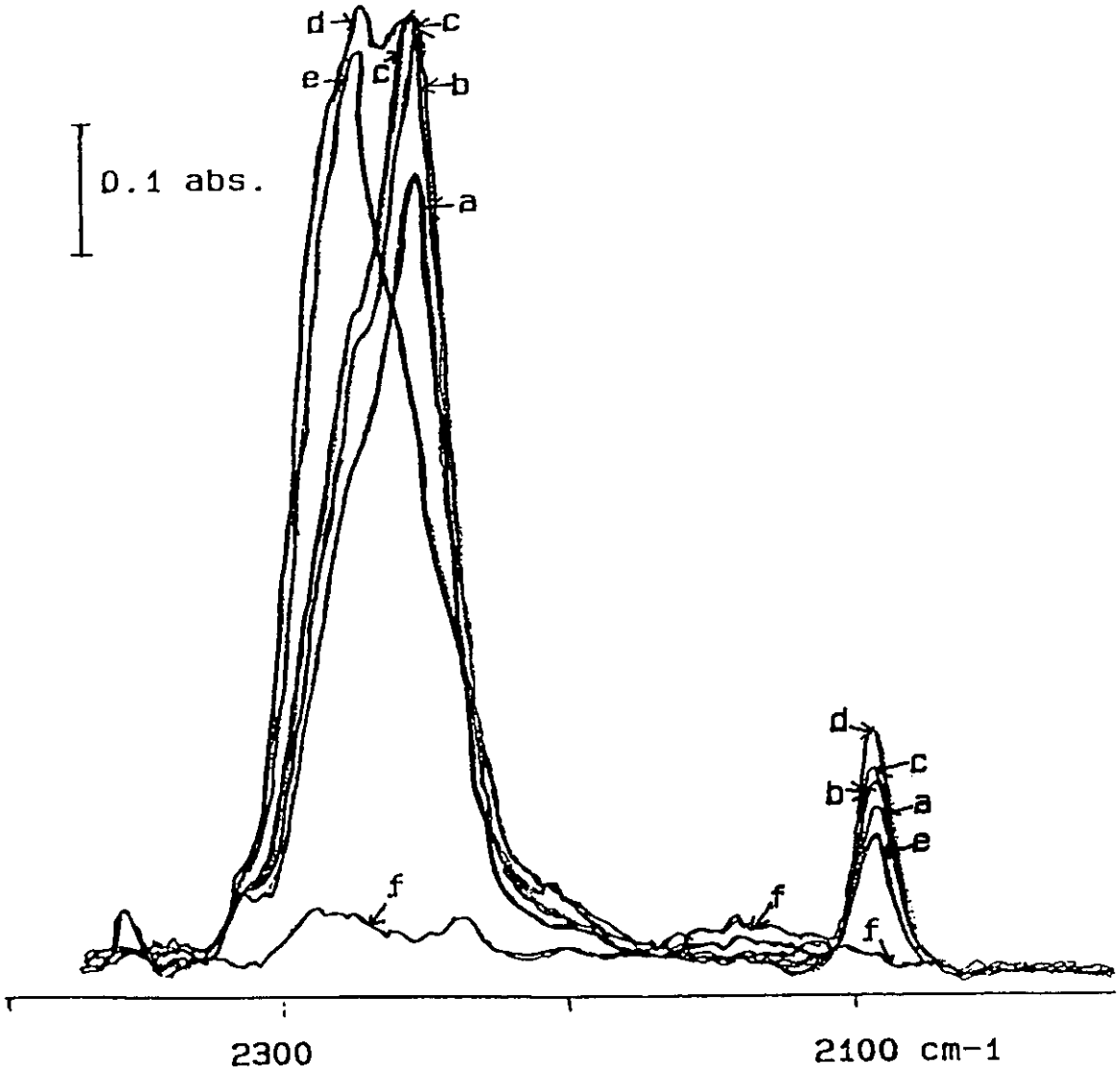

Figure 9.7

Addition of:
a) 25 umole g^{-1} C_2N_2 to Al(800 °C)
followed by evacuation for 0.5 hrs. at
b) 100 °C, c) 200 °C, d) 300 °C,
e) 400 °C, and f) 500 °C.

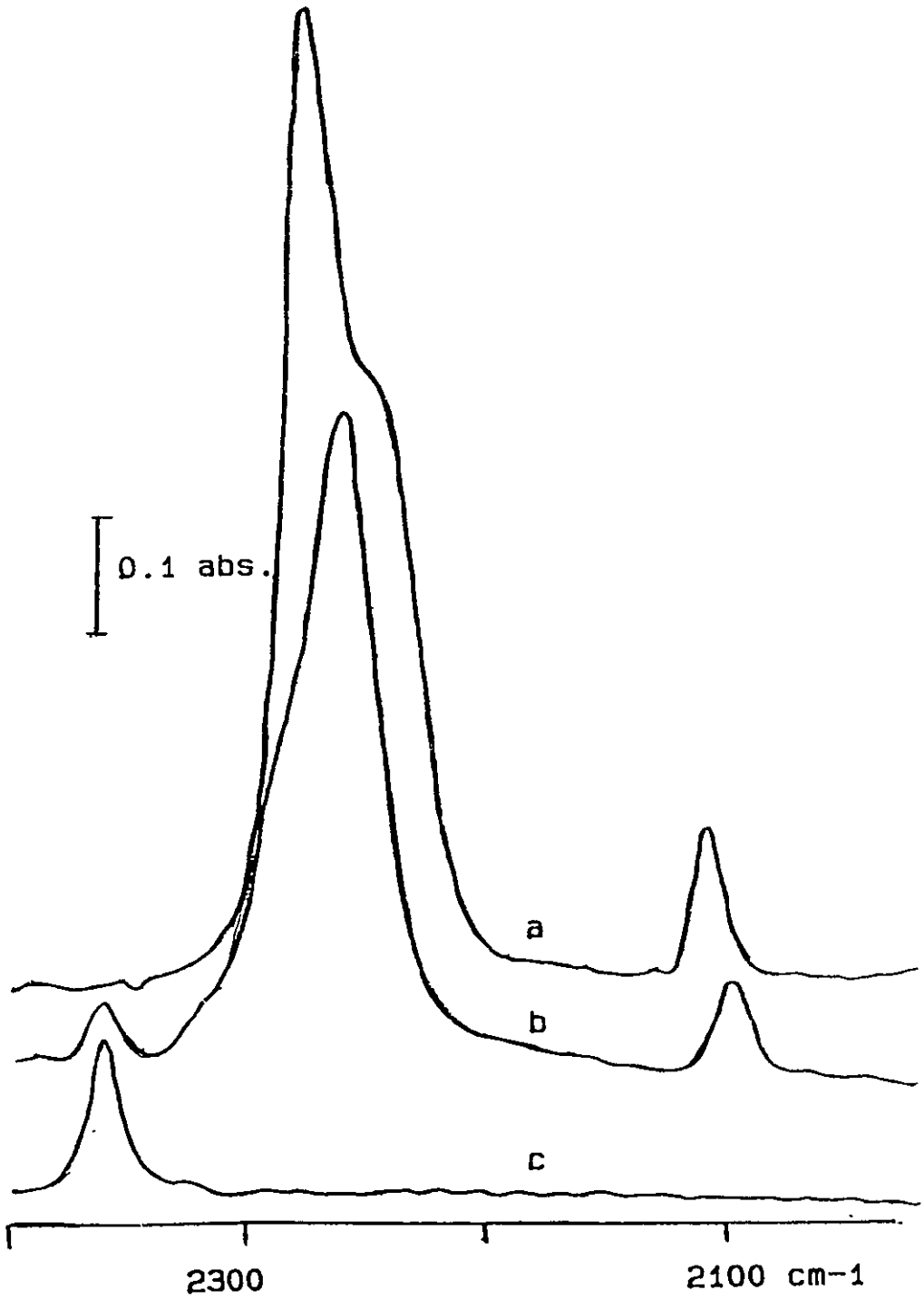

Figure 9.8

Addition of C_2N_2 to:
a) Al(800 °C) predoped with pyridine,
b) Al(800 °C), and
c) Al(800 °C) predoped with BF_3.

TABLE 9.2

Observed wavenumbers and isotopic shifts for the reaction of C_2N_2 on alumina and silica.

OBSERVED	^{13}C	^{15}N	^{18}O	ASSIGNMENT
ALUMINA[a]				
2365	62	21	0	-CN
2315	61	21	0	-CN
2274	60	8	0	-NCO
2254	60	8	0	-NCO
2140	60	22	0	N=C=N
2092	42	32	0	-NC
1620	35	25	0	=C=N
1570	35	10	0	=C=N
1340	10	20	0	-C-N
SILICA[b]				
2353	60	10	-	-NCO
2313	60	10	13	-NCO
2174[a]	70	28	-	N=C=N
2218	51	30	0	-CN
2100	39	36	0	-NC
2078	58	20	0	
1505	0	25	-	-NCO
1470	0	30	34	-NCO

[a] from this thesis.

[b] from Morrow and Cody, ref. 133.

The ^{13}C and ^{15}N shifts in frequency shown in Table 9.2 were obtained by using $^{13}C_2N_2$ and $C_2{}^{15}N_2$. For ^{18}O shifts, the alumina was first heated in $H_2{}^{18}O$ at 400°C several times, followed by degassing at 400°C. Examination of the hydroxyl region of alumina indicated that all Al-OH were converted to Al-^{18}OH. The sample was then degassed at 800°C. Since exchange between bulk and surface oxygen may occur upon final degassing at 800°C, we have no knowledge of the actual ^{18}O concentration at the surface of the alumina.

There are several apparent similarities in the isotopic shifts observed on alumina with those reported for silica [133]. (The shifts reported for silica are also given in Table 9.2.) Morrow and Cody [133] reported that the computed shifts for SiNC, SiCN and SiNCO were insensitive to choice of the value for Si-C or Si-N vibrational stretching modes. Therefore, assuming similar geometry, similar isotopic shifts would be expected for alumina cyano compounds. Bands at 2365 and 2315 cm^{-1} are assigned to Al-CN, 2274 and 2255 to Al-NCO and 2094 to Al-NC stretching modes.

The isotopic results, coupled with the site blocking pyridine and BF_3 data lead us to postulate the following reaction to occur on Al(800°C):

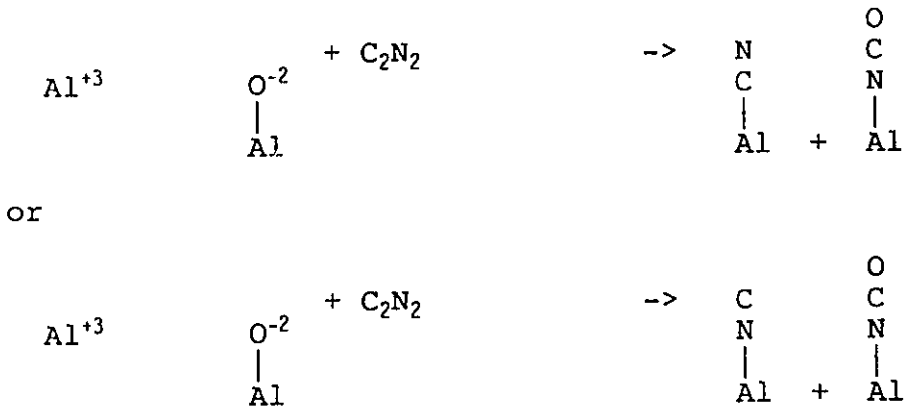

or

(9.f)

The 1620, 1570 and 1340 cm^{-1} bands decreased uniformly during pyrolysis which implies that these bands are due to the same surface compound. On a completely hydroxylated $-Al_2O_3$, approximately 210 umole g^{-1} OH sites exist, and therefore, an approximately equal number of Lewis acid Al^{+3} and basic O^{-2} would be generated upon dehydroxylation. However, we have observed that 1000 umole g^{-1} of C_2N_2 was adsorbed on alumina which indicated that some polymeric buildup must occur to account for this discrepancy.

HCN polymerization on alumina results in bands due to NH_2 and C=C modes in the 1650 to 1550 cm^{-1} region and a band at 1360 cm^{-1} assigned to a -C-N stretching mode [152]. The reaction of ethyl isocyanate with silica produced bands in the 1650 to 1550 cm^{-1} region due to NH_2 and C=O modes [138]. Therefore, based on group frequency analysis, numerous possibilities exist for the assignment of the 1620 and 1570 cm^{-1} bands. The formation of NH_2

can be ruled out immediately since no source of hydrogen is present on Al(800°C). Isotopic data for the bands at 1620, 1570 and 1340 cm^{-1} show that these bands contain both nitrogen and carbon (See Table 9.2 and Figure 9.6). The 1620 and 1570 cm^{-1} bands occur within the region for C=N modes and are assigned accordingly. The lower band at 1340 cm^{-1} cannot be due to the C-N stretch of C-NH_2 although it might be due to a C-N= stretch in a paracyanogen like species (see below).

Cyanogen has been reported to form paracyanogen upon polymerization [156]. Paracyanogen and other conjugated ring systems containing C=N are known to have bands in the 1650 to 1550 cm^{-1} region. Morterra and Low [156] observed that with addition of C_2N_2 to reactive silica, a band at 1553 cm^{-1} formed which they assigned to paracyanogen:

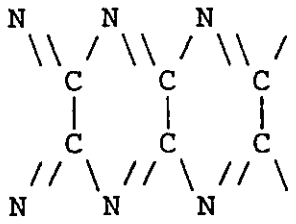

(9.g)

via the following mechanism:

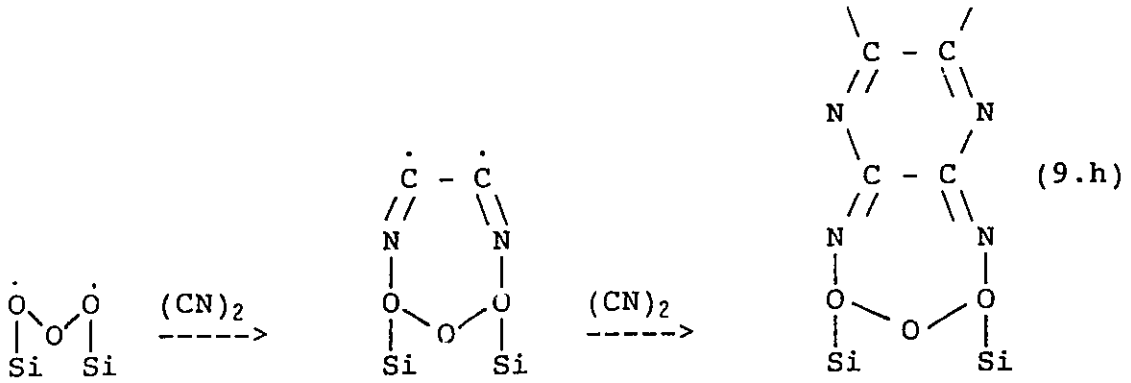

(9.h)

Formation of paracyanogen or a similar type of weakly adsorbed compound would explain the observed increase in the 2400 to 2000 cm^{-1} bands and the decrease in the 1620/1570 cm^{-1} bands during evacuation at room temperature. Removal of paracyanogen would result in Al-CN and Al-NCO formation by the reaction:

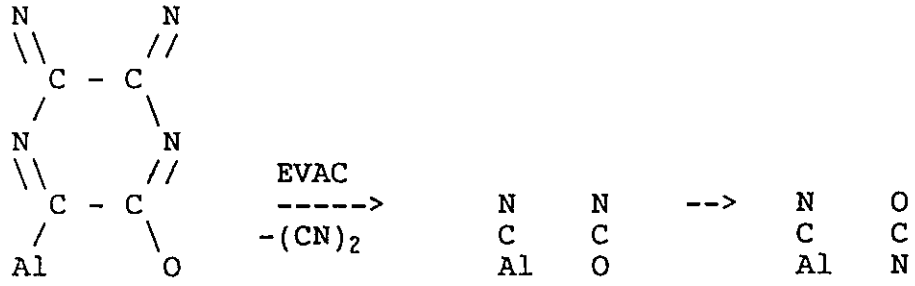

(9.i)

The broad band at 2140 cm^{-1} in Figure 9.7 was more intense if larger quantities of C_2N_2 were used and upon heating above 400°C there was a correlation between its growth and the disappearance of the 2274 cm^{-1} isocyanate band. This is reminiscent of the conversion of the isocyanate band on silica into the carbodiimide (2174 cm^{-1}) upon heating near 450°C.

Further, the isotopic shifts for the silica carbodiimide band were similar to those found for the 2140 cm^{-1} on Al_2O_3.

In a separate experiment, $^{12}C_2N_2$ and $^{13}C_2N_2$ were added sequentially in equal quantities to Al(800°C) at room temperature. Upon pyrolysis at 300°C, the bands at 2254/2194 cm^{-1} shifted to 2274/2214 cm^{-1} and the intensity ratios remained constant. Above 400°C, the 2274/2214 cm^{-1} bands decreased uniformly and two bands at 2140 and 2078 cm^{-1} formed (Figure 9.9). Therefore, we conclude that on Al_2O_3, as with SiO_2, the 2140 cm^{-1} band contains one carbon atom and is due to a carbodiimide type species via the reaction:

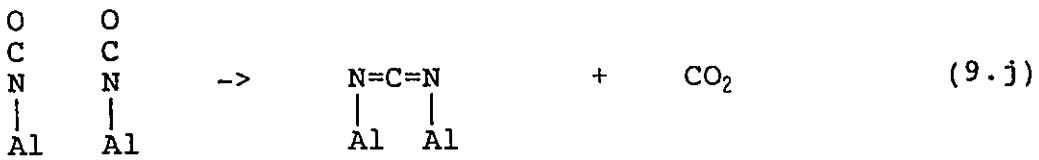

(9.j)

The 2140 cm^{-1} band was stable up to at least 800°C (no measurements at higher temperatures were performed) and was removed in the presence of O_2 at 600°C.

9.2.3 Summary

HCN dissociatively adsorbs on basic oxide sites of alumina and weakly coordinates with acidic aluminum sites. Rapid polymerization of the adsorbed HCN follows. Both types of adsorbed HCN are necessary for polymer formation.

Reaction of C_2N_2 with alumina occurs at room temperature to form Al-NCO, Al-CN, Al-NC and paracyanogen. As observed for SiO_2

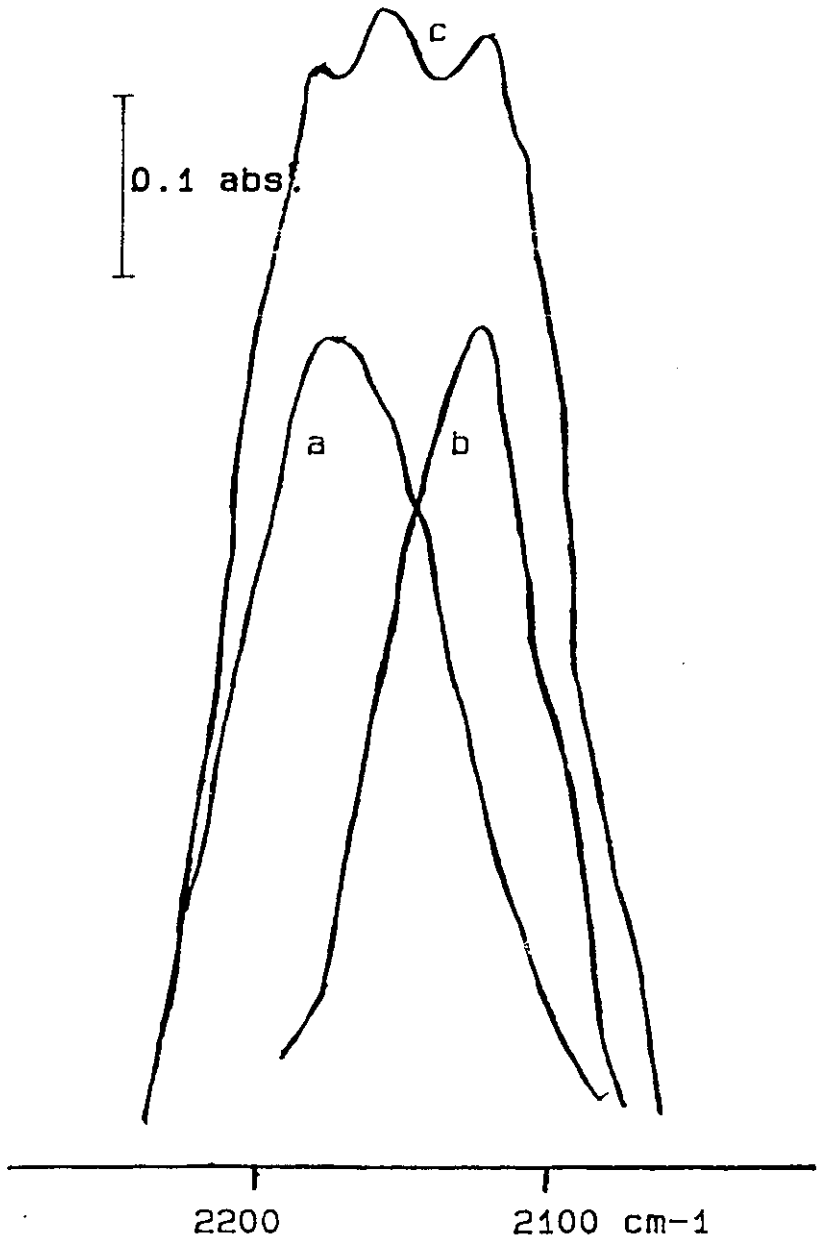

Figure 9.9

Pyrolysis of Al(800 °C) at 400 °C after initial addition of;
a) C_2N_2,
b) $^{13}C_2N_2$, and
c) an equal quantity of $C_2N_2/^{13}C_2N_2$ at room temperature.

carbodiimide formation at 400°C arises from the condensation of adjacent isocyanates.

Chapter 10

COMPUTERIZATION OF A DISPERSIVE INFRARED SPECTROPHOTOMETER

10.1 INTRODUCTION

The introduction of the computer to the scientific laboratory has ushered in new and powerful instrumentation and applications [157-159]. In the field of spectroscopy, the uniting of the computer with infrared (IR) spectrophotometers resulted in the production of the now familiar Fourier Transform Infrared Spectrophotometers (FTIR) which exit today. Prior to obtaining the Bomem DA3 FTIR most of our infrared spectra were recorded on a Perkin-Elmer model 283 dispersive spectrophotometer. A number of advantages were realized for having the spectrophotometer computer controlled. This along with the availability of low cost microcomputers led us to develop computer-based methods for the acquisition and analysis of infrared spectra.

In this chapter, an outline of the method involved in interfacing a microcomputer to a dispersive IR and its applications will be discussed. The oxide supports used in our studies have regions of low transparency in the infrared, thus

making it difficult to observe peaks due to adsorbed species in these regions. By recording spectra digitally we were able to subtract the adsorption due to the oxide support and thus observe bands due solely to adsorbed species. This provided an advantage over the conventional procedure of spectral compensation by means of a blank sample in the reference beam because the computerized subtraction on the same sample before and after treatment yields a more true difference spectrum.

Secondly, by performing repetitive averaging over a limited region, the signal to noise ratio could be improved. In addition, techniques resulting from the computerization of the 283 for recording spectra at elevated temperatures and for studying samples which decompose in the beam area due to localized heating have been developed.

10.2 COMPUTERIZATION

10.2.1 DESCRIPTION OF EQUIPMENT

The microcomputer was an Apple II+ with 64 K RAM memory, language card, two disc drives, and monitor. The ordinate signal (pen displacement) from the 283 was supplied to a Teckmar analog converter (ADC) board. A Teckmar digital converter (DAC) board provided output to an external Kipp and Zonen model BD40 strip chart recorder. Additional input and output functions were provided through TTL inputs (Pb0, Pb1, Pb2) and annunciator

outputs (AN0, AN1, AN2) located on the Apple's game I/O connector [160].

The spectrophotometer was a Perkin-Elmer model 283 with wavenumber marker accessory, repetitive scan accessory and ordinate data processor accessory. Of the three, only the repetitive scan accessory was used in conjunction with the computer to provide repetitive averaging and scanning capabilities. This accessory on the 283 enabled scans to be recorded in a continuous or manual mode over any frequency range. The 283 had no RS-232C communication facilities but contained input and output terminals at the rear of the recording unit [161]. All interfacing between the Apple II+ and the 283 was performed through these terminals. A description of the terminals used is found in Table 10.1.

10.2.2 DATA ACQUISITION

The ADC (Teckmar AD211) provided 12 bit resolution and accuracy. It was jumpered for true differential input which allowed rejection of noise common to both input channels. The ADC was also jumpered for two's complement output. Simple binary or offset binary do not give full resolution (1/4096), but 1/2048 instead. All other jumper options were set for standard operation (i.e. no overlap, external clear enable not used, and no external strobing.) All inputs must be in the range 0 to 5 volts and all data storage programs were written for the ADC located in slot #1 of the Apple II$^+$.

TABLE 10.1

Input and Output Terminals Used
at Rear of 283 Recording Unit

(1) PIN # 1,2 - 1.0 Volt Output with Return - Corresponds to recorder pen deflection including expansion, absorbance, marker pulses, reduced ordinate, offset and response.

(2) PIN # 7,8 - Scan Synchronization - A logic level occurs between these two output positions when the recorder pen is down and alive. A +5 volt level occurs for non-scanning (including filter and grating change) conditions, and a 0 volt level occurs for scanning conditions.

(3) PIN # 9,10 - Cam Pulse Output and Ground - Cam pulses occur every 0.1 cm^{-1} between 4000 and 2000 cm^{-1}, and every 0.05 cm^{-1} between 2000 cm^{-1} and the end of the range. Pulses are +5.0 volts and approximately 1 millisecond wide.

(4) PIN # 12,13 - Auto Sampler Change - Supplies a +5 volt, 250 and 400 millisecond signal as a sample advance signal after a single manual repetative scan has been completed. The signal occurs when the scan has returned to high limits.

(5) PIN # 14,15 - Remote Start - Allows a remote device to initiate a repetitive scan in the manual mode or to start or stop a normal scan. The signal should be a momentary contact closure at least 100 milliseconds wide.

The signal representing the pen displacement is in the range 0 to 1 volt, 1 volt representing 100% transmittance. An instrumentation amplifier is used to provide a gain of 5. The output from the amplifier is then fed to one of the differential input channels (in our case, channel #1). Both the ADC daughter board and amplifier were powered by a 15 volt standard power supply. The daughter board used this supply to provide the analog ground, while the +5 volt and digital ground were taken from the Apple. Coaxial connectors and a chassis for the amplifier and daughter board were used to eliminate noise on all channels.

To record a spectrum, the 283 is first set at the starting wavenumber. An interactive basic program is used to input high and low wavenumber and resolution of the scan. Control is then transferred to machine language subroutines. The starting and stopping of the 283 is done by closing the contacts (pin #14,15) for approximately 0.1 seconds. This is accomplished through a relay switch which is controlled by an annunciator output (AN0) on the Apple.

The synchronization for data acquisition was controlled by monitoring the cam motor pulses which were used to synchronize movement of the chart and grating monocrometer. Under normal operating conditions a 1 millisecond, 5 volt pulse is provided from pin #12,13 every 0.1 cm^{-1} above 2000 cm^{-1} and every 0.05 cm^{-1} below 2000 cm^{-1}. This spectrophotometer output is then fed into the ADC as input channel 0 and a polling subroutine monitors

channel 0 for a value greater than 2048, corresponding to a 2.5 volt signal, which indicates that a pulse has been received.

Two possible resolutions were provided; a) high resolution with a data point every 0.1 cm^{-1}, and, b) low resolution for data every 1 cm^{-1}. A cam pulse counter was used to determine whether a data point was to be acquired. This counter has to be doubled at 2000 cm^{-1} to maintain constant resolution over the entire scan. The ADC performed 12 bit conversions at 30 KHz which was sufficient to collect data at the fastest spectrophotometer speed (cam pulse approximately every 3 milliseconds).

A 5 volt logic between pin #7,8 of the 283 exists for non-scanning conditions (i.e. filter change, grating change). Pin #7 is connected to Pb0 and pin #8 to ground on the Apple's game I/O connector. In this way, a polling routine, after every cam pulse, examines for the grating changes at 2000 and 600 cm^{-1}. A timing loop is used to distinguish between filter changes and grating changes.

Data acquisition proceeded in the following manner. The 283 is started via AN0 from the Apple. Scanning condition is then checked by polling Pb0 and is continuously monitored after every cam pulse for detection of filter and grating changes. The pulse counter decrements when a cam pulse is detected in channel #0 of the ADC. When the pulse counter reaches zero then a data point is collected from channel #1 from the ADC and stored in two successive memory locations. The ADC is allowed to "warm up" and the twelfth value is taken. The 283 is again checked for scanning conditions and the entire data acquisition procedure is

repeated. Once the last data point is taken then the 283 is stopped via AN0.

In addition to data acquisition, other software options include; display of spectra on two high resolution graphic screens with expansion and cursor capabilities, integration of bands, subtraction of spectra, boxcar averaging, conversion from absorbance to transmittance and vice versa, plotting to an external recorder, repetitive scanning, repetitive averaging and storage to and from floppy disc. Data files were a maximum of 8K in length which was sufficient to record over the entire spectral range 4000 cm^{-1} to 200 cm^{-1} at low resolution. A maximum range of approximately 400 cm^{-1} could be used for high resolution. Machine language subroutines were employed when noninteractive manipulation of data files was involved (i.e. display, subtraction, conversion to absorbance, etc.). This greatly increased speed of operation and allowed a more efficient use of the Apple's RAM memory.

10.2.3 REPETITIVE SCANNING

This program has two purposes; a) it allows the transfer of spectra to or from a floppy disc as a function of time (Repscan), and, b) to perform signal averaging (Repavg). Both of these options require the use of the repetitive scan accessory on the 283. The high and low wavenumber were selected manually on the accessory. This is necessary to rewind the 283 to the high wavenumber once a scan was completed. The Repscan program was

very similar to the data acquisition program. The 283 was started and data was collected in the same manner. Upon reaching to low wavenumber value the 283 stopped and returned to the starting wavenumber. A 5 volt 250 to 400 milliseconds pulse from pin #17,18 was produced once the 283 has returned to the high wavenumber and this signal is fed into Pb2 on the Apple where it is detected by a polling routine. The data file is stored to disc and a timing loop is initiated until the next scan. Repetitive scanning has been useful for experiments requiring spectra at fixed intervals over a long time period (e.g. overnight).

For Repavg the average spectrum is calculated for a number of consecutive spectra recorded. This resulting increase in signal to noise ratio would allow us to observe bands of weak intensity or bands in low transparency regions that under normal scanning conditions could not be observed (Figure 10.1). The first scan is recorded exactly as described in Repscan. The second and subsequent scans are recorded immediately after the 5 volt pulse is detected from pin #17,18. The spectra are coadded at the time of acquisition and, upon completion, the average spectral values are then calculated. Since the ADC values range from 0 to 4095, an overflow may occur when more than 16 scans are averaged. In the case, three bytes per data point are used which increased the number of possible coadded scans to 4095. The use of three bytes per data point limits the maximum number of data points to approximately 2700. The calculated average is then stored in two bytes.

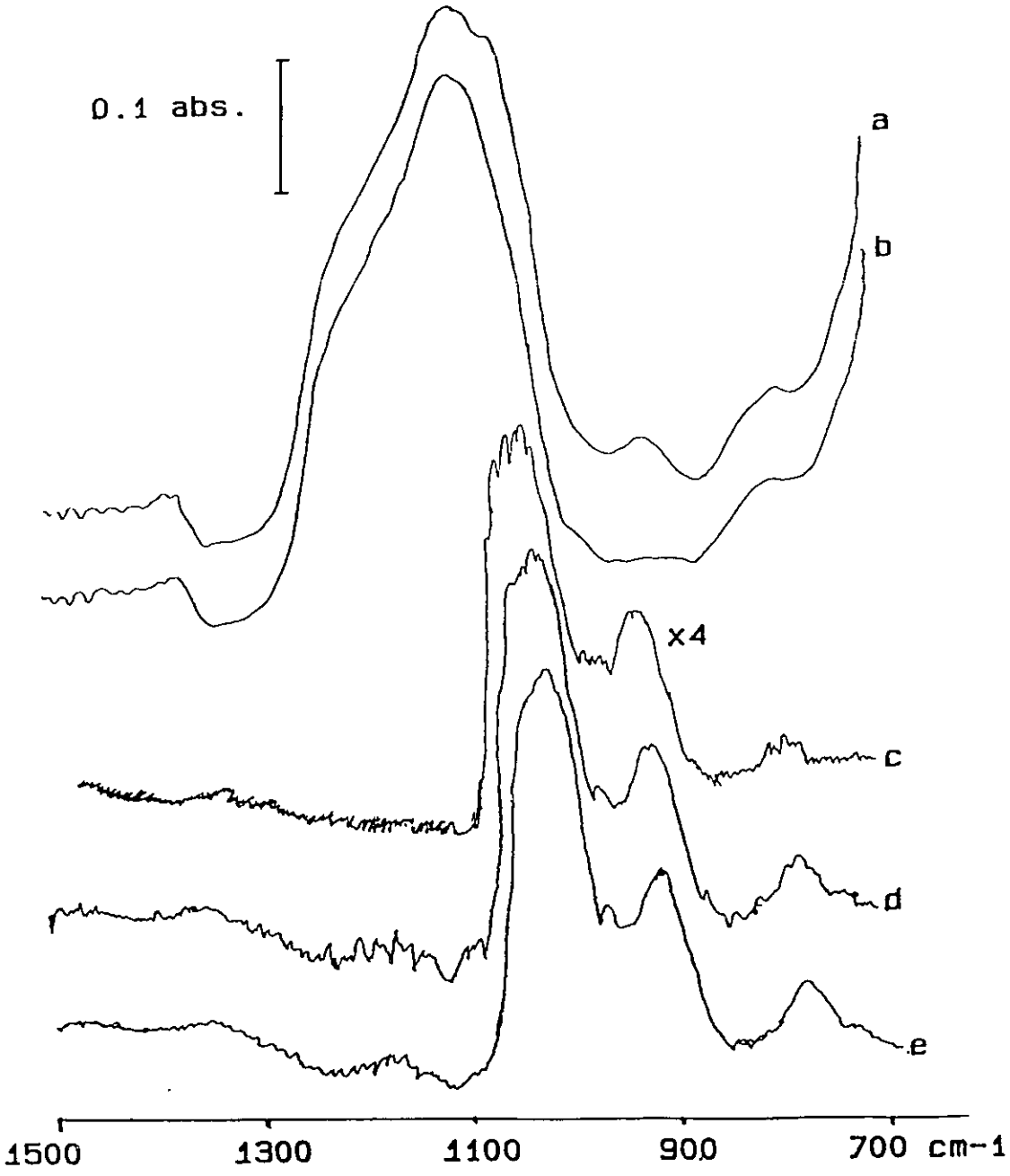

Figure 10.1

a) Silica film degassed at 400 °C, and
b) With excess $TiCl_4$ added to (a).
Difference spectrum (b)-(a), with
c) No spectral averaging,
d) 4 scans averaged, and
e) 16 scans averaged.

10.2.4 ADDITIONAL SOFTWARE

Once a spectrum was stored either by repetitive scanning or data acquisition a number of options involving software manipulations of the data files were available.

10.2.4.1 SUBTRACTION

As stated in the introduction, one of the primary reasons for computerizing the 283 was to enable us to subtract one spectrum from another. By subtracting the absorbance due to the support from one with an adsorbed species, one may obtain spectra due solely to that of the adsorbate which under normal conditions would be difficult to see. The subtraction program is also used for high temperature recording of spectra, for recording spectra of thermally sensitive samples and for the thin film technique described elsewhere [162].

The program first loads two files from the floppy disc into the Apple's memory. These files must be in absorbance. The background file is stored in the 8K memory of the high resolution graphic secondary page thus limiting the display function to one screen. The second file is stored in the 8K allotted to data files and is then transferred into the ram of the language card. The desired range of subtraction and scaling factor was selected via a basic program. The subtracted spectrum is stored in the data file memory location and then displayed on the high resolution graphic screen. This procedure is sometimes repeated

several times using different scaling factors until the desired spectrum is achieved. This can be performed rapidly; the second file is transferred from the language card to the data file memory location, subtraction proceeds and the spectrum is then displayed.

10.2.4.2 DISPLAY

A spectrum or a portion of a spectrum could be displayed on two separate high resolution screens (150 x 280 pixels) and 4 lines of text at the bottom. Both ordinate and abscissa expansion were provided along with wavenumber cursor capabilities. Integration of a band was also available with display. The limits of integration could be defined either with the cursor or via keyboard input. The area below the curve and above a line connecting the two limits is calculated by Simpson's Approximation.

10.2.4.3 PLOT

This function provided output of the displayed spectrum to an external Kipp and Zonen DA40 strip chart recorder. The DAC located in slot #2 on the Apple was jumpered for 0 to 5 volt output which was connected to the high and low pins of the recorder. The ordinate output was under software control such that 0 volts represented the bottom and 5 volts the top of the high resolution screen. The stepper motor of the DA40 could be

operated externally by a 5 volt TTL pulse at least 1 millisecond wide or internally at 200 Hz providing the several chart speeds available. A subroutine generated a pulse through AN1 on the games I/O connector. By varying the number of pulses generated between each conversion and by choosing different chart speeds on the recorder, a large number of possible formats were available for output to the recorder.

10.2.4.4 BOXCAR AVERAGING

This subroutine was used to remove high frequency noise from a spectrum. This was done in the following manner. The value of the first data point was obtained by taking the average of the first four data points. In a similar manner, value of the second data point is the average of the second through to the fifth data point. This manipulation is continued through to the end of the data file. The last three data points are left unchanged.

10.2.4.5 CONVERT TO TRANSMITTANCE OR ABSORBANCE

Conversion between transmittance and absorbance was also available. Absorbance was calculated in base 10. These two functions operated at an approximate conversion rate of 35 data points per second and thus were by far the slowest data manipulation step.

The data files could also be stored and loaded from disc via an interactive basic subroutine.

10.3 APPLICATIONS

10.3.1 HIGH TEMPERATURE SPECTRA

The study of adsorption of gases on oxide surfaces sometimes involve reactions which occur at elevated temperatures. However, above ambient temperatures, infrared emission of the sample may modify the adsorption spectra. Therefore, spectra are usually recorded at or below room temperature. The question arises as to whether the spectrum observed at ambient is truly representative of the reactions which occur or the species present at these elevated temperatures. To overcome this problem, a method for obtaining spectra at elevated temperatures will be described.

The infrared cell used in these <u>in situ</u> temperature studies is shown in Figure 2.3. For a given wavelength(l) and temperature(t) the pen displacement on the 283 operating in transmittance is:

$$(Is(l,t) + E(l,t)) / Ir(l) \qquad (10.a)$$

where Is = Intensity of beam passing through the sample
E = Emission due to the sample
Ir = Intensity of the reference beam

The 283 is a post-sample chopped spectrophotometer and therefore emission and absorption of infrared light by a sample cannot be separated. To overcome this problem the following procedure is performed. The sample is placed in the beam and heated to the

desired temperature. A transmittance spectrum is recorded under normal scanning conditions (Equation 10.a) and stored to disc. The sample beam is then blocked with an opaque object and another transmittance spectrum is recorded. In doing this, we obtain a spectrum due to the emission of the sample according to the following equation:

$$E(1,t)/Ir \qquad (10.b)$$

Thus, by subtracting the emission spectrum in transmittance from that of the unblocked beam spectrum in transmittance one obtains:

$$Is(1,t)/Ir(1) \qquad (10.c)$$

which is the transmittance spectrum due to infrared absorption. The transmittance and emission spectrum of alumina degassed at several temperatures is shown in Figure 10.2. Below 100°C, no emission spectrum was observed. The emission spectra were subtracted to give rise to the transmittance spectra shown in Figure 10.3. Virtually, no differences were observed in the final spectra obtained in this manner.

The spectra of a sulfated alumina in Figure 7.4, was recorded in the same way. To accomplish this, the alumina background and emission were recorded at temperatures between 25°C and 800°C. The true alumina background due to absorption, was calculated by subtraction. Sulfur dioxide (10 umoles) and oxygen (40 umoles) were added to the alumina (100 mg) and heated at 400°C 1 hour. followed by degassing at 400°C 1 hour. The transmittance and emission spectra were then recorded for the sulfated alumina at

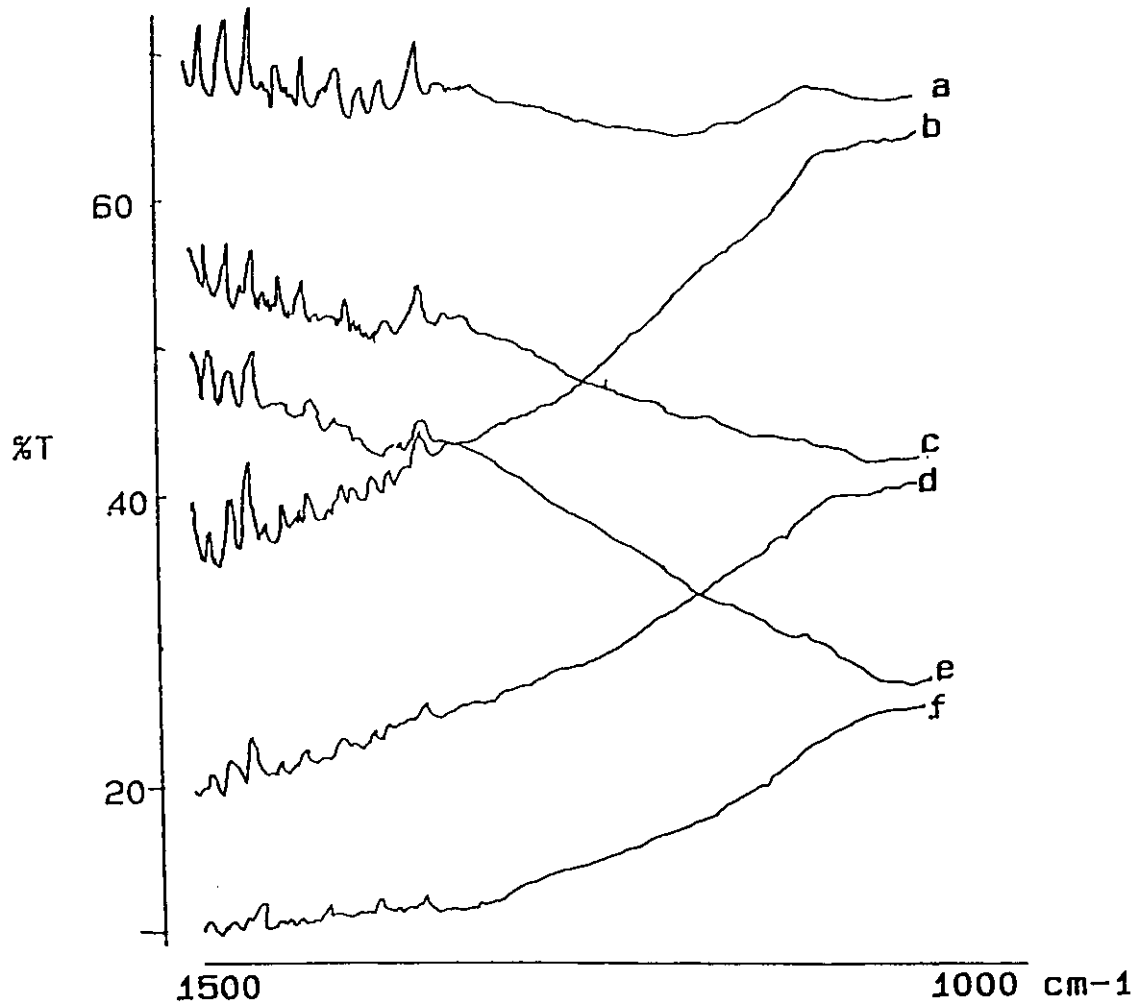

Figure 10.2

Alumina (20 mg cm^{-2}) degassed at 800 °C for 30 minutes.
Transmittance spectra recorded at:
a) 800 °C, c) 600 °C, e) 400 °C,
and the emission spectra recorded at:
b) 800 °C, d) 600 °C, and f) 400 °C.

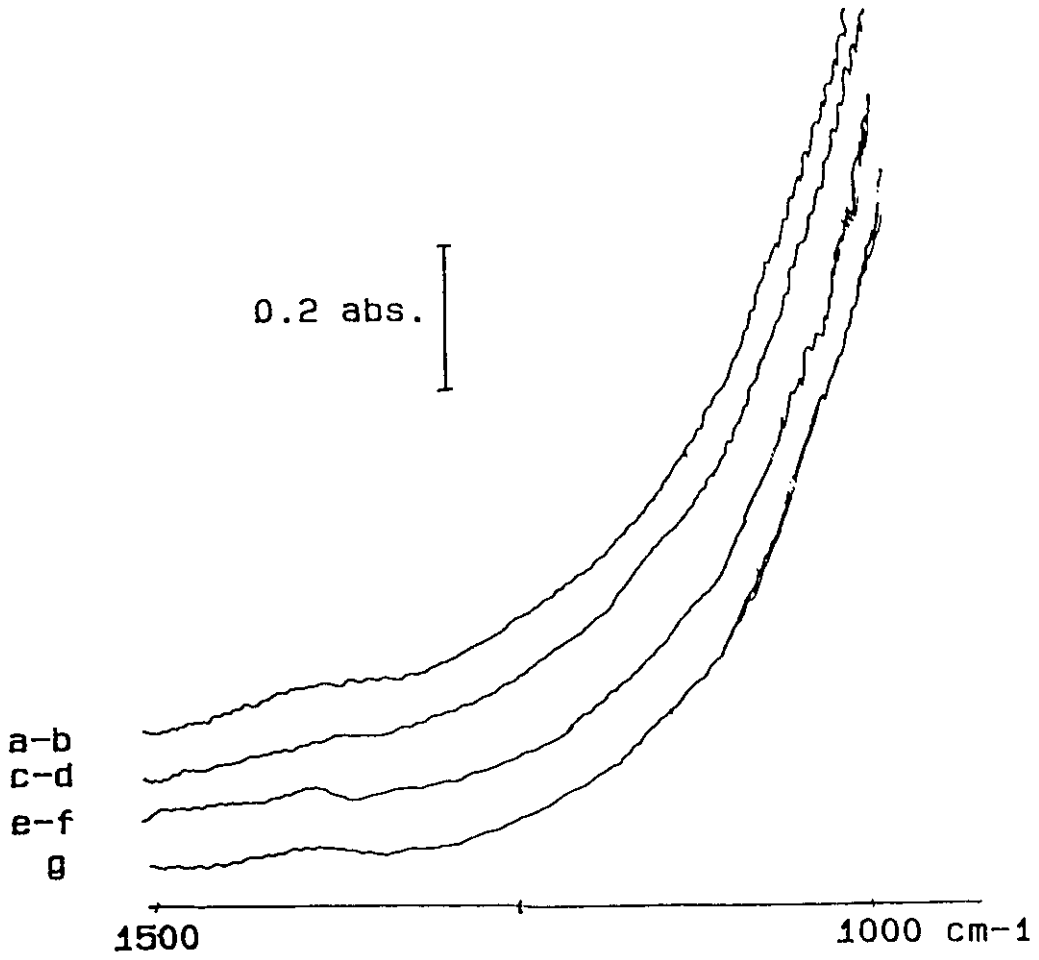

Figure 10.3

Spectra shown in Figure 10.2 after removal of the emission contribution and (g) spectrum recorded at room temperature. Spectra were overlapping in %T and are shown in absorbance with an offset for clarity.

each temperature and the true absorption spectrum was calculated. As before the alumina background was then subtracted resulting in the spectra shown in Figure 7.4. From this result we were able to conclude that the sulfated species observed at room temperature is stable up to 750°C on alumina.

A similar technique has also been developed for the Bomem DA3 FTIR. In this case, the direct emission from the sample to the detector is unmodulated and, hence, does not contribute to the signal. This unmodulated signal would, however, increase the DC level and may cause detector saturation. This effect can be minimized by placing an aperture immediately following the sample.

The emission signal from the sample that enters the interferometer returns to the sample and detector in a modulated state and, therefore, contributes to the overall signal. As with the 283, this signal can be measured independently by blocking the source. This was done by placing a Canadian quarter in one of the filter wheel positions.

10.3.2 TEMPERATURE SENSITIVE SAMPLES

One of the major problems which exists for infrared studies at low temperatures or for thermally sensitive samples is due to localized heating effects caused by the infrared beam. For the 283, a temperature of 95°C has been estimated for a black body sample [162]. It has been shown that the adsorption of diborane on silica can be attributed to a localized heating effect [162].

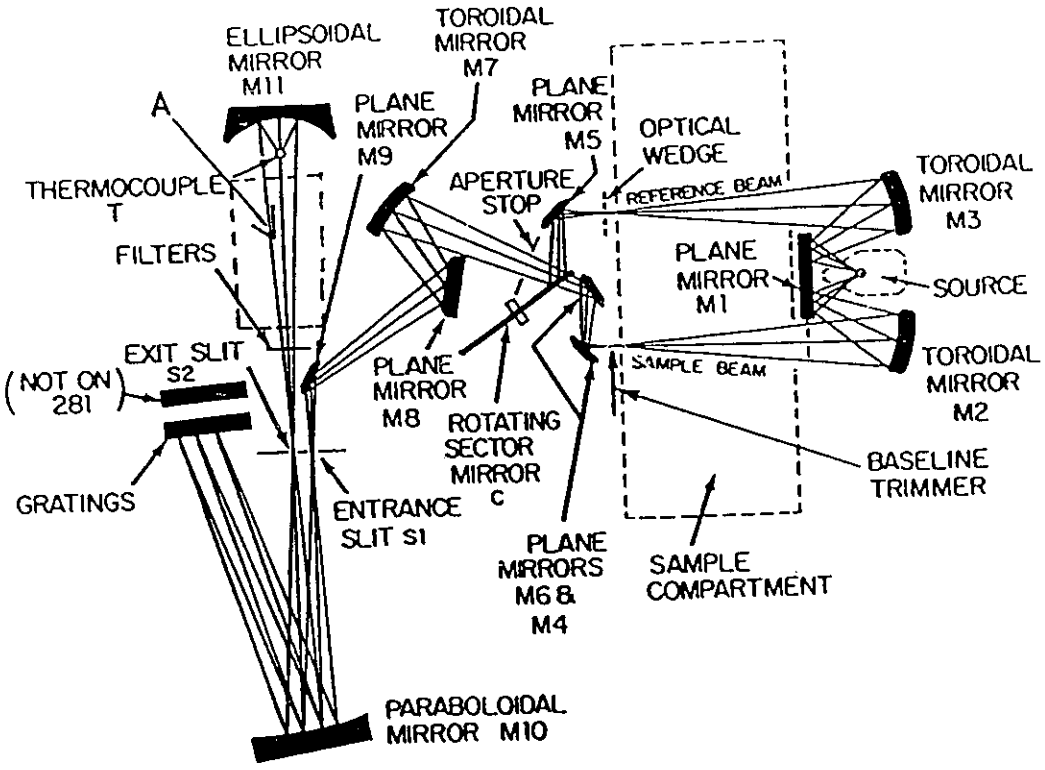

Figure 10.4

The Perkin-Elmer Model 283 Spectrophotometer Optical Bench. The region marked (A) is the sample compartment for thermally sensitive samples.

To circumvent this problem, a technique involving the computerized 283 has been developed. The optical schematic for the 283 is shown in Figure 10.4. The source of radiant energy for the instrument is a length of ceramic tube heated by an internal metallic element. The ceramic is heated to about 1200°C and produces a continuous spectrum of electromagnetic energy covering the region from 4000 to 200 cm^{-1}. This passes directly through the sample, whereas the gratings, exit slit and filters allow only the light of an approximately 3 cm^{-1} bandwidth to reach the detector. A sample placed directly in front of the detector would receive about 1/1000th of the radiant energy normally received in the sample compartment. This decrease would effectively eliminate any localized heating effects of the beam.

The distance between the filters and the detector is approximately 8 cm, which is sufficient space for insertion of most infrared cells. As shown in Figure 10.4, a hole is cut through the top of the optical unit cover to provide access to this region. A reference followed by the sample spectrum is recorded in single beam mode.

An example of the use of this technique is illustrated in Figure 10.5. The adsorption of $Co_2(CO)_8$ on alumina occurs readily at ambient temperature resulting in a red colourization of the alumina. When this sample is placed in the sample beam of the 283, a brown decolourization of the alumina occurs in the beam area during scanning. This brown colour can also be produced by simply degassing the sample between 40 to 80°C. In contrast, no decolourization of the red coloured alumina occurred

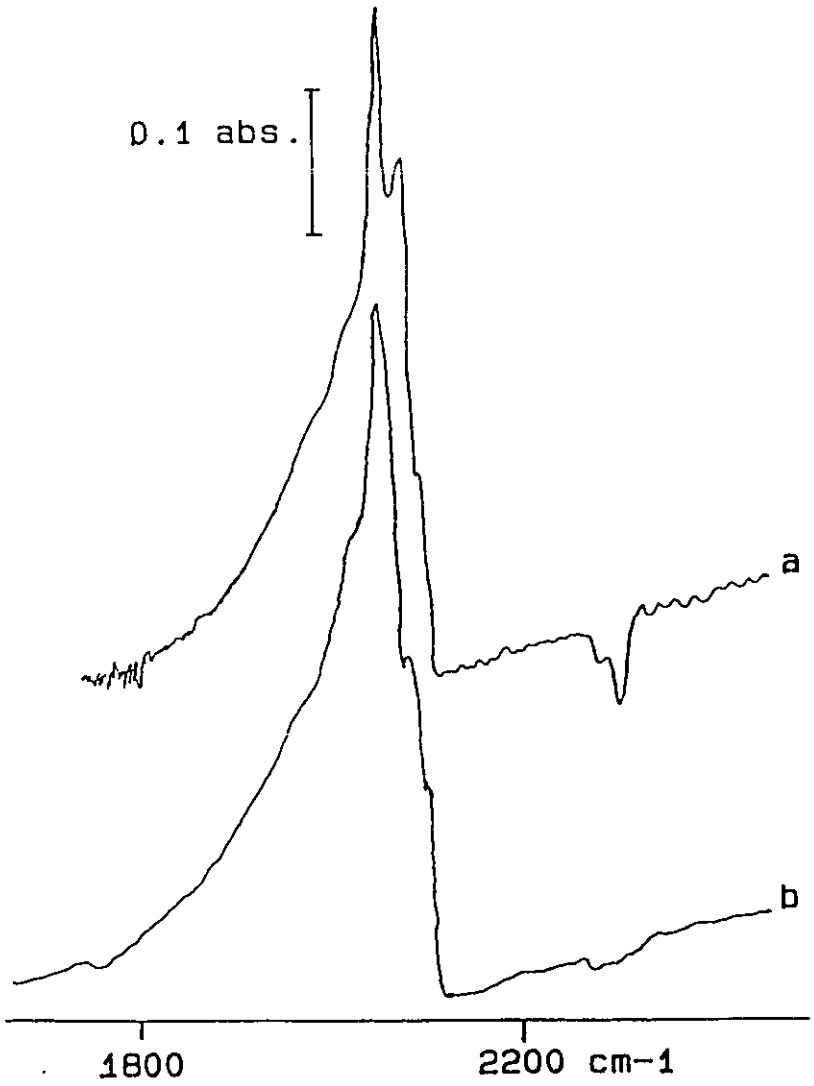

Figure 10.5

Spectra of $Co_2(CO)_8$ added to Al(400 °C).
Spectra recorded in:
a) double beam mode, and
b) in single beam mode with the sample placed at position (A) in Figure 10.4.

when scanning in the modified single beam mode. The resulting infrared spectra, recorded either in the single beam (i.e. sample placed in front of the detector) or double beam, were identical for the brown coloured sample. A different infrared spectrum was observed for the red sample placed in the two sample locations as shown in Figure 10.5.

10.4 SUMMARY

Total hardware cost, excluding the strip chart recorder, was approximately $3000 Canadian. The signals used from the terminals of the 283 could have been taken from the internal circuitry of most dispersive infrared spectrophotometers. Consequently, the hardware setup and programs developed require minor modifications for generalized use. Prior to obtaining our Bomem DA3 FTIR, this setup provided reliable results with extensive use over a two year period.

BIBLIOGRAPHY

1. Semrau K. Sulfur Removal and Recovery from Industrial Processes. (Pfeifier, J.B., Ed.) Advan. Chem. Series 139, Amer. Chem. Soc., Washington, D.C. (1975).

2. Pollution Control and Energy Needs. (Jimeson, R.M., Spindt, R.S., Ed.) Advan. Chem. Series 127, Amer. Chem. Soc., Washington, D.C. (1973).

3. Hyne, J.B., Oil Gas J., 70, 64, (1972).

4. Mohammad Saad, A.B., These (3 eme Cycle), (1986).

5. Dupey G. and Graulier M. Informations Chimie. Special Catalyse, 74, 33, (1969).

6. Dupin, T., Baige, G. and Poisson R., Eur. Pat. Appl. EP., 38, 741, (1980).

7. Nakamoto, K., Infrared and Raman Spectra of Inorganic and Coordination Compounds. Fourth Edition, John Wiley and Sons (1986).

8. Nickless, G., Inorganic Sulfur Chemistry. Elsevier, Amsterdam (1968).

9. Peter, L. and Meyer, B., Inorg. Chem. 24, 3071 (1985).

10. Schmidt, M., Sulfur in Organic and Inorganic Chemistry (Senning, A., Ed.), 71, Marcel Dekker, Inc., New York, (1972).

11. Korosy, L., Gewanter, H.L., Chalmers, F.S. and Vasan, S., Sulfur Removal and Recovery from Industrial Processes (Pfeifier, J.B., Ed.) 192, Advan. Chem. Series 139, Amer. Chem. Soc., Washington, D.C. (1975).

12. Pollard, F., Jones, D.J., Chem. Soc., Spec. Publ. 12, 363 (1959)

13. Sato, S., Higuchi, S. and Tanaka, S., Applied Spectrosc. 39, 822 (1985).

14. Saad, A.B. Mohammed, Thesis, 3 eme cycle, Caen(1986).

15. Blukis, V. and Myers, R.J., J. Phys. Chem. 69, 1154 (1965).

16. Tang, S. and Brown, C.W., Inorg. Chem. 14, 2856 (1975).

17. Janz, G.J., Downey, J.R., Roduner, E., Wasilczyk, G.J., Coutts, J.W. and Elvard, A., Inorg. Chem. 15, 1759 (1976).

18. Currel, B.R, Williams, A.J, Mooney, A.J., and Nash, B.J. New Uses of Sulfer. (West, J.R., Ed.) Advan. Chem. Series 140, Amer. Chem. Soc., Washington, D.C. (1975).

19. Matsuda, S. and Kato, A., Appl. Catal. 8, 149 (1983).

20. Morrow, B.A. and Ramamurthy, P., J. Phys. Chem. 77, 3052 (1973).

21. Lavalley, J.C., Private Communications.

22. Clarke, E.C.W. and Glow, D.N., Canad. J. Chem. 418, 522 (1970).

23. Handbook of Preparative Inorganic Chemistry. (Brauer G. Ed.) Academic Press, New York, (1963).

24. Thomas, C.L., Catalytic Processes and Proven Catalysts. Academic Press, New York (1970).

25. Knozinger, H. and Ratnasamy, P., Catal. Rev. Sci. Eng., 17, 31 (1978).

26. Knozinger, H., Stud. Surf. Sci. Catal. 20, 111 (1985).

27. Kiselev, A.V. and Lygin, V.I., Infrared Spectra of Surface Compounds. Wiley and Sons (1972).

28. Cocke, D.L., Johnson, E.D. amd Merrill, R.P., Catal. Rev. Sci. Eng., 26, 163 (1984)

29. Lippens, B.C. and de Boer, J.H., Acta Cryst. 17, 1312 (1964).

30. Peri, J.B., J. Phys. Chem. 69 220 (1965).

31. Butt, J.B. and Starzec, L.T., J. Catal. 32, 99 (1974).

32. Dabrowski, J.E., Butt, J.B. and Bliss, H., J. Catal. 18, 297 (1970).

33. Jones, L.H., J. Chem. Phys., 22, 217, (1954)

34. Della Gatta, G., Fubini, B., Ghiotti, G. and Morterra, C., J. Catal. 43, 90 (1976).

35. Datta, A. and Cavell, R.G., J. Phys. Chem. 89, 450 (1985).

36. Deo, A.V., Dalla Lana, I.G. and Habgood, H.W., J. Catal. 12, 270 (1971).

37. Lavalley, J.C., Travert, J., Laroche, D. and Saur, O., Compt. Rend. 285C, 385 (1977).

38. Lavalley, J.C., Travert, J., Chevreau, T., Lamotte, J. and Saur, O., J. Chem. Soc., Chem. Comm., 146 (1979).

39. Saur, O., Chevreau, T., Lamotte, J., Travert, J. and Lavalley, J.C., J. Chem. Soc., Faraday Trans. I. 77, 427 (1981).

40. Liu, C.L., Chuang, T.T. and Dalla Lana, I.G., J. Catal. 26, 474 (1972).

41. Slager, T.L. and Amberg, C.H., Can. J. Chem. 50, 3416 (1972).

42. Bartholomew, C.H., Agrawal, P.K. and Katzer, J.R., Adv. Catal. 31, 135 (1982).

43. Deane, A.M., Griffiths, D.L., Lewis, I.A., Winter, J.A. and Tench, A.J., J. Chem. Soc., Faraday Trans. I. 71, 1005 (1975).

44. Berg, R.W., Von Winbos, S. and Boerrum, N.J., Inorg. Chem. 19(9), 2688 (1980).

45. Amenomiya, Y., Morikawa, Y. and Pleizier, G., J. Catal. 46, 431 (1977).

46. Krupay, B.W. and Amenomiya, Y., J. Catal. 67, 362 (1981).

47. Collins, T.U., Johnson, W.H. and Nier, A.O., Phys. Rev. 94, 398 (1954).

48. Lohman, J.B., Reding, F.P. and Horning, D.F., J. Chem. Phys. 19, 252 (1951).

49. Saumagne, P. and Dorval, P., Compt. Rend. 263B, 963 (1966).

50. Falk, M., Spectrochim. Acta 40A, 43 (1984).

51. Chang, C.C., J. Catal. 53, 374 (1978).

52. Karge, H.G. and Dalla Lana, I.G., J. Phys. Chem. 88, 1538 (1984).

53. Datta, A., Cavell, R.G., Tower, R.W. and George, Z.M., J. Phys. Chem. 89, 443 (1985).

54. Vit, Z., Vala, J.F., Malek, J., Appl. Catal. 7, 159 (1983).

55. Karge, H.G., Trevizan de Suarez, S. and Dalla Lana, I.G., J. Phys. Chem. 88, 1782 (1984).

56. Schoonheydt, R.A. and Lunsford, J.H., J. Catal. 26, 261 (1972).

57. Lavalley, J.C. and Benaissa, M., J. Chem. Soc., Chem. Commun., 908 (1984).

58. Karge, H.G., Tower, R.W., Dudzik, Z. and George, Z.M., Stud. Surf. Sci. Catal. 7, 643 (1981).

59. Newman, G. and Powell, D.B., Spectrochimica Acta. 19, 213 (1963).

60. Lavalley, J.C., Janin, A. and Preud'homme, J., React. Kinet. Catal. Lett. 18 No. 1-2, 85 (1981).

61. Hashimoto, S., Inove, G. and Akimoto, H., Chem. Phys. Lett. 107, 198 (1984).

62. Morterra, C., Zecchina, A., Collician, S. and Chiorino, A., J. Chem. Soc., Faraday Trans. I, 1544 (1977).

63. Lavalley, J.C., Lamotte, J., Saussey, H. and Preud'homme, J., Sulfur Lett. 1, 101 (1982).

64. Datta, A. and Cavell, R.C., J. Phys. Chem. 89, 454 (1985).

65. Saussey, H., Lavalley, J.C., Ziolek, M. and Kusawa, J., J. Catal. (submitted)

66. Dudzik, Z. and George, Z.M., J. Catal. 63, 72 (1980).

67. Glass, R.W. and Ross, R.A., Can. J. Chem. 49, 2832 (1971).

68. Gallon, M.A. and Smith, J.M., J. Catal. 38, 206 (1975).

69. Saussey, H., These 3 en cycle, Caen (1984).

70. Hair, M.L., Infrared Spectroscopy in Surface Chemistry. Marcel Deikker Inc., New York (1967).

71. Little, L.H., Infrared Spectra of Adsorbed Species. Acad. Press, London (1966).

72. McFarlane, R.A, Ph.D Thesis, University of Ottawa, Canada (1987).

73. Vol'nov, I., Peroxides, Superoxides and Ozonides of Alkali and Alkaline Earth Metals. Plenum Press, New York (1966).

74. Siriwardane, R.V. and Cook, J.M., J. Coll. and Interface Soc. 108, 414 (1985).

75. Fiujii, K.O. and Takeda, E., Kagaku Kojo 11(5), 81 (1967).

76. Alverez, S., Tabacik, V. and Casabo, J., J. Mol. Structure 130, 235 (1985).

77. George, Z.M., Sulfur Removal and Recovery from Industrial Processes (Pfeiffer, J.B., Ed.), 75, Advan. Chem. Series 139, Amer. Chem. Soc., Washington, D.C. (1975).

78. Fiedorow, R. and Dalla Lana, I.G., J. Phys. Chem. 84, 2779 (1980).

79. Chuang, T.T. and Dalla Lana, I.G., J. Chem. Soc., Faraday Trans. I. 68, 773 (1972).

80. Hirschfeld, T. and Chase, D.B., Appl. Spectrosc. 40, 133 (1986)

81. Tripp, C., and Buijs, H., FT-Raman Application Note, Sept. 1986, Bomem Inc.

82. Hallmark, V.M., Zimba, C.G., Swalen, J.D., and Rabolt, J.F., Spectroscopy 2 40 (1987)

83. Tripp, C. and Buijs, H., FT-Raman Application note, June, 1987, Bomem Inc.

84. Parfitt, G.D., Progr. Surf. Membr. Sci. 11, 181 (1976).

85. Busca, G., Saussey, H., Saur, O., Lavalley, J.C. and Lorenzelli, V., Applied Catal. 14, 245 (1985).

86. Busca, G., Forzatti, P. Lavalley, J.C. and Tronconi, E., Catalysis by Acids and Bases, 15, Elsevier, The Netherlands (1985).

87. Jackson, P. and Parfitt, G.D., Trans. Faraday Soc. 67, 2469 (1971).

88. Tanaka, K. and White, J.M., J. Phys. Chem. 86, 4708 (1982).

89. Griffiths, D.M. and Rochester, C.H., J. Chem. Soc., Faraday Trans. I. 73, 535 (1977).

90. Boehm, H.P., Dicuss. Faraday Soc. 52, 264 (1971).

91. Boehm, H.P. and Herrman, M., Anorg. Allgem. Chimie 352, 156 (1967).

92. Steijns, M. and Mars, P., Ind. Eng. Chem. Prod. Res. Dev. 16, 35 (1977).

93. Saur, O., Bensitel, M., Saad, A.B. Mohammed, Lavalley, J.C., Tripp, C.P. and Morrow, B.A., J. Phys. Chem. 90, 980 (1986).

94. Saussey, H., Saur, O. and Lavalley, J.C., Jou. Chim. Phys. 81(4), 261 (1984).

95. Mashchenko, A.I., Pariiskii, G.B. and Kazanskii, V.B., Kinet. Katal. 9(1), 151 (1966).

96. Beck, D.D, White, J.M., and Ratcliffe, C.T, J. Phys. Chem. 90, 3132 (1986).

97. Goodsel, A.J., Low, M.J.D. and Takezawa, N., N. Environ. Sci. Technol. 6, 268 (1972).

98. Carleton, F.B., Quinn, H.A. and Rooney, J.J., J. Chem. Soc., Chem. Commun., 231 (1973).

99. Gilmore, T.A. and Rooney, J.J., J. Chem. Soc., Chem. Commun., 219 (1975).

100. Carleton, F.B., Gilmore, T.A. and Rooney, J.J., Prog. Int. Congr. Catal. I. 6, 291 (1976).

101. Ono, Y., Takagiwa, H. and Fukuzumi, S., J. Catal. 50, 181 (1977).

102. Khulbe, K.C. and Mann, R.S., J. Catal. 51, 364 (1978).

103. Parkyns, N., Proc. 5th Internat. Cong. Catal., Palm Beach, 205 (1972).

104. Dohy, D. and Lucazeau, G., J. Mol. Structure 79, 419 (1982).

105. Rosynek, M.P., Smith, W.D. and Hightower, J.W., J. Catal. 23, 204 (1971).

106. Gravlier, M. and Papee, D., Energy Process, Canad. Natur. Gas. Process, Calgary, 1 (1974).

107. Saussey, H., Vallet, A. and Lavalley, J.C., Mat. Chem. Physics 9, 457 (1983).

108. Preud'homme, J., Lamotte, J., Janin, A. and Lavalley, J.C., Bull. Soc. Chim. France I., 433 (1981).

109. Przystajko, W., Fiedorow, R. and Dalla Lana, I.G., Applied Catal. 15, 265 (1985).

110. Kayo, A., Yamaguchi, T. and Tanabe, K., J. Catal. 83, 99 (1983).

111. Jin, T., Machida, M., Yamaguchi, T. and Tanabe, K., Inorg. Chem. 23, 4396 (1984).

112. Nagase, Y., Jin, T., Hattori, H., Yamaguchi, T. and Tanabe, K., Bull. Chem. Soc. Jpn. 58, 916 (1985).

113. Andersson, S., Pompe, R. and Vannerberg, N.G., Applied Catal. 16, 49 (1985).

114. McArthur, D.P., Simpson, H.D. and Baron, K., Oil and Gas Journal, 70 (1983).

115. Byrne, J.W., Speronello, B.K. and Leuenberger, E.L., Oil and Gas Journal, 101 (1984).

116. Quet, C., Tellier, J. and Voirin, R., Stud. Surf. Sci. Catal. (Catal. Deact.) 6, 323 (1980).

117. Lavalley, J.C., Personal Communication.

118. Morterra, C., Chiorino, A. and Zecchina, A. and Fisicaro, E., Gazz. Chim. Ital. 109, 691 (1979).

119. Ross, S.D., Inorganic Infrared and Raman Spectra. McGraw-Hill, London (1972).

120. Ryan, R.R., Kubas, G.J., Moody, D.C. and Eller, P.G., Struct. Bonding (Berlin) 46, 47 (1981).

121. Colthup, N.B., Daly, L.H. and Wiberley, S.E., Introduction to Infrared and Raman Spectroscopy. Academic Press Inc., New York (1964).

122. Pinchas, S. and Laulicht, I., Infrared Spectra of Labelled Compounds. Academic Press Inc., London (1971).

123. Horn, R.W., Weissberger, E. and Collman, J.P., Inorg. Chem. 9, 2367 (1970).

124. Moody, D.C. and Ryan, R.R., Inorg. Chem. 16, 2473 (1977).

125. Sacks, M.D., Tseng, T.Y. and Lee, S.Y., Amer. Ceramic Soc. Bull. 63, 301 (1984) and references therein.

126. Nishimura, M., Asukura, K., and Iwasawa, Y., J. Chem. Soc. Chem. Comm. 1660 (1986)

127. Bensital, M., Saur, O., Lavalley, J.C., and Morrow, B.A., Mater. Chem. Phys., (in press)

128. Cotton, F.A. and Wilkinson, G., Advanced Inorganic Chemistry. John Wiley and Sons, 4th Edition, New York (1980).

129. Hanrahan, E.S., J. Inorg. Nucl. Chem. 26, 1757 (1964).

130. Udupa, M.R., Thermochim. Acta. 57, 377 (1982).

131. Saad, A.B. Mohammed, D.O.A. (1984).

132. Ruttenberg, F.E. and Low, M.J.D., J. Amer. Ceramic. Soc., 56, 241 (1973).

133. Morrow, B.A. and Cody, I.A., J. Chem. Soc., Farad. Trans. I, 71, 1021 (1975).

134. Petit, J.C. and James, H., Thermochim. Acta., 69, 323 (1985).

135. Petit, J.C. and James, H., J. Chimie. Phys. 82, 481 (1985).

136. Ito, T., Nozaki, T. and Ishikawa, H., Optical Properties, 127, 2053 (1980).

137. Farkis, A. and Mills, G.A., Adv. Catal. 13, 393 (1962)

138. Eley, D.D., Kiwanuka, G.M. and Rochester, C.H., J. C. S., Faraday I, 69, 2062 (1973).

139. Bloomfield, C.A. and Little, L.H., Can. J. Chem., 51, 1771 (1973).

140. Morrow, B.A., Cody, I.A. and Lee, L.S.M., J. Phys. Chem., 79, 2405 (1975).

141. Unland, M.L., J. Phys. Chem., 79, 610 (1975).

142. Dalla Betta, R.A. and Shelef, M., J. Molec. Catal., 1, 431 (1976).

143. Shelef, M., Catal. Rev. - Sci. Eng., 11, 1 (1975).

144. Unland, M.L., J. Catal. 31, 459 (1973).

145. Arai, H. and Tominaga, H., J. Catal., 43, 131 (1976).

146. Solymosi, F. and Rasko, J., J. Catal., 49, 240 (1977).

147. Nayama, H., Tanaka, M., Iida, H. and Echigoya, E., Bull. Chem. Soc., Jap., 49, 2047 (1976).

148. Klimisch, R.L. and Barnes, G.J., Environ. Sci. Technol., 6, 543 (1972).

149. Solymosi, F., Volgyesi, L. and Sarkany, J., J. Catal., 54, 386 (1978).

150. Solymosi, F. and Bansagi, T., J. Phys. Chem., 83, 552 (1979).

151. Kortum, G. and Delfs, H., Spetrochim. Acta., 20, 405 (1964).

152. Low, M.J.D. and Ramamurthy, P., J. Res. Inst. Catalysis, Hokkaido Univ., 16, 535 (1968).

153. Long, D.A. and George, W.O., Spectrochim. Acta., 20, 1799 (1964).

154. Rhee, K.H., and Basila, M.R., J. Catal., 1, 433 (1968).

155. Schwab, G.M, and Kral, H., Proc. Int. Congr. Catal., 1, 433 (1965).

156. Morterra, C. and Low, M.J.D., Annals of the New York Academy of Sciences, 220 (1973).

157. Lykos, P., Computer Networking and Chemistry. ed. A.C.S. Symposium Series, 19, American Chemical Society, Washington (1975).

158. Personal Computers in Chemistry. ed. Lykos, P., Wiley, New York (1980).

159. Computers in Chemical and Biochemical Research. Vol. 2, ed. Klopfenstern, C.E. and Wilkins, C.L., Academic Press, New York (1974).

160. Apple II Reference Manual. Apple Computer Inc. (1979).

161. Model 283 Infrared Spectrophotometer Reference Manual. Perkin-Elmer, Norwark, Connecticut, U.S.A. (1975).

162. Morrow, B.A., Tripp, C.P. and McFarlane, R.A., J. Chem. Soc., Chem. Commun., 1282 (1984).

163. Morrow, B.A. and McFarlane, R.A., Langmuir 2, 315 (1986)